The Synthesis of Novel Block Copolymers via Atom Transfer Radical Polymerisation for Use as Stabilisers in Non-Aqueous Dispersion Polymerisations

Kate E Belsey

A thesis submitted to the University of Kent in partial fulfilment of the requirements for the degree of Doctor of Philosophy.

University of Kent
Canterbury
Kent
CT2 7NH

June 2015

Abstract

Colloidal polymeric particle dispersions have found many industrial applications, one of which is as the 'ink' particles within electrophoretic displays. Traditionally these displays have shown high resolution, increased battery life and excellent readability in sunlight, when compared with more commonly used displays, such as liquid crystal displays (LCDs). However, commercially available examples have only demonstrated black and white displays, or screens with coloured filters over the black and white particles, resulting in 'washed out' colours. The development of a full colour electrophoretic display holds great industrial potential to advance the field of electrophoretics, as well as available technology.

A stabiliser is required during the synthesis of said particle dispersions, in order to control the parameters of the particles, as well as to ensure they remain stable and do not aggregate or settle out. Numerous different stabilisers have been successfully employed, although each has disadvantages and difficulties associated with it. This work describes the development of a block copolymer stabiliser of poly(methyl methacrylate) and poly(octadecyl acrylate). The stabiliser itself was synthesised using controlled radical polymerisation techniques, namely atom transfer radical polymerisation (ATRP). ATRP allowed for the molecular weight, composition and distribution of chain lengths to be tailored to meet certain requirements. The stabilisers were then employed in non-aqueous dispersion (NAD) polymerisations, to synthesise dispersions of monodisperse, cross-linked and dyed particles, with good size control and spherical packing. Initial dispersions showed desirable characteristics for electrophoretic fluids, but exhibited a thermoresponsive gelation once allowed to stand for a period of time. The nature of this gelation process was investigated, before modifications were made to the structure of the stabiliser. This new stabiliser was then used in NAD polymerisations, which resulted in particles which still possessed all the desirable properties previously observed, without the gelation. These particles were then tested successfully for their application in electrophoretic displays.

Acknowledgements

Firstly I must thank Dr Simon Holder for the endless amount of invaluable support, guidance and knowledge he has provided me with throughout this PhD – without him I would not have made it to this point. I also need to thank Dr Serena Corr for her help as associate supervisor.

Thank you to Louise, Claire, Mark, Henry and everyone else at Merck Chilworth for working with me during my PhD – for hosting me in your labs, for the guidance with experiments, patents and writing, and also for the CASE conferences in lovely hotels!

I would like to thank everyone who has been part of the (extended) Holder/310 group over my time here, all for very different (but equally important) reasons: Beulah for convincing me I could do it and starting me on the polymer pathway; Aaron for the days of keeping me sane in the lab and for guiding me for the longest; Marc for suffering with me for the entirety of this PhD – the fact we are submitting together is hilarious but fitting; girl Charlie for always listening, always being there, always telling me that I'm right (even when I'm not) and always having chocolate; boy Charlie for being the happiest, most positive and lovely person I know; Gemma for the endless cups of tea and long chats (often about fish); Darren for the Asda discount, the late night sampling runs and the most unique taste in shirts; Danielle for being my favourite minion of all time and staying in touch even though you're now the enemy; Liv for being so very clumsy and regularly creating words; Christina for keeping me sane recently and for being an amazing travel buddy; as well as the newest additions to our lab family: Trevor, Ollie, Chrissie, Alex, Yarry and Francesco. This thesis is because of all of you. Thank you also to Sean, for making very long and painful conferences bearable, and even enjoyable (usually in the bar and not in the lecture theatre!).

I owe a huge amount to everyone in the department who has become accustomed to bailing me out on short notice due to lack of organisation – *occasionally* on my part – JJ, Bernard, Ian, Trevor, Spartaco, Dave, Roy, Pat, Debs, James, Dean, Mike, Ann: thank you all so much. I need to thank Barry and Ewan for their support, and for sharing their knowledge and experiences with me. I also need to say thank you to

Ian Brown for all his TEM help, and to Michelle and Mark for being so wonderful with their amazing NMR at short notice. I should also thank all the undergrads who always made Tuesday the most interesting day of the week, and a day with no fires was a good day (JJ I'm still sorry about the hole in your bench from my first day demonstrating!).

I am very lucky to have a long list of people who have been a huge support network to me over the past 3(ish….okay 4) years. Chrissie, Bernie, Charlotte, Lewis and Alex – thank you for being a like a second family to me, always opening your home to me and cheering me up on the bad days. Jess – thank you for being there for the last 16 years (wow that's scary), for always listening and for being there whenever I need you. Jade, Rachel and Jess – thank you for our (almost) monthly meetings, and for listening to my moanings! Jill – thank you for the catchups, the cake, and more importantly the wine! (and now Beth cuddles!) Liz – thank you friend for our random coffees and dinners, we really must do it more often. To David and Pauline for always being so optimistic and supportive. I am indebted to all of you.

To everyone at the golf club, particularly the bar staff, who were a huge part of my life throughout my degree and throughout my PhD, thank you for listening to my rants and putting up with me being so nerdy (I can still make you aspirin).

Finally, to my family. Colin and Linda – thank you for welcoming me, for the coffees and for always having time to listen. Grandma Mert and Auntie Diane – thank you for always believing in me, even when I don't believe in myself. To those who aren't here to see me get to this point (Grandpa Don, Grandpa Peter, Grandma Eve, Grandpa Jack) – I hope I make you proud. To Daniel, who is already a big shot developer - I will always have this thesis! To my mum, for being my inspiration and for always, always supporting me. And finally to Matt, who is the reason I have made it – I love you, and you are my everything. This is for all of you.

Declaration

I declare that this thesis is my own work and effort, and has been written in my own words. Due care has been taken to properly reference the work of others wherever necessary.

Kate Belsey
29 January 2015

Abbreviations

ARGET	Activators regenerated by electron transfer
ATRA	Atom transfer radical addition
ATRP	Atom transfer radical polymerisation
DCM	Dichloromethane
DLS	Dynamic light scattering
DMSO	Dimethylsulfoxide
dNbpy	2,2-dinonyl-4,4,-dipyridyl
DP	Degree of polymerisation
EBIB	Ethyl α-bromoisobutyrate
EBPA	Ethyl α-bromophenylacetate
EGDMA	Ethylene glycol dimethacrylate
FTIR	Fourier-transform infra-red spectroscopy
FRP	Free radical polymerisation
GPC	Gel permeation chromatography
I_{Eff}	Initiator efficiency
ISET	Inner sphere electron transfer
k_{act}	Activation rate coefficient
K_{ATRP}	Rate coefficient of ATRP
k_{deact}	Deactivation rate coefficient
k_p	Propagation rate coefficient
k_t	Termination rate coefficient
LCST	Lower critical solution temperature
MALDI-TOF	Matrix-assisted laser desorption ionisation time of flight spectrometry
Me_6TREN	Tris(2-(dimethylamino)ethyl amine
MA	Methyl acrylate
MMA	Methyl methacrylate
M_n	Number average molecular weight
M_p	Peak average molecular weight
M_t	Metal centre in ATRP
M_w	Weight average molecular weight

NAD	Non-aqueous dispersion
NMP	Nitroxide mediated polymerisation
NMR	Nuclear magnetic resonance spectroscopy
ODA	Octadecyl acrylate
ODMA	Octadecyl methacrylate
OSET	Outer sphere electron transfer
PHSA	Poly(hydroxystearic acid)
PMDETA	N,N,N’,N’,N’’-pentamethyldiethylenetriamine
PMMA	Poly(methyl methacrylate)
P_m•	Active polymer chain with radical
P_n•	Active polymer chain (of different chain length) with radical
PODA	Poly(octadecyl acrylate)
PPMI	N-(n-propyl)-2-pyridylmethanimine
PRE	Persistent radical effect
RAFT	Reversible-addition fragmentation chain transfer
RI	Refractive index
SARA	Supplemental activator and reducing agent
SEC	Size exclusion chromatography
SEM	Scanning electron microscopy
SET	Single electron transfer
T_m	Melting transition temperature
T_g	Glass transition temperature
THF	Tetrahydrofuran
UCST	Upper critical solution temperature

Table of Contents

Chapter 1: Introduction to Polymers

1.1 Introduction to Polymerisation Techniques

1.1.1 Free Radical Polymerisation

Of the multitude of polymerisation methods, the free radical polymerisation of vinyl (double bond containing) monomers has probably been one of the most successful. It is frequently used in industry, due to the wide range of monomers and solvents which can be used. There are three main steps to free radical polymerisation (FRP) – initiation, propagation and termination, as shown in Scheme 1.1.

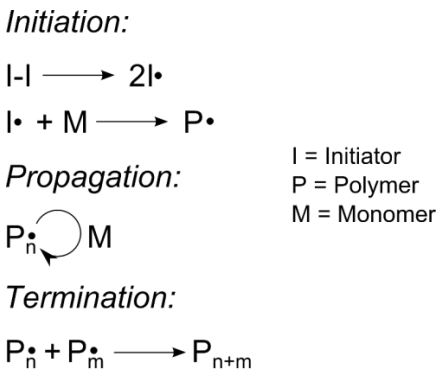

Scheme 1.1: The three stages of free radical polymerisation, where P_n and P_m are two different polymer chains, and • denotes a radical.

First, a bond within an initiator molecule undergoes homolytic fission, leaving two radical initiator groups. This fission can occur through thermal decomposition or photoinitiation with the addition of UV light, amongst other methods. These then go on to react with a monomer molecule containing a double bond, which breaks to form a radical active centre. The rate of initiation is defined as:

$$R_i = 2fk_d[I] \tag{1.1}$$

where k_d is the rate constant of initiator decomposition.

This active radical comes into contact with other monomer molecules during the propagation stage, steadily increasing the polymer chain one monomer unit at a time,

with the radical moving to the end of the chain each time. The rate of propagation is defined as:

$$R_p = k_p[M][P\cdot]$$

(1.2)

The reaction terminates when two polymer radicals meet each other, known as radical-radical coupling or bimolecular termination, which effectively removes the propagating radical. Termination can also occur through radical transfer from the propagating chain to solvent, polymer or monomer molecules. Other side reactions are observed during FRP – one of these is a process whereby the propagating radical can be transferred to a different active polymer chain, leaving a double bond at the end of one chain and terminating the other. This side reaction is known as disproportionation. The rate of termination is defined as:

$$R_t = 2K_t[P\cdot]$$

(1.3)

where K_t is the sum of the termination via combination, disproportionation and radical transfer.

By combining these three equations, the rate of propagation can be determined as a function of both the monomer and initiator concentration using the equation:

$$R_p = k_p\left(\frac{fk_d}{k_t}\right)^{\frac{1}{2}}[M][I]^{\frac{1}{2}}$$

(1.4)

Although FRP is advantageous as it is carried out under mild conditions and is simple to achieve, it has been shown to produce polymers with very broad molecular weight distributions. The disproportionation and bimolecular termination reactions occur unpredictably, meaning that the product polymer is often also of a very different molecular weight to that which was being targeted by the synthesis. FRP also does not allow for the synthesis of polymers which can be extended to make block copolymers. This inability to control the architecture, the molecular weights and the dispersity of polymers was one of the reasons that controlled polymerisation methods were developed.

1.1.2 Controlled Radical Polymerisation

Whilst conventional radical polymerisation can be conducted on a large scale in order to produce polymers on a commercial scale, emerging applications often require polymers which are more well-defined than those obtained via FRP. For this reason, polymer science moved into developing synthetic routes which provided more control over the properties of the polymer produced – molecular weight, dispersity and composition. A number of routes were discovered, which were termed 'reversible-deactivation radical polymerization', often also known as 'controlled radical polymerisations' or 'living radical polymerisations'. However, this latter name is not strictly accurate, as truly 'living' polymerisations do not allow for any termination reactions to occur; whilst these new controlled polymerisations do exhibit a significantly reduced degree of termination in comparison to FRP, these reactions do still occur. The name 'living' originally came from work into anionic polymerisations, where under ideal conditions termination did not occur, allowing propagation to continue until all monomer was consumed – this work was also one of the first methods of synthesising block copolymers.[1]

In order for a polymerisation to be described as living, it must meet a number of criteria, laid out by Quirk and Lee.[2] These conditions are:

1. Chain growth continues until all monomer has been consumed, and can continue if monomer is later added.
2. Molecular weight increases linearly with conversion.
3. Irrespective of the conversion, the concentration of the active species remains constant.
4. Distributions of molecular weight are narrow (M_w/M_n <1.5).
5. Sequential monomer addition leads to synthesis of block copolymers.
6. The functionality of the polymer chain end is preserved.

Atom transfer radical polymerisation (ATRP), reversible-addition fragmentation chain transfer polymerisation (RAFT) and nitroxide mediated polymerisation (NMP) were three of the routes which received a significant amount of interest amongst research groups. All of these methods are designed around a dynamic equilibrium between active (propagating) and dormant (terminated) species, which is the main feature allowing control over the product polymer. The equilibrium is designed to

ensure the concentration of active species is low during the polymerisation, typically resulting in defined molecular weights and a low dispersity.

1.1.3 Nitroxide Mediated Polymerisation

Nitroxide mediated polymerisation (NMP) was developed by Hawker in 1994[3], and is based around an equilibrium between dormant alkoxyamines, and the active propagating species typical of other controlled polymerisation mechanisms.[4] The nitroxide temporarily traps radicals to allow the reaction to progress, before returning to the dormant, end-capped species. NMP was originally shown to only be valid with styrene based monomers when 2,2,6,6-tetramethyl-1-piperidinyloxy (TEMPO) was used,[5] which facilitated the development of other nitroxides for use as radical generators.[6] TEMPO is often described as the 'persistent radical' in NMP, comparable to a similar process in ATRP (to be discussed in section 1.1.5). Scheme 1.2 shows a typical bimolecular NMP reaction, which requires the addition of a radical initiator, in this case benzoyl peroxide (BPO). As part of the development of novel reagents, unimolecular mediators were later designed which acted as both the initiating group and the end cap.[7]

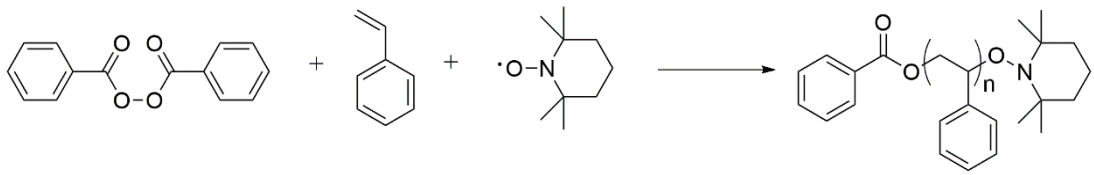

Scheme 1.2: A typical bimolecular NMP reaction, using TEMPO as the mediator, benzoyl peroxide as the initiator and styrene as the monomer (adapted from reference [8]).

There are, however, a number of disadvantages associated with NMP as a synthetic route. Polymerisations often have to be conducted at relatively high temperatures (>100ºC); the understanding of the kinetic processes for using polymers synthesised in this way is very limited, and the range of monomers which can be used are restricted.[9] The first example of a methacrylate homopolymerisation via NMP at relatively mild reaction conditions was published very recently in comparison to the length of time that NMP has been considered a valuable technique.[10] For this reason, NMP has not yet been adopted as a frequently used technique in industry.

1.1.4 Reversible-Addition Fragmentation Chain-Transfer Polymerisation

Reversible-addition fragmentation chain-transfer polymerisation (RAFT) was developed by Rizzardo in 1998.[11] It is a pseudo-living reaction, meaning that it has living characteristics but utilises a conventional free radical initiator. Scheme 1.3 shows the mechanism for the RAFT process, where a radical is formed from an initiator, which reacts with monomer molecules to form the start of a polymer chain. The radical on this polymer chain can be temporarily added to the carbon centre of the RAFT agent to form a dormant species (known as the reversible chain transfer), before the radical returns to the propagating species to continue the polymerisation. This is the dynamic equilibrium for the RAFT process, comparable to those in ATRP and NMP. During reinitiation, the free radical leaving group R reacts with monomer molecules to form another growing polymer chain, meaning that the polymerisation and chain transfer can occur on both sides of the RAFT agent.

A chain transfer agent is required for the polymerisation, and these are typically dithioesters, dithiocarbamates and dithiobenzoates.[11] The choice of RAFT agent is critical in controlling the molecular weights and dispersities of the polymers synthesised. The agent requires three properties: 1) a reactive C=S bond; 2) a stabilising 'Z' group; and 3) a free radical leaving group 'R'.[8] The specific RAFT agent selected is often tailored due to the monomer and solvent of the system. This method has also been shown to produce block copolymers and copolymers with varying complex morphologies, due to the polymer retaining its functionality after reaction completion and purification.[12]

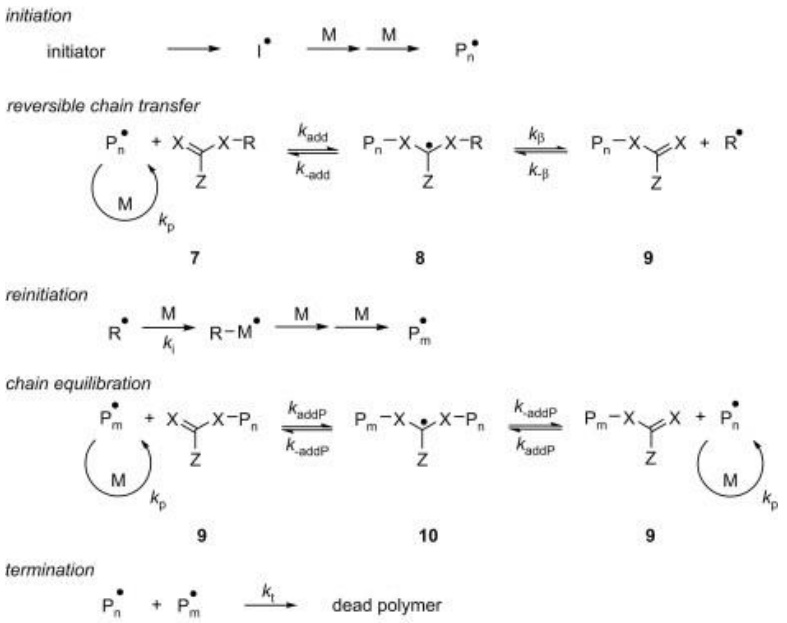

Scheme 1.3: Mechanism of RAFT polymerisation (reproduced from reference [12]), where X is typically sulphur.

One of the original disadvantages of using RAFT polymerisation was the presence of the sulphur moieties in the product polymer. This resulted in polymers which smelled unpleasant, and were often highly coloured due to the RAFT agents used. However, it was later shown that it is possible to regenerate chain transfer agents after a RAFT polymerisation by using free radical sources,[13] as well as to functionalise them, by processes such as thermal elimination or reaction with nucleophiles.[14] This was seen to remove the bright colours, as well as the added benefit of new, desirable functionalities. The majority of polymers synthesised by RAFT contain thioester groups, which are undesirable in industrial processes. Other disadvantages of RAFT include the fact that the RAFT agents are not commercially available and therefore need to be synthesised, and that the polymerisations typically need to be stopped at 70-90% conversion in order to reduce the effect of bimolecular termination (which is increased by the use of a free radical initiator).

As this work focuses on ATRP, the rest of this discussion will concern this method only.

1.1.5 Atom Transfer Radical Polymerisation

Atom transfer radical polymerisation (ATRP) is a type of controlled, living polymerisation, discovered by the research groups of Sawamoto[15] and Matyjaszewski[16] at around the same time in 1995. Sawamoto reported the use of iron and ruthenium based catalysts, whilst Matyjaszewski favoured the use of copper catalysed systems, with the essential principle being the same. Ruthenium based catalysts are expensive, whilst iron based systems were not always seen to be as effective as the use of other metal halide systems. For these reasons, together with the sheer volume of research documenting the use of Cu(I) and Cu(II) systems, throughout this work the activating/deactivating system will be referred to as Cu(I)/Cu(II).

ATRP has been shown to provide control over the molecular weights of the product polymers, and to give dramatically lower dispersities than are observed for a typical FRP. It is often seen as an extension of atom transfer radical addition also known as ATRA, shown in Scheme 1.4, where L_n is a ligand, X is a halide group and M_t is the metal centre. ATRA is the addition of a radical to an unsaturated molecule, which can then revert back to the dormant molecule. This is typically only a one step addition, as opposed to ATRP which is a number of additions in succession.[17]

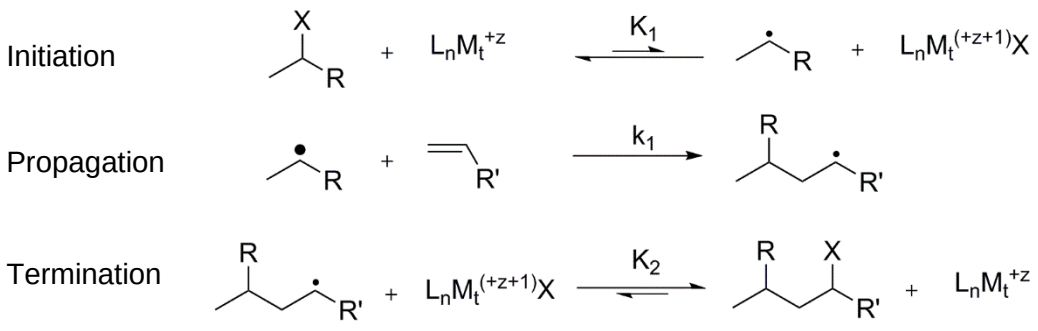

Scheme 1.4: Mechanism of atom transfer radical addition (ATRA) (reproduced from reference [17]).

The mechanism for polymerisation (Scheme 1.5) revolves around a dynamic equilibrium between the metal halide catalyst and the growing polymer chain during the propagation step. A metal halide (typically) catalyst, aliphatic amine ligand, halide initiator, monomer and solvent are combined under an inert atmosphere. The halide from the initiator transfers to the metal-ligand complex (increasing the oxidation state of the metal), leaving behind an active radical on the initiator group –

shown by the activation rate coefficient, K_{act}. This radical can then propagate with monomer available in the system, increasing the chain length of the polymer. The halide then returns to 'cap' the growing polymer chain, making it dormant – this is represented by the deactivation rate coefficient, k_{deact}.

The strength of the carbon-halide bond means that the activation energy to produce this radical is large. This causes the equilibrium to be heavily shifted towards the formation of dormant chains, meaning there is only ever a low concentration of radicals available to react within the system. It is this general 'inactivity' that allows the reaction to progress slowly, and with great control over the chain length and dispersity.

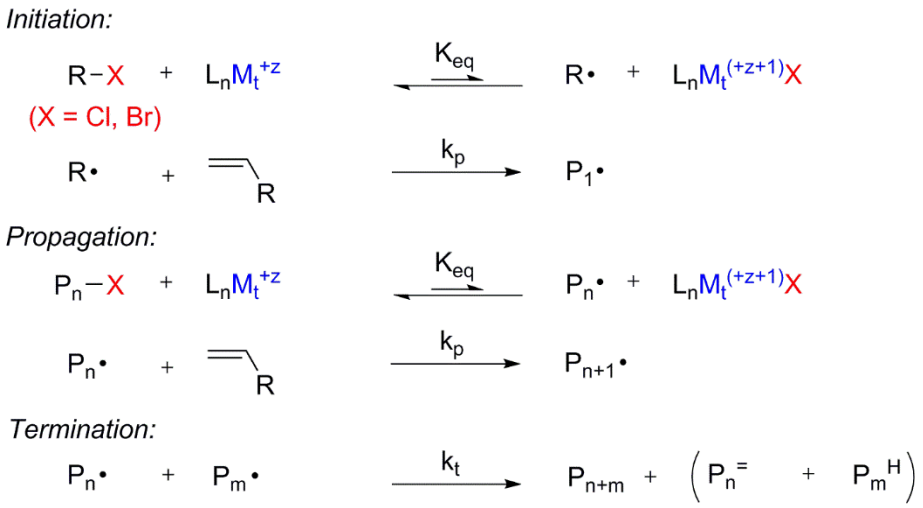

Scheme 1.5: Illustration of the steps involved in ATRP (reproduced and updated from reference [17]).

When all monomer has been consumed, the product polymer chains which have not undergone side reactions will be halide-terminated, allowing for them to be used as macro-initiators for other polymerisations. This functionality means that ATRP is a very valuable method for the facile synthesis of block copolymers – the polymer can either be isolated, purified and then added to another reaction, or a second monomer can be added straight to the initial reaction (when all monomer has been consumed), giving a 'one-pot' method for block copolymerisation.[18, 19]

Termination either occurs when all monomer has been consumed, or through bimolecular termination. Although bimolecular termination is theoretically almost eliminated by using ATRP, as the scarcity of active polymer chains in solution means the probability of two chains meeting in order to terminate is much lower, it is

still seen to occur in ATRP systems. Another undesirable termination reaction during ATRP is the formation of a carbon-carbon double bond, from the exclusion of the halide moiety. Both of these termination processes are shown in Scheme 1.6, with the termination rate coefficient, k_t. These steps suggest there are 3 electron transfer reactions which are crucial to ATRP: disproportionation of the ATRP activator; the oxidation or reduction of radicals to carbocations and carboanions; and the radical coordination to the ATRP catalyst.[20]

One of the key features of ATRP is the persistent radical effect (PRE) – Scheme 1.8 shows the proposed mechanism for PRE. In ATRP, the persistent radical is the Cu(II) species. It is based around the principle that, typically towards the beginning of a reaction, bimolecular termination is often observed as there is no deactivating Cu(II) present. This radical-radical coupling results in an increase of the deactivating Cu(II) species present in the reaction medium, which cannot be reduced back to Cu(I) species.[21] This shifts the equilibrium to the left, increasing the control of the ATRP system.

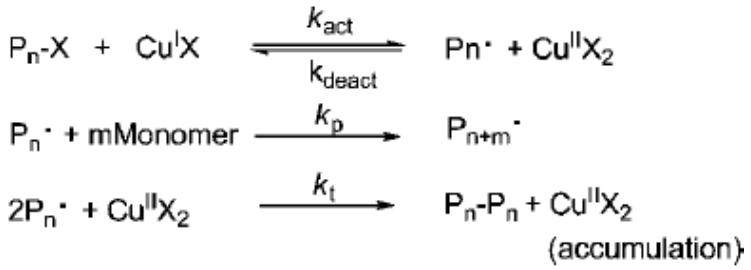

Scheme 1.6: Processes involved in the persistent radical effect, leading to a build-up of the deactivator, Cu(II).

1.1.5.1 Kinetics of ATRP

As previously mentioned, the control over molecular weight and dispersity is maintained by a dynamic equilibrium between activation and deactivation, shown in Figure 1.1.

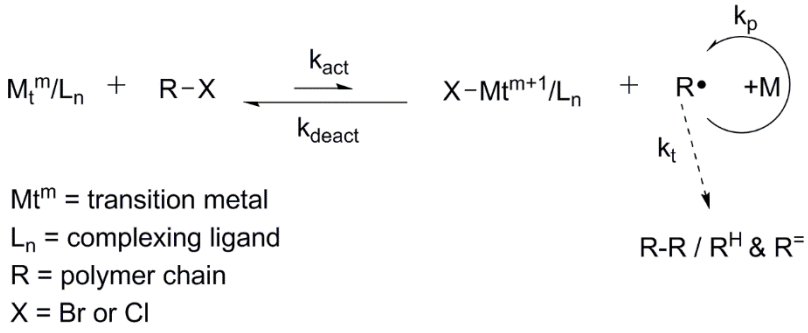

Figure 1.1: The dynamic equilibrium involved in ATRP (reproduced and updated from reference [16]).

This equilibrium can be described by the equilibrium constant of ATRP, defined as:

$$K_{ATRP} = \frac{k_{act}}{k_{deact}} = \frac{[P\cdot][Cu(II)X]}{[PX][Cu(I)]} \tag{1.5}$$

where k_{act} is the equilibrium constant of activation, and k_{deact} is the equilibrium constant of deactivation. K_{ATRP} must be kept low (between 10^{-4} and 10^{-9}) in order to achieve control over the reaction and reduce termination reactions seen more often in conventional radical polymerisations. It has been suggested that this means that the components in ATRP are probably 2 orders of magnitude less active than those in conventional FRP.[22] If k_{act} is too low, then the reaction will proceed slowly (if at all). If K_{ATRP} is too large, due to a high k_{act}, then control will not be maintained, and termination reactions will occur alongside the propagation steps. On the other hand, if k_{act} is very low, giving a very small K_{ATRP}, then if the polymerisation proceeds at all, it will be incredibly slow. The rate of polymerisation, k_p, is defined by:

$$R_p = k_p[P*][M] \tag{1.6}$$

where k_p is the rate coefficient of propagation, P* is the concentration of propagating radicals, and M is the concentration of monomer.

The overall equilibrium is composed of 4 sub-equilibria, shown in Figure 1.2. K_{ET} represents the process of electron transfer, K_{EA} the electron affinity of the halide, K_{BH} the homolysis of the alkyl halide bond, and K_x the association of the halide to the metal ligand complex.

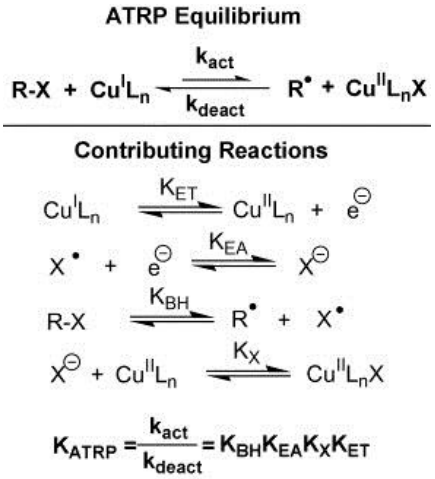

Figure 1.2: the overall equilibrium and the four sub-equilibria of ATRP.

Kinetic plots are often presented as evidence that an ATRP reaction is truly living – the pseudo-first-order nature of the reaction (where the concentration of monomer is significantly greater than of the active radical P*) suggests that a semilogarithmic plot of monomer conversion against time should be linear. This linearity signifies that the reaction is progressing in a controlled manner, with uniform growth of polymeric chains as monomer is consumed. Towards the end of a reaction, this linear plot is sometimes observed to flatten out, and eventually reach a plateau, as monomer consumption nears completion and termination reactions increase. These reactions increase due to catalyst which has been irreversibly oxidised, and the reduction of available monomer for propagation. Similarly, a plot of molecular weight against conversion would be expected to be linear, if initiation has occurred effectively – both of these plots are shown in Figure 1.3.

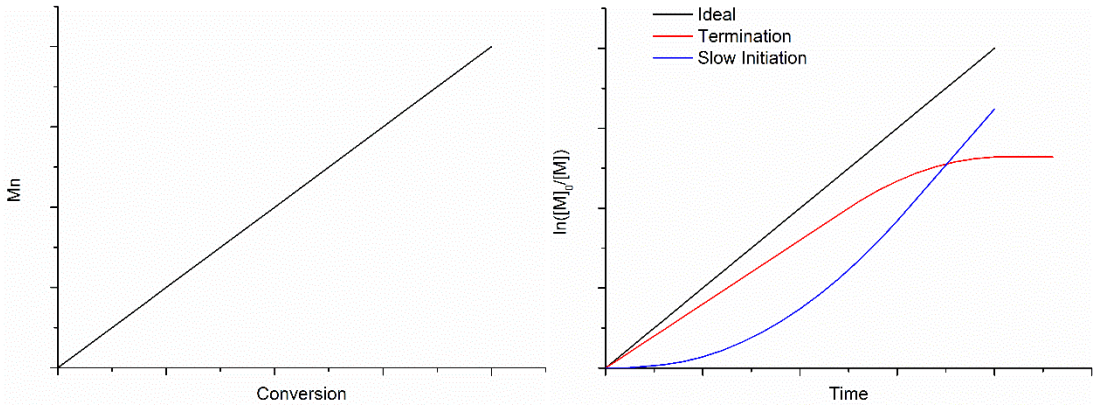

Figure 1.3: Linear kinetic plots following the progression of a polymerisation. On the left, conversion against molecular weight, and on the right a semilogarithmic plot of time against conversion. The right hand plot also shows how the kinetics would be affected if other unwanted processes occurred during the reaction.

An equation related to these kinetic plots describes the relationship between conversion and all the other parameters included in the ATRP system. This equation only holds true for when there is a low concentration of radicals and the rate of termination is low, and is defined as:

$$ln\left(\frac{[M]_0}{[M]_t}\right) = \frac{k_p k_{act}[RX]_0[Cu^I]_0}{k_{deact}[Cu^{II}]_0} t \quad (1.7)$$

with $[Cu^I]$ being the concentration of copper (I) species, $[Cu^{II}]$ being the concentration of copper (II) species, and all other parameters as are previously defined.[23]

In order to obtain the desired control over the reaction, each component of the ATRP system must be carefully selected. The choice of monomer, catalyst, initiator, ligand and solvent, together with the reaction temperature and the molar ratios of each component added, have a dramatic effect over the product polymer.

1.1.5.2 Monomers

The monomer in ATRP reactions is often selected for its properties once polymerised, and then the other features of the system are optimised around that monomer choice. Monomers which have been successfully polymerised via ATRP include a range of styrenes,[24-26] acrylates,[27-29] methacrylates[30-33] and many others. Each monomer has its own K_{ATRP}, and its own radical propagation rate. This means that in order to maintain control over the polymerisation, both the concentration of active radicals and the rate of radical deactivation must be controlled.[34]

One of the other features of ATRP is that it is affected by the reactivity of individual monomers. Whilst conventional radical copolymerisation of two monomers simultaneously would produce a 'random' copolymer, the same reaction in an ATRP system would result in a gradient copolymer. This is due to the reactivity of the two monomers: if they have very similar reactivities, then the monomers will be randomly distributed throughout the chain, however if one is considerably more reactive than the other, this monomer will react preferentially, creating a

composition drift. Another way to synthesise gradient copolymers is by controlling the feed ratios of each monomer during the reaction.[22, 28]

1.1.5.3 Catalysts

The catalytic system in ATRP is composed of a metal halide and an aliphatic amine ligand. The selection of each of these components can dramatically affect the control over the polymerisation.

The metal halide (in most cases, Cu-X) selected for ATRP needs to have 2 valence states which are 1 electron apart, and an affinity for halogens. This allows the metal centre to be oxidised from Cu(I) to Cu(II) when it accepts the halide from the initiator or growing polymer chain, and then reduced back to Cu(I) when the halide returns to the chain, rendering it temporarily dormant again. This oxidation process causes an increase in coordination number for the copper, and it has been suggested that Cu(I) is tetracoordinate, while Cu(II) is pentacoordinate, shown in Figure 1.4.[17, 35]

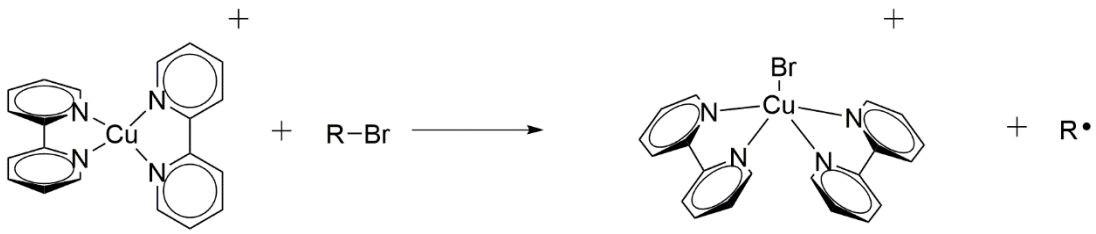

Figure 1.4: Proposed arrangement of ligand and catalyst system (reproduced from reference [36]).

The activity of the catalyst depends upon both the affinity of the halide atom to the ligand complex (k_X). This is also directly affected by the selection of the ligand in the system. For complexes with similar k_X values, the redox potentials can be used as a measure of the catalytic activity. CuCl species typically exhibited lower redox potentials than CuBr species, and these redox potentials were seen to decrease as the number of coordination sites present on the ligand increased.[37]

Although K_{ATRP} for CuBr would be expected to be up to several orders of magnitude greater than for the same system but containing CuCl, due to the difference in bond dissociation energy of the C-Br and C-Cl bonds, the difference is actually considerably smaller due to the higher electron affinity of the chlorine.[38]

The ligand in an ATRP reaction is responsible for a number of the properties of the system, including the steric, electronic and solubility properties of catalysts in ATRP, and as such they also have an effect on the equilibrium constants.[39] A wide range of ligands have been developed, and the selection of a suitable ligand often depends on the metal centre to be used within the catalyst.[22] For example, copper catalysed systems tend to be successful when a multi-dentate nitrogen based ligand is used, which can also be used for iron based systems, while ruthenium systems often use more complicated ligand catalyst complexes, such as incorporating half-metallocenes and alkylidenes.

The first examples of ligands used for ATRP were bipyridines, which were shown to control the molecular weight of the polymers.[16] It was later shown that adding substituents onto bipyridine ligand improved the solubility of the copper halide in the polymerisation, and led to a dramatic reduction of dispersity.[40] This also increased the k_{act} from 0.066 to 0.20.[41] However, the reaction times were slow for these bidentate ligands. This led to the development of tri and tetradentate ligands, and ligands with branched structures, such as PMDETA, HMTETA and Me_6TREN. Me_6TREN forms one of the most active complexes, with a k_{act} value of 450 $M^{-1}s^{-1}$. These studies led to the proposal of a general order of reactivity for ligand complexes: tetradentate (cyclic-bridged) > tetradentate (branched) > tetradentate (cyclic) > tridentate > tetradentate (linear) > bidentate ligands.[41]

New ligands with a N=C-C=N (diimine) structure were investigated – a range of Schiff base ligands were synthesised via the condensation of amines with other functional molecules, amongst them pyridine carboxaldehydes.[42] This work showed that steric crowding of the catalyst (by adding branching to the ligand) decreases k_p and leads to an increased weight distribution, whilst increasing the length of the alkyl substituent on the pyridine ring leads to better solubility in non-polar systems.[42] The low lying π^* orbital present in these ligands enables them to stabilise metal centres due to two properties – their ability to remove electron density from the metal centre, and their ability to change their conformation when they are coordinating with the metal in two different oxidation states.

One of these ligands has been used in numerous examples of ATRP reactions - N-(n-propyl)-2-pyridyl(methanimine) (PPMI).[33, 43-45] This particular ligand resulted in

linear evolution of molecular weight with regards to conversion, but caused an induction period as well as an increase in dispersity from increased termination reactions. This induction period was likely due to the formation of an active initiator. The molecular weight was seen to be dependent on the concentration of Cu(I) in the system.[36]

A number of ligands and their activities are displayed in Figure 1.5. – one general trend that can be observed is that ligands containing more nitrogen groups typically exhibit a higher activity.[23] The choice of each component must allow for enough activity that the reaction proceeds fairly quickly, without being so active that the reaction progresses in an uncontrolled manner.

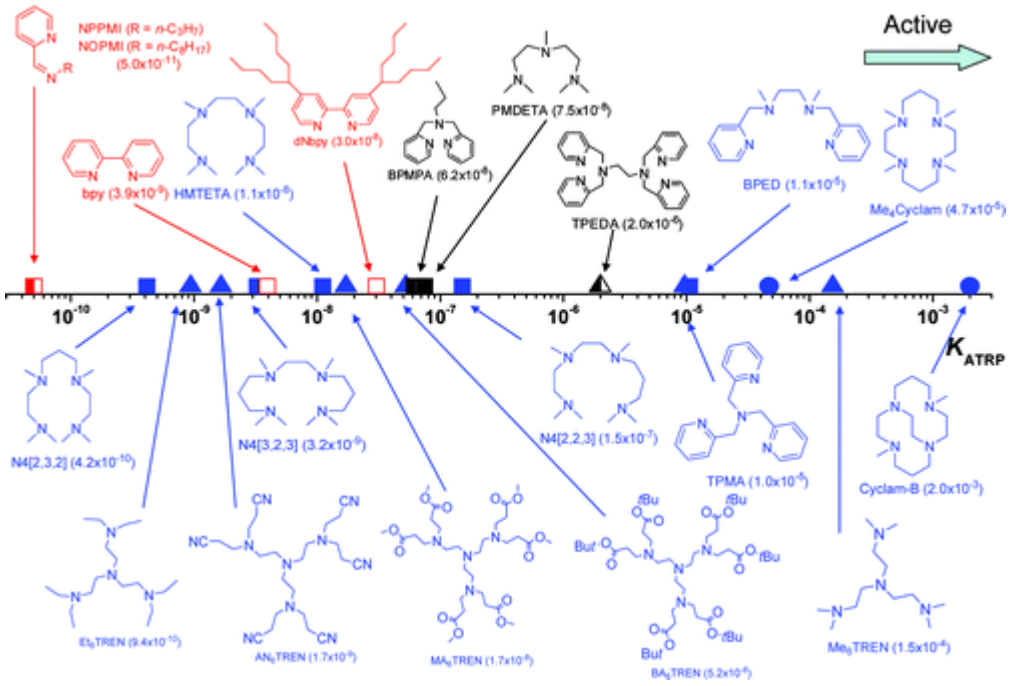

Figure 1.5: K_{ATRP} constants for various ligands when used in conjunction with Cu-X catalyst, EBIB initiator, in acetonitrile (Reprinted with permission from W. Tang et al, Journal of the American Chemical Society, 2008, 130, 10702-10713. Copyright 2008 American Chemical Society[23]).

Values for K_{ATRP} have been measured experimentally for systems in acetonitrile. When CuBr was used as the catalyst and ethyl 2-bromoisobutyrate (EBIB) was used as the initiator, values of K_{ATRP} for bpy, PMDETA and Me_6TREN were $3.9x10^{-9}$, $7.46x10^{-8}$, and $1.54x10^{-4}$ respectively.[46] This highlights the necessity to select a ligand with an activity that is suitable for the polymerisation system. It has already been mentioned that K_{ATRP} needs to be kept low in order to maintain control over the

system, and the activity of PMDETA here is clearly just on the boundary of keeping the necessary control.

ATRP reactions can be carried out in bulk, but the presence of solvent increases the control over molecular weight and dispersity. Non-polar aromatic solvents are the most suitable for polymerisations of methyl methacrylate, but this causes difficulties if bipyridine is selected as a ligand. Bipyridine is only sparingly soluble in solvents such as toluene, giving a slow uncontrolled polymerisation. This issue was circumvented and the system made more homogenous by the addition of long alkyl substituents to positions away from the coordinating sites of the ligand.[22]

1.1.5.4 Initiators

The degree of polymerisation (DP) is mainly controlled by the initiator used in the reaction, and is defined as:

$$DP = \frac{M_n}{M_0} = \frac{\Delta[M]}{[I]_0} \tag{1.8}$$

where M is the monomer, I is the initiator, and M_n is the molecular weight of the product polymer. The DP is calculated by dividing M_n by the molecular weight of one monomer unit, and if initiation occurs efficiently it is also proportional to the concentration of monomer in relation to the concentration of initiator added at the start of the reaction.

Initiators for ATRP typically contain an alkyl halide (R-X) group, which is usually next to an electron withdrawing group. This substituent activates the R-X bond, increasing its polarity which in turn leads to the formation of a more stable radical.[47] However, if these groups stabilise the R-X too strongly, little or no initiator efficiency is seen, whilst simple alkyl halides with no stabilising groups often exhibit multiple initiation sites or chain transfer reactions. The trend for these groups, in order of increasing activity, is amide<ester≈aryl<cyano. An initiator is also often selected with a similar structure to that of the monomer to be polymerised, such as ethyl 2-bromoisobutyrate (EBIB) for the polymerisation of methyl methacrylate. Initiators with halides attached to a tertiary carbon exhibit the highest activities,

followed by secondary and then primary arrangements. This is due to the tertiary carbon stabilising the radical more effectively than less substituted carbon centres.[22]

In order to maintain control over the polymerisation, the process of initiation must occur more rapidly than the process of propagation. This is to ensure that all initiator molecules form radicals and chain-extend uniformly – if initiation is slow, some chains will begin to grow before others, resulting in a broad dispersity and uncontrolled molecular weights. A number of ATRP initiators and their activities are shown in Figure 1.6. No initiators are shown containing an iodine group – this is due to the inherent instability of the Cu(II)-I bond, so whilst the k_{act} is similar for iodine containing initiators, the K_{ATRP} is significantly lower.

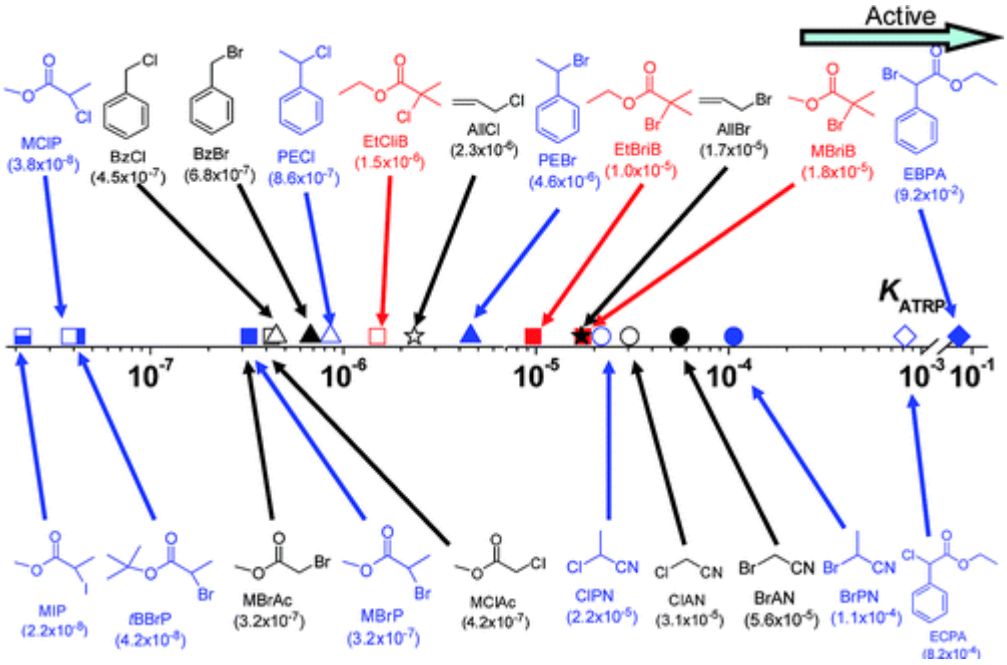

Figure 1.6: K_{ATRP} constants for various initiators, when used in conjunction with Cu-X catalyst, TPMA ligand, in acetonitrile (Reprinted with permission from W. Tang et al, Journal of the American Chemical Society, 2008, 130, 10702-10713. Copyright 2008 American Chemical Society[23]).

Selection of the halogen group on the initiator is also often dictated by the monomer to be polymerised. For example, methyl methacrylate works particularly well with chlorinated initiators, due to it forming a stable, tertiary conjugated radical. Methyl acrylate and styrene based monomers are typically seen to prefer bromine or iodine based initiators.[22] It has also been shown that choosing an initiator with a different halide group to the halide on the catalyst can result in improved control over the polymer. The polymerisation of methyl methacrylate catalysed by benzyl bromide

and copper(I) chloride was shown to synthesise polymers of well defined, targeted molecular weights, whilst the same system catalysed by benzyl chloride and copper (I) bromide was uncontrolled. This difference was attributed to the fact that benzyl bromide was initiated rapidly due to the weak C-Br bond, but the active polymer chain was then capped by a chloride radical, forming a much stronger C-Cl bond, meaning propagation was then considerably slower.[48]

Initiators with more than one initiating site have been developed, in order to synthesise branched or star polymers. It has been possible to synthesise well-defined star polymers with fluorescent porphyrin cores.[25] The use of 3, 5, 8 and 21 arm initiators in the polymerisation of methyl methacrylate was investigated, with comparisons between branched and linear polymers drawn from multi-detector size exclusion chromatography (SEC).[49]

One of the advantages of ATRP is the ability to use initiators which contain the necessary halide leaving group, but also a functional group at the other end to produce functional end-capped polymers. Using 2-hydroxyethyl 2-bromoisobutyrate[38, 50] as an initiator produced PMMA-Br macroinitiators of low dispersities (around 1.2), which could then be block polymerised with *n*-butyl acrylate to give PMMA-*b*-PBA with a hydroxy functionality at one end and a bromide functionality at the other end.[30] The synthesis of the bifunctional hydroxy initiator has been reported – reducing the ratio of the ethylene glycol used in the synthesis (in excess with regards to bromoisobromobutyrate) results in some mono-hydroxy initiator, but a larger proportion of the bifunctional initiator.[51]

1.1.5.5 Chain-end Fidelity

As previously discussed, whilst ATRP significantly reduces termination and side reactions, it does not eradicate them completely. Both the elimination and bimolecular termination reactions result in a loss of the Br- end group from the polymeric chains, removing the capability to use these polymers as macroinitiators for further reactions. For this reason, monitoring and controlling the chain-end fidelity obtained via ATRP became a significant area of interest.

Kinetic models were developed to take into account all of the parameters of controlled polymerisations, including viscosity, thermal initiation and elimination reactions. These models suggest that an increase in conversion leads to a lower dispersity, but also a lower activity, particularly after 80% conversion. One particularly valuable observation was that an increase in solvent volume was proportional to an increase in bimolecular termination. However, whilst an elimination reaction results in the loss of end group activity, it will still result in a polymer with a narrow dispersity and targeted molecular weight – this means high Đ or linear evolution of molecular weight does not necessarily indicate a polymer sample with high functionality.[52]

It has been proposed that after 60% conversion, the chain end fidelity in controlled/living free radical polymerisations is significantly reduced.[53] Monitoring of chain end fidelity by high resolution NMR techniques showed that to achieve ~80% functionality, the reaction should not proceed past around 70%, and a particularly significant loss of Br endcaps was observed after 90% conversion. This work took into consideration a number of possible side reactions which would result in the loss of the halogen group, such as elimination and bimolecular termination. Elimination reactions were seen to contribute to this loss of activity after 40% conversion is reached, whilst bimolecular termination occurs early on but is not seen to continue after around 10% conversion.[54]

Numerous attempts have been made to improve the end group fidelity maintained at high conversion by adjusting the reaction parameters. It has been shown that reducing the reaction temperature of the polymerisation of MMA from 90ºC to 60ºC resulted in a more linear kinetic plot, with high functionality being confirmed by NMR.[30]

Aside from allowing further polymerisation stages, terminal halide functionality also allows for subsequent reactions to give different functional end groups. Nucleophilic substitution for methanethiosulfate groups has been reported, which then enabled further functionalization with thiols.[55] Block copolymers have also been synthesised with a hydroxy-functionalised initiator, and substitution of the bromide end cap with 5-amino-1-pentanol allowed for the synthesis of telechelic polymer chains.[30]

1.1.5.6 The Removal of the Copper Species

One of main drawbacks of ATRP as a synthesis method is the amount of copper used during synthesis, and the need to remove this catalyst from the resulting polymer. Copper complexes are especially soluble in polar solvents, so an effective method of catalyst removal is the use of solvents such as methanol to precipitate the desired polymer chains, whilst leaving the copper in solution.[56] It has also been possible to separate catalyst from polymer by the formation of a biphasic system, where one phase is 'polymer rich', and the catalyst remains in the other phase.[51, 57]

One approach was the use of ion-exchange resins, typically containing acidic groups. Using a cationic, macroporous exchange resin, Dowex MSC-1, over 95% of bromide containing catalysts with PMDETA could be removed from reaction mixes in less than although the removal efficiency was found to be dependent on temperature, polarity of solvent and individual properties of each resin, such as the bead size and degree of cross-linking.[58] These findings were supported by work on PDMAEMA, which found that resins (Dowex MSC-1 and Chelex 20) could be used to leave just 1 ppm copper in the product polymer, whilst maintaining nearly 85% yield. However, achieving levels of catalyst this low required contact with the resin overnight, meaning this procedure is still time-consuming.[59]

An alternative method of removal was using zinc powder. The powder was activated to remove the oxide layer from the surface, before being added to the reaction mixture with 0.2 g silica gel. After stirring for less than 5 minutes, the solution had become colourless, and when examined by AAS, only 0.25 ppm copper remained in the reaction mixture. On precipitation, the polymer was white and showed no traces of zinc or copper by AAS, suggesting all zinc complexes remained in solution during the precipitation process. This method left the halogen end cap on the synthesised polymer, although could be manipulated to become a valid route to debrominating the product polymer.[60]

Purifying poly(ethyleneimine) (PEI) via conventional catalyst removal techniques has proven to be difficult due to its ability to complex strongly with the copper catalysts used in ATRP. For this reason, and due to its considerably lower toxicity than conventional ligands, hyperbranched poly(ethyleneimine) was converted into a 'macroligand' for use in the ATRP of MMA. A ratio of 4:1 (the amine groups on

the macroligand to copper) was used, which resulted in copper becoming trapped within the precipitated PMMA. However, on increasing the ratio to 10:1, colourless polymer was obtained, with less than 17 ppm of residual copper present, low dispersities (1.2-1.4) and near-linear kinetic plots. The catalyst complex remains in solution when the polymer is precipitated out, and can be recovered by evaporating off the reaction solvent.[61]

Whilst there are a number of valid methods of catalyst removal, the ability to recycle this catalyst would make the process more viable for use in industry. One example of such a method was the use of copper (II) species, namely $CuBr_2$. The copper species was added to an ATRP reaction mixture after polymerisation had reached completion, and was allowed to stir for 3 hours, before being passed through a microfilter. It was shown that this process did not result in a change in polymer characteristics, but reduced the copper content of the product from 240 ppm to just 30 ppm. The catalyst could then be removed from the filter plug, reduced back to Cu(I) and reused.[62]

1.1.5.7 Activator ReGenerated by Electron Transfer ATRP

Activator regenerated by electron transfer ATRP (ARGET-ATRP) is a form of ATRP where another component is added to the reaction which is designed to reduce the persistent radical effect, by reducing some of the deactivator back to the activator (Scheme 1.7).[63]

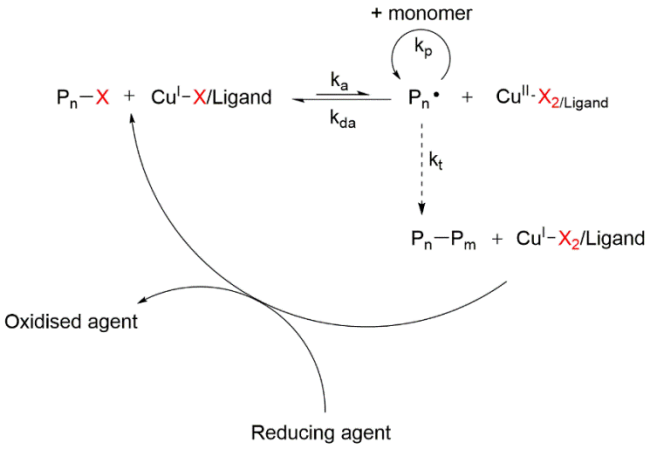

Scheme 1.7: Mechanism for ARGET-ATRP, where a reducing agent is added in order to regenerate the activating species (reproduced from reference [63]).

Reducing agents such as tin(II) 2-ethyl hexanoate and sugars have been successfully employed, and are added in significant excess with regards to the amount of copper required (often only parts per million). For example, only 2 ppm of copper was necessary in the polymerisation of MMA, resulting in polymers with targeted molecular weights and relatively controlled Đ (1.36), whilst a slight increase in copper concentration, to 50 ppm, provided a significantly narrower distribution (1.16).[63] The reduction of Cu(II) to Cu(I) with nitrogen based ligands has also been observed and followed using UV-Vis spectroscopy, which was then used in ATRP polymerisations of MMA. No Cu(I) species was added to the reaction mixture, yet controlled polymerisation was observed when the system was homogenous, with the excess amount of ligand acting both as the solubilising ligand and the reducing agent. However, when a heterogenous system was observed, considerably less excess ligand was necessary, due to the fact that not all the copper was solubilised, meaning more ligand was already free to act as a reducing agent.[64]

The use of a reducing agent also allows for a limited amount of oxygen to be present within the reaction, a feature not often observed for ATRP systems. The reducing agent can counteract the rapid oxidation of Cu(I) to Cu(II) and reduce it back to Cu(I), although tuning the amount of reducing agent added is crucial. Too much reducing agent results in less control over the system, whilst not enough means some of the air is not consumed, and no polymerisation is observed.[65]

1.1.6 Copper (0) Mediated Controlled Polymerisations

One of the major disadvantages of ATRP, particularly for use in industrial processes to produce consumer products, is the amount of copper required in each reaction. Whilst ARGET-ATRP reduces the concentration of copper somewhat, it also requires the addition of a separate reducing agent, some of which are health hazards which again are undesirable for industrial products. This was one of the main driving forces behind a number of developments in controlled radical polymerisation – one of these was the use of zero-valent copper, which can be conducted following one of two different proposed mechanisms. There is a debate in the current literature as to whether the actual mechanism is that of SARA-ATRP or SET-LRP, but for the

purposes of this work they will be treated as two different categories of polymerisation.

1.1.6.1 Supplemental activator and reducing agent ATRP

Supplemental activator and reducing agent ATRP (SARA-ATRP) is based around the mechanism of conventional ATRP, but with the addition of Cu(0) species to act as an extra activator (mechanism shown in Figure 1.7). This process means that the amount of Cu(II) necessary in the system is significantly reduced.

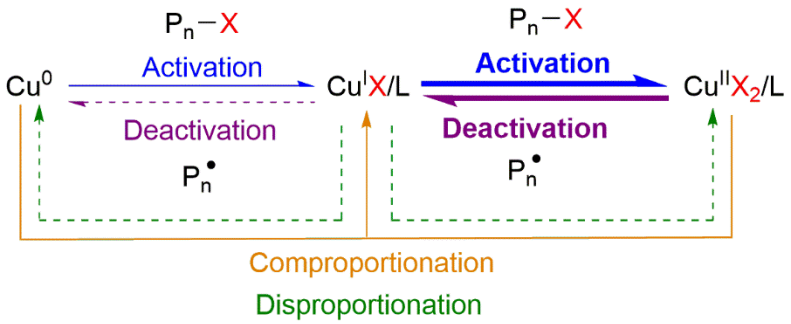

Figure 1.7: Scheme showing the processes occurring during SARA-ATRP – dashed lines are those which are not considered to happen, with the bold lines being those which are dominant (reproduced from reference [66]).

Copper (II) halide catalysts have been used in conjunction with copper (0) wire to polymerise methyl methacrylate and then to carry out a block polymerisation with methyl acrylate. This reduced the amount of copper halide required to less than 2500 ppm, and some of the best results were achieved with only 250 ppm (dispersity of 1.14, initiator efficiency of 102%). It was also observed that a smaller amount of copper (0) resulted in higher conversions, lower dispersities and slower, more controlled reaction rates.[67] This was supported by work to polymerise styrene in toluene, which found that copper (0) alone caused the reaction to be uncontrolled from the start, giving low conversions and high molecular weight, polydisperse polymers. They found that the addition of a small amount of copper (II) resulted in product polymers with considerably lower dispersities, and *ca.* 80% conversion.[68]

Work has demonstrated that metallic iron, magnesium and zinc are all suitable supplemental activators for polymerisations of acrylates, as well as acting as reducing agents.[69] Sodium dithionite, a sulphite known for its reducing capability,

was also used as a supplemental activator in the ATRP of MA – this was a potential step towards industrialising the SARA-ATRP process, as sulphites are already used in numerous industrial processes due to being environmentally friendly.[70]

Polymerisation of methyl methacrylate in toluene was carried out with just Cu(0) as the catalysing species. It was suggested that the Cu(0) activates the alkyl halide initiator and forms a Cu(I) species, which then goes on to mediate the ATRP using the same equilibrium between Cu(I) and Cu(II) as is typically observed. Copper powder still remained at the end of these reactions, suggesting that even though a stoichiometric amount of initiator, ligand and copper are added, less than one molar equivalent of the copper is actually involved during the polymerisation. It has also been shown that bimolecular termination occurs more often at the beginning of an ATRP reaction.[52, 54] This led to experiments where the Cu(0) was allowed to activate the alkyl halide in the absence of monomer, to allow the dynamic equilibrium to be reached. When monomer was subsequently added, no rapid polymeric termination was observed, and polymers with narrow molecular weight distributions were still obtained. However, in this method bimolecular termination of initiating molecules reduced the initiator efficiency and often polymers of higher molecular weights than targeted were also observed.[71]

1.1.6.2 Single Electron Transfer Living Radical Polymerisation

Single electron transfer living radical polymerisation (SET-LRP) is another example of a controlled/'living' polymerisation, the mechanism for which is shown in Scheme 1.8.

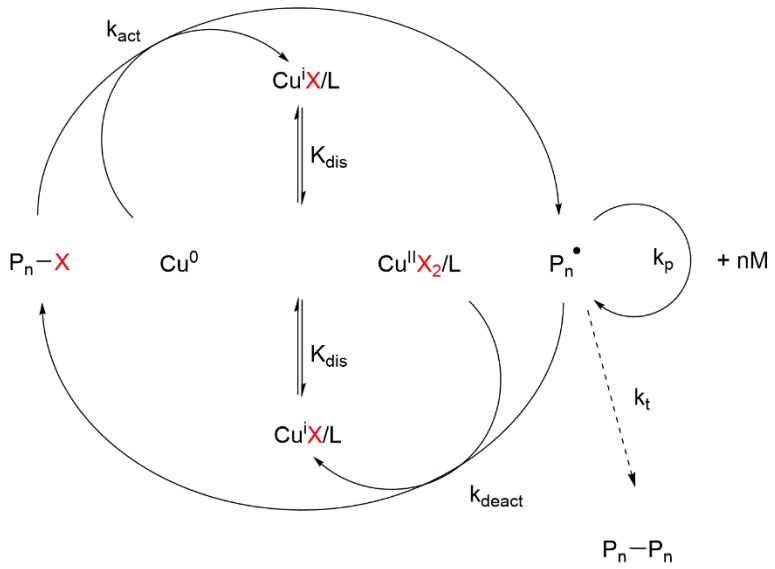

Scheme 1.8: The mechanism for SET-LRP (reproduced from reference [72]).

The key step in SET-LRP is the in situ disproportionation of Cu(I) to the deactivator Cu(II) and the catalyst Cu(0). As shown in Scheme 1.10, in SET-LRP it is the Cu(0) species which is the activator of the dormant polymer chains, not the Cu(I) species. The Cu(II) species is still the deactivator, returning the halide to the active radical species and temporarily end-capping it again. Both of these processes result in the production of Cu(I), which spontaneously disproportionates back to Cu(0) and Cu(II). These reactions typically require milder conditions than those for ATRP – they are usually carried out at ambient temperature, and in polar solvents such as water and dimethylsulfoxide (DMSO) as opposed to alkanes usually used in ATRP.

The Cu(0) species can either be added to the reaction in powder or wire form, or can be created in situ, as 'nascent' Cu(0) species, from the disproportionation of Cu(I) species. This in situ disproportionation was demonstrated by the addition of CuBr to tris[2-(dimethylamino)ethyl]amine (Me_6TREN) in water – very quickly reddish Cu(0) powder was seen to fall out of solution, and the liquid turned to a deep blue colour, indicated $CuBr_2$ in solution.[73]

One of the reasons for solvent choice is whether or not the solvent will allow for the disproportionation of the Cu(I) species, as it is crucial that the solvent does not stabilise the Cu(I). When ligand is present, DMSO has been shown to facilitate disproportionation due to the fact that the ligands form stronger complexes with Cu(II) species. However, Cu(I) species have been shown to be stable even in the presence of ligands in other solvents, such as acetonitrile. When identical

polymerisations of MA were conducted in DMSO and acetonitrile, DMSO resulted in polymer chains with high end fidelity and linear conversion with regard to time. However, the reaction containing acetonitrile was shown to slow down over time, as well as exhibiting a dramatic increase in functionality as the reaction progressed. This work demonstrated that the choice of solvent can determine which mechanism the reaction follows, and thus whether it is ATRP or SET-LRP.[74]

Another differentiation between traditional ATRP and SET-LRP is the mechanism by which the copper reacts with the alkyl halide – either via an outer sphere electron transfer (OSET) or via an inner sphere electron transfer (ISET), both shown in Scheme 1.9. It has been proposed that during ATRP, an ISET process occurs, where the alkyl halide and the metal catalyst centre form a transition state, before the alkyl radical is formed. However, it has been suggested that in systems where zero-valent copper is used, that bond fragmentation occurs with no transition state, before the electron transfer occurs and the alkyl radical is produced.[75]

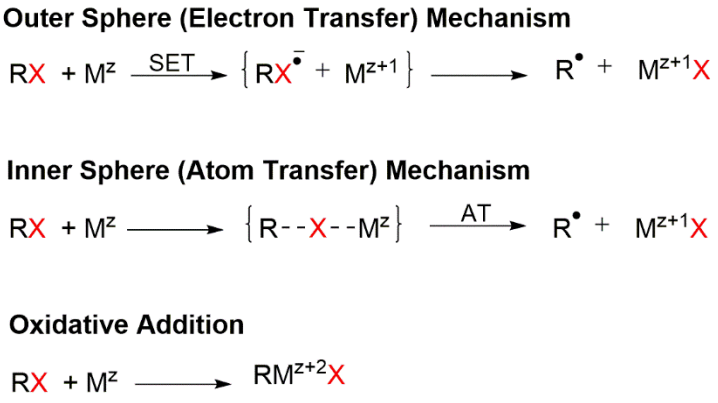

Scheme 1.9: Possible mechanisms for electron transfer between catalysts and alkyl halides (reproduced from reference [75]).

One of the key differences between copper (0) mediated SARA ATRP and SET is shown in Scheme 1.10. SARA is based around the principle that alkyl halides are activated by Cu(I), and that disproportionation is not observed, but that comproportionation is. However, SET suggests that it is the Cu(0) species which activates the halides, and that Cu(I) does in fact disproportionate.[66] The debate as to which mechanism is actually correct is likely to continue for some time, as considerable amounts of evidence are regularly being published in support of both theories.

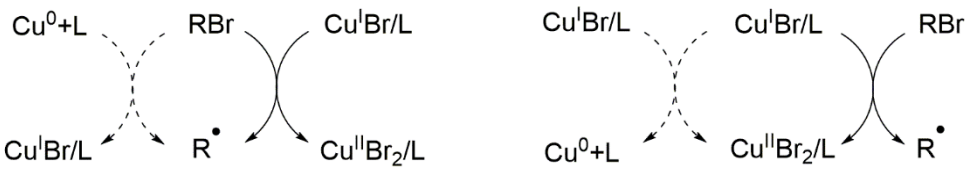

Scheme 1.10: Mechanism showing the main differences between the mechanisms for SARA-ATRP (solid lines) and SET-LRP (dashed lines) (reproduced from reference[66]).

It has been shown that if a polymerisation is conducted with just Cu(0) species present, the distribution of molecular weights obtained would be very broad. An identical polymerisation with just Cu(II) species was not seen to produce any polymeric product. However, with both Cu(0) and Cu(II) species added at the beginning of the reaction, complete conversion, control over molecular weights and narrow dispersities were obtainable.[73]

Numerous investigations have been carried out into the effect each component of a SET system has on the product polymer. Copper (0) mediated copolymerisation of methyl methacrylate and styrene in DMF was carried out at ambient temperature, producing copolymers of low dispersity when 2,2-dichloroacetophenone (DCAP) was used as an initiator, whilst exhibiting the characteristics of a controlled living polymerisation. This method was found to be dependent on solvent and initiator choice, with the use of DMSO as solvent or methyl 2-bromopropienate (MBP) resulting in uncontrolled polymerisation[76] – this solvent dependency has been shown in a number of systems.[57, 74, 77] Sequential polymerisation was also investigated – when the conversion of methyl acrylate reached a certain level, more monomer was added. Chain extension was successful for the first three additions, and whilst the fourth addition resulted in no chain growth, the presence of the bromine end cap was confirmed, suggesting the reaction had slowed significantly. Each addition of monomer was then accompanied by Cu(0) wire – which resulted in an improved rate of polymerisation. This work supports the theory that SET results in polymers with higher end group activity.[78]

The use of Cu(0) wire in the polymerisation of methyl acrylate, and the chain end fidelity as the reaction progressed, has been analysed using ESI-MS (electrospray ionisation-mass spectroscopy) as opposed to MALDI, due to the reduced degradation seen during the ESI process.[79] This work demonstrated that up to 98% fidelity could

be maintained with 100% monomer conversion, particularly when Cu(II) species were added at the beginning of the reaction.[53]

It has been proposed that copper wire used in SET-LRP reactions is often coated in a layer of copper oxide, Cu_2O, which is a slower catalyst for polymerisation than the zero-valent copper.[80] A method for removing this layer and activating the surface of the wire has been reported –the Kp was seen to dramatically increase whilst maintaining the control over the product polymer when the wire was treated with hydrazine hydrate for just 10 minutes prior to being used in a polymerisation. The Kp was seen to decrease as the wire was exposed to air, but even after exposure times of a week, the Kp was still higher for the activated wire than the wire which had not been treated.[81]

One of very few examples in the literature of the SET polymerisation of MMA investigated the use of a mixed metal (iron and copper powders) catalyst system. This work showed that whilst Fe alone produced an uncontrolled polymerisation, at certain ratios of Fe:Cu, the rate of polymerisation slowed slightly and control over weight and dispersity was increased. It was suggested that the Cu_2O (mentioned previously) which builds up on the surface of the copper wire was removed by the reduction of the Fe, activating the wire.[77] The lack of published work documenting successful SET-LRP of methacrylates is thought to be due to disproportionation causing early bimolecular termination, a feature which is not often observed in SET polymerisations of acrylates. However, the polymerisation of long chain methacrylates, such as lauryl methacrylate, was demonstrated in isopropyl alcohol (IPA) due to the formation of a biphasic system. The IPA was seen to solubilise the monomer but not the polymer formed, causing the mixture to separate – this also resulted in the catalyst being in a separate phase to the product, making the amount of copper left in the product significantly less than usually observed.[57]

Fluorinated alcohols (such as trifluoroethanol - TFE) have been successfully used as solvents in SET systems. It was been demonstrated that Cu(0) wire could be used alone, with no Cu(I) or Cu(II) added, and that even if the wire was not pre-activated (by treatment with HCl or hydrazine) then self-activation could be observed. The fluorinated solvents were thought to modify the surface of the wire which resulted in an increased surface area – explaining the ‘self-activation’ when reactions were

carried in the fluorinated solvents. Control over molecular weight and dispersity could be attained via polymerisation in these solvents, or when polymerisations were carried out in DMSO after the wire was activated in TFE.[82]

One of the fundamental difficulties with the majority of controlled polymerisations is the requirement of an anaerobic environment. In the case of SET, this is due to the formation of copper oxides on the surface of the wire, which can catalyse the polymerisations, but at a significantly slower rate than Cu(0). This in turn limits the industrial potential of the synthetic route, as these conditions can be difficult to maintain on a large scale. However, it has been shown that it is possible to conduct SET reactions under aerobic conditions, if hydrazine hydrate is added in sufficient excess to the reaction mixture. The mechanism for this process is shown in Scheme 1.11. It has been suggested that the hydrazine hydrate activated the copper oxides back to Cu(0), as well as potentially activating any Cu(II), reducing the concentration of the deactivator present.[83]

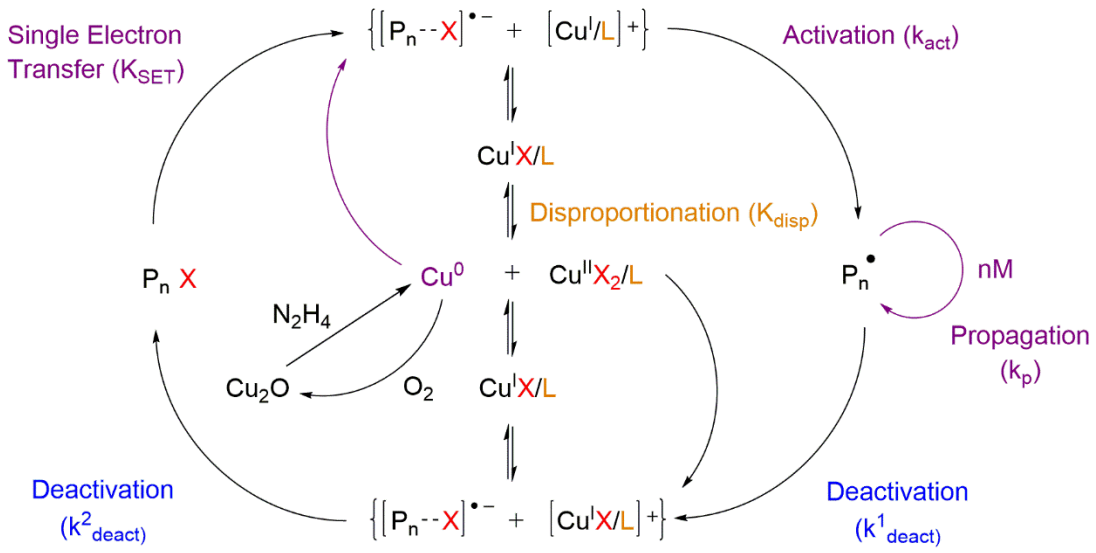

Scheme 1.11: The mechanism of SET-LRP conducted in the presence of air, showing the activation of copper oxides to Cu(0) (reproduced from reference [83]).

It has also been reported that SET is an 'immortal' system. It was shown that the polymerisation could not be irreversibly terminated by exposure to oxygen, and that one freeze thaw cycle was sufficient to return the reaction to anaerobic conditions and to allow the reaction to proceed with the same level of control over molecular weight and dispersity as before the oxygen exposure. The only difference observed

was that the reaction rate was slightly slower, presumably due to the formation of Cu_2O.[84]

This vast body of work into SET-LRP shows that, whilst SET can be a very valuable polymerisation method (particularly with regards to milder reaction conditions, lower catalyst loading and increased chain end fidelity), the reaction conditions must be precisely tuned in order to achieve the required control over the system. It has also shown considerably less success in maintaining control over product characteristics for the polymerisation of methacrylates.

These methods do not totally eradicate the need for copper to be present in the reaction, but the method for removal of copper wire is considerably easier than that of halide powders, and the lower concentration of copper (II) can be removed more quickly than for conventional ATRP.

1.1.7 Metal Free ATRP

One of the most exciting recent developments in ATRP chemistry is the publication of some work into 'metal-free atom transfer radical polymerisation'.[85] This stemmed from similar work into polymerisation using photoredox catalysts where an iridium based catalyst (tris[2-phenylpyridinato-C2,N]iridium(III)) was used, which absorbed visible light to form an $Ir(ppy)_3\cdot$ radical, which was capable of reducing an alkyl halide initiator to form an initiating radical.[86] In this latest work, 10-phenylphenothlazine (PTH) was selected as the catalyst due to its photoactive nature, as well as its low cost and availability – the proposed mechanism is shown in Scheme 1.14. Product polymers were successfully synthesised with molecular weights close to those targeted, low dispersities (as low as 1.12), and comparable chain end fidelity to those obtained via conventional ATRP. Kinetics were also shown to be linear, indicating the 'living' nature of the polymerisations.[85]

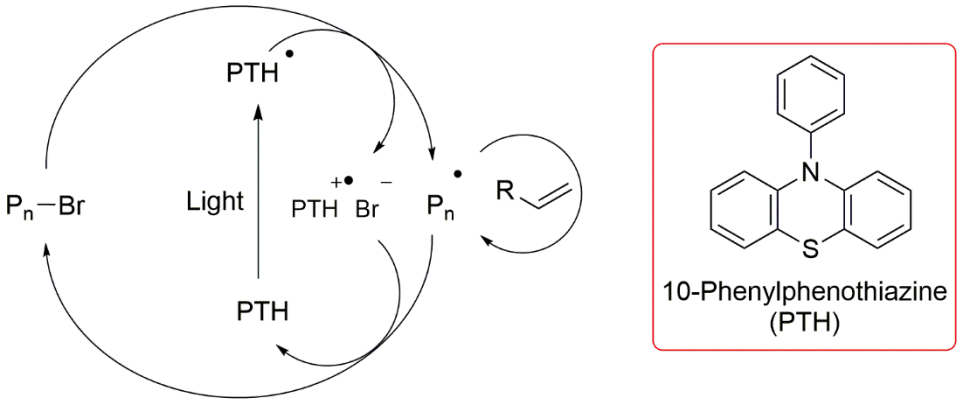

Scheme 1.12: Proposed mechanism for metal-free ATRP where PTH is the catalyst which is activated by visible light (reproduced from reference [85]).

Whilst little detail is given into the ease and success of catalyst removal from the system, this novel method for synthesising well-defined polymers without the need for a metal catalyst could potentially open a number of new possibilities with regards to industrialising ATRP.

1.2 Methods of Polymer Analysis

1.2.1 Size Exclusion Chromatography

The most common method of polymer analysis is through size exclusion chromatography (SEC), also referred to as gel permeation chromatography (GPC). SEC separates polymeric samples in relation to their hydrodynamic volume or size, and provides details of the molecular weight of the sample.

The polymeric sample is dissolved into a suitable solvent, and then injected into the machine. The continuous phase (often THF, chloroform or water) passes through columns packed with particles with pores of a known size (the stationary phase). High molecular weight polymer chains elute from the columns first, whilst lower molecular weight chains elute more slowly due to being freely able to pass inside the pores of the stationary phase. The eluted polymer chains are then analysed by a detector – common examples include refractive index, light scattering and UV detectors.[87]

GPC is calibrated against known molecular weight standards. The accuracy of the measurements can be affected if a calibrant is used which is not of a similar structure to the sample to be analysed. This is because hydrodynamic volume is dependent on the type of polymer.[88]

1.2.2 MALDI-TOF Spectroscopy

Matrix-assisted laser desorption ionisation time-of-flight mass spectrometry (MALDI-TOF) is a soft ionisation form of mass spectrometry. A sample is dissolved up with a cationization salt (such as silver trifluoroacetate -AgTFA) in a suitable matrix (such as dithranol) and applied to a metal target, before the sample is irradiated by a laser. This results in the fragmentation of the sample – these fragments are ionised before they are accelerated into a mass spectrometer for analysis.[89]

MALDI has been used to analyse polymer samples in a number of ways. Firstly, it can be used to confirm the distribution of polymeric chains, although typically samples need to be smaller than 5000 Da to allow for accurate identification of species.[90] It has also been used to monitor the chain end fidelity of a polymer, with different species identified for polymers containing active halide end groups, double bonds due to elimination and species which had undergone bimolecular termination.[53]

The choice of salt combined with the matrix and the polymeric sample has also been shown to affect the number of species observed. It was demonstrated that using AgTFA in the MALDI analysis of polystyrene resulted in numerous unknown species, which were not present when NaTFA was used instead.[91]

1.2.3 Dynamic Light Scattering

Dynamic light scattering (DLS) is a method used to calculate particle sizes due to the amount of light that they scatter. Particles are known to move by Brownian motion, and this random movement is typically due to collisions with molecules of solvent in the environment around the particles. Smaller particles will exhibit larger Brownian

motion, as they can move faster in solution, and only require a weak collision to induce movement. This motion is defined by the translational diffusion coefficient, which can be used to calculate particle size.

The hydrodynamic diameter d(H) can be obtained from the Stokes-Einstein equation:

$$d(H) = \frac{kT}{3\pi\eta D} \tag{1.9}$$

where D is the translational diffusion coefficient, k is Boltzmann's constant, T is temperature and η is viscosity.[92] The translational diffusion coefficient takes into account both the core of a particle, and its surface structure, as well as charge and concentration. This equation indicates that to calculate the particle size accurately, temperature must be precisely controlled and the viscosity of the solvent must also be known at that temperature.

When particles scatter light from the laser onto the detector within the spectrometer, a pattern of areas which are lit up form on the detector, creating a 'speckle pattern' interspersed with darker areas which are not being hit by scattered light. As particles move in solution, this pattern also moves. The detector records the changing light patterns, or fluctuations, and uses these to calculate an average light intensity. If these intensities change rapidly, then small particles are present in the solution, as these particles tend to exhibit higher Brownian motion. The inverse is therefore also true – larger particles which move more slowly will result in a smaller change in average light intensity at the detector. These changing light intensities are then used to calculate particle sizes within the sample.[93]

Concentrated samples, or those which are opaque, will scatter considerably more light than more dilute solutions of smaller particles. This means that the most effective measurement is achieved by measuring scattering at a point close to the front wall of the cuvette. The opposite is true for the dilute solutions – measurements should be taken from a greater distance inside the cuvette, to maximise the amount of scattering from the sample. This can be manually controlled, although it is common for apparatus to take preliminary measurements in order to determine the best depth at which to record measurements. If a sample is too concentrated, it is possible that light will be scattered by more than one particle

before it is detected, known as multiple scattering. For this reason, it is common for DLS apparatus to measure light that is scattered back at nearly 180º to the incident light, reducing both the distance the light has to travel through the sample, and the amount of multiple scattering occurring.

Another factor to be considered when obtaining measurements is the rate of sedimentation for the sample – if a dispersion is not particularly stable and particles tend to settle to the bottom of the cuvette, the first measurement taken could vary significantly from the last, meaning the averages would be skewed. This makes it essential to keep the sample as evenly distributed during measurement as possible, although for some systems a 'sedimentation constant' has been calculated which can then be taken into account for future measurements.[94] Similarly, once a sample has formed a gel, little or no Brownian motion can be observed, meaning that aggregates within gels cannot be 'sized' using dynamic light scattering techniques.

DLS can produce a number of different particle size distributions – the most commonly discussed are number, volume and intensity distributions. Figure 1.8 shows how these distributions would vary for the same sample. This sample contains particles of 5 nm and particles of 50 nm in equal amounts. Looking at the number average (N_{ave}) on the left, the peaks would be of the same relative percentage as there are an equal number of each size of particle. For the volume average (V_{ave}), the area of the peak corresponding to the 50 nm particles is now 1000 times that of the 5 nm peak, because the volume of these particles is 1000 times the volume of the smaller ones. The intensity average on the right (I_{ave}) is now 1000000 times larger for the 50 nm particles, as larger particles scatter considerably more light than smaller ones (from Rayleigh's approximation of scattering[95]).

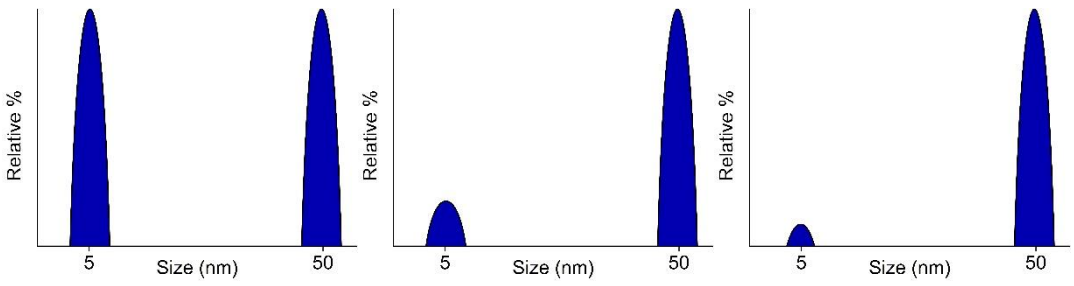

Figure 1.8: representative distributions of the same sample, showing: a) number, b) volume; and c) intensity distributions (reproduced from reference).

The DLS spectrometer only records the intensity, and both the N_{ave} and V_{ave} are then calculated from this data. These different representations of the same sample can prove problematic – if not interpreted correctly, both the V_{ave} and I_{ave} distributions would imply that there are considerably more of the larger particles present. One further parameter, $Z_{ave,}$ can be obtained from DLS data, which takes into account both the hydrodynamic radius and the scattered light. However, as the scattered light is larger for larger particles, Z_{ave}, V_{ave}, and I_{ave} are all larger than N_{ave} values, with N_{ave} giving a more accurate depiction of the distribution of particle sizes within a sample. For this reason, N_{ave} will be reported throughout this work, together with dispersity.

1.2.4 Differential Scanning Calorimetry

Differential scanning calorimetry (DSC) is a technique used to monitor thermal transitions within a sample.[96] The heat flow into a sample is measured in relation to a known reference sample, and this difference can give information about transitions such as heat capacity, temperatures of crystallisation and melting and reactions progressing within the sample. The advantage of DSC over other calorimetric methods is that the sample is enclosed into a pan made of stable, highly conductive material such as aluminium, removing the effects of heat transfer which would be seen for the larger, unenclosed samples needed for techniques such as differential thermal analysis (DTA). The pans must be highly conductive, in order to reduce thermal lag (temperature difference between the sample and the sensor) and temperature gradient (different temperatures at different points in the sample).[97]

DSC produces thermograms for each sample, plotting heat flow (often in terms of mW or mW/mg) against temperature. These plots show the amount of energy supplied to the system in order to maintain the sample at a given temperature. During an endothermic transition, such as melting, the sample absorbs heat from the surroundings, making it cooler than the reference sample, giving a minimum on the curve. In contrast, for an exothermic transition such as crystallisation, energy is released from the sample, causing it to be warmer than its surroundings, meaning a maximum is produced on the plot. DSC data is often presented with two values – the onset temperature of the transition, as well as the peak of the transition. Figure

1.9 shows typical transitions as seen on a DSC thermogram, as well as the areas under (or above) the curve, used to calculate the ΔH values for each transition.

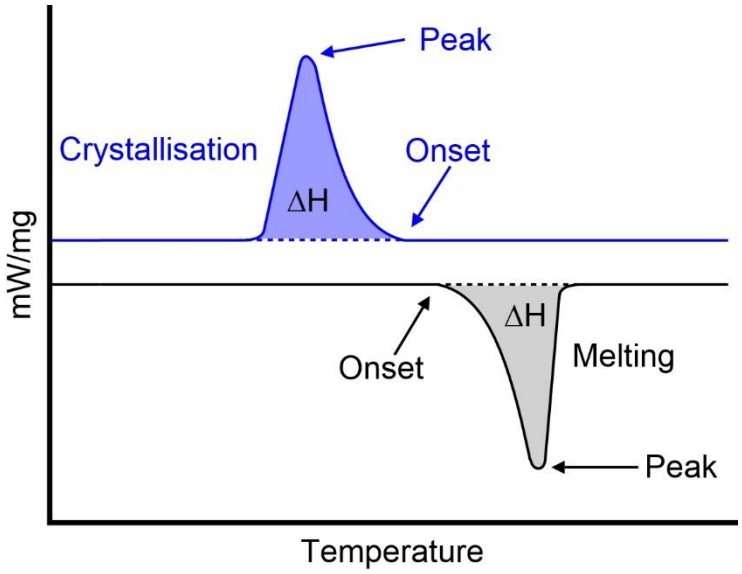

Figure 1.9: DSC thermograms showing melting and crystallising transitions.

The glass transition temperature of a polymer (or its T_g) is the temperature above which it is softened and becomes pliable – below this temperature, the polymer is a 'glass', or amorphous solid. T_g is determined by a number of structural properties, such as steric hinderance, side groups, symmetry and flexibility of the polymer chain.[98] The T_g of an amorphous or semicrystalline material will be considerably broader than for a crystalline material. T_m is the temperature of melting, although this is often observed as a range, due to the range of molecular weights in a polymer sample. Above this temperature, all crystalline regions are seen to become amorphous. The actual value of T_m can vary depending on the processes that the sample has previously been subjected to (known as its thermal history)[95], but typically increases as side chains along the polymer backbone become longer. This transition can often be linked to the heat of fusion, or H_f, which is the heat required to induce melting.

The analysis of copolymers by DSC can provide valuable information about the composition of the copolymer, particularly when monomers are combined which, when polymerised to form homopolymers, have noticeably different T_g values. A block copolymer would typically show two transitions, corresponding with the T_g for each component in the polymer, indicating the clear phase separation. However, a truly random copolymer would usually only give one thermal transition, somewhere

between the values for the two homopolymers, indicating one mixed phase with no separation.[99] This is the case when the two monomers have relatively similar reactivity ratios. However, the thermogram for a gradient copolymer, where there is a large difference between the reactivities of the monomers, would be expected to resemble the block copolymer thermogram, due to composition drift along the chain.

As previously mentioned, the degree of crystallinity can be obtained via DSC measurements, and is defined as:

$$X_c = \frac{\Delta H_f(T_m)}{\Delta H_f^0(T_m^0)} \tag{1.10}$$

where X_c is the degree of crystallinity, ΔH_f is the heat of fusion at the melting point T_m, and $\Delta H_f^0(T_m^0)$ is the heat of fusion for the purely crystalline material measured at the melting point.[100] This can further be extended to calculate the number of carbon atoms in side chains of a polymer which contribute to the crystallisation process, by calculating:

$$\Delta H_f = \Delta H_{fe} + b(n) \tag{1.11}$$

where ΔH_{fe} is the heat of fusion for the side chains of the molecules and b corresponds to the contribution of each additional carbon atom.[101]

1.2.5 Rheology

Rheology is the study of deformation and flow of materials under an applied force. Rheometers can typically be operated in two modes, each of which provides different information about the sample being analysed. In *rotational* mode, the viscosity of a sample can be measured, providing information about the flow of the material, whilst in *oscillatory* mode, information about the deformation and stability of the sample can be obtained.

The higher viscosity a material has, the more resistance to flow, and vice versa – viscosity can be defined as:

$$Viscosity = \frac{Shear\ stress}{Shear\ rate}$$

(1.12)

Shear stress is the force which is being placed on the material (calculated as force over surface area), while shear rate (change in strain over change in time) is the speed at which the material moves. This means a material of low viscosity will have a higher shear rate under the same amount of stress than a material with high viscosity.

A material which is '*shear thinning*' displays a lower viscosity when it is exposed to a larger shear stress – some of these materials possess a '*yield stress*', which is the amount of shear required in order for them to flow. A material which is '*thixotropic*' is one which becomes more viscous when allowed to stand, but returns to a less viscous state when stirred or agitated.[102]

The *complex modulus* (G*) is a measure of the toughness of a material, which is measured in pascals, and is calculated by:

$$Modulus = \frac{Shear\ stress}{Strain}$$

(1.13)

A sample with a high modulus is one with a high resistance to strain, meaning the sample is stiffer than one with a lower modulus.

Phase angle (δ) is calculated by measuring the time difference between the maximum force being applied at the maximum strain being measured. This in turn gives an indication of how 'solid-like' or 'liquid-like' a sample is. When a sample is completely solid – also known as a purely elastic material - the phase angle is zero as both the stress and strain are exactly in phase. However, when a material is liquid – also known as a purely viscous material – the stress and strain are out of phase, giving a phase angle of 90º. Most materials do not fall at the extremes of this scale, but can exhibit both properties. A material which behaves like a liquid in some situations and a solid in others is known as *viscoelastic*, with a material which has as much liquid character as solid character possessing a phase angle of 45º and being described as a gel. The stress and strain for both elastic and viscous materials are

shown in Figure 1.10, showing the solid with both characteristics in phase, and the liquid with the characteristics ¼ of a cycle out of phase.

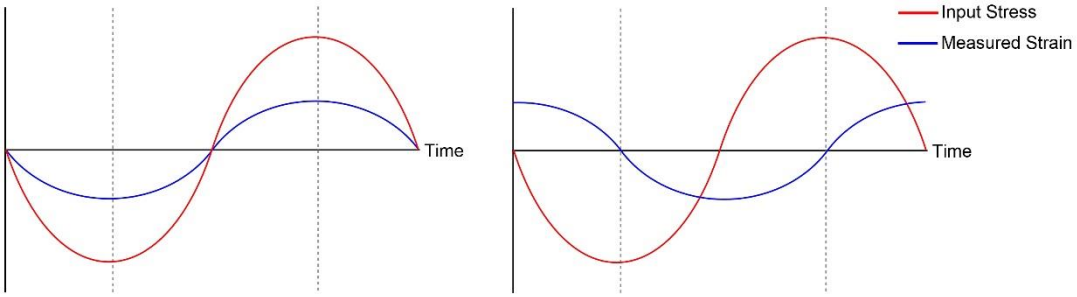

Figure 1.10: The input stress and measured strain for: left - a purely elastic (solid) material where stress and strain are in phase; and right – a purely viscous (liquid) material where stress and strain are ¼ of a cycle out of phase.

The modulus and phase angle are often combined to give two more parameters which are commonly used in rheological measurements. G' is the storage modulus, which is highest in solid-like materials, while G'' is the loss modulus, highest in liquid-like materials. This is reflected in the fact that when G' > G'', the phase angle is less than 45º, consistent with a solid-like material.[102]

Before viscoelastic measurements are conducted for a set of samples, it is important conduct an amplitude sweep by increasing the size of the oscillations. This determines the linear viscoelastic region (LVR), which is the range over which G' remains constant. Once strain is applied which exceeds the LVR, the sample will break or bend, making further measurements less valuable. For this reason, all measurements should be carried out within the LVR.

1.3 Conclusions

Continuous advances in medicine, technology and materials drive the development of materials with increasingly tailored properties. Conventional radical polymerisation techniques no longer provide enough control over composition and morphology which is necessary to meet the demands of these industries. This led to the rapidly expanding field of controlled radical polymerisations.

The development of ATRP, SARA and SET-LRP (amongst other polymerisation techniques) has opened up endless possibilities for composition, morphology and

properties of polymers. This is evident by the wealth of publications and research into the development of these systems, as well as their relevance to practical and industrial applications.

One further area of polymer science is the synthesis of particles via precipitation, emulsion and dispersion polymerisations. This area of colloidal polymeric materials, together with its dependence on stabilisers which are often well-defined copolymers synthesised via the techniques just discussed, will be discussed in chapter 2.

1.4 References

1. M. Szwarc, M. Levy and R. Milkovich, *Journal of the American Chemical Society*, 1956, **78**, 2656-2657.
2. R. P. Quirk and B. Lee, *Polymer International*, 1992, **27**, 359-367.
3. C. J. Hawker, *Journal of the American Chemical Society*, 1994, **116**, 11185-11186.
4. M. K. Georges, R. P. N. Veregin, P. M. Kazmaier and G. K. Hamer, *Macromolecules*, 1993, **26**, 2987-2988.
5. G. Moad, E. Rizzardo and D. H. Solomon, *Macromolecules*, 1982, **15**, 909-914.
6. D. Benoit, V. Chaplinski, R. Braslau and C. J. Hawker, *Journal of the American Chemical Society*, 1999, **121**, 3904-3920.
7. N. V. Tsarevsky and B. S. Sumerlin, *Fundamentals of Controlled/Living Radical Polymerization*, Royal Society of Chemistry, 2012.
8. H. Arslan, *Block and Graft Copolymerisation by Controlled/Living Radical Polymerization Methods, Polymerization*, InTech, 2012.
9. C. J. Hawker, A. W. Bosman and E. Harth, *Chemical Reviews*, 2001, **101**, 3661-3688.
10. C. Detrembleur, C. Jerome, J. De Winter, P. Gerbaux, J.-L. Clement, Y. Guillaneuf and D. Gigmes, *Polymer Chemistry*, 2014, **5**, 335-340.
11. J. Chiefari, Y. K. Chong, F. Ercole, J. Krstina, J. Jeffery, T. P. T. Le, R. T. A. Mayadunne, G. F. Meijs, C. L. Moad, G. Moad, E. Rizzardo and S. H. Thang, *Macromolecules*, 1998, **31**, 5559-5562.

12. G. Moad, E. Rizzardo and S. H. Thang, *Polymer*, 2008, **49**, 1079-1131.
13. S. Perrier, P. Takolpuckdee and C. A. Mars, *Macromolecules*, 2005, **38**, 2033-2036.
14. H. Willcock and R. K. O'Reilly, *Polymer Chemistry*, 2010, **1**, 149-157.
15. M. Kato, M. Kamigaito, M. Sawamoto and T. Higashimura, *Macromolecules*, 1995, **28**, 1721-1723.
16. J. S. Wang and K. Matyjaszewski, *Macromolecules*, 1995, **28**, 7901-7910.
17. T. E. Patten and K. Matyjaszewski, *Adv. Mater. (Weinheim, Ger.)*, 1998, **10**, 901-915.
18. D. Nagai, A. Fujii, B. Ochiai, A. Sudo and T. Endo, *Journal of Polymer Science Part A: Polymer Chemistry*, 2008, **46**, 1990-1997.
19. H. Wei, S. Perrier, S. Dehn, R. Ravarian and F. Dehghani, *Soft Matter*, 2012, **8**, 9526-9528.
20. N. V. Tsarevsky, W. A. Braunecker and K. Matyjaszewski, *Journal of Organometallic Chemistry*, 2007, **692**, 3212-3222.
21. H. Fischer, *Chemical Reviews*, 2001, **101**, 3581-3610.
22. M. Ouchi, T. Terashima and M. Sawamoto, *Chemical reviews*, 2009, **109**, 4963-5050.
23. W. Tang, Y. Kwak, W. Braunecker, N. V. Tsarevsky, M. L. Coote and K. Matyjaszewski, *Journal of the American Chemical Society*, 2008, **130**, 10702-10713.
24. M. Rajan, U. S. Agarwal, C. Bailly, K. E. George and P. J. Lemstra, *Journal of Polymer Science Part A: Polymer Chemistry*, 2005, **43**, 575-583.
25. L. H. High, S. J. Holder and H. V. Penfold, *Macromolecules*, 2007, **40**, 7157-7165.
26. K. Matyjaszewski, K. Davis, T. E. Patten and M. Wei, *Tetrahedron*, 1997, **53**, 15321-15329.
27. K. L. Beers and K. Matyjaszewski, *J. Macromol. Sci., Pure Appl. Chem.*, 2001, **A38**, 731-739.
28. K. R. Vidts, B. Dervaux and F. E. Du Prez, *Polymer*, 2006, **47**, 6028-6037.
29. G. Street, D. Illsley and S. J. Holder, *Journal of Polymer Science Part a-Polymer Chemistry*, 2005, **43**, 1129-1143.
30. H. Zhang, X. Jiang and R. van der Linde, *Polymer*, 2004, **45**, 1455-1466.

31. D. M. Haddleton, A. J. Clark, M. C. Crossman, D. J. Duncalf, A. M. Heming, S. R. Morsley and A. J. Shooter, *Chemical Communications*, 1997, 1173-1174.
32. D. M. Haddleton, J. Lad and S. Harrisson, *Abstracts of Papers of the American Chemical Society*, 2002, **224**, 039-POLY.
33. V. Raghunadh, D. Baskaran and S. Sivaram, *Polymer*, 2004, **45**, 3149-3155.
34. K. Matyjaszewski and J. Xia, *Chemical Reviews*, 2001, **101**, 2921-2990.
35. K. Matyjaszewski, *Curr. Opin. Solid State Mater. Sci.*, 1996, **1**, 769-776.
36. D. M. Haddleton, C. B. Jasieczek, M. J. Hannon and A. J. Shooter, *Macromolecules*, 1997, **30**, 2190-2193.
37. J. Qiu, K. Matyjaszewski, L. Thouin and C. Amatore, *Macromolecular Chemistry and Physics*, 2000, **201**, 1625-1631.
38. W. Jakubowski, J. F. Lutz, S. Slomkowski and K. Matyjaszewski, *Journal of Polymer Science Part A: Polymer Chemistry*, 2005, **43**, 1498-1510.
39. A. K. Nanda and K. Matyjaszewski, *Macromolecules*, 2003, **36**, 1487-1493.
40. J. X. Timothy E. Patten, Teresa Abernathy and Krzysztof Matyjaszewski, *Science*, 1996, **272**, 866-868.
41. W. Tang and K. Matyjaszewski, *Macromolecules*, 2006, **39**, 4953-4959.
42. D. M. Haddleton, M. C. Crossman, B. H. Dana, D. J. Duncalf, A. M. Heming, D. Kukulj and A. J. Shooter, *Macromolecules*, 1999, **32**, 2110-2119.
43. A. J. Clark, G. M. Battle, A. M. Heming, D. M. Haddleton and A. Bridge, *Tetrahedron Letters*, 2001, **42**, 2003-2005.
44. Z.-H. Luo, H.-J. Yu and T.-Y. He, *Journal of Applied Polymer Science*, 2008, **108**, 1201-1208.
45. W. Tang, A. K. Nanda and K. Matyjaszewski, *Macromol. Chem. Phys.*, 2005, **206**, 1171-1177.
46. W. Tang, N. V. Tsarevsky and K. Matyjaszewski, *Journal of the American Chemical Society*, 2006, **128**, 1598-1604.
47. M. Mishra and Y. Yagci, *Handbook of Vinyl Polymers: Radical Polymerization, Process, and Technology, Second Edition*, Taylor & Francis, 2008.
48. K. Matyjaszewski, D. A. Shipp, J.-L. Wang, T. Grimaud and T. E. Patten, *Macromolecules*, 1998, **31**, 6836-6840.

49. A. B. James, M. H. David and C. R. Becer, in *Progress in Controlled Radical Polymerization: Materials and Applications*, American Chemical Society, 2012, vol. 1101, pp. 81-98.
50. N. Rossi, R. Jones and S. Holder, *Journal of Polymer Science Part A: Polymer Chemistry*, 2003, **41**, 30-40.
51. C. Boyer, A. Atme, C. Waldron, A. Anastasaki, P. Wilson, P. B. Zetterlund, D. Haddleton and M. R. Whittaker, *Polymer Chemistry*, 2013, **4**, 106-112.
52. J.-F. Lutz and K. Matyjaszewski, *Macromolecular Chemistry and Physics*, 2002, **203**, 1385-1395.
53. F. Nyström, A. H. Soeriyadi, C. Boyer, P. B. Zetterlund and M. R. Whittaker, *Journal of Polymer Science Part A: Polymer Chemistry*, 2011, **49**, 5313-5321.
54. J. F. Lutz and K. Matyjaszewski, *Journal of Polymer Science Part A: Polymer Chemistry*, 2005, **43**, 897-910.
55. C. Boyer, A. H. Soeriyadi, P. J. Roth, M. R. Whittaker and T. P. Davis, *Chemical Communications*, 2011, **47**, 1318-1320.
56. Y. Shen, H. Tang and S. Ding, *Prog. Polym. Sci.*, 2004, **29**, 1053-1078.
57. A. Anastasaki, C. Waldron, V. Nikolaou, P. Wilson, R. McHale, T. Smith and D. M. Haddleton, *Polym. Chem.*, 2013, **4**, 4113-4119.
58. K. Matyjaszewski, T. Pintauer and S. Gaynor, *Macromolecules*, 2000, **33**, 1476-1478.
59. I. Ydens, S. Moins, F. Botteman, P. Degée and P. Dubois, *e-Polymers*, 2004, **4**, 414-420.
60. F. Canturk, B. Karagoz and N. Bicak, *Journal of Polymer Science Part a-Polymer Chemistry*, 2011, **49**, 3536-3542.
61. Z. Shen, Y. Chen, H. Frey and S. E. Stiriba, *Macromolecules*, 2006, **39**, 2092-2099.
62. S. Faucher, P. Okrutny and S. Zhu, *Macromolecules*, 2006, **39**, 3-5.
63. W. Jakubowski and K. Matyjaszewski, *Angew. Chem., Int. Ed.*, 2006, **45**, 4482-4486.
64. Y. Kwak and K. Matyjaszewski, *Polymer International*, 2009, **58**, 242-247.
65. K. Matyjaszewski, H. Dong, W. Jakubowski, J. Pietrasik and A. Kusumo, *Langmuir*, 2007, **23**, 4528-4531.

66. D. Konkolewicz, Y. Wang, P. Krys, M. Zhong, A. A. Isse, A. Gennaro and K. Matyjaszewski, *Polym. Chem.*, 2014, **5**, 4409-4430.
67. A. J. D. Magenau, Y. Kwak and K. Matyjaszewski, *Macromolecules*, 2010, **43**, 9682-9689.
68. B. D. Hornby, A. G. West, J. C. Tom, C. Waterson, S. Harrisson and S. Perrier, *Macromolecular Rapid Communications*, 2010, **31**, 1276-1280.
69. Y. Zhang, Y. Wang and K. Matyjaszewski, *Macromolecules*, 2011, **44**, 683-685.
70. C. M. R. Abreu, P. V. Mendonça, A. C. Serra, A. V. Popov, K. Matyjaszewski, T. Guliashvili and J. F. J. Coelho, *ACS Macro Letters*, 2012, **1**, 1308-1311.
71. A. G. West, B. Hornby, J. Tom, V. Ladmiral, S. Harrisson and S. Perrier, *Macromolecules*, 2011, **44**, 8034-8041.
72. V. Percec, T. Guliashvili, J. S. Ladislaw, A. Wistrand, A. Stjerndahl, M. J. Sienkowska, M. J. Monteiro and S. Sahoo, *Journal of the American Chemical Society*, 2006, **128**, 14156-14165.
73. Q. Zhang, P. Wilson, Z. Li, R. McHale, J. Godfrey, A. Anastasaki, C. Waldron and D. M. Haddleton, *J. Am. Chem. Soc.*, 2013, **135**, 7355-7363.
74. G. Lligadas, B. M. Rosen, M. J. Monteiro and V. Percec, *Macromolecules*, 2008, **41**, 8360-8364.
75. V. Percec, A. V. Popov, E. Ramirez-Castillo and O. Weichold, *J. Polym. Sci., Part A: Polym. Chem.*, 2003, **41**, 3283-3299.
76. J. Gao, Z. Zhang, N. Zhou, Z. Cheng, J. Zhu and X. Zhu, *Macromolecules*, 2011, **44**, 3227-3232.
77. L. Zhou, Z. Zhang, W. Wang, Z. Cheng, N. Zhou, J. Zhu, W. Zhang and X. Zhu, *J. Polym. Sci., Part A: Polym. Chem.*, 2012, **50**, 936-943.
78. A. Anastasaki, C. Waldron, P. Wilson, R. McHale and D. M. Haddleton, *Polymer Chemistry*, 2013, **4**, 2672-2675.
79. A. T. Jackson, A. Bunn, I. M. Priestnall, C. D. Borman and D. J. Irvine, *Polymer*, 2006, **47**, 1044-1054.
80. V. Percec, B. Barboiu and M. van der Sluis, *Macromolecules*, 1998, **31**, 4053-4056.
81. N. H. Nguyen and V. Percec, *J. Polym. Sci., Part A: Polym. Chem.*, 2010, **48**, 5109-5119.

82. S. R. Samanta, H.-J. Sun, A. Anastasaki, D. M. Haddleton and V. Percec, *Polymer Chemistry*, 2014, **5**, 89-95.
83. S. Fleischmann, B. M. Rosen and V. Percec, *J. Polym. Sci., Part A: Polym. Chem.*, 2010, **48**, 1190-1196.
84. X. Jiang, B. M. Rosen and V. Percec, *J. Polym. Sci., Part A: Polym. Chem.*, 2010, **48**, 2716-2721.
85. N. J. Treat, H. Sprafke, J. W. Kramer, P. G. Clark, B. E. Barton, J. Read de Alaniz, B. P. Fors and C. J. Hawker, *Journal of the American Chemical Society*, 2014, **136**, 16096-16101.
86. B. P. Fors and C. J. Hawker, *Angewandte Chemie International Edition*, 2012, **51**, 8850-8853.
87. S. Mori and H. G. Barth, *Size Exclusion Chromatography*, Springer, 1999.
88. P. C. Painter and M. M. Coleman, *Essentials of Polymer Science and Engineering*, DEStech Publications, Incorporated, 2008.
89. H. Pasch and W. Schrepp, *MALDI-TOF Mass Spectrometry of Synthetic Polymers*, Springer, 2003.
90. A. M. Belu, J. M. DeSimone, R. W. Linton, G. W. Lange and R. M. Friedman, *Journal of the American Society for Mass Spectrometry*, 1996, **7**, 11-24.
91. K. Kim, A. Hasneen, H.-j. Paik and T. Chang, *Polymer*, 2013, **54**, 6133-6139.
92. I. Teraoka, *Polymer Solutions: An Introduction of Physical Properties*, Wiley Online Library, 2002.
93. B. J. Berne and R. Pecora, *Dynamic Light Scattering: With Applications to Chemistry, Biology, and Physics*, Dover Publications, 2013.
94. M. M. Kops-Werkhoven and H. M. Fijnaut, *The Journal of Chemical Physics*, 1981, **74**, 1618-1625.
95. J. M. K. G. Cowie and V. Arrighi, *Polymers: Chemistry and Physics of Modern Materials*, CRC Press, 2008.
96. J. D. Menczel and R. B. Prime, *Thermal Analysis of Polymers: Fundamentals and Applications*, Wiley, 2014.
97. G. Höhne, W. Hemminger and H. J. Flammersheim, *Differential Scanning Calorimetry*, Springer, 2003.
98. D. J. Walton and J. P. Lorimer, *Polymers*, Oxford University Press, 2000.

99. K. A. O'Leary and D. R. Paul, *Polymer*, 2006, **47**, 1226-1244.

100. Y. Kong and J. N. Hay, *Polymer*, 2002, **43**, 3873-3878.

101. N. A. Plate and V. P. Shibaev, *J. Polym. Sci., Macromol. Rev.*, 1974, **8**, 117-253.

102. H. A. Barnes, J. F. Hutton and K. Walters, *An Introduction to Rheology*, Elsevier, 1989.

Chapter 2: Introduction to Colloids

2.1 Introduction

Colloidal materials are systems where one phase is dispersed within another – the dispersed phase is typically made up of droplets of liquid or solid particles which are between 1 nm and 10 μm in size, and the continuous phase can be either solid, liquid or gaseous. One of the key properties of colloidal systems are their high surface area to volume ratios, due to the small size of the dispersed phase.[1]

Of particular interest to this work are liquid-liquid and solid-liquid colloidal systems. A liquid in liquid dispersion is known as an emulsion, which comprises a surfactant or emulsifier and two phases, typically oil and water. An emulsifier is required to reduce the surface tension between phases and act as a barrier or interface.[2] Which phase is dispersed and which one is continuous is dictated by the relative volumes, the choice and concentration of emulsifier and the temperature of the system. Bancroft's rule states that the surfactant will be the most soluble in the continuous phase, meaning the phase that solubilises the surfactant less will become the dispersed phase.[3] A special category of emulsions exists where the stabiliser itself is a particle – these are known as Pickering emulsions. Emulsions can also be formed via the swelling of latex particles by the uptake of monomer, which can then be polymerised, causing a slight shrinkage in particle size – polymeric colloidal dispersions will be discussed in detail in section 2.3.

A solid in liquid dispersion is often described as a 'sol', and the most commonly applied examples of this system are inks and paints. Whilst liquid droplets in emulsions are spherical due to the surface tension, this is not necessarily true for a solid dispersed phase, although the system can be designed in order to tune the shape of the particles.[1] Solid in liquid dispersions are also often divided into lyophilic and lyophobic systems – lyophilic systems are inherently stable and particles can be dispersed relatively simply, whilst lyophobic systems are often less stable and exhibit coagulation (although this can sometimes occur over a long time period.[2]

The stability and properties of all of these systems are related to four key factors – Brownian motion, interactions between particles and between phases, and the effects of gravity over time.

2.2 Stability and Behaviour of Colloidal Dispersions

The random movement of particles within a system is known as 'Brownian motion', and is due to collisions with other particles or solvent molecules. It has been shown that small particles move rapidly through a solution due to a higher rate of interactions or collisions with solvent molecules within the system in comparison to larger particles. If these small particles are not stable, it is possible that during a collision they can aggregate - this aggregation typically falls into one of two categories, flocculation and coagulation. Whilst these terms are often used interchangeably, flocculation is a looser aggregation of the disperse phase which can typically be broken up by agitation, but coagulation is often described as a 'merging' of particles, occasionally leading coalescence, or complete merging.[2]

Interactions between particles can be hindered by a number of stabilisation methods, either by repulsion caused by surface charge, or by a steric layer causing a physical barrier. When a particle in suspension possesses a charge, countercharges from the solvent are held loosely around it in what is known as an 'electrical double layer'. A number of different models for this layer have been developed, taking into account different parameters of the system.[4] The first layer of the counterions is closely packed to the particle, in a region known as the Stern layer, with the arrangement of the next layer of counterions being diffuse, due to the inherent movement of the ions in solution.[5] Typically, charged dispersions have low solids contents, as once the concentration of particles increases past a certain point, they will be forced to come into contact with other particles, resulting in aggregation.

The potential between particle surface and the liquid is known as the zeta potential. When a particle moves in solution, the Stern layer of counterions moves with it, whilst the diffuse layer stays with the continuous phase, causing this difference in potential.[5]

Charged particles in solution can also undergo electrophoresis, which is the movement of the charged particles under the influence of an electric field, due to the Lorentz force.[6]

Electrophoretic mobility, or how a particle moves when subjected to an electric field, is related to the viscosity and dielectric constant of the solvent, together with the Zeta potential of the particle, and can be defined by the Henry equation:

$$U_E = \frac{2\varepsilon\xi}{3\eta}.F(ka) \tag{2.1}$$

where ε is the dielectric constant of the solvent, ζ is the Zeta potential, η is the viscosity of the solvent and F(ka) comes from the Huckel approximation. This approximation gives a value of 1 for particles which are smaller than 1 micron, and are in a medium which has a low dielectric constant. Generally, a Zeta potential of greater than 60 is desirable for the colloids to remain stable over a long time frame.

When a solvated layer of a stabiliser forms a steric barrier around colloidal particles, this is known as steric stabilisation. For this to be an effective method of preventing aggregation, there must be a high surface coverage of the particle, as well as strong adsorption of the stabiliser onto the surface. Sufficient extension of loops and chains of the stabiliser out into the solvent is also crucial, meaning regions of the stabiliser must be soluble in the continuous phase. Two different mechanisms of steric stabilisation have been proposed – interpenetration of the stabiliser chains of two different particles, or the compression of the chains between the particles. Both would lead to a repulsive force due to an increase in pressure and free energy in the system. This balances with the van der Waals forces present which would lead to particle attraction – in reality it is thought that both interpenetration and compression occur at the same time. Figure 2.1 is a schematic illustrating both electrostatic and steric stabilisation.

At the centre of Figure 2.1 is a representation of DVLO theory[7, 8], developed by Derjaguin, Verwey, Landau and Overbeek. It is a measure of the balance between the attractive and repulsive forces experienced by a particle. The plot shows the energy levels at certain distances from each particle – the energy required to place

two particles next to each other in a stable system should be high enough that the repulsive forces overcome this attraction, preventing aggregation from occurring.

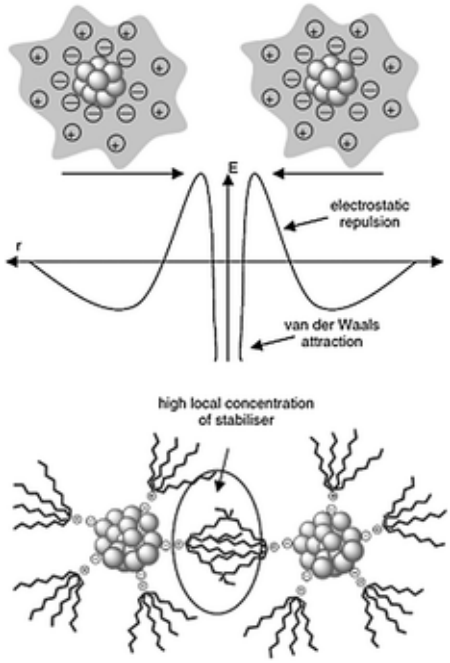

Figure 2.1: schematic to show: **top –** electrostatic repulsion and; **bottom –** steric stabilisation of colloidal particles (Reproduced with permission from C.-J. Jia and F. Schuth, Physical Chemistry Chemical Physics, 2011, 13, 2457-2487)[9].

Instability can also arise from bridging (where a stabiliser molecule becomes adsorbed onto the surface of more than one particle), or depletion, whereby free chains in solution cause exclusions from areas between particles.[1] All of these factors in instability can be affected by the temperature of the dispersion.

Gravitational effects arise due to a difference in density between the dispersed phase and the continuous phase. A large density difference between the two can result in sedimentation (when the disperse phase falls downwards and settles at the bottom) or creaming (where the disperse phase migrates upwards and forms a layer at the top). There is a point at which both upwards (gravitational) and downwards (upward drag and buoyancy) forces acting on the particle are equal, known as the terminal velocity. If there are no interactions between particles, the terminal velocity can be defined by the Stokes equation:

$$v_s = \frac{2r^2(\rho_L - \rho_p)g}{9\mu_L} \tag{2.2}$$

where r is the radius of the particle, g is due to gravity, ρ_p and ρ_L are the densities of the particle and the continuous phase , and μ is the viscosity of the continuous phase. It has also been suggested that in order to prevent sedimentation, two solvents with differing specific gravities can be combined in quantities that will match the specific gravity of the particles, although this is often only effective at a specific temperature.[5]

2.3 Synthesis of Polymeric Colloidal Dispersions

Whilst colloidal dispersions can be made up of organic or inorganic components, the most relevant area of colloids to this work is systems where the disperse phase is polymeric particles. There are a number of different synthetic routes to polymeric colloidal systems, but some of the most commonly utilised are emulsion, precipitation and dispersion polymerisation. These are differentiated between by a number of criteria, namely the mechanism and kinetics of polymerisation, the shape and size of particles produced, and the state of the reaction mixture at the beginning of the reaction.[10]

2.2.1 Emulsion Polymerisation

Emulsion polymerisation was developed in the 1930's within the rubber industry[11, 12] resulting in a number of patents. It showed great promise for industrial and commercial applications, and was adopted by the coatings industry as polymer particles could be produced which were insoluble but dispersed in water, giving a route to non-toxic, non-flammable paints. Prior to this, paints were organic based, which posed numerous health risks.

The components of an emulsion polymerization are a solvent (usually water), a monomer (immiscible with the reaction solvent), an initiator (soluble in reaction solvent) and a surfactant or emulsifier. This surfactant is amphiphilic, possessing a hydrophobic tail and a hydrophilic head, leading to the formation of aggregates, such as micelles and vesicles. A micelle is an assembly of amphiphilic molecules, where the 'solvent-phobic' (lyophobic) regions are at the centre, and the 'solvent-philic'

(lyophilic) regions are orientated outwards to come into contact with the solvent. These assemblies form when the concentration of a surfactant is above its critical micelle concentration (CMC).[13] These micelles with hydrophobic centres solubilise the monomer, creating monomer droplets with surfactant molecules at their surface. Polymerisation occurs as radicals the water-soluble initiator diffuse into the monomer-containing micelles, causing polymer growth (Figure 2.2).[14, 15] The micelles which form are typically between 5 and 10 nm in diameter, whilst the solubilised droplets of monomer are often as large as 10 µm.

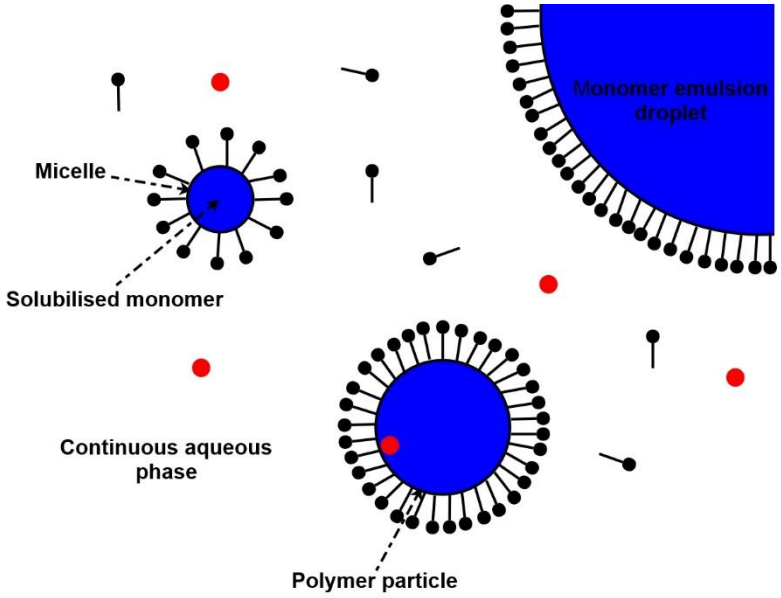

Figure 2.2: Schematic of emulsion polymerisation, showing the micellisation of monomer droplets by surfactant molecules (black molecules with tails), and water soluble initiators (red circles) migrating inside the micelles to initiate polymerisation (reproduced from reference [16]).

The polymerisation is typically divided into three stages, or intervals I, II and III. During interval I, initiator molecules diffuse into the monomer swollen micelles, causing nucleation. During interval II, monomer diffuses from the droplets into the particles nucleated from micelles, where polymerisation is occurring rapidly. Towards the end of the reaction, in interval III, particles no longer have access to such a ready supply of unreacted monomer, leading to a drop in rate of polymerisation.[17] At the beginning of a reaction, the majority of the monomer is found within droplets, but as polymerisation progresses, and the reaction enters interval II, the monomer diffuses from the droplets into micelles, until all monomer has become incorporated into the micelles at around 50 to 80% conversion. Polymerisation then continues until all monomer within micelles has been reacted to

form polymer. Particles synthesised are typically in the range of 1-10 μm in size, although particles smaller than 1 micron can be obtained via a slightly different reaction pathway, known as miniemulsion.[17, 18]

Micelles are more effective at capturing free radicals to induce polymerisation than monomer droplets are. This is due to the relatively large surface area that micelles possess in comparison to the droplets. A number of kinetic studies have been undertaken on emulsion systems, which assumed that a micelle could only tolerate the presence of one radical moiety at a time, and that if a second radical were to diffuse into the micelle, this would terminate the polymerisation reaction. If another radical were to enter, the reaction would begin again, meaning the emulsion polymerisation is a series of on-off steps until the consumption of all monomer. This implied that only half of the polymeric particles will contain an active radical at any point in the reaction.[16, 19]

Polymeric surfactants for emulsion polymerisation vary greatly in composition of the hydrophobic block, with monomers such as polystyrene, poly(methyl methacrylate) and poly(propylene oxide) used, whilst the hydrophilic block is most often made up by poly(ethylene oxide) – PEO.[20] However, if particle dispersions in non-aqueous solvents are required, other polymerisation methods are necessary.

2.2.2 Precipitation Polymerisation

In precipitation polymerisation, both the monomer and initiator are soluble in the reaction solvent, but the polymer is insoluble, so when a critical molecular weight is reached, the chains precipitate out.[21] The absence (or small quantity) of a stabiliser in precipitation polymerisation means that these chains tend to aggregate or flocculate, producing particles with a wide size distribution, due to the lack of control that emulsion polymerisation is seen to provide. On occasion, these reactions can be carried out without the presence of a solvent – this is possible when a polymer is insoluble in its own monomer.

One particular advantage of precipitation polymerisation from an industrial perspective over other techniques is the rapid rate of reaction and high molecular weight polymers which are obtained.[22] The system can also be tuned in order to

improve the dispersity of the product particles, such as by the addition of a cross-linker rather than a stabiliser. One mechanism for particle growth highlighted the necessity for reactive groups to be present on the surface of the particle, suggesting particle growth was entropic rather than enthalpic, i.e. a precipitated particle chain will not just adsorb to an unreactive particle surface. It was proposed that this indicated that the surface of the particle was actually a 'solvent-swollen, partially cross-linked gel layer', and that this alone was sufficient to sterically stabilise the particles.[23]

2.2.3 Dispersion Polymerisation

Dispersion polymerisation could be described as precipitation polymerisation but with the addition of a stabiliser. Both the monomer and initiator are soluble in the reaction medium, but at a critical length the polymer chains which form are insoluble, meaning they precipitate out of solution. These then aggregate to form particles, with the stabiliser acting as a barrier between the particle and solvent interface. The first examples of using stabilisers to regain the control in dispersion polymerisation were with graft copolymers[24, 25], which showed it was possible to add a polymeric stabiliser to prevent aggregation, and also indicated a potential link between temperature and flocculation.[26]

Whilst polymerisations in aqueous solutions became well documented, advances in organic media were slower to develop. The first real example of dispersion polymerisation in non-aqueous materials (non-aqueous dispersion or NAD) was not until the 1960's[27], before it received a significant increase in attention in the 1970's as knowledge and understanding developed.[21, 26, 28]

2.2.4 Non-Aqueous Dispersion Polymerisation

NAD is based around the same principle as precipitation polymerisation, where the monomer and initiator are soluble in the continuous solvent phase, while the polymer which forms is insoluble and therefore precipitates out of solution. These precipitated polymer chains begin to coagulate and form discrete particles, with the

stabiliser forming a barrier at the surface of the particle (Figure 2.3). This prevents the particles aggregating, and allows monomers access to the growing polymer chains whilst keeping the polymer inside and new oligomers out.[29]

To achieve these properties successfully, the stabiliser is seen to have one anchor component which becomes part of the growing particle, and a liquid soluble component to remain at the solvent/particle interface. There has been a range of research (discussed later, section 2.2.4.3) into suitable stabilisers for NAD, some of which have been graft or random copolymers[24, 29, 30], but the research most relevant to this work has been with the use of block copolymers.[20, 31, 32]

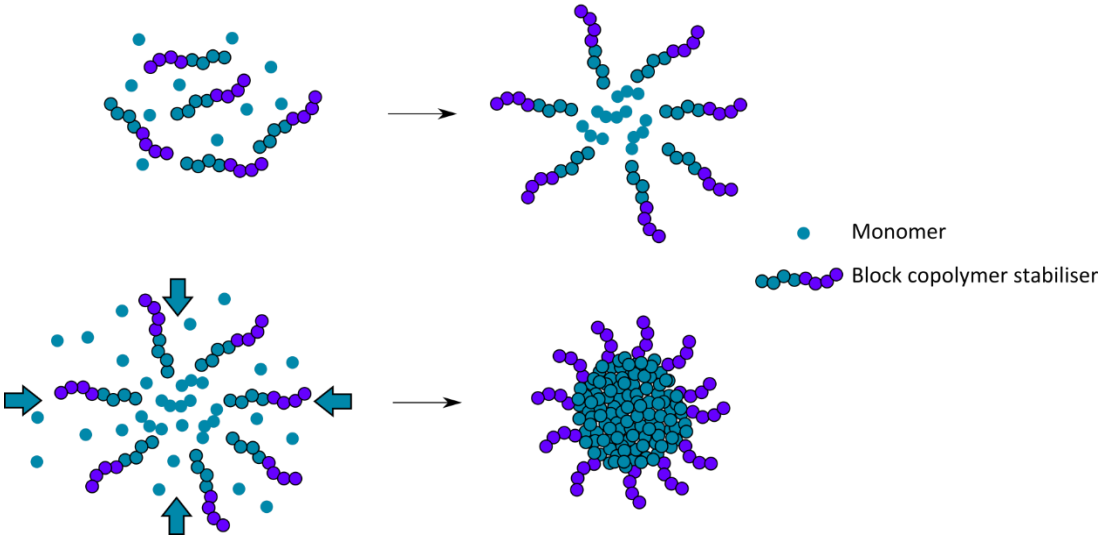

Figure 2.3: Schematic of NAD polymerisation, reproduced from reference [29]. **Top:** oligomer and polymer chains begin to form (blue) and coagulate with the help of stabilisers (blue and purple) forming a barrier; **Bottom:** polymerisation continues within the stabiliser barrier with monomer able to enter but the polymeric chains are trapped - stabiliser chains eventually become incorporated into the particle.

Figure 2.4 shows some SEM images of PMMA particle dispersions. The concentration of stabiliser used in each synthesis varied, resulting in a change in particle size – this trend will be discussed in more detail in section 2.2.4.4. These particles could be described as 'ideal' particles synthesised by NAD, as (with the exception of image 4), the particles are seen to be monodisperse, relatively spherical, and are hexagonally close packed.

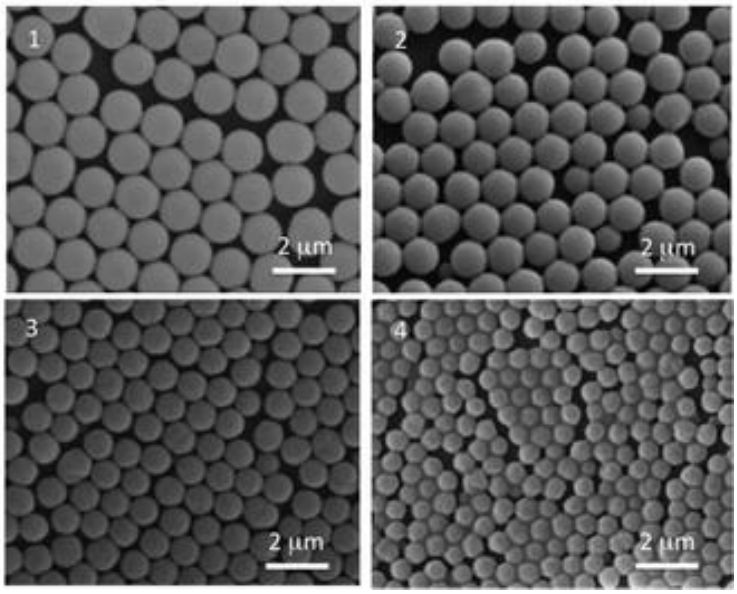

Figure 2.4: SEM images of examples of PMMA particles in dodecane synthesised by NAD polymerisation. Each image is for a different weight percentage stabiliser: 1) 2.5 wt %; 2) 5 wt %; 3) 10 wt %; and 4) 20 wt % (Reproduced with permission from A. P. Richez, et al, Langmuir, 2014, 30 (5), 1220-1228 – Open Access).[33]

Studies into the mechanism of the dispersion polymerisation suggest that once polymeric chains have reached their critical length and precipitated out of solution, Brownian motion causes them to come into contact with one another, leading to aggregation. The stabiliser begins to cover the particle surface, until this aggregation can no longer occur due to steric repulsion. This model for particle formation was found to be in good agreement with experimental data, with the model able to predict concentration of particles in relation to concentration of monomer.[34]

2.2.4.1 Initiator

Radical initiators such as benzoyl peroxide (BPO) and bis(4-t-butylcyclohexyl)peroxy dicarbonate (p-TCP)[35] themselves are often seen to have high cross-linking properties, which could make them unsuitable for dispersion polymerisations if they are seen to distort the particles too much. Of these radicals, AIBN is shown to have the lowest cross-linking efficiencies (28 times less than BPO), and as such has been shown to have success in producing monodisperse, spherical particles. Particle size increased with increased initiator addition, due to the larger number of radicals and growing polymer particles at the start of the

reaction which will aggregate.[36] However, although BPO is known to have high cross-linking effects, it has been shown that it can be used successfully in NAD polymerisations to synthesise monodisperse particles, with dispersities as small as 4% being reported.[37]

The use of a polysiloxane macroinimer (dimethyl siloxane copolymerised with an azo group) has been described. This research emphasised the importance of the solubility parameters of initiators and stabilisers in order to achieve stable dispersions rather than aggregates as seen previously, with further support for the theory that on increasing initiator concentration, particle size decreases.[38]

The use of a poly(oxyethylene) macroinimer (PEO MIM) was investigated in an ethanol and water dispersion system. The macroinimer acting as three of the necessary components of a dispersion polymerisation at once - a comonomer, stabiliser and initiator. This meant that only monomer and solvent needed to be added for the reaction to progress. However, unstable dispersions were produced with large particles seen to flocculate and aggregate for polymerisations of both styrene and methyl methacrylate.[39] Whilst this method was not for non-aqueous dispersion, if a similar macroinimer could be developed to work in non-aqueous systems, it would provide a valuable, simple synthetic route, removing a number of the necessary elements of the NAD process.

2.2.4.2 Solvent

The model for the mechanism of dispersion polymerisation suggests that the choice of solvent was crucial, as it needed to be one in which the monomer and initiator were soluble, but also one in which the polymer was insoluble.[29] It has been widely acknowledged that the solubility of PMMA in a range of solvents is greatly influenced by its molecular weight – this is the factor which controls at which stage in the reaction polymer chains will begin to precipitate out. Numerous studies have shown that hexane is the best anti-solvent to allow the precipitation and recovery of the smallest polymer chains, while methanol is seen to leave a greater proportion of chains behind in solution.[40, 41] The use of diethyl ether was also investigated, but was

found to be too expensive, hazardous, and did not increase the removal of contaminants or the range of chain lengths precipitated.[40]

The majority of studies indicated that alkane solvents produce particles with desirable properties (low particle size distribution and good control over particle size). However, the choice of alkane systems has varied, but hexane/dodecane[24, 29, 32] has been used with great success, heptane or cyclohexane (chosen specifically because of their solubility parameters).[38] It was also shown that solvents such as toluene and cyclohexanone are unsuitable as they possess comparable solubility parameters to PMMA, meaning precipitation did not occur.

The use of mixed solvents was further investigated – heptane and toluene were added together at varying concentrations in order to adjust the solubility parameter of the mixture. This enabled control over the state the product remained in; at the highest concentrations of toluene to heptane, the solubility parameter was seen to be at its highest and therefore a polymer solution was observed, in comparison to the dispersion of particles seen at low or zero toluene content.[38]

2.2.4.3 Stabiliser

The best architecture for a NAD stabiliser depends upon the interactions that occur at the particle/solvent interface. It has been suggested that block copolymers act as the most efficient stabilisers, due to their two distinct regions – an "anchor component" which becomes incorporated into the particle itself, and a "liquid soluble component" which remains at the barrier. A gradient or random copolymer might be made of the same two constituents, but because of their composition, interactions at the surface could potentially be hindered. In Figure 2.5 depicting possible arrangements of stabilisers at the particle surface, the block copolymer is shown to cover the surface but with space to allow monomer in whilst preventing oligomer or polymer chains from aggregating other than inside the particles. The gradient copolymer shows similar interactions, but because of the backbone of "anchor" monomer, it covers a much larger surface area of the particle, leaving only a small number of sites for monomer to enter the particle. By the same principle, if there is a small amount of surface coverage (usually due to too low a concentration of

stabiliser), the steric stabilisation is often not great enough to prevent particles flocculating and produces an unstable, fused dispersion with little or no discrete particles.

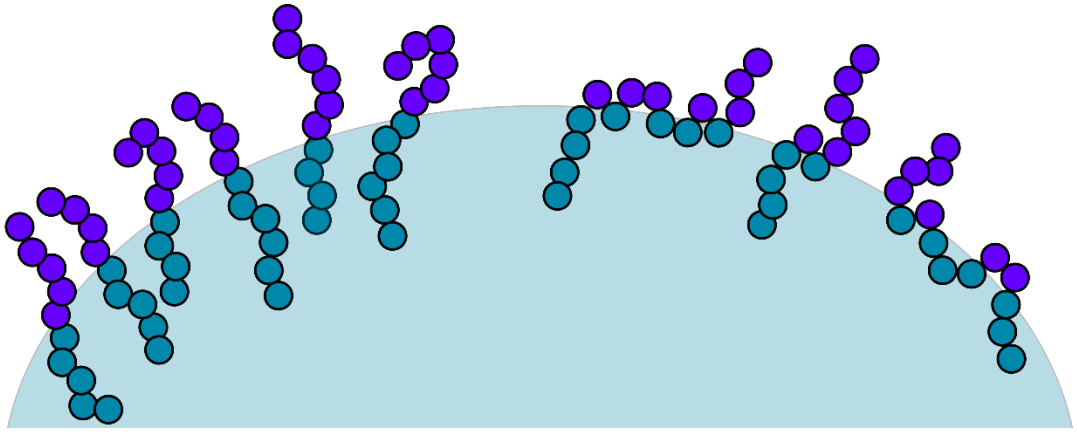

Figure 2.5: arrangement of stabilisers at particle/solvent interface. **Left:** Block copolymer arrangement; **right:** Gradient copolymer arrangement.

In the first documented examples of NAD in the 1960's, ordinary surfactants such as Lissapol-N (shown in Figure 2.6) and common soap surfactants were employed as stabilisers.[27] However, as understanding of surface coverage and the mechanism of stabilisation developed, together with more advanced methods of polymeric synthesis, a new range of specialist stabilisers were synthesised. This was to add functionality to the stabilisers, as well as to allow precise control over the dispersions formed.

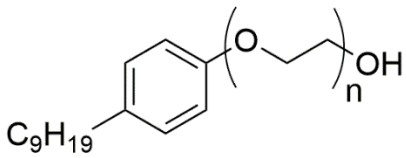

Figure 2.6: the structure of Lissapol-N, also known as 4-nonylphenyl-polyethylene glycol.

Graft and homopolymer stabilisers

A comb stabiliser of a poly(hydroxystearic acid) backbone, with methyl methacrylate and glycidyl methacrylate chains grafted to it (PHSA-*g*-PMMA-PGMA), was developed for use in dispersion polymerisations. These syntheses

particles with wide ranging diameters (178 nm to 2.6 μm) and dispersities as low as 3.9% were synthesised (shown in Figure 2.7). The stabiliser could be covalently linked into particles by a distillation reaction after the dispersion reaction had reached completion. This work also provided evidence for the concept that by varying the monomer concentration, particle size could be accurately controlled.[24, 42] Later research suggested a lack of reproduceability in the stabiliser synthesis, potentially due to the number of complicated steps. However, this work proposed a number of measures which could be taken to improve the success of the synthesis.[43]

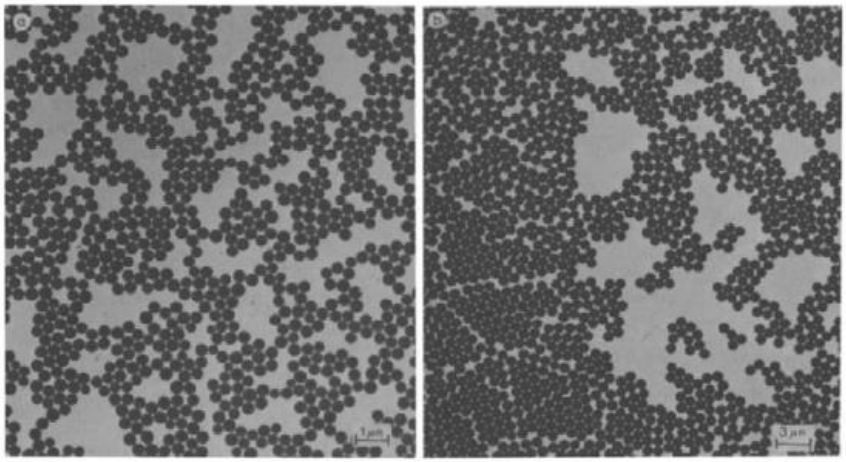

Figure 2.7: PMMA particles stabilised by PHSA-*g*-PMMA-PGMA (Reproduced with permission from L. Antl, J. W. Goodwin, R. D. Hill, R. H. Ottewill, S. M. Owens, S. Papworth and J. A. Waters, Colloids and Surfaces, 1986, 17, 67-78).[24]

The use of poly(hydroxystearic acid)-*graft*-poly (methyl methacrylate) (PHSA-*g*-PMMA) (Figure 2.8) was investigated. This stabiliser was shown to produce highly monodisperse particles (as low as 2% dispersity) with a great deal of control over particle size on varying reaction conditions - by varying solvent to monomer ratio, particles from 500 nm to 1.5 μm were synthesised. However, it has often proven difficult to synthesise the stabiliser as the reaction process is long and complex.[29, 44] This stabiliser is also seen to only have weak interactions with the particle surface.[45]

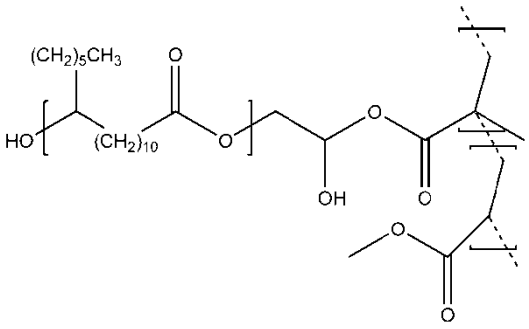

Figure 2.8: the structure of PHSA-g-PMMA.

Another variation was the use of poly(dimethylsiloxane) (PDMS) with methacryloxypropyl terminated groups as a stabiliser for dispersions of PMMA particles (Figure 2.9). It was seen as being an improvement on PHSA-*g*-PMMA stabilisers as the synthesis of this stabiliser was much simpler. When used in NAD polymerisations, PDMS based stabilisers were seen to produce stable colloidal dispersions of particles over 1 μm.[46] There were no obvious disadvantages to the use of PDMS based stabilisers, although the inability to produce particles smaller than 1 micron could potentially limit the applications that the synthesised dispersions could be used for.

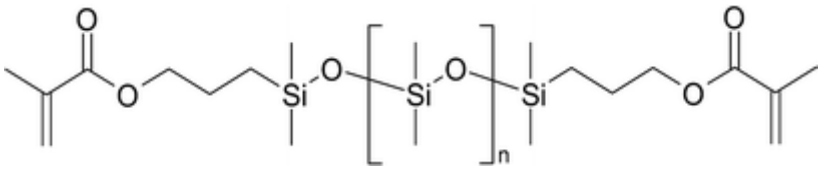

Figure 2.9: Structure of methacryloxypropyl terminated PDMS.[46]

Block copolymers

PDMS block copolymers with polystyrene (PDMS-*b*-PS) were used to synthesise PMMA particles, and were shown to be stable between a temperature range of -82 and 56ºC,[47] with a linear relationship between the particle size and stabiliser concentration. Dispersities were low and, by stopping the reaction prematurely, stable distributions of particles as small as 100 nm could be obtained. This research also indicated that the "ASB" or "anchor/soluble balance" was critical to the stability of the dispersion – if the value of anchor components relative to the liquid soluble

components was greater than 4.4, the resulting dispersion would not be stable. This was because longer liquid soluble (lyophilic) blocks stabilised a larger surface area of the particle.[28]

The conclusions drawn from this selection of research was that there was the need for a stabiliser with a simple synthesis (if not commercially available) which produced particles possessing all of the desired qualities. This led to the development, amongst others, of a poly(methyl methacrylate)-block-poly(octadecyl acrylate) (PMMA-*b*-PODA) stabiliser (Figure 2.10) which was suggested as a possible replacement for the current industrial standard (PHSA-*g*-PMMA), with its long alkyl chains to act as the liquid soluble component and provide the steric stabilisation shell. [32, 37] It was reported that particles with dispersities as low as 3.8% and close hexagonal packing could be synthesised, and that by varying the proportions of monomer, solvent and stabiliser, particle size could be varied from 62 nm to 1.19 µm.[32, 37]

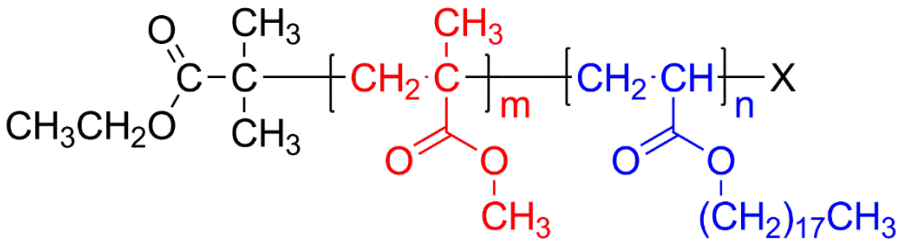

Figure 2.10: structure of PMMA-*b*-PODA.

This work also showed that random copolymers could, under certain conditions, produce stable dispersions with low dispersities. However, this was likely due to the fact that MMA and ODA have very different reactivities, meaning the 'random' copolymers were technically gradient copolymers, which exhibit a composition drift. This meant that there were likely to be long regions of PODA blocks in the copolymers, allowing them to stabilise the particles in a similar manner to normal block copolymers. A schematic representation of block, random and gradient copolymers is shown in Figure 2.11. However, work into this stabiliser did not extend to the ability to functionalise either the stabiliser or the particles, such as the incorporation of dyes and other functionalities.

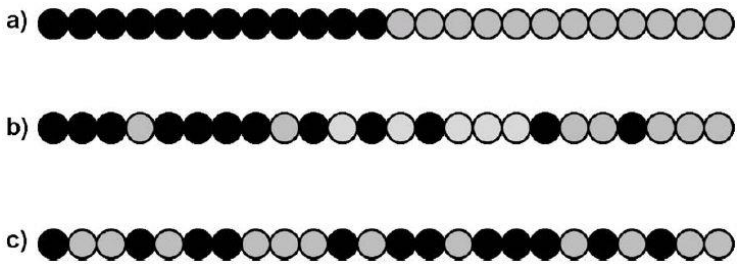

Figure 2.11: schematic demonstrating the arrangement of two different types of monomer unit in: a) block copolymer; b) gradient copolymer; and c) a random copolymer.

There have been countless other categories of stabiliser used for non-aqueous dispersion polymerisation, whilst this section covered a select few. The stabilisers highlighted here give an overview of the main categories of stabiliser (graft and block copolymers) as well as the effects that changing stabiliser concentration and architecture can have on dispersions of particles. Particular attention was paid to those stabilisers containing PHSA, as these were used as a direct comparison for stabilisers synthesised in this work. There are a number of reviews which cover the vast amount of literature on different types of stabilisers in greater depth.[20, 45]

Recent developments suggested it would be possible to produce monodisperse particles without the addition of any stabiliser to the synthesis. Research found that by using a cationically charged monomer (structure shown in Figure 2.12) in a copolymerisation with styrene but without a stabiliser, cationic particles were produced without the need to either remove a stabiliser or bind it into particles after synthesis. These particles were between 560 nm and 9 μm, and in some cases with standard deviations as low as 3%. The quality of these particles was however greatly influenced by the concentration of initiator and solvent composition.[48]

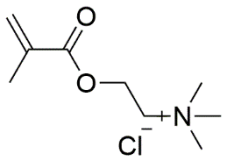

Figure 2.12: structure of the cationically charged monomer used to produce stable dispersions without the need for a stabiliser.

2.2.4.4 Particle Size

Dispersion polymerisation is acknowledged as being a simple synthetic route to monodisperse particles down to less than 1 μm in size, in some cases as small as 100 nm. The easiest method to predict and control the size of the product particles is to vary the monomer:solvent ratio, or monomer:stabiliser ratio.

The most common finding was that by increasing the ratio of monomer in relation to the solvent, larger particles were formed.[36, 49] This was supported by research with similar findings, which also indicated that with an increase in stabiliser concentration with respect to monomer concentration, particle size was seen to decrease.[24, 37, 46] A larger concentration of stabiliser is capable of stabilising a much larger particle surface area, which is achieved by smaller particles being synthesised.

Increasing the molecular weight of a stabiliser has also been shown to produce smaller particles, due to a more complete surface coverage.[28] Graft copolymers typically have little or no control over product particle size, which could be due to the stabiliser covering a greater surface area of the growing particle, preventing access for monomer molecules to reach the polymerisation. This also leads to an increased dispersity.[37]

2.2.4.5 Cross-linker

Many syntheses of particles have also included a cross-linking substituent, usually divinyl benzene (DVB) or ethylene glycol dimethacrylate (EGDMA).[50-52] Cross-linkers are often used to ensure particles keep their strength and structure when being transferred between solvents for various applications. This transfer is typically from a solvent with a solubility parameter similar to that of the particles, to one which is a much closer match to the particles, but the cross-linking groups help to prevent dissolution from occurring. These reactants contain groups - commonly vinylic groups - which cause chains to cross-link, often leading to loss of spherical nature, uneven looking particle surfaces and an increase in dispersity. It is not uncommon for discrete particles to be completely absent from the reaction mixture at the end of a polymerisation, as high concentration of cross-linker can lead to dramatic aggregation, resulting in large agglomerations of many individual particles. At

exceptionally high concentrations (up to 90 mol% of EGDMA), pores were seen to form in the particle surfaces, leaving a rough, porous surface, shown in Figure 2.13.[53]

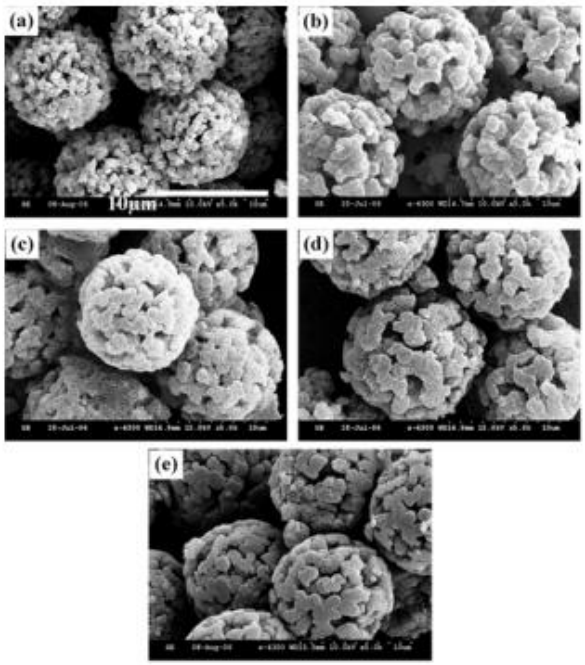

Figure 2.13: SEM images showing the rough, porous surface of particles containing exceptionally high concentrations of EGDMA: a) 10 mol %; b) 25 mol %; c) 50 mol %; d) 75 mol%; and e) 90 mol % (Reproduced with permission from D. Kim et al, Macromolecular Research, 2009, 17, 250-258).[53]

Some research has found there is no real correlation between cross-linker concentration and particle size (diameter)[54, 55] – a potential explanation for this is that it is more difficult for monomer to become incorporated into cross-linked structures (suggesting no change in size will be observed). However, other groups have shown that the addition of cross-linker does lead to an increase in particle size (in some cases up to 100% increase in comparison to uncrosslinked particles)[37, 52] due to crosslinks causing larger nuclei and in turn larger product particles. It has also been shown that the solvent make-up dictates how much of an effect the EGDMA will have.[52]

Adding the cross-linker at a later stage in PS particle synthesis has been shown to prevent the often observed broadening of dispersities. It has been shown that by adding EGDMA (with a new batch of monomer and solvent) after initiation has occurred and less than 5% monomer has reacted, a monodisperse distribution of particles can be achieved (shown in Figure 2.14), although similar results were not

noted for DVB.[55] This can be described as a two-stage dispersion polymerisation. Although this seemed to be a valuable synthetic discovery, it was later shown that a narrow dispersity can be seen even on addition of EGDMA at the start of the reaction, suggesting that this variable is affected considerably by the reaction system involved.[37]

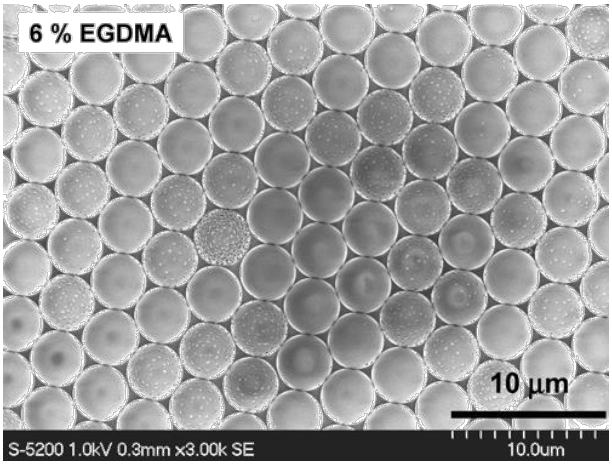

Figure 2.14: SEM image showing the monodisperse PS particles synthesised by adding EGDMA at a later stage in the polymerisation. Surface roughness can also be observed in the image. (Reproduced with permission from J. S. Song and M. A. Winnik, Macromolecules, 2005, 38, 8300-8307. Copyright American Chemical Society 2005).[55]

2.2.4.6 Incorporation of functional groups

Several approaches have been adopted to add functional moieties (such as dyes and fluorescent molecules) to the particles synthesised by dispersion polymerisation methods. One method was to form PMMA particles in the absence of dye, and then to swell them in a solvent containing rhodamine perchlorate dye. However, although these product particles were seen to incorporate the fluorescent dye, they were also seen to exhibit long range repulsion.[56]

Polymerisation of monomers with two functional groups, one which was polymerisable, and one which fluoresced is generally a more successful approach in producing fluorescent dispersions. Specially designed fluorescent monomers (such as 4-methylaminoethylmethacrylate-7-nitrobenzo-2-oxa-1,3-diazol (NBD-MAEM) and RITC-aminostyrene (RAS)) have been used in random copolymerisations with methyl methacrylate, producing particles of low dispersity (<7%) and diameters of

<500nm. These monomers with a polymerisable group became 'locked on' to the particles when the polymerisable group reacted with a monomer on the surface of a particle. Particle dispersions were also obtained which contained a fluorescent group without the polymerisable moiety, but these required an individual distillation step to 'lock on' to the particles.[44, 49] However, synthesis of the specialised monomers was seen to be time consuming and complex.

For this reason, it was suggested that a 'one pot' method of producing fluorescent particles would be a valuable development. Fluorescent moieties were successfully incorporated into a dispersion of PMMA particles in dodecane, and on several washes with solvent were not seen to leach out of the particles. This was thought to be due to their limited solubility in hydrocarbons, forcing them to remain in the PMMA particles which are more polar. It was also shown that if a dye was soluble in the monomer phase at the beginning of a reaction, then the presence of the dye was less likely to affect particle formation.[42] This method was further developed to give a truly one-step synthesis without the need for a lengthy 'locking in' step, also lowering the dispersity – longer reaction times are seen to disrupt and broaden narrow particle size distributions.[29]

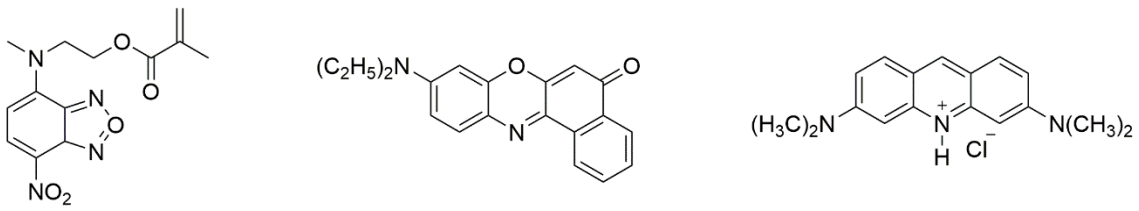

Figure 2.15: structures of some of the functional groups added to particle dispersions: NBD-MAEM (left), Nile Red (centre) and Acridine Orange (right).

2.2.4.7 Supercritical carbon dioxide

In recent years, there has been a significant amount of research into dispersion polymerisation in supercritical carbon dioxide ($scCO_2$). $ScCO_2$ exists at the critical point between high temperature (above 305 K) and high pressure (above 73 atm). This has proved popular due to the ever increasing focus on reducing the damage done to the environment by the use of harmful organic processes and volatile solvents in industry. Carbon dioxide therefore offers a valuable solution, due to its

accessible, inexpensive nature and its natural abundance.[13, 57] At increased pressure and temperature CO_2 is seen to possess properties of both its liquid and gaseous states, which can be utilised in terms of the solubility of both reactants and products in either CO_2 phase.[58] Furthermore unlike organic solvents, CO_2 can be readily removed by a drop in pressure and temperature.

The first published example of a polymerisation under $scCO_2$ was the polymerisation of fluorinated acrylate monomers, which was a homogenous system.[59] However, in recent years, more success has been achieved in the use of heterogeneous polymerisation. This is due to the "CO_2-phobic" nature of most polymers, making dispersion or emulsion polymerisations a far more attractive synthetic route. This supported the use of block or graft copolymers as stabilisers, as seen in usual dispersion methods, due to their ability to possess both "philic" and "phobic" regions.

Evidence suggested that fluoro- or silicon-based polymers were the most soluble in $scCO_2$[60], with poly(fluoroalkyl methacrylate) (PFMA)[61], Krytox[62] or poly(1,1-dihydroperfluorooctyl acrylate) (PFOA)[60] being suitable choices for the CO_2-philic block. The need for these stabilisers was demonstrated by a polymerisation carried out in the absence of a block copolymer, producing a low yield and a broad dispersity, with the majority of product polymer precipitating and solidifying at the bottom of the reaction vessel.[61] This research also indicated the trends for both larger molecular weight stabilisers and a higher concentration of stabiliser to give products of a larger molecular weight with a narrow dispersity, while increasing the monomer concentration resulted in larger diameters with a much broader dispersity.

Research has also been undertaken into the synthesis of cross-linked microparticles in scCO, demonstrating that with the use of a suitable stabiliser at various concentrations and varying concentrations of cross-linker, it was possible to achieve particles of narrow dispersity and controlled size in much the same way as a traditional dispersion polymerisation under nitrogen atmosphere.[63, 64] With a higher concentration of stabiliser, the particles showed the most desirable properties (spherical nature, low aggregation and extremely low dispersity), potentially due to the greater surface area coverage of the forming particles.[64] However, this is disputed by the theory that when smaller particles are formed, high stabiliser

coverage did not counteract the unstable nature of particles which led to aggregation.[63] It was also suggested that particle size could be controlled by varying the concentration of monomer or initiator in the synthesis.

2.4 Applications of Colloidal Dispersions

Colloidal dispersions find uses in numerous areas of everyday lives – from paints, inks, cleaning solutions and thickening agents, to incorporation into food products and water treatments. However, whilst they are valuable for a large number of general areas, there are a number of very niche applications for which they have become particularly successful – one of these is electrophoretic displays.

2.4.1 Electrophoretic Displays

The electrophoresis of colloidal particles discussed previously (section 2.2) has recently found an application in display technologies, known as electrophoretic displays (EPDs).

EPDs have become increasingly more common in everyday life, finding applications in areas such as electronic book readers, mobile phone screens and advertising media. They are advantageous over other forms of electronic screens such as liquid crystal displays (LCDs), as they are designed to be read in bright sunlight without the user observing a glare, and they are also typically cheaper to manufacture. They have a battery life which can extend up to at least a month, due to the fact that they only draw power for the split second at which the displayed image changes. They are a type of 'bistable display', which means that the device retains an image even when the power is switched off.

EPDs are made up of charged particles within a fluid, with electrodes placed above and below. When an electric field is applied, the particles are either attracted or repelled, which creates an image for the user to see. White particles cause the reflection of light, whilst black particles absorb the light.[65-67] The scattering length for the light is very short (around 1μm) giving a high reflectivity and contrast – this

is similar to the contrast difference between black ink on white paper, hence the alternative name given to EPDs - 'E-paper'.[68]

As the technology has progressed, a number of different compositions for screens have been developed which will be discussed below.

2.4.1.1 Types of Display

The first example of an electrophoretic display was developed by Gyricon in 1978.[69] This utilised Janus particles, or particles which have two distinct regions of different colours and properties. In this case, the particles had one hemisphere which was black and one which was white, with each half being oppositely charged. These particles were then encapsulated by oil, and placed into thin, transparent shells, before being arranged into a thin layer. A change in the electric field on either side of the layer caused the spheres to rotate, with the different coloured hemispheres being used to create an image (Figure 2.16).[70]

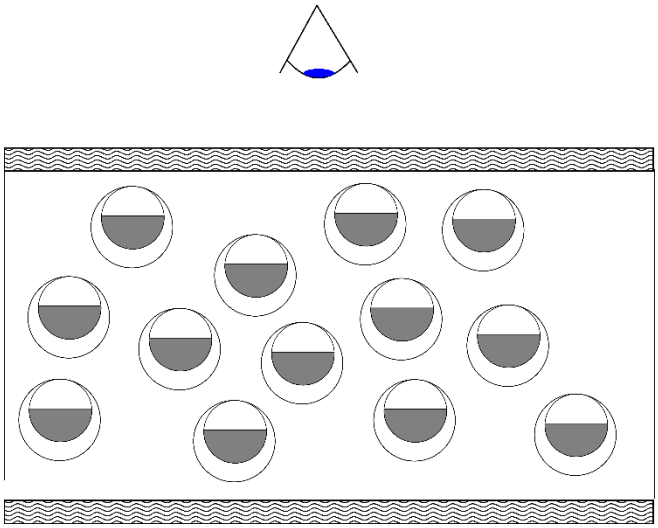

Figure 2.16: schematic of a Gyricon electrophoretic display, reproduced from reference.[71] Janus particles encapsulated in oil are placed in a transparent shell, and an applied electric field causes these spheres to rotate.

Another means of achieving two coloured systems was described in 1973 by a research group in Japan. They detailed a possible method which included two different coloured particles, but focused on a system where the liquid was one colour, by utilising oil soluble dyes in an organic solvent, and the particles were a

contrasting colour. They typically used titanium dioxide (white) or hansa yellow (an organic azo compound) to achieve this effect.[72] The device worked by the migration of the charged particles through the dielectric fluid when an electric field was applied. If the particles were attracted to the display side, the user would see the colour of the particles (white in the schematic Figure 2.17), and if the particles were repelled from the display then the user would see the colour of the dielectric fluid (black in the schematic). This format has since been mirrored in a range of other devices,[65, 66, 73] and was the basis of the SiPix microcup system (shown in Figure 2.9), which was developed to enable a 'roll-to-roll' production process.[74]

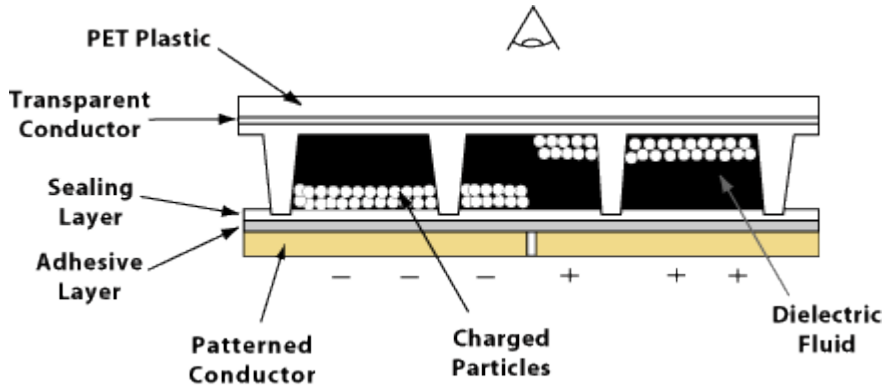

Figure 2.17: schematic of SiPix microcup electrophoretic display, reproduced from reference.[74]

E-Ink developed a system based around microcapsules containing a transparent, colourless fluid, together with particles of two opposing charges, usually coloured black and white. These microcapsules were placed between two sets of electrodes, one of which was transparent to allow the user to view the display. When current was passed through either set of electrodes, this would cause the particles to either be repelled or attracted, creating an image at the display surface (shown in Figure 2.18).

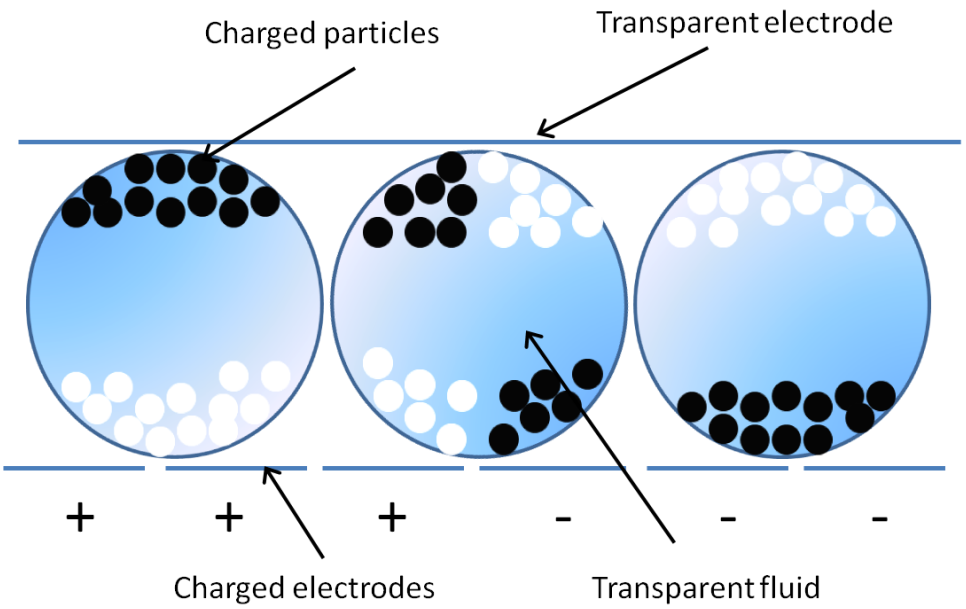

Figure 2.18: schematic of E-Ink electrophoretic display, reproduced from reference.[75]

Whilst this type of display has successfully been incorporated into a number of commercial products (such as the Amazon Kindle[76] and the Barnes and Noble Nook[77]), this has only been demonstrated for black and white systems. Initially, a system known as E-Ink Triton Imaging Film was developed to enable a coloured display, whereby a colour filter was placed over the black and white screen. Whilst this was effective in creating a coloured display, the reflected light intensity was reduced, resulting in faded, 'washed out' colours as opposed to the bright, full colours achieved using other display technologies such as organic light emitting diodes (OLED). This can be improved by the use of backlight, but this in turn increases the power required to use the device.

There is, however, the potential to adapt these electrophoretic systems to incorporate coloured particles in order to create full colour displays. Indeed there has recently been work into three coloured systems, where charge density has been utilised to allow for different rates of particle movement.[78, 79] There has also recently been an example of a system which simultaneously used white, cyan, magenta and yellow particles, not within the microcapsules but instead in a system known as independently movable coloured particles (IMCP).[79]

This work focuses on the development of coloured electrophoretic fluids to be used within the 'E-Ink' type schematic, so further discussion will be solely based around this. There have already been a number of patent applications from Merck

Chemicals Ltd in this area,[80-82] based around the synthesis of polymeric particles (typically methacrylates) with polymerisable dyes incorporated into the particles.

2.4.1.2 Specifications for EPDs Utilising the E-Ink Technology

Firstly, the choice of solvent used within the display is crucial. The solvents need to be organic and inert, meaning they can be used at a range of temperatures without nearing their boiling points, as well as being unreactive towards the particles, the microcapsules and the electrical effect of the electrodes. The solvent also needs to have a low dielectric constant to allow the maximum electric field to form between the electrodes – fluids with a high dielectric constant would cause a drop in the electric field strength and in turn allow the particles to move more efficiently. The dielectric constant is a measure of how easily an ion dispersed within that solvent dissociates. An ionic species will strongly associate within a solvent with a low dielectric constant, which are also typically non-polar solvents.

Table 2.1: the boiling points and dielectric constant of common solvents.

Solvent	Boiling Point (°C)	Dielectric Constant ε (at 25°C)[83]
Water	100	78.54
Ethanol	78.2	24.30
Cyclohexanone	155.4	18.30
Chloroform	61.2	4.81
Toluene	110.6	2.38
Dodecane	216.3	2.01
Hexane	68.7	1.89

There are also a number of specifications which the particles must meet. Firstly, different types of particles have been designed to be compatible with the organic solvents necessary for EPD. Approaches to this include pigments which have polymer chains bound to or grown from their surface,[84] particles synthesised to encapsulate pigments inside,[85] and particles which are synthesised before dye is diffused into them.[78] These particles must then possess a number of properties.

Size – Particles should (usually) be between 400 and 1000 nm in diameter – they are required to be this small to allow them to scatter light effectively when they are packed at the electrode. Larger particles would also be likely to have a higher rate of settling. Particle size is also seen to have an effect on the Zeta potential of a dispersion.

Size distribution – Particles should have a narrow size distribution. This is to allow for good hexagonal packing of particles at the screen surface to give a high depth of colour, as well as to provide a 'clean' switch when the current is passed through the electrodes. If particles of varying sizes were to be placed inside the microcapsules, these would move at different speeds through the liquid, due to the drag on the particle changing as a function of size.

Density – in order for displays to be viable for long periods of time, it is crucial that particles within a dispersion do not sediment and settle at the bottom of capsules. For this reason, the density of the particles in relation to the density of the solvent is a key parameter in the design of the display. The rate of settling can be calculated using the Stokes-Einstein equation of settling as mentioned previously.

Refractive Index – scattering of light within the display arises from the difference between the refractive index (RI) of the particles and the RI of the surrounding solvent. The greater the 'mismatch' between the refractive indices, the higher the optical scattering and therefore the opacity of the fluid.[66] This is desirable, as it will result in a greater contrast, increasing the 'paper-like' quality of the display.

Switching speed – The time taken for a switch to occur can be estimated by:

$$t_{switching} = \frac{h}{\mu E} = \frac{h^2}{\mu V} \tag{2.3}$$

where μ is the electrophoretic mobility, h is the cell gap and V is the applied voltage. This switching speed is one of the limitations of electrophoretic displays, preventing it from being suitable for applications where high speed video replay is required.

Adsorption to electrodes – electrophoretic technologies only require the application of current when an image is to be changed. This means that particles are required to remain at the electrodes for considerable periods of time after this initial pass of

current, and so must adsorb to the surface. However, this adsorption must be reversible, as if they are held too strongly at the electrodes, the image will not change as desired – this often results in 'ghosting', where a new image is displayed but a trace of the old image is still visible.[86]

Charge – in order for the particles to move within an electrophoretic display, they must possess a charge. However, PMMA particles which have previously been mentioned do not have their own charge. For this reason, a charge carrier agent (such as polybutene-succinimide[87]) is often added to the particle dispersions when they are made into electrophoretic inks.

Colour – the colour properties of electrophoretic inks can be tuned by controlling the percentage dye content of the particles, and the volume fraction of the particles in the electrophoretic fluid. It is also crucial that dye does not leach from the particles into the surrounding medium, as this would affect the image produced. Traditionally, inorganic pigments were used, such as titanium dioxide and carbon black – however, to incorporate the full spectrum of colours, organic dyes, particularly those which are polymerisable, look to be the most suitable.

2.5 Conclusions

Synthetic routes to dispersions of polymeric particles with a narrow size distribution have been developed. Control over each of the parameters of these reactions, including concentration of monomer and stabiliser in relation to solvent, and particularly the design of specialised stabilisers for NAD polymerisations, can produce particles with a wide range of properties. The size and dispersity of the particles can all be controlled by modifying the conditions of the reaction. It is also essential to ensure that the dispersions are stable over a long period of time, typically by a combination of steric stabilisation and electrostatic repulsion.

Market research has already identified a specific gap in the market for low power, high lifetime displays which are cheap to manufacture, and these have been successfully sold for a number of years.[88] Thus far, they have been employed in E-readers and mobile phone screens. If this technology could be advanced to enable full colour displays, the number of possible applications for these displays could

dramatically increase. Aside from making children's books, magazines and textbooks accessible on E-readers, they could be a low cost, low energy advertising medium, and could even be used on wall surfaces as a way to change the colour of rooms – black and white systems have already been developed into 'smart' window systems.

However, it is clear that whilst conducting NAD polymerisations, there are a wide variety of parameters which must successfully be controlled. The choice of each component within the dispersion, together with their behaviour under the influence of an electric field, will dictate how effective the dispersions could be as electrophoretic fluids.

2.6 References

1. J. Goodwin, *Colloids and Interfaces with Surfactants and Polymers: An Introduction*, Wiley, 2004.
2. G. Barnes and I. Gentle, *Interfacial Science: An Introduction*, OUP Oxford, 2011.
3. B. Kronberg, K. Holmberg and B. Lindman, *Surface Chemistry of Surfactants and Polymers*, Wiley, 2014.
4. S. U. Pickering, *J. Chem. Soc., Trans.*, 1907, **91**, 2001-2021.
5. A. L. Dalisa, B. Singer and S. Ross, *IEEE Trans. Electron Devices*, 1976, **23**, 1256-1256.
6. A. T. Hubbard, *Encyclopedia of Surface and Colloid Science*, Taylor & Francis, 2002.
7. B. Derjaguin and L. Landau, *Progress in Surface Science*, 1993, **43**, 30-59.
8. E. J. W. Verwey, J. T. G. Overbeek and J. T. G. Overbeek, *Theory of the Stability of Lyophobic Colloids*, Dover Publications, 1999.
9. C.-J. Jia and F. Schuth, *Physical Chemistry Chemical Physics*, 2011, **13**, 2457-2487.

10. J. C. Salamone, *Concise Polymeric Materials Encyclopedia*, Taylor & Francis, 1998.

11. Process for Manufacturing Artificial Rubber, F. Hofman, 1909.

12. Synthetic Rubber and Method of Making It, R. P. Dinsmore, 1929.

13. J. L. Kendall, D. A. Canelas, J. L. Young and J. M. DeSimone, *Chem. Rev. (Washington, D. C.)*, 1999, **99**, 543-563.

14. F. A. Bovey, I. M. Kolthoff, A. I. Medalia. E. J. Meehan, *Emulsion Polymerization*, Interscience Publishers, New York, 1955.

15. D. C. Blackley, *Emulsion Polymerisation*, Applied Science Publishers Ltd, London, 1975.

16. J. M. K. G. Cowie and V. Arrighi, *Polymers: Chemistry and Physics of Modern Materials*, CRC Press, 2008.

17. C. S. Chern, *Prog. Polym. Sci.*, 2006, **31**, 443-486.

18. M. S. El-Aasser and P. A. Lovell, *Emulsion polymerization and emulsion polymers*, J. Wiley, 1997.

19. W. V. Smith and R. H. Ewart, *The Journal of Chemical Physics*, 1948, **16**, 592-599.

20. G. Riess and C. Labbe, *Macromolecular Rapid Communications*, 2004, **25**, 401-435.

21. K. E. J. Barrett, *Dispersion Polymerization in Organic Media*, John Wiley and Sons, London, 1975.

22. H. S. Mickley, A. S. Michaels and A. L. Moore, *Journal of Polymer Science*, 1962, **60**, 121-140.

23. J. S. Downey, R. S. Frank, W.-H. Li and H. D. H. Stöver, *Macromolecules*, 1999, **32**, 2838-2844.

24. L. Antl, J. W. Goodwin, R. D. Hill, R. H. Ottewill, S. M. Owens, S. Papworth and J. A. Waters, *Colloids and Surfaces*, 1986, **17**, 67-78.

25. J. Stejskal, P. Kratochvil and C. Konak, *Polymer*, 1991, **32**, 2435-2442.

26. M. D. Croucher and M. L. Hair, *Colloids and Surfaces*, 1980, **1**, 349-360.

27. Dispersion Polymerisation, D. J. W. Osmond, GB 893429, 1962.

28. J. V. Dawkins and G. Taylor, *Polymer*, 1979, **20**, 599-604.

29. H. Hu and R. G. Larson, *Langmuir*, 2004, **20**, 7436-7443.

30. R. P. A. Dullens, E. M. Claesson and W. K. Kegel, *Langmuir*, 2004, **20**, 658-664.

31. F. L. Baines, S. Dionisio, N. C. Billingham, S. P. Armes, *Macromolecules*, 1996, **29**, 3096-3102.

32. H. V. Harris and S. J. Holder, *Polymer*, 2006, **47**, 5701-5706.

33. A. P. Richez, L. Farrand, M. Goulding, J. H. Wilson, S. Lawson, S. R. Biggs and O. J. Cayre, *Langmuir*, 2014.

34. M. Yasuda, H. Seki, H. Yokoyama, H. Ogino, K. Ishimi and H. Ishikawa, *Macromolecules*, 2001, **34**, 3261-3270.

35. S. Fujii, H. Minami and M. Okubo, *Colloid Polym. Sci.*, 2005, **284**, 327-333.

36. W. Yang, J. Hu, Z. Tao, L. Li, C. Wang and S. Fu, *Colloid Polym. Sci.*, 1999, **277**, 446-451.

37. H. V. Penfold, S. J. Holder and B. E. McKenzie, *Polymer*, 2010, **51**, 1904-1913.

38. K. Nakamura, K. Fujimoto and H. Kawaguchi, *Colloid Surf. A-Physicochem. Eng. Asp.*, 1999, **153**, 195-201.

39. U. Yildiz, *Macromolecular Symposia*, 2002, **179**, 297-304.

40. C. A. Barson, J. C. Bevington and B. J. Hunt, *European Polymer Journal*, 1996, **32**, 1055-1059.

41. J. C. Bevington, B. J. Hunt and C. A. Barson, *European Polymer Journal*, 1998, **34**, 1387-1389.

42. A. I. Campbell and P. Bartlett, *Journal of Colloid and Interface Science*, 2002, **256**, 325-330.

43. M. T. Elsesser and A. D. Hollingsworth, *Langmuir*, 2010, **26**, 17989-17996.

44. G. Bosma, C. Pathmamanoharan, E. H. A. de Hoog, W. K. Kegel, A. van Blaaderen and H. N. W. Lekkerkerker, *Journal of Colloid and Interface Science*, 2002, **245**, 292-300.

45. A. P. Richez, H. N. Yow, S. Biggs and O. J. Cayre, *Prog. Polym. Sci.*, 2013, **38**, 897-931.

46. S. M. Klein, V. N. Manoharan, D. J. Pine and F. F. Lange, *Colloid Polym. Sci.*, 2003, **282**, 7-13.

47. D. H. Everett and J. F. Stageman, *Faraday Discussions of the Chemical Society*, 1978, **65**, 230-241.

48. Q. Q. Liu, Y. L. Li, S. H. Shen, Z. H. Zhou, B. L. Ou and S. L. Tang, *J. Macromol. Sci. Part A-Pure Appl. Chem.*, 2011, **48**, 518-525.

49. R. S. Jardine and P. Bartlett, *Colloid Surf. A-Physicochem. Eng. Asp.*, 2002, **211**, 127-132.

50. J. Choi, S. Y. Kwak, S. Kang, S. S. Lee, M. Park, S. Lim, J. Kim, C. R. Choe and S. Hong, *Journal of Polymer Science Part A: Polymer Chemistry*, 2002, **40**, 4368-4377.

51. K. C. Lee and S. Y. Lee, *Macromolecular Research*, 2007, **15**, 244-255.

52. H. T. Zhang, H. Huang, R. Lv and M. Chen, *Colloid Surf. A-Physicochem. Eng. Asp.*, 2005, **253**, 217-221.

53. D. Kim, D. Y. Lee, K. Lee and S. Choe, *Macromolecular Research*, 2009, **17**, 250-258.

54. J. X. Huang, X. Y. Yuan, X. L. Yu and H. T. Zhang, *Polymer International*, 2003, **52**, 819-826.

55. J. S. Song and M. A. Winnik, *Macromolecules*, 2005, **38**, 8300-8307.

56. A. D. Dinsmore, E. R. Weeks, V. Prasad, A. C. Levitt and D. A. Weitz, *Appl. Opt.*, 2001, **40**, 4152-4159.

57. M. R. Giles, J. N. Hay, S. M. Howdle and R. J. Winder, *Polymer*, 2000, **41**, 6715-6721.

58. A. I. Cooper and J. M. DeSimone, *Current Opinion in Solid State and Materials Science*, 1996, **1**, 761-768.

59. J. M. Desimone, Z. Guan and C. S. Elsbernd, *Science*, 1992, **257**, 945-947.

60. Z. B. Guan and J. M. Desimone, *Macromolecules*, 1994, **27**, 5527-5532.

61. W. P. Hems, T. M. Yong, J. L. M. van Nunen, A. I. Cooper, A. B. Holmes and D. A. Griffin, *Journal of Materials Chemistry*, 1999, **9**, 1403-1407.

62. M. R. Giles, R. M. T. Griffiths, D. J. Irvine and S. M. Howdle, *European Polymer Journal*, 2003, **39**, 1785-1790.

63. W. X. Wang, R. M. T. Griffiths, A. Naylor, M. R. Giles, D. J. Irvine and S. M. Howdle, *Polymer*, 2002, **43**, 6653-6659.

64. T. Casimiro, A. M. Banet-Osuna, A. M. Ramos, M. N. da Ponte and A. Aguiar-Ricardo, *European Polymer Journal*, 2005, **41**, 1947-1953.

65. A. L. Dalisa, *IEEE Trans. Electron Devices*, 1977, **24**, 827-834.

66. B. Fitzhenryritz, *IEEE Trans. Electron Devices*, 1981, **28**, 726-735.

67. J. Kostelec and R. Liebert, *American Ceramic Society Bulletin*, 1974, **53**, 606-606.

68. B. Comiskey, J. D. Albert, H. Yoshizawa and J. Jacobson, *Nature*, 1998, **394**, 253-255.

69. N. K. Sheridon, Google Patents, 1978.

70. J. M. Crowley, N. K. Sheridon and L. Romano, *Journal of Electrostatics*, 2002, **55**, 247-259.

71. M. C. Tam, Google Patents, 2008.

72. I. Ota, J. Ohnishi and Yoshiyam.M, *Proceedings of the IEEE*, 1973, **61**, 832-836.

73. V. Novotny and M. A. Hopper, *Journal of the Electrochemical Society*, 1979, **126**, 2211-2216.

74. R. Sprague and Sist, *SiPix Microcup Electrophoretic Epaper for Ebooks*, 2009.

75. E Ink Technology: How E Ink Works. (accessed 12 March 2014), www.eink.com/how_e_ink_works.html.

76. Amazon Kindle Product Specification. (accessed 4 April 2013), http://www.amazon.co.uk/kindle-ereader-ebook-reader/dp/B007HCCOD0.

77. Nook by Barnes & Noble. (accessed 13 March 2014), http://www.barnesandnoble.com/u/nook/379003208/.

78. M. Wang, C. Lin, H. Du, H. Zang and M. McCreary, *SID Symposium Digest of Technical Papers*, 2014, **45**, 857-860.

79. N. Hiji, Y. Machida, Y. Yamamoto, Y. Satoh, S. Ootani, T. Satoh and K. Shigemura, *SID Symposium Digest of Technical Papers*, 2012, **43**, 85-87.

80. Particles for electrophoretic displays, S. Butterworth, L. D. Farrand, M. J. Goulding, B. Saunders, J. H. Wilson and S. G. Yeates, WO 2012152392 A1, 2012.

81. Coloured particles for electrophoretic displays, L. D. Farrand, M. J. Goulding, J. H. Wilson, A. N. Smith, M. James and D. Walker, US 8743451 B2, 2014.

82. Particles for electrophoretic displays, L. D. Farrand, M. James, M. Koch, A. N. Smith, J. H. Wilson, M. J. Goulding and D. Walker, EP 2393851 A2, 2011.

83. A. A. Maryott, E. R. Smith and S. National Bureau of, *Table of dielectric constants of pure liquids*, National Bureau of Standards, Washington D.C., 1951.

84. N. Miyagawa, S. Nakamura, M. Wang and T. Kitamura, *Journal of Imaging Science and Technology*, 2010, **54**, 10506-10501.

85. S. W. Oh, C. W. Kim, H. J. Cha, U. Pal and Y. S. Kang, *Advanced Materials*, 2009, **21**, 4987-+.

86. G. Feng and M. J. Gormish, *SID Symposium Digest of Technical Papers*, 2008, **39**, 697-700.

87. Particles for electrophoretic displays, L. D. Farrand, M. James, E. J. Markham, C. Topping and J. H. Wilson, 2012.

88. M. Kuo, *Digitimes*, 2010

Chapter 3: Synthesis of PMMA-b-PODA and its Use as a Stabiliser

3.1 Introduction

The synthesis of copolymers for use as stabilisers in non-aqueous dispersion polymerisation has been documented widely in literature. These are typically block or graft copolymers (as discussed in Chapter 2), and are often synthesised using controlled polymerisation techniques to ensure they have a well-defined structure and are of a narrow distribution. The selection of each component of the stabiliser is dictated by the particles which are to be stabilised, the medium they are to be dispersed in, and desirable properties of the dispersions. This chapter details the synthesis of a number of stabilisers of varying molecular weights and compositional ratios, and the investigation of their use in non-aqueous dispersion polymerisations of PMMA particles in dodecane.

3.1.1 Dispersion Polymerisations of PMMA

Poly(methyl methacrylate) (PMMA) is a transparent, stiff plastic, made up of methyl methacrylate units bonded together. A number of routes to its synthesis were first documented by a patent filed by ICI in 1931, which also reported its use as a thermoplastic.[1] This one patent has since been cited in numerous other applications for intellectual property, covering areas such as insulation[2], optical lenses[3] and surgical material.[4] This wide range of applications for PMMA comes from the valuable properties of the material – it has been shown to be biocompatible, easy to manipulate and relatively simple to synthesise.

There are numerous examples in the literature of dispersions of PMMA particles in non-polar solvents.[5-10] It has already been demonstrated that selecting the correct reaction parameters and components resulted in the synthesis of very monodisperse particles, with the ability to control the size of the resulting particles simply by

varying the reaction conditions. These PMMA particles have also successfully been demonstrated to be a viable alternative to the inorganic particles used in the conventional electrophoretic displays.

Whilst the majority of the particle criteria necessary for them to be used in EPDs (discussed in Chapter 2) are controlled by the synthesis conditions, a number of them can be directly linked to the stabiliser used. The concentration of stabiliser in relation to the amount of monomer system can provide control over particle size, and the lengths of each block in a copolymer stabiliser can dictate the stability of the resulting particle dispersion. The selection of the stabiliser controls properties such as the resistance of the particles to aggregation or sedimentation.

One of the difficulties in incorporating dyes into polymeric particles is the leaching of the dyes into the dispersion medium.[11] Typically the dyes are just encapsulated or entangled in the polymer chains forming the particle. However, the use of a dye with a polymeric moiety (similar to that of the MMA monomer unit in the particles) would allow for the covalent incorporation of the dyes into the particles, reducing the risk of any leaching occurring.

The choice of non-polar solvent was mainly application driven – electrophoretic displays require a solvent which has a relatively low boiling point as well as a low freezing point, to allow a device to function in most environments. These solvents are also typically less reactive than polar solvents, potentially adding to the lifetime and stability of any systems they are incorporated into. Dodecane, the solvent of choice for the particle dispersions, has a boiling point of 216ºC and a freezing point of -10ºC.[12] It also has a refractive index (RI) of 1.419,[13] whilst PMMA has a RI of 1.491[14] (both measurements recorded at a wavelength of approximately 590 nm). As discussed in chapter 2, the difference in RI between solvent and particles has a pronounced effect on the light scattering properties, and in turn the image clarity of the final device.

3.1.2 Synthetic Routes to Polymeric Stabilisers

In an industrially driven project with a specific application in mind, the selection of a synthetic route is often crucial in order to maintain desired properties in the

synthesised material. With regards to polymerisation, this decision is often based on which controlled living radical technique (ATRP, SET, RAFT or NMP) will result in the most suitable polymers.

RAFT was eliminated as a potential method due to a number of drawbacks. One of the main objectives of the project was the ability to synthesise full colour particles, by the addition of polymerisable dyes. RAFT chain transfer agents are typically brightly coloured (often red or orange), and they become incorporated into the product polymer themselves. This would result in all stabilisers being coloured before their use in polymeric dispersions, theoretically limiting the capability to produce dispersions of all colours. Another drawback is that the chain transfer agents often have an unpleasant smell, due to the sulphur moieties they possess. It has been demonstrated that it is possible to regenerate chain transfer agents after a RAFT polymerisation,[15] as well as to functionalise them,[16] which also removes the undesirable colours. Whilst RAFT does allow for chain extension and block copolymerisation by maintaining end group activity, some chain termination is still observed.[17]

ATRP was selected for the stabiliser synthesis for a number of reasons – firstly, it has been shown to provide control over chain length and dispersity of polymer chains, as well as the possibility to extend these chains by block copolymerisation.[18] It is suitable for polymerising a wide range of monomers, and the parameters of the reaction can be controlled by changing any of the key components of the reaction (solvent, initiator, ligand and catalyst). Recent developments have led to new polymerisation techniques which potentially circumvent some of the difficulties seen in ATRP systems. For this reason, copper (0) mediated ATRP in non-polar solvents and single-electron transfer polymerisation (SET) were also selected as possible synthetic routes which could also result in higher end group fidelity, and reduce the concentrations of copper compounds in both the reactions and the products.[19]

3.1.3 Poly(methyl methacrylate)

The anchor component of a stabiliser for use in NAD polymerisations needs to have a strong affinity for the dispersed phase (in this case, the PMMA particles), as well as an aversion to the continuous phase (in this case, dodecane).

PMMA has already been presented as the anchor component in a number of other stabilisers for non-aqueous dispersion polymerisations of MMA.[20, 21] There is a wealth of examples in the literature of the synthesis of well-defined PMMA via ATRP, and its use as a macroinitiator from which to synthesise block copolymers.[22-26] PMMA is an obvious choice for the anchor component of PMMA particles as it will have a strong affinity for the PMMA chains precipitating out during the polymerisation and forming particles.

The length of the PMMA anchor component in relation to the length of the lyophilic block was seen to affect the dispersity of particles produced in dispersion polymerisations.[21]

3.1.4 Poly(methyl methacrylate)-block-poly(octadecyl acrylate)

Octadecyl acrylate (also known as stearyl acrylate) is a non-polar, hydrophobic monomer which possesses a bulky 18-carbon long alkyl chain which, when incorporated into a polymer chain, enables side chain crystallisation.[27] These properties make it a strong candidate for the lyophilic portion of a steric stabiliser for dispersions in alkane solvents. The synthesis of the homopolymer poly(octadecyl acrylate) (PODA) via ATRP has been reported,[28] as well as its incorporation into diblock copolymers.[29] Whilst initially polymer chains were seen to precipitate out of solution (due to incompatibility with the solvent best suited to the catalyst/ligand system), changing the ligand to a disubstituted bipyridine derivative improved the solubility of the polymer chains. However, it was noted that the addition of Cu(II) at the beginning of the reactions was necessary to reduce the Kt (constant of termination), which otherwise was exceptionally high, potentially due to a steric effect of the alkyl chain, which 'protected' the radical from termination.[28]

The use of copolymers with one octadecyl (meth)/acrylate block as stabilisers for polymer nanocomposites,[30] and for polymeric particle dispersions[31] have also been discussed in literature, where the ODMA was selected for its ability to solubilise polymers in alkane mixtures. Poly(methyl methacrylate)-*block*-poly(octadecyl acrylate) (PMMA-*b*-PODA) – shown in scheme 3.1 - has been reported a number of times, and successfully used as a stabiliser for dispersion polymerisations.[32, 33]

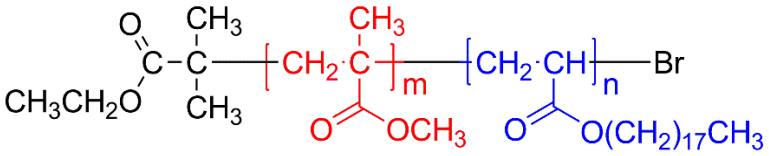

Scheme 3.1: the structure of PMMA-*b*-PODA stabiliser synthesised via ATRP.

As previously discussed, other stabilisers have been successfully used in NAD polymerisations, although not without drawbacks. The synthesis of PMMA-*b*-PODA presented contains considerably fewer stages than stabilisers which have been used more commonly, such as PHSA-*g*-PMMA[7], and this work looks to optimise the synthesis.

3.2 Aims and Objectives

The aim of the work outlined in this chapter was to synthesise precisely controlled block copolymers for use as stabilisers in non-aqueous dispersion polymerisations (NAD). Firstly, a specialised ligand was synthesised following literature procedures, which was then used in the atom transfer radical polymerisation (ATRP) of methyl methacrylate, with the aim of creating a PMMA macroinitiator with an active bromide end cap (PMMA-Br). This PMMA-Br was then used in the synthesis of a variety of block copolymers.

The resulting block copolymers were then used in the NAD polymerisation of methyl methacrylate. Initially these reactions followed a protocol designed by Claire Topping at Merck's Chilworth Technology Centre, which was optimised for use with the PHSA-*g*-PMMA stabiliser. Once the method was shown to be successful with PMMA-*b*-PODA used as the stabiliser instead, the ratios of reaction components were systematically varied to investigate the versatility of the system.

The wt % of monomer and stabiliser were varied to explore the effect on particle size and dispersity, and additives such as crosslinker (ethylene glycol dimethacrylate) and polymerisable dyes were incorporated into some of the dispersions. When dyed, cross-linked, monodisperse particles had been synthesised, these dispersions were subjected to preliminary tests designed by Merck to test their viability as electrophoretic fluids.

3.3 Experimental

3.3.1 Materials and Apparatus

Propylamine (Aldrich, 98%), 2-pyridinecarboxaldehyde (Aldrich, 99%), 2-bromo-2-methylpropionyl bromide (Aldrich, 98%), ethylene glycol anhydrous (Aldrich, 99.8%), triethylamine (Aldrich, 99%), copper (I) bromide (Aldrich, 98%), copper (I) chloride (Aldrich, 97%), copper (II) chloride (Aldrich, 97%), N,N,N',N'',N''-pentamethyldiethylenetriamine (PMDETA) (Aldrich, 99%), 4,4′-dinonyl-2,2′-dipyridyl (dNbpy) (Aldrich, 97%), ethyl-2-iso-bromobutyrate (EBIB) (Acros Organics, 98%), tris[2-(dimethylamino)ethyl]amine (Me_6TREN) (Aldrich, 97%), ethyl α-bromophenylacetate (Aldrich, 97%), methacrylic acid (Aldrich, 99%) 2,2'-azobis(2-methylbutyronitrile) (V-59) (Wacko Chemicals, 99%), octanethiol (Aldrich, 98.5%), ethylene glycol dimethacrylate (Aldrich, 98%) and copper wire (0.5 mm ⌀, Aldrich) were used without further purification. Magnesium sulphate (Aldrich), aluminium oxide (Acros Organics, activated, neutral, Brockmann 1, for chromatography, 50-200 μm), hexane (Fisher, laboratory grade), dichloromethane, diethyl ether, toluene, methanol, xylene and tetrahydrofuran (all Fisher, analytical grade) were used as received. Commercially available polymerisable dyes (magenta and red) were used as received from Merck Chemicals. In order to remove inhibitors, methyl methacrylate (Aldrich, 99%) and ethyl hexyl acrylate (Alfa Aesar, 98%) were passed directly through an aluminium oxide column, and octadecyl acrylate (Aldrich, 97%) was heated to 60°C; stirred with alumina overnight; and hot filtered.

^{1}H and ^{13}C nuclear magnetic resonance (NMR) spectra were recorded using a JEOL ECS-400 spectrometer at 30°C from solutions in $CDCl^3$.

FTIR spectra were obtained using a Shimadzu IRAffinity-1. All measurements were taken from 400-4000 cm^{-1} for 256 scans, with a golden gate component used when measuring spectra of solids.

Molecular weight characteristics of polymers were estimated relative to PMMA standards by gel permeation chromatography (GPC) using a PL-GPC 50 supplied by

Polymer Laboratories Ltd, in conjunction with a refractive index detector. All determinations were carried out at 40°C with tetrahydrofuran (THF) as a mobile phase at a flow rate of 1 ml min-1, using a 50 mm x 7.8 mm 10 µm PLgel guard column and 2 x 300 mm x 7.8 mm 5 µm PLgel Mixed-C columns.

Dynamic light scattering (DLS) measurements were carried out on colloidal solutions at a range of temperatures using a Zeta-sizer nano series (Nano-ZS) machine, supplied by Malvern Instruments. The z-average, number average and dispersity were measured at temperatures between 10°C and 45°C at a height of 0.85 cm, with measurements taken over a period of 90 seconds with an automatically generated number of scans, ranging from 12-19.

Scanning electron microscope (SEM) images were taken using a JCM-5000 Benchtop SEM (Neoscope), at a specimen height of 55 mm, an acceleration voltage of 15 kV and under high vacuum. Particles were sputtered by gold for 120 seconds at 18mA before being assessed in the SEM chamber. Particle sizes were measured using Image J software version 1.42q, with diameters of over 100 particles for each dispersion measured from 8-bit, binary watershed images using a feret distribution.

MALDI-TOF spectra were obtained using a Bruker ultrafleXtreme MALDI-TOF/TOF. Samples were spotted on a MTP 384 ground steel sample target and data was collected using Bruker's flexcontrol software between 800 and 8000 m/z in positive ion mode. Data was the summation of 4000 laser shots with an extraction delay of 110 ns, samples were accelerated with an ion source 1 voltage of 25 kV, ion source 2 voltage of 22.4 kV and lens voltage of 7.8 kV and reflected with a reflector 1 voltage of 26.45 kV and reflector 2 voltage of 13.4 kV and ions detected with a detector voltage of 2.4 kV. Data was processed using Bruker's flexanalysis software.

3.3.2 Synthesis of N-(n-propyl)-2-pyridyl(methanimine) (PPMI) Ligand

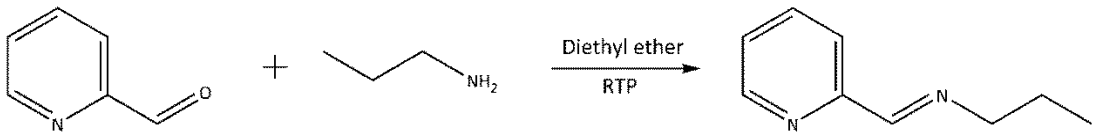

Scheme 3.2: Synthesis of N-(n-propyl)-2-pyridyl(methanimine)

PPMI was synthesised following a literature procedure.[23] Propylamine (88 ml, 0.730 mol) was added dropwise to a mixture of 2-pyridinecarboxaldehyde (60 ml, 0.730 mol) and diethyl ether (90 ml) with stirring on ice. On complete addition of propylamine, magnesium sulphate was added and the reaction allowed to stir for two hours at 25°C. The reaction mixture was filtered before solvent was removed under vacuum. The product was then purified by distillation under vacuum, to leave a golden yellow oil (54% yield).

^{1}H NMR (400 MHz, $CDCl_3$, ppm) δ: 0.95 (triplet, 3H, C**H$_3$**-CH_2-), 1.74 (multiplet, 2H, CH_3-C**H$_2$**-), 3.61 (triplet, 2H, N-C**H$_2$**-CH_2), 7.23 (triplet, 1H, N=CH-C**H**), 7.66 (triplet, 1H, N=CH-CH=C**H**), 8.00 (doublet, 1H, N-C-C**H**-CH), 8.38 (singlet, 1H, N-C-C**H**=N), 8.61 (doublet, 1H, C-N=C**H**).

^{13}C NMR ($CDCl_3$, ppm) δ: 11.7 (**C**H_3-CH_2), 23.7 (CH_3-**C**H_2), 63.1 (CH_3-CH_2-**C**H_2) 120.9 (pyridyl N-CH-**C**H), 124.4 (pyridyl N-C-**C**H), 136.3 (pyridyl N-CH-CH-**C**H), 149.2 (N=**C**H), 154.5 (pyridyl N-**C**H), 161.5 (pyridyl N-**C**).

FTIR – ν_{max}/cm^{-1} 3053 (aromatic C-H), 2960, 2929, 2873 (alkyl C-H), 1649 (C=N), 1587, 1566 (C=C), 1336 (aromatic C-N), 1226 (alkyl C-N).

3.3.3 Synthesis of PMMA

Poly(methyl methacrylate) was chosen to be the lyophobic block of the stabilisers. This was partly due to the wealth of research into its synthesis via conventional radical polymerisation as well as controlled living polymerisations, but also working on the basis that the polymeric dispersions would be of methyl methacrylate. This ensured that the stabilisers would interact favourably with the polymeric particles as they were forming, and increase the likelihood that they would become entangled and continue to act as steric stabilisers.

3.3.3.1 Synthesis of PMMA Macroinitiator by ATRP (M1-M21)

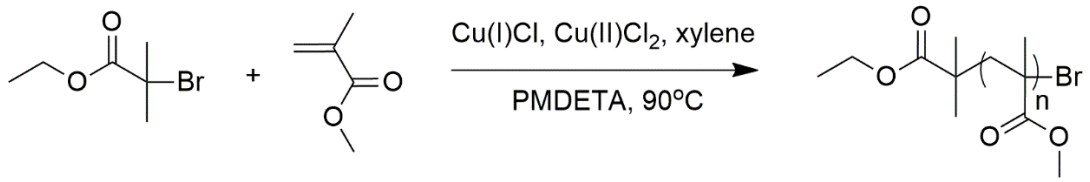

Scheme 3.3: Synthesis of PMMA-Br via conventional ATRP.

A typical procedure was as follows. Nitrogen gas was bubbled through a mixture of MMA (70g, 0.699 mol), copper (I) chloride (1.065 g, 0.011 mol), copper (II) chloride (0.072 g, 0.538 mmol), PMDETA (5.592 g, 0.033 mol) and xylene (140 ml) for an hour. Nitrogen gas was bubbled through a separate flask of ethyl-2-*iso*-bromobutyrate (EBIB) (1.57 ml, 0.011 mol) simultaneously. The mixture was then subjected to 4 freeze-pump-thaw cycles and then heated to 90°C, before ethyl-2-iso-bromobutyrate was injected, and the reaction mixture stirred at temperature for 150 minutes. The reaction mixture was diluted with THF, run down an alumina column and THF was removed under vacuum. The polymer was redissolved in THF and precipitated into cold stirring hexane twice to give a white powder.

The quantities of the reactants, and the choice of initiator, ligand, catalyst and solvent were varied for individual reactions. Details of the products for these reactions can be found in Tables 3.1 and 3.2

^{1}H NMR (400 MHz, $CDCl_3$, ppm) δ: 0.9 (broad doublet, 3H, C(C**H$_3$**), 1.75 (broad doublet, 2 H, C-C**H$_2$**-C), 3.6 (singlet, 3H, O-C**H$_3$**).

^{13}C NMR ($CDCl_3$, ppm) δ: 14.2 (**C**H_3-CH_2), 18.8 (**C**H_3-C-CO), 22.7 (**C**H_3-C-**C**H_3), 31.6 (CH_3-**C**-C=0), 44.6 (CH_3-**C**-CH_3), 44.9 (**C**H_2-C-C=O), 51.9 (**C**H_3-O), 54.5 (CH_3-**C**H_2), 177.0 (O-**C**=O-C), 178.2 (O=**C**-OCH_3).

3.3.3.2 Synthesis of PMMA Macroinitiator by Copper (0) Mediated ATRP (M22-M24)

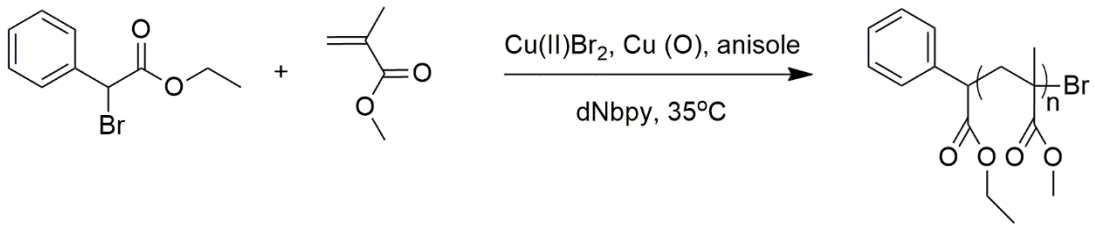

Scheme 3.4: Synthesis of PMMA-Br via copper (0) mediated ATRP

A typical procedure was as follows. Nitrogen gas was bubbled through a mixture of methyl methacrylate (25 g, 0.249 mol), ethyl α-bromophenyl acetate (0.934 g, 3.84 mmol), 4,4′-dinonyl-2,2′-dipyridyl (0.785 g, 1.92 mmol), copper (II) bromide (0.429

g, 1.92 mmol) and anisole (25 ml) for 30 minutes, before the mixture was subjected to three freeze-pump-thaw cycles. After the last thaw, 55.23 mm copper (0) wire was added to the mixture under positive nitrogen pressure, and the reaction mixture was stirred at 35°C for 12 hours. The reaction mixture was diluted with THF, run down an alumina column and THF was removed under vacuum. The polymer was redissolved in THF and precipitated into cold stirring hexane twice to give a white powder.

The choice of ligand, the scale of the reaction and the time of the reaction were varied for individual syntheses. Details of the products for these reactions can be found in Table 3.3.

^{1}H NMR (400 MHz, $CDCl_3$, ppm) δ: 0.83 (broad doublet, 3H, C(C**H$_3$**), 1.19 (broad triplet, 3H, C**H$_3$**-CH_2) 1.79 (broad doublet, 2 H, C-C**H$_2$**-C), 3.54 (singlet, 3H, O-C**H$_3$**), 3.76 (multiplet, 1H, C**H**-Ph), 4.02 (multiplet, 2H, CH_3-C**H$_2$**), 7.00-7.21 (multiplet, 5H, **Ph**).

^{13}C NMR ($CDCl_3$, ppm) δ: 14.2 (**C**H_3-CH_2), 25.4 (**C**H_3-C-CO), 44.6 (CH_3-**C**-C=0), 51.9 (**C**H_2-C-C=O), 52.6 (Ph-**C**H), 53.1 (**C**H_3-O), 68.1 (CH_3-**C**H_2), 127.6, 128.7, 128.9 (**Ph**), 176.3 (O-**C**=O-C), 177.8 (O=**C**-OCH_3).

3.3.3.3 Synthesis of PMMA Macroinitiator by SET-LRP (M25-M28)

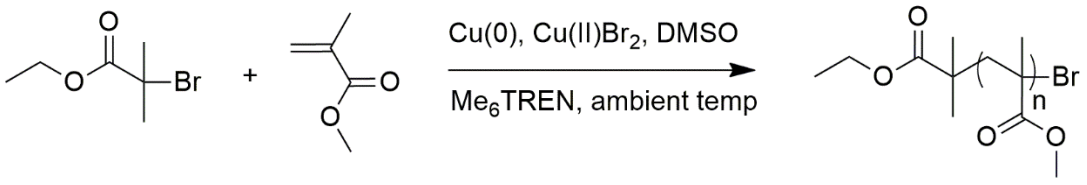

Scheme 3.5: Synthesis of PMMA-Br via SET polymerisation.

A typical procedure was as follows. Nitrogen gas was bubbled through a mixture of methyl methacrylate (25 g, 0.249 mol), ethyl α-bromoisobutyrate (0.749 g, 3.84 mmol), tris[2-(dimethylamino)ethyl]amine (Me_6TREN) (0.106 g, 0.461 mmol), copper (II) bromide (0.043 g, 0.192 mmol) and dimethylsulfoxide (25 ml). 25 cm of copper (0) wire (preactivated with concentrated hydrochloric acid for 10 minutes) was added to the mixture under a positive nitrogen pressure. The reaction was then

allowed to progress at ambient temperature, with stirring and under nitrogen, for 24 hours, before the reaction mixture was diluted with THF, run down an alumina column and THF was removed under vacuum. The polymer was redissolved in THF and precipitated into cold stirring hexane twice to give a white powder.

The choice of initiator, ligand and solvent were varied for individual syntheses. Details of the products of these reactions can be found in Table 3.4.

^{1}H NMR (400 MHz, $CDCl_3$, ppm) δ: 0.9 (broad doublet, 3H, C(C**H$_3$**), 1.75 (broad doublet, 2 H, C-C**H$_2$**-C), 3.6 (singlet, 3H, O-C**H$_3$**).

^{13}C NMR ($CDCl_3$, ppm) δ: 14.2 (**C**H_3-CH_2), 19.0 (**C**H_3-C-CO), 22.7 (**C**H_3-C-**C**H_3), 33.4 (CH_3-**C**-C=0), 43.5 (CH_3-**C**-CH_3), 44.8 (**C**H_2-C-C=O), 52.1 (**C**H_3-O), 55.7 (CH_3-**C**H_2), 177.2 (O-**C**=O-C), 177.9 (O=**C**-OCH_3).

3.3.4 Synthesis of Block Copolymers

3.3.4.1 Synthesis of PMMA-*b*-PODA by ATRP (S1-S5)

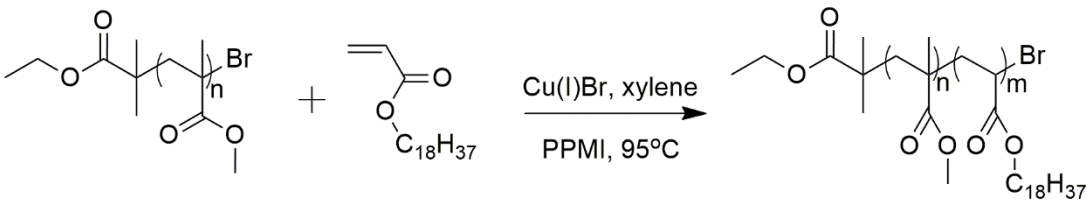

Scheme 3.6: Synthesis of PMMA-*b*-PODA.

A typical procedure was as follows. Nitrogen gas was bubbled through a mixture of ODA (14.352 g, 0.0442 mol), copper (I) bromide (0.106 g, 1.37 mmol), PPMI (0.219 g, 1.47 mmol) and toluene (15 ml) for an hour. This mixture was then subjected to 4 freeze-pump-thaw cycles with heat added in the thaw stage to reach above melting point of ODA, before the mixture was heated to 95°C. Nitrogen was bubbled through a separate flask of PMMA-Br (5.000 g, 0.737 mmol) in toluene (10 ml) simultaneously. The solution of PMMA-Br in toluene was then injected and the reaction allowed to stir at temperature under nitrogen atmosphere for 6 days. The mixture was diluted with THF, run down an alumina column and the solvent

removed under vacuum. The polymer was then redissolved in DCM and precipitated into cold stirring methanol twice to give an off-white (brownish) powder.

The choice of macroinitiator and the scale of the reaction were varied for individual syntheses. Details of the products of these reactions can be found in Table 3.5.

^{1}H NMR (400 MHz, $CDCl_3$, ppm) δ: 0.9 (multiplet, 4H, C**H$_3$**-$C_{16}H_{32}$ and CH_3-$(CH_2)_{16}$-CH_2-O-CO-C**H**), 1.0 (broad doublet, 3H, CH_3-O-CO-C(C**H$_3$**)), 1.2-1.4 (broad singlet, 32H, CH_3--(C**H$_2$**)$_{16}$-CH_2), 1.6 (broad singlet, 2H, CH_3-$(CH_2)_{16}$-CH_2-O-CO-CH-C**H$_2$**), 1.8 (broad singlet, 2H, CH_3-O-CO-C-C**H$_2$**), 3.6 (broad singlet, 3H, O-C**H$_3$**), 4.0 (broad singlet, 2H, CH_3-$(CH_2)_{16}$-C**H$_2$**-O).

^{13}C NMR ($CDCl_3$, ppm) δ: 14.2 ($(CH_2)_{17}$-**C**H_3), 22.8 (CH3-C-CO), 25.7 ($(CH_2)_{16}$-**C**H_2-CH_3), 26.0 (O-CH_2-CH_2-**C**H_2), 29.5 (CH_3-**C**-C=0), 29.9 (O-CH_2-**C**H_2), 31.1 ($(\mathbf{C}H_2)_{12}$-CH_2-CH_2-CH_3), 32.1 (CH_3-CH_2-**C**H_2), 44.6 (CH_3-$(CH_2)_{16}$-CH_2-O-CO-CH-**C**H_2), 51.9 (**C**H_3-O-CO), 68.1 (O-**C**H_2-$(CH_2)_{16}$-CH_3), 177.8 (O-**C**=O).

3.3.4.2 Synthesis of PMMA-*co*-PODA (C1 & C2)

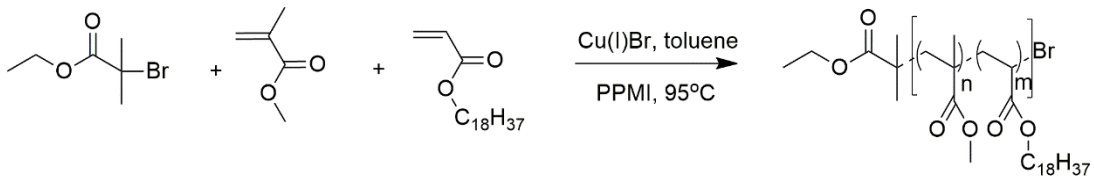

Scheme 3.7: Synthesis of PMMA-*co*-PODA random copolymers via ATRP.

A typical procedure was as follows. Nitrogen was bubbled through a mixture of methyl methacrylate (8.00 g, 0.0799 mol), octadecyl acrylate (12.00 g, 0.0380 mol), copper (I) bromide (0.0846 g, 0.5895 mmol) PPMI (0.1747 g, 1.179 mmol) and toluene (23 ml) for 1 hour. This mixture was subjected to three freeze-pump-thaw cycles, before being heated to 95°C. Nitrogen was bubbled through a separate mixture of EBIB (0.2259 g, 0.5895 mmol) and toluene (2 ml) simultaneously for an hour. The solution of EBIB in toluene was then injected and the reaction allowed to stir at temperature under nitrogen atmosphere for 24 hours. The mixture was diluted with THF, run down an alumina column, and the solvent removed under vacuum. The polymer was then redissolved in DCM and precipitated twice into cold stirring methanol to give a clean white powder.

The ratios of each monomer were varied for individual syntheses. Details of the products of these reactions can be found in Table 3.6.

^{1}H NMR (400 MHz, $CDCl_3$, ppm) δ: 3.6 (broad singlet, 2H, CH_3-$C_{16}H_{32}$-C**H$_2$**), 3.5 (broad singlet, 3H, C**H$_3$**-O), 1.8 (multiplet, 2H, CH_3-$C_{16}H_{32}$-CH_2-O-CO-CH-C**H$_2$**), 1.6 (broad singlet, 2H, CH_3-O-CO-C(CH_3)-C**H$_2$**), 1.3 (multiplet, 32H, CH_3-C_{16}**H$_{32}$**-CH_2), 1.0 (singlet, 1H, CH_3-$C_{16}H_{32}$-CH_2-O-CO-C**H**), 0.9 (multiplet, 3H, C**H$_3$**-$C_{16}H_{32}$-CH_2), 0.8 (multiplet, 3H, CH_3-O-CO-C(C**H$_3$**)).

3.3.5 Synthesis of Particle Dispersions by NAD

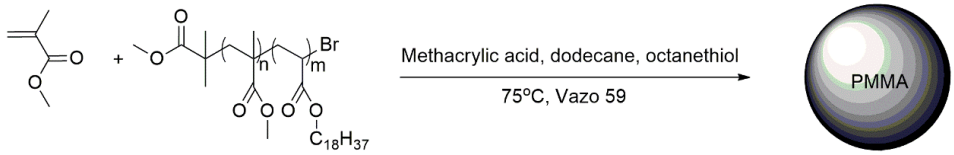

Scheme 3.8: Synthesis of PMMA particles by non-aqueous dispersion polymerisation.

A typical procedure was as follows. Methyl methacrylate (20.580 g, 0.205 mol), copolymer stabiliser (1.050 g, 0.508 mmol), octanethiol (0.125 ml, 0.715 mmol), methacrylic acid (0.416 ml, 4.859 mmol) and dodecane (25.195 g, 0.146 mol) were added together and heated to 70°C under nitrogen. V-59 initiator (0.200 g, 1.036 mmol) was then added, and the mixture was stirred under nitrogen for two hours, before being removed from the heat and allowed to cool to room temperature. The reaction mixture was then passed through 50 μm cloth (purchased from Sefar) to remove fused particles, and washed in dodecane, centrifuged and redispersed three times before analysis by SEM and DLS.

The ratios of monomer to solvent and the choice of stabiliser were varied for individual syntheses. Details of the products of these reactions can be found in Table 3.7.

3.3.6 Synthesis of Cross-linked or Dyed Particle Dispersions by NAD

Ethylene glycol dimethacrylate (EGDMA) or commercially available cross-linking dyes (scheme 3.9) were used in different molar ratios (1 and 5% with regards to monomer) in the typical particle syntheses detailed in 3.3.5. These components were

added to the mixture before the heating step. Details of the products of these reactions can be found in Table 3.7

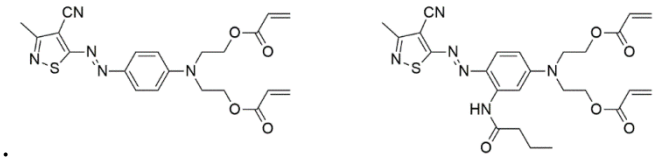

Scheme 3.9: commercially available polymerisable dyes used in NAD polymerisations; left – red, right – magenta 1.

All particle dispersions were analysed by SEM and DLS to determine particle size and dispersity.

3.4 Results and Discussion

3.4.1 Synthesis of PPMI ligand

The NMR spectrum for the ligand after purification (Figure 3.1) showed all of the expected peaks for the desired product. Peaks for the starting materials pyridine carboxaldehyde and propyl amine were absent, confirming completion of the reaction, and peaks corresponding to diethyl ether were no longer present. This demonstrated the purity of the product after isolation, drying and distillation under vacuum. The structure was also confirmed by the presence of aromatic signals on the FTIR spectrum.

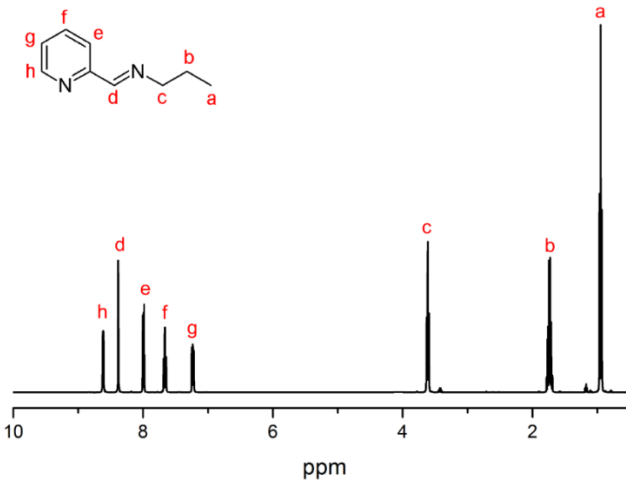

Figure 3.1: ^{1}H NMR spectrum of PPMI ligand, showing peak assignments.

3.4.2 Synthesis of PMMA-Br

Poly(methyl methacrylate) macroinitiators were synthesised via a number of controlled polymerisation methods, varying the reaction conditions and reagents to investigate the change in chain length, dispersity and end group activity. The results of this systematic variation of ATRP reactions are shown in Tables 3.1 and 3.2, whilst macroinitiators synthesised by Cu(0) mediated ATRP are in Table 3.3, and by SET-LRP are in Table 3.4. The text coloured red is to indicate which parameter was changed from the previous synthesis to investigate the effect of that component. Target M_n was calculated from the addition of the molecular weight of the initiator to the number of monomer units added to synthesis per initiator molecule. I_{eff} was calculated from the theoretical M_n (percentage conversion of the target M_n) divided by the measured M_n of the sample.

Figure 3.2 shows the assigned ^{1}H NMR spectrum for PMMA initiated by EBIB – there are observable signals due to groups from the initiator, but they are less apparent than those from the polymer backbone. This is because they represent considerably fewer protons than those in the main polymer structure. Multiple peaks are also observed for single proton environments, which were attributed to the different tacticities (discussed in chapter 1).

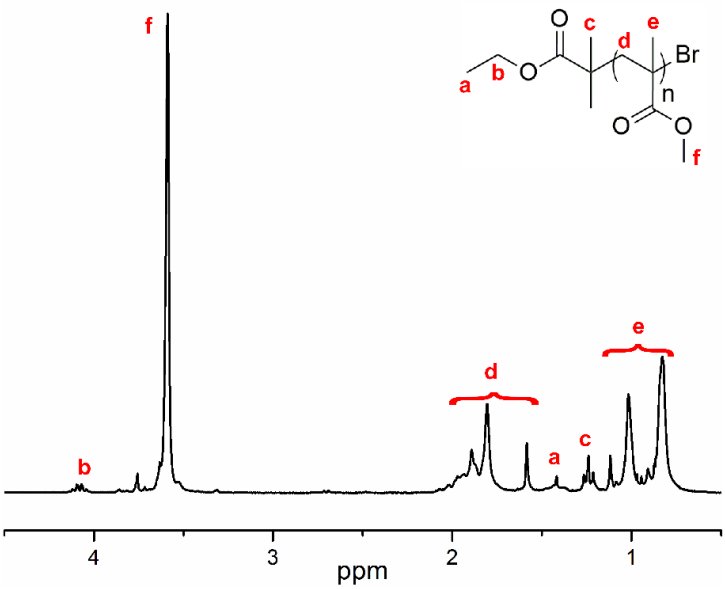

Figure 3.2: ^{1}H NMR spectrum of PMMA-Br (M3) synthesised by ATRP with EBIB as the initiator, showing full peak assignments.

The initial small scale PMMA syntheses (M1-M6), using ethyl-2-iso-bromobutyrate (EBIB) as an initiator, PPMI as a ligand and CuBr as the catalyst system, were conducted following a published method of ATRP synthesis of PMMA macroinitiators.[32] These syntheses were shown to produce polymer samples with narrow weight distributions. However, the reactions progressed quickly, with M_n values observed to be higher than targeted – for this reason, the time at which the reaction was stopped was reduced from 48 hours to 6 hours, in order to isolate PMMA chains of smaller molecular weights.

It was then necessary to scale up the synthesis of PMMA, due to the industrial nature of the project and the need for large amounts of macroinitiator from which to synthesise multiple block copolymer stabilisers. On scaling up this reaction (M7-M10), chains were seen to be significantly above the desired molecular weights even after a shorter period of time had passed – in some cases just 45 minutes. This was likely due to a poor initiator efficiency (I_{Eff}), which was not calculated as conversions were not recorded for these polymerisations. This could have been caused by a low K_{act} for the system. If K_{ATRP} was higher than K_{act}, this would lead to some chains initiating and growing rapidly, consuming monomer before the remainder of the initiator molecules could form radicals. The other alternative would be an excess of bimolecular termination, although this would likely have caused higher dispersity values than were observed. There has also been some evidence that the initiation or propagation stages of ATRP can be exothermic,[34] which would have a greater effect on a larger scale reaction, and would increase the equilibrium constants for the system.

The ligand was then changed from PPMI to PMDETA, due to the increased activity of PMDETA in comparison to PPMI (M9 and M10). Whilst an increase in dispersity was observed, which is due to the increased K_{ATRP} of PMDETA when compared to K_{ATRP} of PPMI,[35] there was no reduction in chain length which would indicate an increase in I_{Eff}. This again was evidence of poor initiation, meaning that the rate of polymerisation was dramatically higher than the rate of initiation.

The targeted M_n values were varied between syntheses for a number of reasons. Firstly, literature into the stabilisation of PMMA particles by PMMA-*b*-PODA block copolymers showed that a DP of approximately 60 resulted in stable particle

dispersions. This indicated that the initial syntheses M1 – M3, targeting DP values of around 25, would not necessarily have provided PMMA blocks which were long enough for effective stabilisation. Also, ATRP is known to result in a loss of chain end fidelity after 80% conversion, so the targeted molecular weights were increased from around 5000 $gmol^{-1}$ to around 6500 $gmol^{-1}$. This meant that stopping reactions at around 80% conversion (for an accurately controlled polymerisation) would result in polymer chains of the actual desired length.

Table 3.1: PMMA-Br macroinitiators, synthesised by ATRP ([a] – measured by GPC).

Macroinitiator	Initiator	Ligand	Catalyst	Solvent	Monomer (g)	Time (hrs)	Temp (°C)	Target M_n	M_n [a]	M_w/M_n [a]
M1	EBIB	PPMI	CuBr	Toluene	10	48	60	2700	3790	1.16
M2	EBIB	PPMI	CuBr	Toluene	10	26	60	2700	3440	1.15
M3	EBIB	PPMI	CuBr	Toluene	10	6	60	2700	2630	1.12
M4	EBIB	PPMI	CuBr	Toluene	10	72	60	5200	4340	1.19
M5	EBIB	PPMI	CuBr	Toluene	10	4	60	3700	3120	1.14
M6	EBIB	PPMI	CuBr	Toluene	10	4	60	6200	4890	1.14
M7	EBIB	PPMI	CuBr	Toluene	100	2.1	60	3700	6600	1.15
M8	EBIB	PPMI	CuBr	Toluene	100	0.75	60	3700	5100	1.19
M9	EBIB	PPMI	CuBr	Toluene	100	24	50	6200	12100	1.16
M10	EBIB	PMDETA	CuBr	Toluene	100	0.75	60	3700	5080	1.67

3.4.2.1 Optimisation of Macroinitiator Synthesis

As the chains were consistently higher than targeted, an initiator with a higher activity was selected, ethyl α-bromophenylacetate (EBPA). EBPA was shown to have a K_{act} of almost 2000 times greater than the K_{act} value for EBIB in the same system ($5.3x10^3$ and 2.7 respectively).[36] This is due to the benzyl group increasing the stability of the radical which is produced, allowing initiation to occur more effectively. This led to another, more dramatic, increase in Đ to 2.2 (M11), which would typically be too high to be considered 'controlled' polymerisation. The results of these polymerisations are shown in Table 3.2.

Changing the reaction solvent to xylene was seen to bring back control over the dispersity and reduced the Đ to 1.29 (M11 and M12). This was attributed to the fact that catalyst systems have been shown to be less soluble in xylene than toluene, causing reactions to progress more slowly.[37] However on scaling up this system, the same difficulties were observed and the chain length increased from 4640 to 11780.

This logic was also employed when modifying the catalyst system – initially CuBr was used, but all reactions up to M12 were seen to progress rapidly and give molecular weights considerably higher than targeted. For this reason, CuCl was used as the catalyst (M14), which reduced the dispersity from 1.81 (M13) to 1.14, but molecular weight was still observed to be too high. This led to the addition of 5% $Cu(II)Cl_2$ being added to the polymerisations (M15 to M21), which reduced the M_n of the products, maintained the low dispersity and also increased the calculated I_{eff}. However, I_{eff} was still observed to be lower than desired (at around 0.5). For this reason, EBIB was again used as the initiator (M17 to M21) as opposed to EBPA, to reduce K_{act} of the system and increase the control over the molecular weights. By stopping the reaction at around 70% conversion in order to maintain chain end fidelity (discussed in Section 3.4.2.3), macroinitiators were obtained with low dispersities (approximately 1.2) and chain lengths which corresponded to the targeted M_n values. These syntheses were M20 and M21, highlighted in blue in Table 3.2.

Table 3.2: PMMA-Br macroinitiators synthesised by ATRP with varying reactants. ([a] – measured by GPC, [b] – calculated from 1H NMR). Highlighted blue are the 'optimised' syntheses.

Macroinitiator	Initiator	Ligand	Catalyst	Solvent	Monomer (g)	Time (hrs)	Temp (°C)	Target M_n	M_n [a]	M_w/M_n [a]	Conversion (%) [b]	I_{eff}
M11	EBPA	PMDETA	CuBr	Toluene	20	72	50	6750	4980	2.21	38	0.51
M12	EBPA	PMDETA	CuBr	Xylene	20	72	50	6750	4640	1.29	35	0.51
M13	EBPA	PMDETA	CuBr	Xylene	100	3	50	6750	11780	1.81	83	0.48
M14	EBPA	PMDETA	CuCl	Xylene	20	24	50	6750	12430	1.14	97	0.53
M15	EBPA	PMDETA	$CuCl/CuCl_2$	Xylene	20	52.5	50	6750	12490	1.13	62	0.34
M16	EBPA	PMDETA	$CuCl/CuCl_2$	Xylene	20	6	90	6750	9610	1.16	78	0.55
M17	EBIB	PMDETA	$CuCl/CuCl_2$	Xylene	20	6	90	6700	9120	1.21	79	0.58
M18	EBIB	PMDETA	$CuCl/CuCl_2$	Xylene	20	6	90	6700	6310	1.19	64	0.68
M19	EBIB	PMDETA	$CuCl/CuCl_2$	Xylene	20	7	90	6700	9300	1.23	75	0.54
M20	EBIB	PMDETA	$CuCl/CuCl_2$	Xylene	70	2.5	90	6700	6790	1.22	66	0.65
M21	EBIB	PMDETA	$CuCl/CuCl_2$	Xylene	70	2.5	90	6700	6700	1.24	66	0.66

Attempts were then made at synthesising macroinitiators via Cu(0) mediated ATRP and SET-LRP (results of which are shown in Tables 3.3 and 3.4). The macroinitiators synthesised using Cu(0) mediated ATRP (M22-M24) were all seen to have very low dispersities (between 1.11 and 1.18), but the molecular weights were all higher than targeted. They were also observed to be considerably slower than polymerisations via conventional ATRP (shortest reaction time of 18 hours in comparison to 150 minutes). Although the weight distribution was narrower than for ATRP, it was decided that the increased control was not worth the extra reaction time, particularly in research intended for a commercial application. For this reason, no further Cu(0) mediated ATRP reactions were conducted.

Table 3.3: PMMA-Br macroinitiators synthesised by Cu(0) ATRP. ([a] – measured by GPC, [b] – calculated from 1H NMR).

Macroinitiator	Initiator	Ligand	Catalyst	Solvent	Monomer (g)	Time (hrs)	Temp (°C)	Target M_n	M_n [a]	M_w/M_n [a]
M22	EBPA	dNbpy	$CuBr_2$/Cu(0)	Anisole	5	18	35	20250	11270	1.18
M23	EBPA	dNbpy	$CuBr_2$/Cu(0)	Anisole	10	24	35	6750	9930	1.11
M24	EBPA	dNbpy	$CuBr_2$/Cu(0)	Anisole	25	72	35	6750	9900	1.11

PMMA macroinitiators were also synthesised using SET-LRP (shown in Table 3.4). All samples (M25-M28) were seen to have larger dispersities than macroinitiators synthesised by either ATRP technique. Whilst the polymer chains for M25 and M28 were both lower than targeted, suggesting the level of control was comparable to the optimised ATRP method, M26 and M27 were still considerably higher than targeted. The use of EBPA as an initiator did result in a reduced dispersity, but also dramatically increased the M_n value, indicating rapid propagation. Whilst the chain end fidelity of these macroinitiators was investigated by MALDI (section 3.4.2.3), it was decided not to synthesise further polymers with SET due to the increased dispersity.

Table 3.4: PMMA-Br macroinitiators synthesised by SET-LRP ([a] – measured by GPC, [b] – calculated from 1H NMR).

Macroinitiator	Initiator	Ligand	Solvent	Target DP	Time (hrs)	Temp (°C)	Target M_n	M_n [a]	M_w/M_n [a]
M25	EBIB	Me_6TREN	DMSO	65	24	25	6700	2535	1.56
M26	EBIB	Me_6TREN	DMSO	65	24	25	6700	9000	1.49
M27	EBPA	Me_6TREN	DMSO	65	24	25	6750	11660	1.28
M28	EBIB	Me_6TREN	DMSO	65	2	25	6700	5609	1.51

3.4.2.2 Kinetics of Macroinitiator Synthesis

After control over the molecular weight and dispersity of the macroinitiators was obtained, it was necessary to confirm that the polymerisations were indeed controlled, and could be described as 'living'. Sampling reactions were conducted, whereby samples of the polymerisation were removed on an hourly basis, and NMR and GPC spectra were obtained. The GPC traces (Figure 3.3) showed an initial induction period, before a steady increase in molecular weight as the reaction progressed until completion at approximately 24 hours. The large peak at around 200 was attributed to the MMA monomer, and as the polymeric chains started to grow the intensity of this peak was seen to decrease and become bimodal due to the formation of slightly longer chains. This bimodality was seen to disappear when the polymeric chains became sufficiently long enough to be isolated from the monomeric peak.

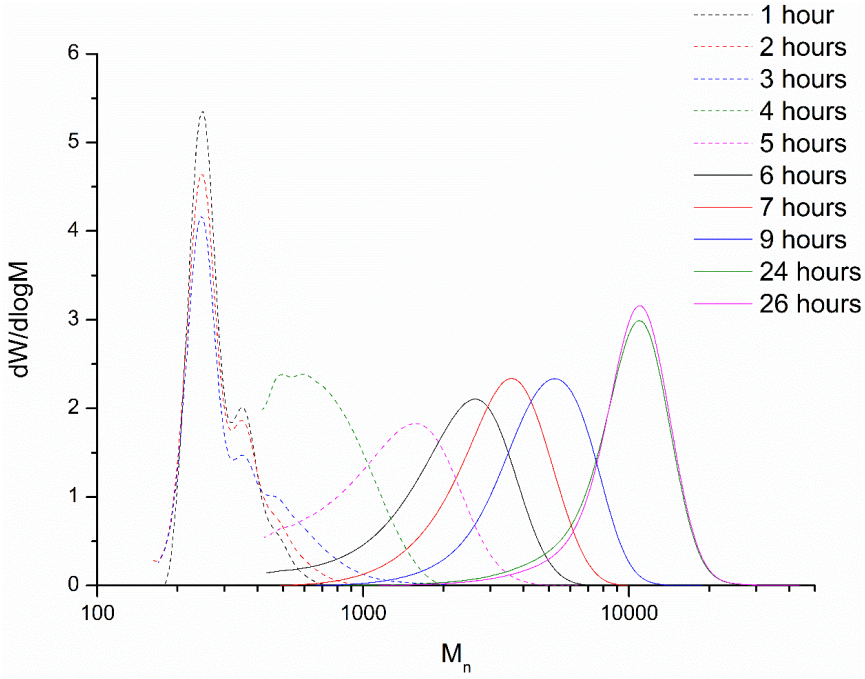

Figure 3.3: GPC traces following the reaction of M15 over a period of 24 hours – small samples of reaction were removed at various intervals and analysed via GPC and NMR.

Two sets of data are typically plotted to confirm the 'livingness' of the reaction – the percentage conversion against molecular weight, and the reaction time against the log values of the conversion ($[M_o]/[M]$). Figures 3.4 and 3.5 show these plots for the synthesis of macroinitiator M16 – both were linear confirming that a controlled

polymerisation was occurring. The theoretical plot for conversion against M_n for the 'ideal' system was included in Figure 3.4. The experimental plot was observed to be higher than the theoretical, which was supported by the I_{eff} value of 0.55.

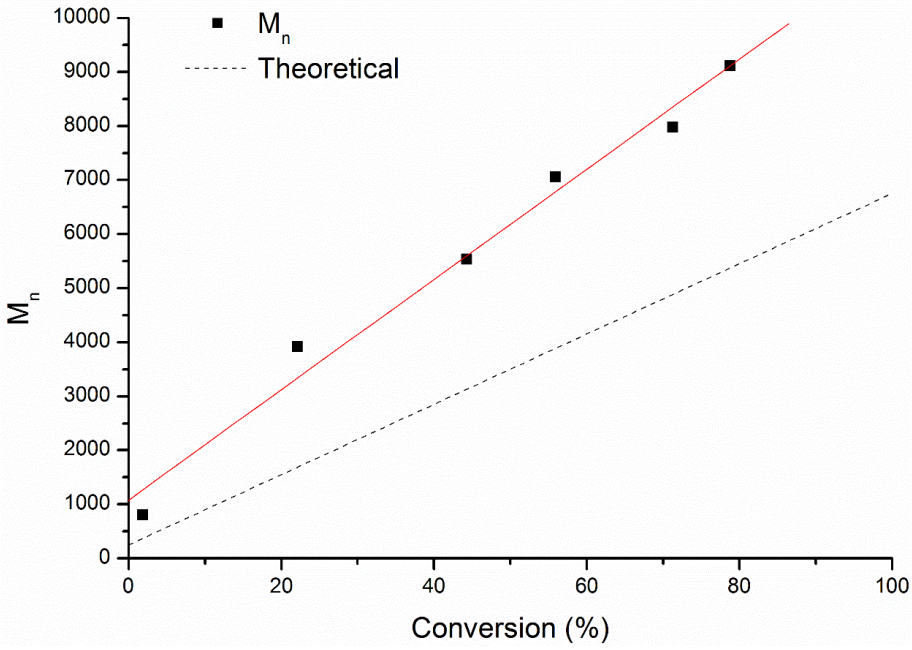

Figure 3.4: A plot to show the M_n of the product polymer M16 with increasing conversion, in comparison to the theoretical values if the initiator efficiency and other parameters were all ideal.

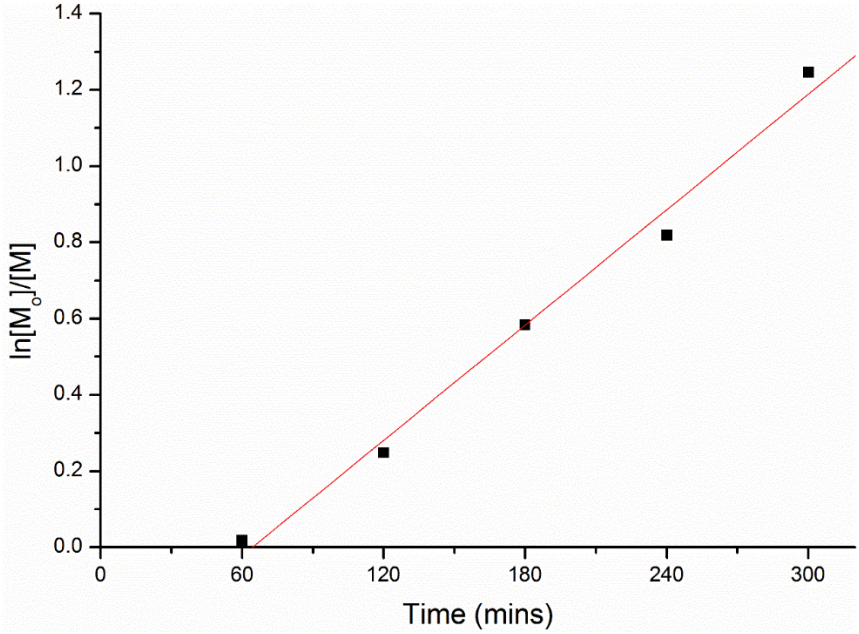

Figure 3.5: A plot to show the $\ln[M_o]/[M]$ over time during the ATRP reaction (M16).

Varying the reaction conditions and reagents has already been shown to alter the kinetics of a controlled polymerisation by affecting the K_{act}, K_{ATRP} and K_{deact}. Figure 3.6 shows the effect on the kinetic plot of altering the initiator, catalyst system and temperature of the reactions (M15-M18). The catalyst system was changed from CuBr to CuCl due to the higher bond dissociation energy of C-Cl than C-Br, with the aim of reducing the rate of propagation after the first initiation had occurred. The plot for M15 was not observed to be linear for the entire duration of the polymerisation –M_n was seen to increase rapidly up to around 15% conversion, before flattening out. This indicated that the reaction was not controlled, and that the concentration of radicals was not constant throughout the reaction.

The addition of $CuCl_2$ to further shift the equilibrium to the left by increasing the rate of deactivation[38] was seen to bring the kinetic plot closer to the predicted values. Changing the initiator back to EBIB from EBPA, reducing K_{act} of the system, also reduced the discrepancy between theoretical and experimental values, supported by the increasing I_{eff} values reported in Table3.2.

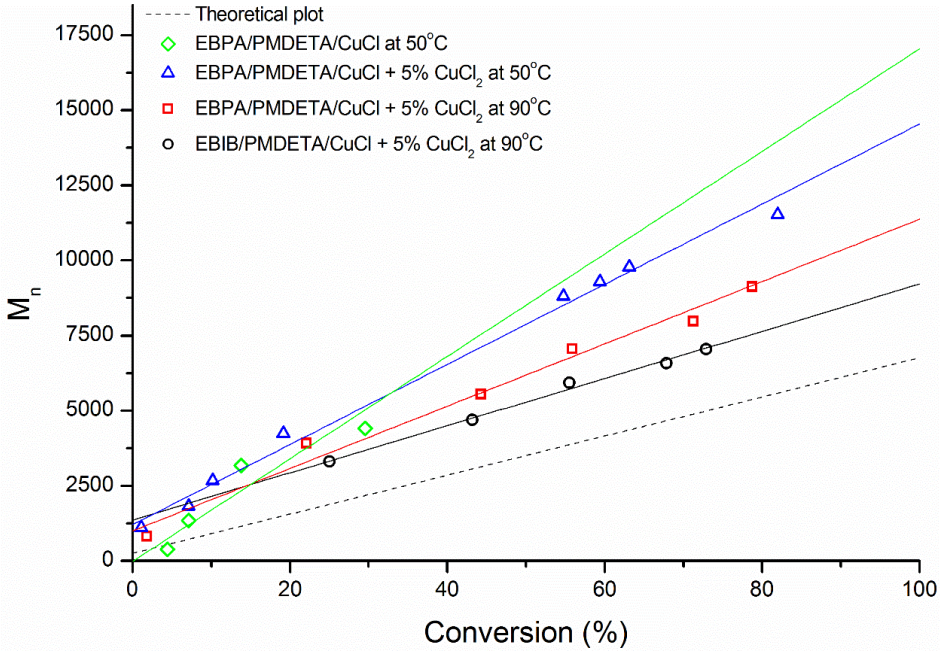

Figure 3.6: A plot to show the M_n against conversion for a number of different ATRP reactions (◊ is M15, Δ is M16, □ is M17, ○ is M18), showing how changing reaction conditions and components improves the initiator efficiency and reaction parameters, to bring them closer to the theoretical ideal M_n.

3.4.2.3 Investigation into Chain End Fidelity

Macroinitiators were synthesised and then tested for chain end fidelity by conducting chain extension reactions. PMMA-Br synthesised via ATRP was added as the initiator to a typical ATRP of methyl methacrylate, and any change in molecular weight and dispersity was followed by periodically removing samples from the reaction for both GPC and ^{1}H NMR. Figure 3.7 shows the GPC traces from one such chain extension reaction. Both the traces for 16 hours and 120 hours are seen to be bimodal, with the majority of the peak exhibiting a considerably larger M_w than that of the macroinitiator. The smaller shoulder to the left of the peak corresponds to the longer polymeric chains of the macroinitiator – these chains were not seen to form block copolymers, indicating that the C-X end group functionality may not have been present in these samples. This was likely due to bimolecular termination or elimination reactions, which was investigated by MALDI.

Removing these short, inactive chains from the sample after reaction completion was also problematic, as they typically precipitated out at the same time as the longer, extended chains. There has been a considerable amount of research into specifically choosing solvents to precipitate into, some of which can selectively cause heavier chains to precipitate out, whilst leaving the shortest chains solvated.[39, 40] Methanol is one such solvent, and was therefore chosen to separate the inactive PMMA chains from the block copolymer chains. To ensure the separation was as efficient as possible, a 'back precipitation' was also carried out. This method involved dissolving the polymer sample in tetrahydrofuran, stirring it on ice, and then adding the non-solvent dropwise, as opposed to adding the polymer dropwise to a predetermined volume of non-solvent. This 'back precipitation' meant that once the volume of methanol added reached a critical level, the longest polymer chains precipitated out. The polymer was then filtered and dried before being analysed by GPC. This resulted in a sample which was no longer bimodal, and had a considerably lower Đ than before this purification step.

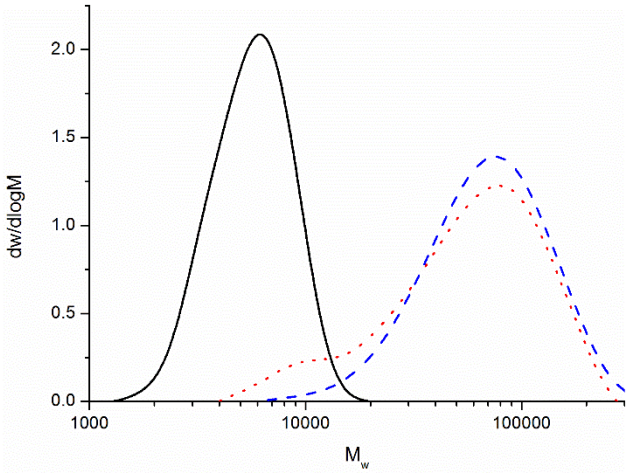

Figure 3.7: GPC trace to show the chain extension of M8: black = PMMA macroinitiator; red = chain extension after 120 hours; blue = after backwards precipitation.

This need to remove unreacted PMMA was not unexpected however. One of the most documented difficulties with synthesising macroinitiators via living radical polymerisation is the ability to retain end group fidelity. As previously mentioned, a number of studies have found that when conducting ATRP reactions, it was essential to stop the reaction at around 80% conversion in order to preserve the halide end-cap. This is in spite of the fact that the nature of this category of controlled polymerisation reactions suggests that the likelihood of bimolecular radical termination is dramatically reduced, due to the limited number of radicals present in the reaction system at any time.[18] It has been suggested that as the reaction nears completion, the number of monomer molecules available to react decreases to such an extent that the bimolecular termination reactions become more common, as well as other side reactions.[41] This was the reason that the targeted chain length became higher than the actual desired chain length – if the reaction was to be stopped at around 80% conversion, then the targeted molecular weight would need to be 25% higher than this point, in order to produce polymeric chains of the correct length.

Chain end fidelity of polymers synthesised via ATRP has been previously monitored by MALDI-TOF spectroscopy. Two segments of MALDI data for macroinitiator M21 synthesised via ATRP are shown in Figures 3.8 and 3.10. Figure 3.8 shows that two species were present in the PMMA sample, and that these species repeat every 100.12 g mol^{-1}, corresponding to the repeating unit of MMA. Due to the side reactions, radical transfer and termination reactions possible during an ATRP reaction, there are a number of possible end groups. Figure 3.10 shows a species at

around 1640, which corresponds with a chain of 15 MMA monomer units joined together with an EBIB initiator group present at one end and a final MMA unit which has undergone an elimination reaction, which resulted in a double bond forming and the loss of H-Br. This elimination has been commonly reported for polymers synthesised via ATRP. However, as elimination has typically been observed to occur from 40% conversion,[42] it is unlikely that this method of termination could be eradicated altogether. It would be expected that the other species would correspond to the same PMMA chain with an active –Br end cap. However, the other species is at 1625, whilst a –Br capped chain would fall at approximately 1719.

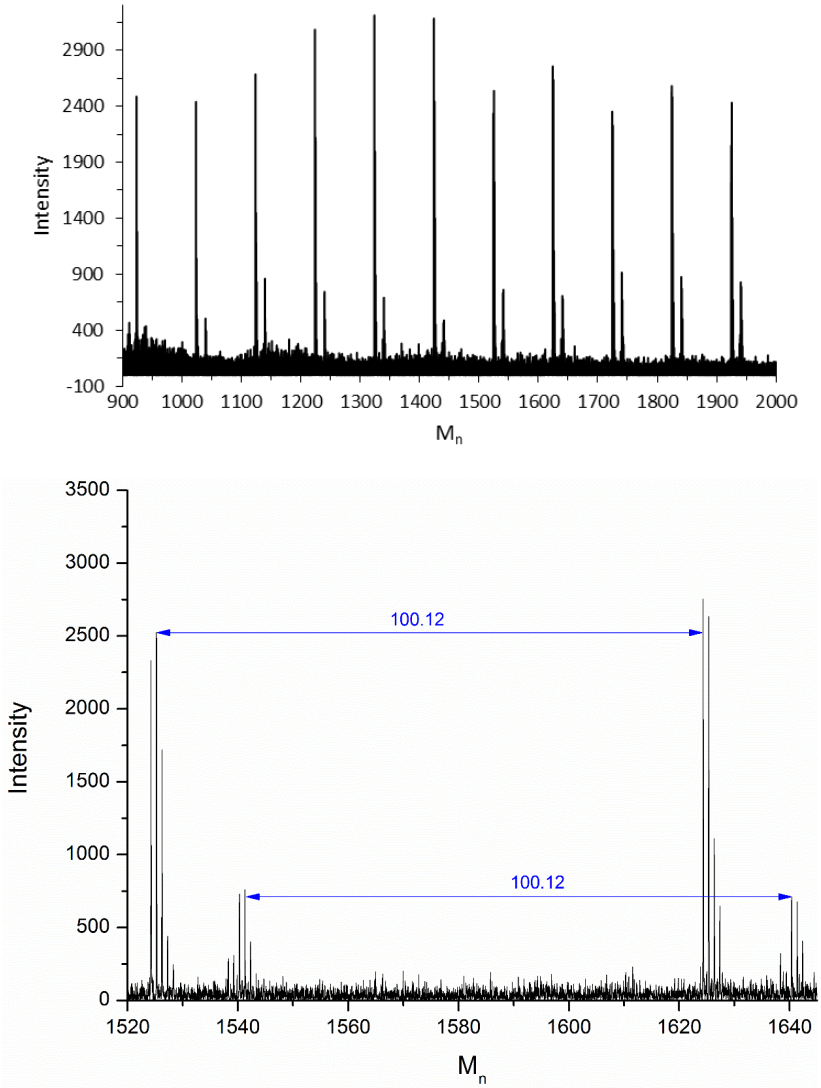

Figure 3.8: MALDI spectra of M21, showing: top – distribution of M_n over large molecular weight range; and bottom - two main species present in the sample, each with a repeating unit of 100.12, indicating they are related to the chain of PMMA.

One particular observation for PMMA samples was that they underwent a thermal decomposition at temperatures above 150ºC, resulting in the elimination of methyl bromide from one end of the chain which led to cyclisation and the formation of a lactone group (structure shown in Figure 3.9).[43] The predictions for a PMMA chain of 15 MMA units which has cyclised to form a lactone group, falls at 1626, which corresponds to the other species seen in Figure 3.10. The relative intensities of the two species in Figure 3.10 suggest that whilst some PMMA chains underwent elimination reactions (species at 1640), the majority of chains retained their active Br- end group.

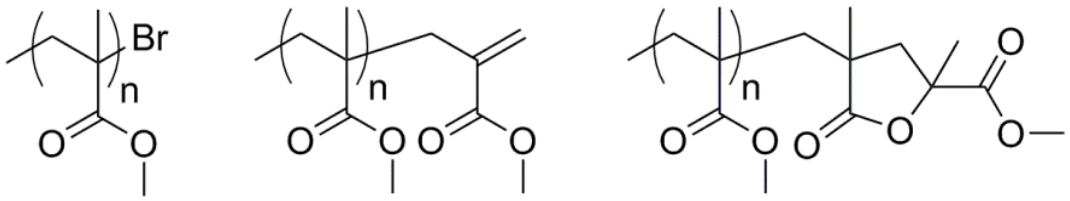

Figure 3.9: Structures of the possible end groups for PMMA synthesised by ATRP: active -Br end cap (left); double bond due to elimination (centre) and lactone cyclic group due to thermal decomposition (right). (Reproduced from reference [43]).

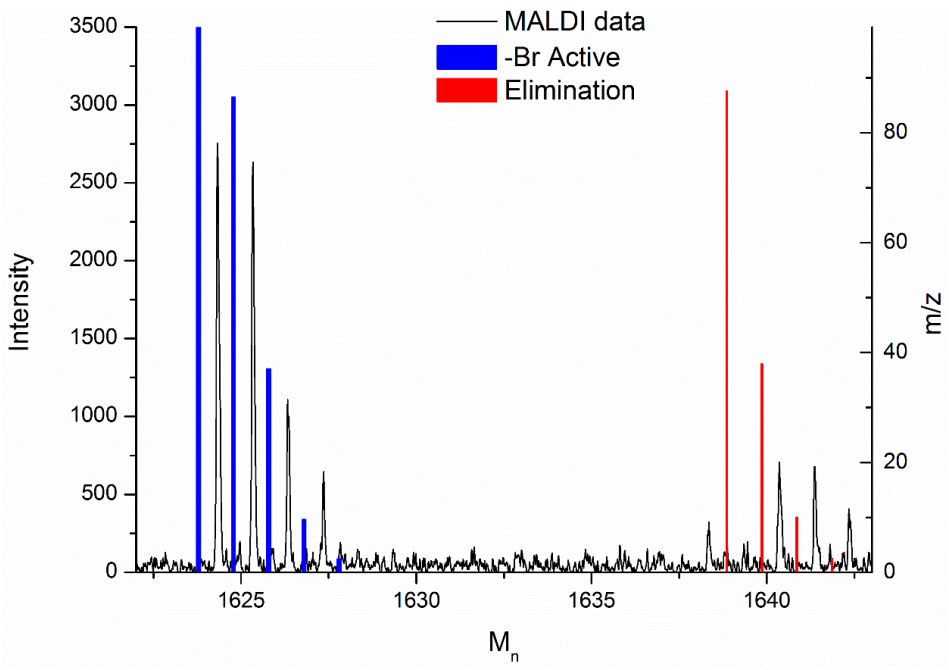

Figure 3.10: MALDI spectrum of M21, showing an expansion of the species in PMMA samples, together with predictions for a PMMA chain which did have an active Br end group that has been cyclised to form a lactone, and predictions for chains which have lost their active end group through an elimination reaction.

One of the main reasons that SET-LRP is often used in place of ATRP is that it has been shown to give near perfect chain-end fidelity due to a greater control over the equilibrium constants. Figure 3.11 shows the MALDI spectrum for PMMA synthesised using SET – it was immediately evident that three species were present. As with ATRP, one species corresponded to chains which lost their Br- during MALDI via cyclisation (shown in blue), and one species corresponded to chains which underwent elimination (shown in red). However, a third species was observed at around 1755. This species was seen to correlate to a chain of 15 MMA units with an EBIB initiator group at *both* ends, indicating bimolecular termination. This is a process which would not typically be expected during SET polymerisations of acrylates, which have been shown to have near perfect Br- activity.[44] However, there have been no examples in the literature demonstrating this level of control over methacrylates (unless fluorinated monomers or solvents are used[45]), which is in agreement with the data presented here.

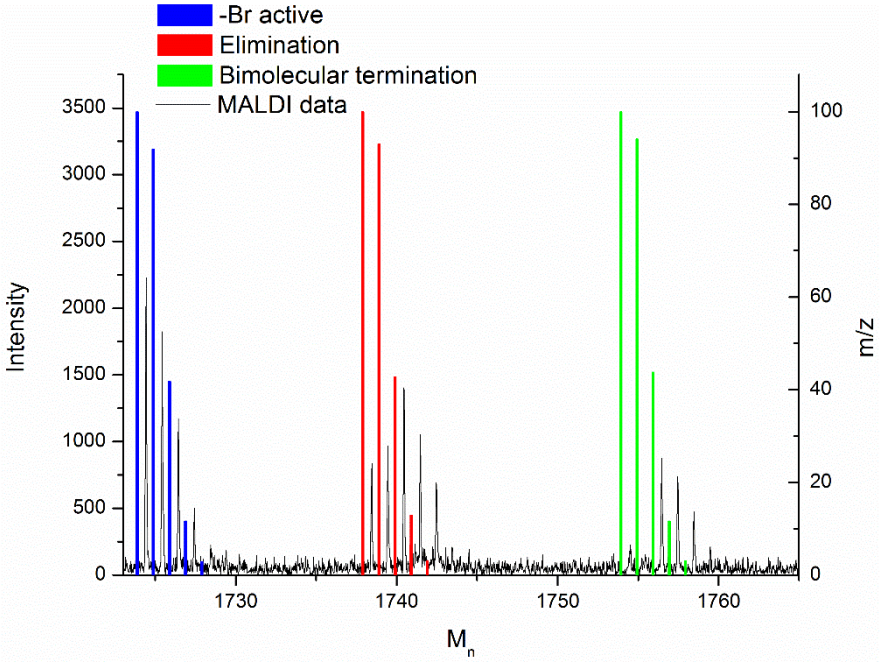

Figure 3.11: MALDI spectrum of M31, showing an expansion of the species of the PMMA samples, together with predictions for chains which were active but have been cyclised during MALDI, chains which have undergone elimination, and chains which have undergone bimolecular termination.

The MALDI data indicated that each synthesis of PMMA macroinitiators by SET-LRP resulted in three different polymeric species – those with active –Br end caps, those with double bonds at the end due to elimination, and those which had

undergone bimolecular termination. However, samples synthesised by conventional ATRP were observed to only possess two species – those with active Br- end caps and those which had undergone elimination. Although this was an unexpected result due to the added control typically exhibited by SET-LRP, it suggested that further optimisation of the SET method would be required in order to produce macroinitiators with the desired level of activity. For this reason, the optimised ATRP method was used for macroinitiator syntheses in the remainder of this work.

3.4.3 Synthesis of PMMA-b-PODA and PMMA-g-PODA

A number of block copolymers were synthesised by chain extension of PMMA-Br macroinitiators with a second monomer, octadecyl acrylate (Table 3.5). The majority of the block copolymers discussed in this section were synthesised using macroinitiator M8, although a large number of PMMA syntheses were conducted. This many reactions were necessary in order to optimise the method to synthesise macroinitiators of controlled molecular weights and narrow dispersities, but M8 was shown to be a suitable length with end group activity allowing for extension to block copolymers. For this reason, M8 was used in order to give preliminary results on block copolymer synthesis and their use as stabilisers, whilst the optimised method was used to produce the stabilisers which will be discussed in Chapters 4 and 5. Figure 3.12 shows the NMR spectrum for stabiliser S5, with the peaks corresponding to each block assigned – the peaks previously assigned to the initiator group can still be observed, but the CH_2 next to the ester is still visible at approximately 4.1 ppm, but the CH_3 signals at 1.3 and 1.4 fall underneath the large signal for the CH_2 protons in the ODA long alkyl chain.

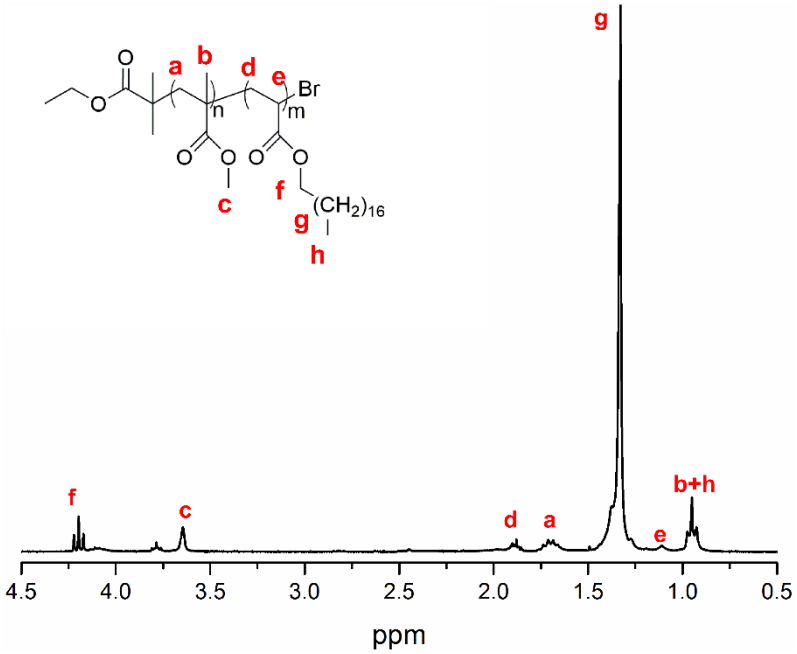

Figure 3.12: ^{1}H NMR spectrum of PMMA-*b*-PODA stabiliser S2 synthesised by ATRP with M8 as the initiator, showing peak assignments.

Figure 3.13 shows the GPC traces for the PMMA macroinitiator M8, and the PMMA-*b*-PODA block copolymer synthesised from it. It demonstrates that, after back precipitation, a monomodal sample was obtained without the presence of unreacted PMMA chains.

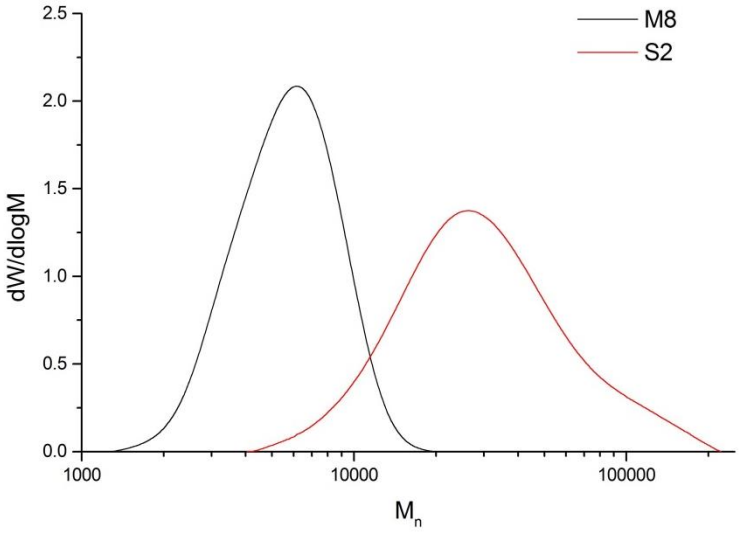

Figure 3.13: GPC traces showing the macroinitiator M8 (black) and the block copolymer S2 (red).

Table 3.5: Syntheses of PMMA-*b*-PODA stabilisers via chain extension of PMMA-Br macroinitiators.

Stabiliser	Macroinitiator	Macroinitiator (g)	Monomer (g)	Target DP of ODA	Target M_n	M_n	M_w/M_n
S1	M8	0.5	3.18	100	37550	33760	1.23
S2	M8	7	19.1	30	14840	23390	1.61
S3	M8	7	26.75	60	24570	31130	1.42
S4	M8	7	44.58	100	37550	54180	1.52
S5	M21	5	14.35	60	26180	12280	1.60

The synthesis of random copolymers is a one-step polymerisation which often results in a polymer with properties between those of the individual components. However, the control over polymerisation seen in ATRP does not always result in a truly random copolymer. This is due to a difference in reactivity ratio between the two monomers within the system. If there is a large difference in reactivity, the more reactive monomer is seen to polymerise first, causing the start of the chain to be richer in one monomer. During the middle of the polymerisation, as the concentration of the reactive monomer decreases, the chain is typically more random, and when all of this monomer has been reacted, the other end of the chain will be richer in the less reactive monomer. This is known as a gradient copolymer, which can be seen as an intermediate between block and random copolymers.

There has been no direct comparison in the literature between the reactivities of methyl methacrylate and octadecyl acrylate when used to synthesise a copolymer, although a number of studies have compared these monomers in relation to other common monomers. In a copolymerisation of ODA with methyl acrylate (MA), ODA was shown to be half as active as MA (with a reactivity ratio of 0.84 in comparison to 1.56 for MA)[46], while a copolymerisation of MA with MMA showed MA to be half as active as MMA.[47] It could potentially be inferred that MMA would be significantly more active than ODA. Consideration of diffusion rates also indicates this to be likely, as ODA is considerably more bulky than MMA, causing it

to move more slowly and be more sterically hindered. These predictions indicate that a copolymer of ODA and MMA synthesised by ATRP would in fact be a gradient copolymer rather than a random copolymer. For this reason, the copolymerisation of methyl methacrylate and octadecyl acrylate will result in a gradient copolymer (PMMA-*g*-PODA) rather than a copolymer (PMMA-*co*-PODA). Two gradient copolymers were synthesised via ATRP, with differing ratios of MMA to ODA. The exact ratios of the monomers were calculated from the NMR spectra obtained (Table 3.6).

Table 3.6: Gradient copolymers of MMA and ODA synthesised via ATRP.

Stabiliser	Mass MMA (g)	Mass ODA (g)	M_w/M_n	Đ	Intended molar ratio MMA:ODA	Observed molar ratio MMA:ODA
C1	4	16	83810	1.67	45:55	62:38
C2	8	16	59990	1.39	68:32	45:55

Full peak assignments for the random copolymer C2 can be seen on Figure 3.14 – due to a number of peaks overlapping, calculations for the ratio of MMA to ODA proved difficult. The most isolated peaks were the ester CH_3 in the MMA portion centred around 3.6 ppm, and the CH_3 at the end of the 18C chain of the ODA. The integrals of these peaks were then compared to give an overall ratio. It was observed that the ratios of MMA to ODA tended to lie much further towards a high concentration of MMA than the ratios initially added to the syntheses. It is possible that the reaction had not reached completion after 24 hours, as long chain acrylates are seen to react much slower than shorter chain monomers. This would mean that the copolymer had an MMA rich end, a random portion in the centre, and then a slightly shorter ODA rich end than would have been obtained had the reaction been allowed to continue. It is possible that the lower the concentration of the ODA block, the lower its stabilising ability.

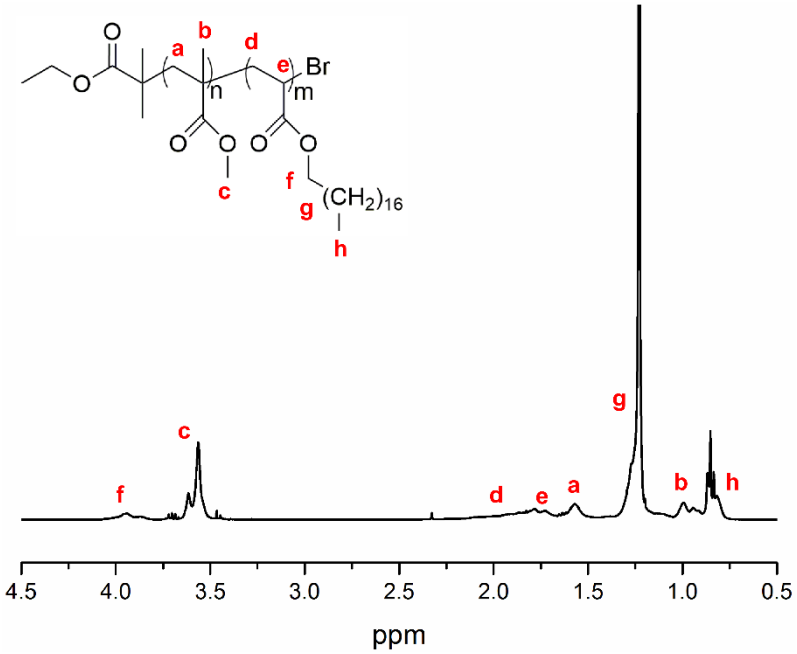

Figure 3.14: ^{1}H NMR spectrum of PMMA-co-PODA (C2) synthesised by ATRP, showing peak assignments.

3.4.5 Synthesis of Particle Dispersions

All particle dispersions were synthesised at Merck Chilworth with the assistance of Claire Topping, using an Asynt kit to allow for multiple syntheses in parallel. The protocol followed had been previously developed at Merck Chemicals,[48] and was optimised for dispersions stabilised by PHSA-*g*-PMMA. The original method was similar to that described in section 3.3.5, but with the PHSA-*g*-PMMA stabiliser used in place of the PMMA-*b*-PODA stabilisers presented in this work. The only other change to the method involved the stage in the process at which the mixture was heated. In the original method, the hydroxystearic acid based stabiliser was seen to be soluble in dodecane at room temperature, so all components were added together before heating. For the dispersions synthesised using the octadecyl acrylate based stabilisers, the reaction mixture was heated to temperature before the addition of the initiator. This was due to the observation that the PMMA-*b*-PODA and PMMA-*co*-PODA stabilisers were not soluble at room temperature. Had the reaction mixture not been heated before the addition of the initiator, the block copolymers would not have been in solution in order to act as stabilisers from the start of the dispersion reaction.

Table 3.7 shows the results of a number of particle dispersions synthesised using the stabilisers shown in Tables 3.5 and 3.6. The dispersions stabilised by PMMA-*b*-PODA stabilisers were seen to produce stable particle dispersions which were monodisperse, and this was still observed on the addition of small molar percentages of cross-linkers and dyes.

Table 3.7: Dispersions of PMMA particles synthesised using PMMA-*b*-PODA and PMMA-*g*-PODA stabilisers. DLS measurements could not be obtained for areas shaded grey due to samples being retained at Merck Chemicals for EPD analysis.

Dispersion	Stabiliser	Wt % monomer	Reactant	D_{SEM}	% SD_{SEM}	D_{DLS}	$Đ_{DLS}$
D1	S2	42	None	1073	37.84	1632	0.141
D2	C2	42	None	-	-	2470	33.8
D3	S4	42	None	673	9.36	1233	0.133
D4	S3	42	None	909	8.05	1838	0.135
D5	S5	42	None	1082	17.1	1325	0.259
D6	S3	39	None	341	9.97	604.6	0.03
D7	S3	47	None	1191	19.48	2629	0.236
D8	S3	42	1% EDGMA	511	17.22	738.8	0.008
D9	S3	42	5% EDGMA	-	-	-	-
D10	S3	42	5% Red	702	8.97	936.7	0.196
D11	S3	42	5% Magenta 1	779	8.86		

A difference was consistently observed between the particle diameters measured by SEM and DLS – the explanation for this is similar to the discrepancy between NMR and GPC discussed in 3.4.2. During the SEM sample preparation, particles are deposited onto a stub and before they are sputtered with gold, the chamber is evacuated, removing all solvent. This means that the particle sizes measured are the dry, discrete particles. However, the DLS measurements are for the particles whilst in dodecane solution – this means that the sizes are actually of the hydration sphere of the particles, resulting in larger particle diameters being recorded.

The method for deriving dispersity from DLS data should also be mentioned, as it is not as self-explanatory as the % standard deviation obtained via SEM analysis. The suppliers of the sizing equipment, Malvern, define dispersions with dispersities of less than 0.08 to be 'a near monodisperse distribution, those between 0.08 and 0.7 as 'mid-range values of Đ', and anything above 0.7 to be a 'very broad distribution of particle sizes'. It is, however, possible to convert Đ to standard deviation, as the formula for Đ is:

$$Đ = \left(\frac{\sigma}{d}\right)^2$$

where σ is the standard deviation, and d is the mean diameter of the particles.

3.4.5.1 Gradient vs Block Copolymers

The bulk of work into stabilisers for dispersion polymerisations focuses on the use of either block or graft copolymers, with very little work into random or gradient copolymers. For this reason, gradient copolymers were synthesised at ratios of MMA to ODA which were comparable with some of the block copolymers synthesised, and were then used in NAD polymerisations of MMA.

Figure 3.15 shows the SEM images of the dispersions synthesised using block (S2) and gradient (C2) copolymers containing 20 % MMA. The block copolymer was seen to produce particles which were relatively spherical, but with quite a high dispersity due to a number of very small particles within the dispersion. It should be noted that this particular stabiliser, D1, was added to the particle synthesis pre-solvated in tetrahydrofuran (THF) due to difficulties precipitating it within the time constraints of working in an industrial lab during a week visit. THF is known to be a very good solvent of most polymers, including PMMA, which could have resulted in the polydisperse nature of the particles, particularly as the large particles taken in isolation have a very low dispersity. The particles synthesised using the gradient copolymer exhibited rough surfaces and were less spherical than those stabilised by the block copolymer. There were very few particles which could be sized accurately as the majority of the particles formed small agglomerates rather than discrete particles. This was supported by DLS measurements, which gave particle sizes of

2470 nm, which could potentially be the result of measuring a mixture of polydisperse, discrete particles together with larger aggregates.

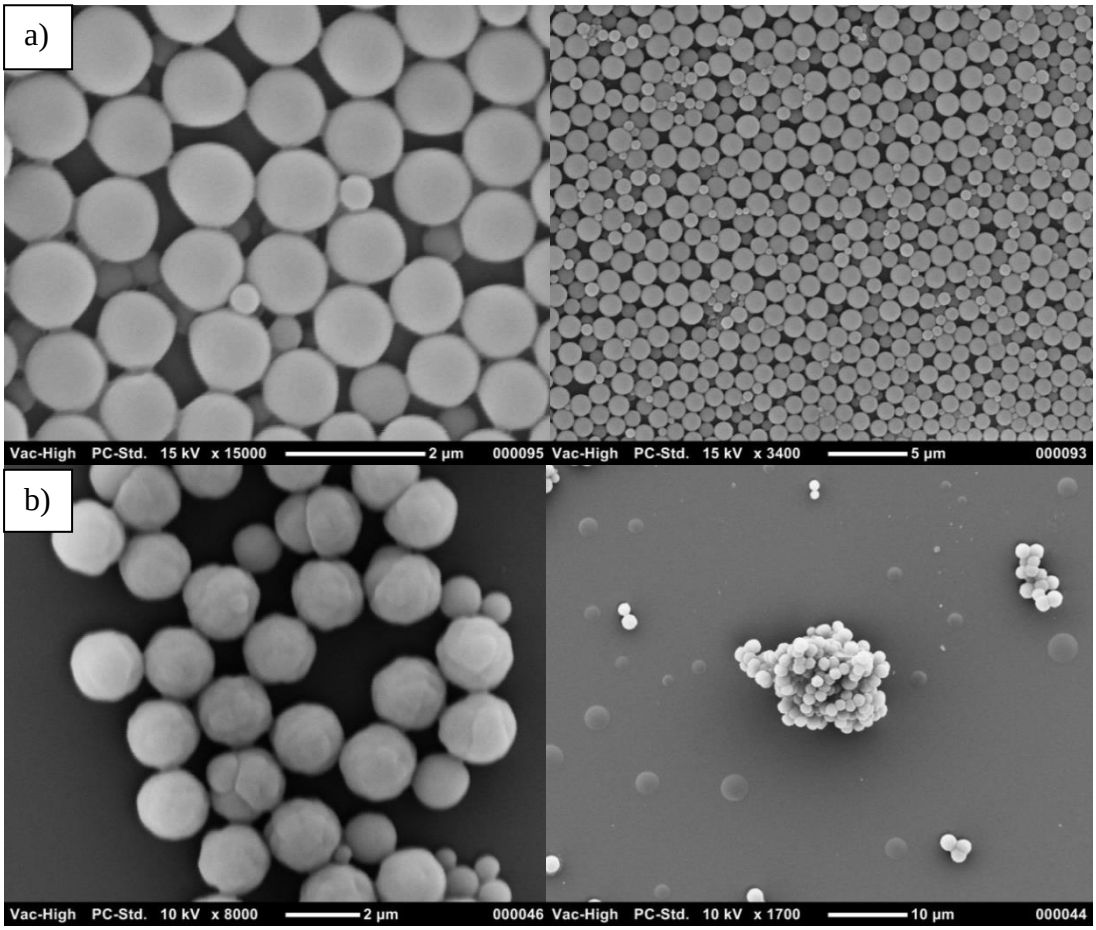

Figure 3.15: SEM images of PMMA particles; a) (top) D1 – using block copolymer; b) (bottom) D2 – using gradient copolymer; both with a molar ratio MMA:ODA ~ 20:80.

A possible explanation for the less desirable properties of particles stabilised by the gradient copolymer in comparison to the block copolymer is represented in Figure 3.16. The block copolymer has been designed with two defined regions – the lyophilic region which remains at the interface between the forming particle and the solvent, and the lyophobic region, which becomes entangled into the particle itself. The defined regions of the two behaviours allow for the monomer units to pass through the solvated lyophilic region into the particle to allow polymerisation to progress, whilst maintaining an effective barrier against longer oligomeric chains. However, the most likely arrangement of the gradient copolymers means that a greater proportion of the surface is obscured. This could hinder the ingress of monomer, resulting in smaller, uneven particles, as well as a higher dispersity.

Although the conformation of random and gradient copolymers was expected to make them less efficient as stabilisers, the results presented here were in contrast to observations made by previous work. Random copolymers were seen to successfully stabilise dispersions of PMMA particles, but this behaviour was attributed to a composition drift in the stabiliser, resulting in blocks of octadecyl acrylate units. This would allow the stabiliser to act in a similar manner to a conventional block copolymer.[32, 33]

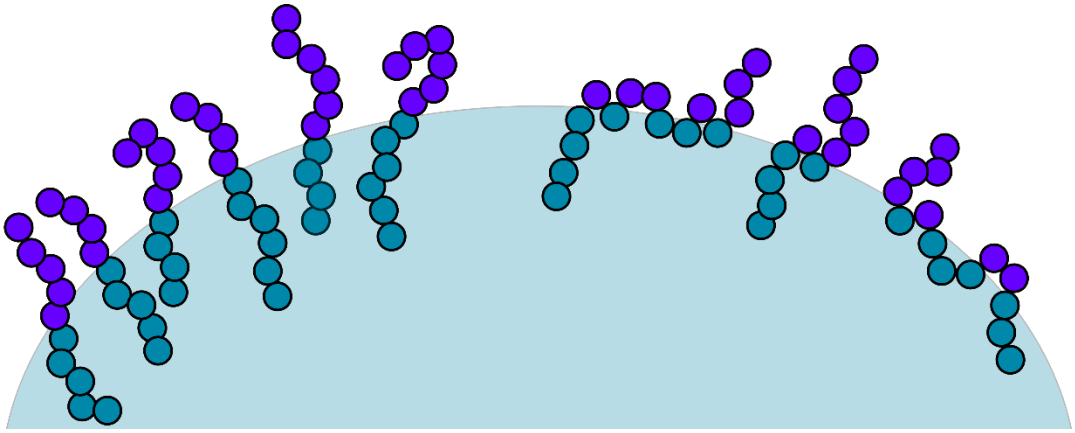

Figure 3.16: schematic showing the potential arrangements of stabiliser molecules at the particle/solvent interface, with block copolymers on the left and gradient copolymers on the right.

3.4.5.2 Ratio of PMMA to PODA

Block copolymers were synthesised at different molar ratios of MMA to ODA, which were then used in dispersions to investigate the effect on the size and the morphology of the particles. Figure 3.17 shows the SEM images obtained for these dispersions. Initially, an increase in the percentage of MMA in the block copolymer was seen to result in an increase in particle size - from 10 molar % to 20 molar % (with all other conditions remaining the same), particles increase from 670 nm to 1070 nm. It appeared that a maximum particle size was reached at around 1100 nm (shown in Figure 3.18). Increasing the concentration of MMA to 55 wt % did not result in any further increase in size. However, as no stabilisers were investigated which possessed between 20% and 55% MMA content, it was difficult to predict the size of particles between these two points, and the plot shown in Figure 3.18 could either indicate a plateau was reached at around 20% MMA, or that the point at 55%

MMA was on the downward slope of a curve which reached a maximum at some stage between these two points. Since we were interested in the synthesis of particles of 1 μm or less, no further research was conducted into the effect on particle size.

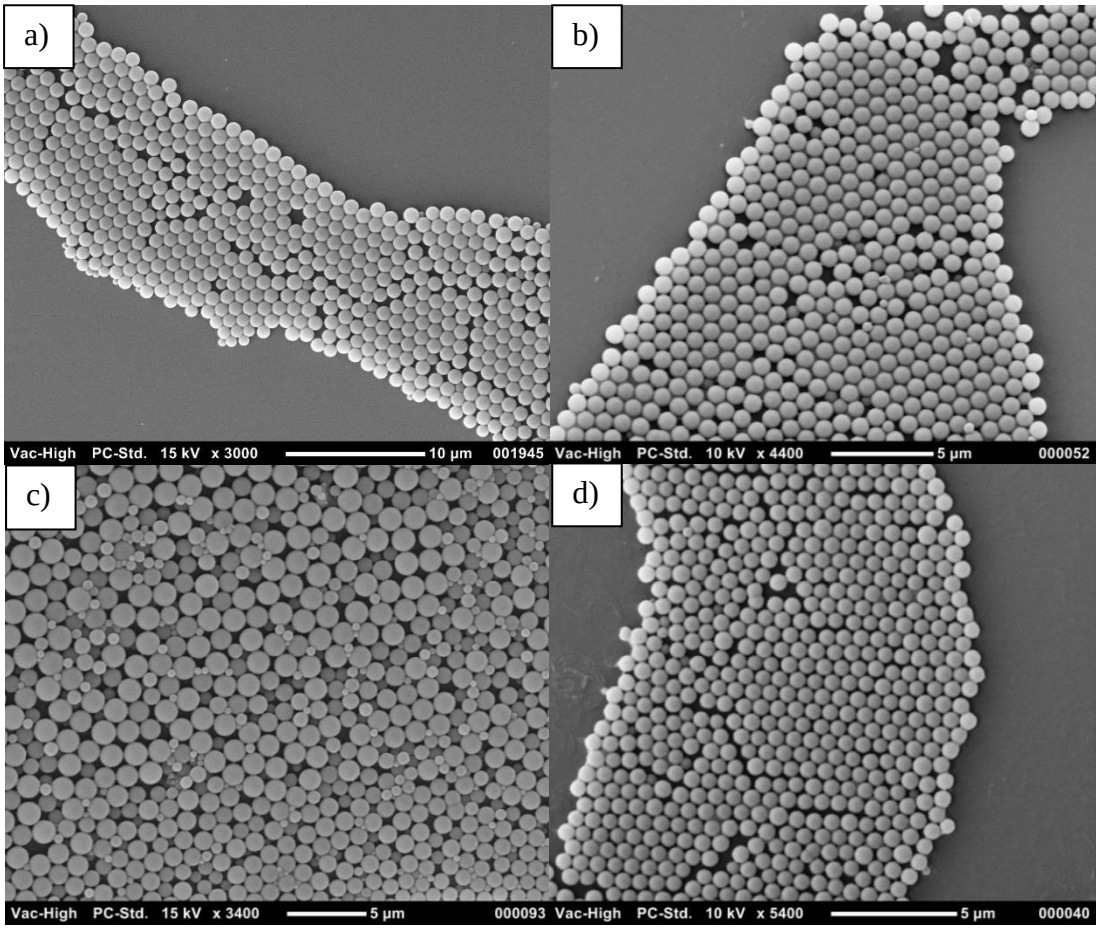

Figure 3.17: SEM images of dispersions with varying ratios of MMA to ODA; D3 with 10% MMA; D4 with 15% MMA; D1 with 20 % MMA; and D5 with 55% MMA.

There has not been much discussion in the literature regarding the ratio between the lyophilic and lyophobic blocks of stabilisers for dispersion polymerisations. However, there has been discussion as to the length of the lyophobic block and how this affected the stability of particles. It was shown that copolymers of styrene and butadiene led to agglomeration of particles at 8% of the lyophobic block even when this was greater than 10000 $gmol^{-1}$. In contrast, shortening this block to 8000 $gmol^{-1}$ still resulted in stable particles when the stabiliser contained 20% of the lyophobic component.[49] This was supported by work which indicated that higher molecular weight copolymers resulted in unstable systems regardless of composition,[50] and

studies reporting that only 15% anchor component was necessary for efficient stabilisation.[51]

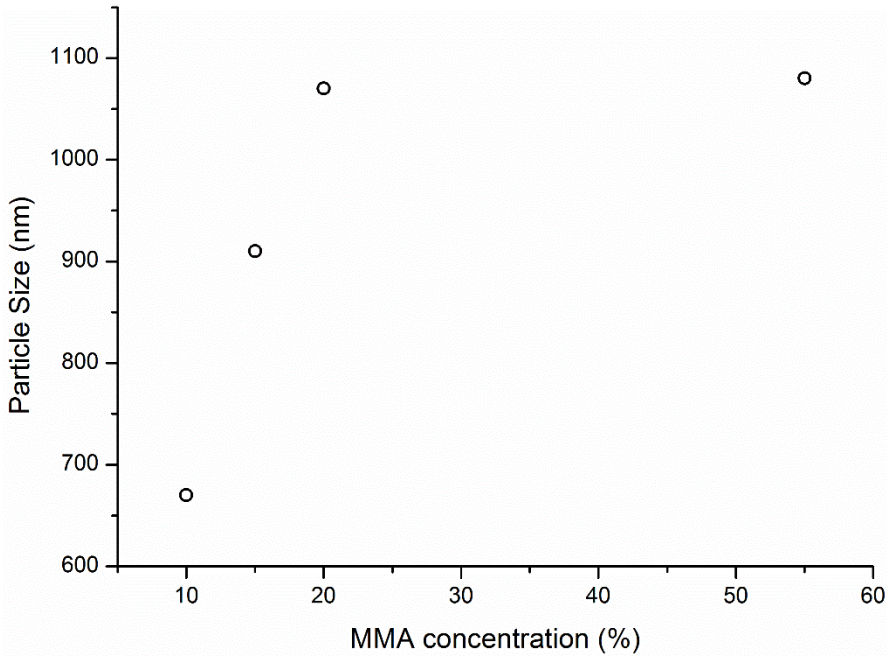

Figure 3.18: Changing particle size with relation to the concentration of MMA in the block copolymer stabiliser.

It should be noted that dispersity typically remained low (below 15 %) and consistent regardless of particle size, with the exception being the particles in D1, due to the aforementioned THF content of the reaction.

3.4.5.3 Amount of monomer:solvent

Numerous studies have reported that the amount of monomer added to a particle synthesis dictates the size of the resulting particles. Syntheses of polystyrene[52] and poly(methyl methacrylate)[21, 53] particles have shown that both the diameter and dispersity of particles increases with an increase in monomer concentration. This is in agreement with observations made in these syntheses – monomer concentration was systematically increased from 39 to 42 to 47 weight percent, and a steady increase in particle size was observed (Figure 3.19). Whilst the dispersion containing 47 % monomer did indeed show a substantially higher dispersity (19.5 %) than that of the dispersion with 39 % (10.0 %), no significant difference was

observed on increasing monomer concentration from 39 to 42 % - in fact, dispersity was marginally lower at 8.1 %.

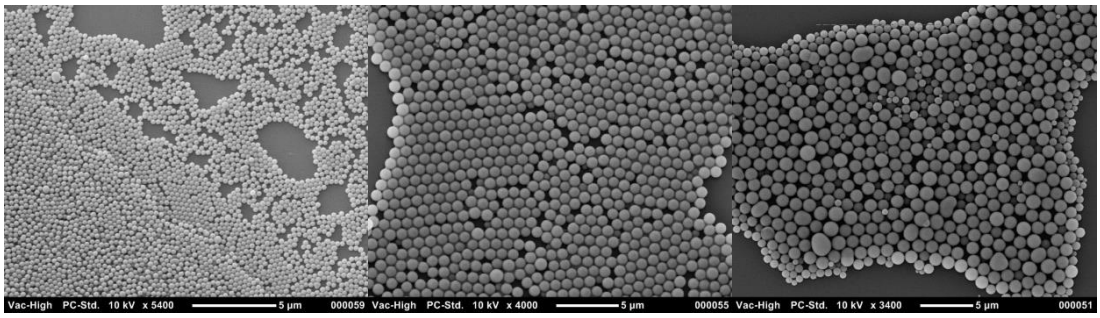

Figure 3.19: SEM images of dispersions synthesised using varying ratios of monomer to solvent; from left to right - D6 with 39 wt % monomer; D4 with 42 wt %; and D7 with 47 wt %.

A number of theories have been developed to suggest why dispersions become less stable above a certain percentage of monomer. Work looking at nanoparticles suspended in solution for drug delivery applications proposes an 'upper limit' of around 40 % solid content. It is suggested, in this work, that for particles to remain stable and dispersed, a defined volume must be excluded around each particle – above 40 % solid content, this volume becomes too large for the amount of solvent present in the system, leading to the agglomeration of particles.[54] This particularly holds true for these sterically stabilised particles, as they have polymeric chains projecting into the solvent medium which would have a tendency to become entangled with other particles in their proximity.

3.4.5.4 Addition of colour and cross linker

Many examples of cross-linked particles can be found in the literature,[55-58] with a number of sources reporting that the addition of the cross-linker, such as divinylbenzene or ethylene glycol dimethacrylate lead to a change in morphology. Typically, the more cross-linker incorporated, the greater the distortion of the particles, leading to a larger dispersion of sizes, as well as less ordered packing due to their non-spherical nature. Figure 3.20 shows the successful incorporation of EGDMA into the PMMA particles – the addition of 1 % increased the dispersity from 8 % to 17 %, but caused a decrease in particle size from 900 nm to 510 nm. However, increasing the amount of EGDMA to 5 % resulted in very few spherical

particles being synthesised – the majority of the reaction aggregated into one mass, and the few particles that were separate were very polydisperse. This suggests that there is an upper limit to the amount of cross-linker which can be incorporated into the dispersions before significant retardation is seen.

Whilst some work has suggested that very small amounts of cross-linker is sufficient to cause severe coagulation (only 0.6 wt %),[59, 60] other sources have successfully added much higher quantities into the dispersions without dramatically adverse effects.

A similar effect is expected on the addition of cross-linking dyes – the dye molecules are larger than the EGDMA, although they contain the same number of cross-linking functional groups. Figure 3.20 also shows SEM images for dispersions synthesised with 5 % red and magenta dyes.

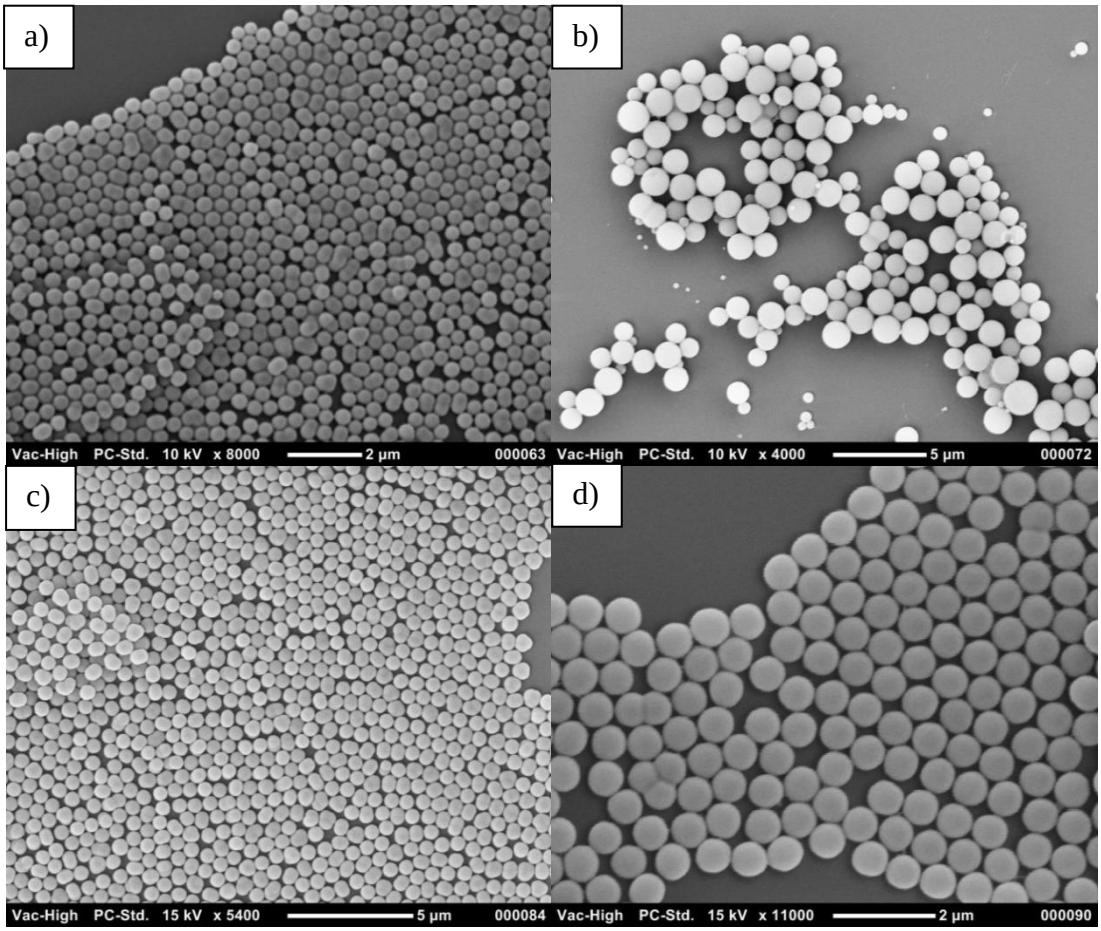

Figure 3.20: SEM images of dispersions incorporating EGDMA or cross-linking dyes; a) D8 with 1 % EGDMA; b) D9 with 5 % EGDMA; c) D10 with 5 % MM10; d) D11 with 5 % MR5.

Whilst it is clear that D11 resulted in monodisperse, spherical PMMA particles which exhibited some of the desired packing properties, this was not the case for the entire dispersion. Some areas were seen to contain large aggregates of particles – the individual particles can still be seen, and they have retained their spherical nature, but they appear to have fused together (Figure 3.21). DLS analysis could not be performed on this sample to confirm the presence of larger aggregates when in solution, as the sample was retained at Merck Chemicals for electrophoretic testing.

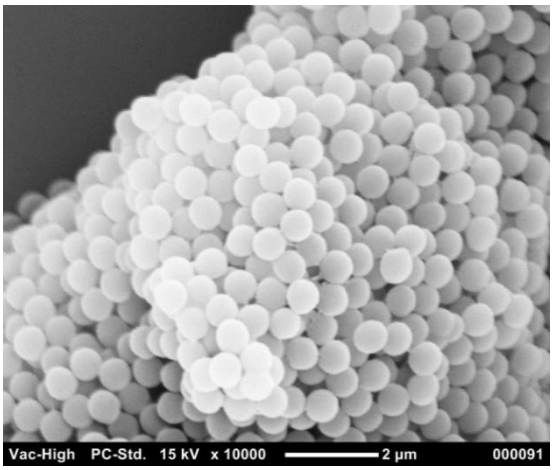

Figure 3.21: SEM images to show the agglomeration of dyed particles in dispersion D11.

3.4.5.5 Other properties of dispersions

It was observed that the smaller particles (particularly those synthesised at 39 wt % monomer) and the aforementioned red particles synthesised with MR5 were less inclined to redisperse into the dodecane after a period of settling, and seemed to agglomerate. This is consistent with theories that suggest that smaller particles, or those which are more highly cross-linked, are more inherently unstable and therefore more likely to aggregate.[61] Some of the dispersions were allowed to stand for a period of time, and were then imaged using SEM for a second time. Whilst the particle size and dispersity were seen to remain relatively consistent, suggesting no reaction is occurring during the aggregation, the packing behaviour of the particles has become less desirable, with particles exhibiting 'clumping' rather than layering (Figure 3.22). Although the aggregation observed could potentially be an artefact of the SEM preparation, the samples were thoroughly redispersed before SEM analysis.

This, together with later observations of interactions between the particles, supported the conclusion that the observed aggregation did arise from particle interactions rather than some other process.

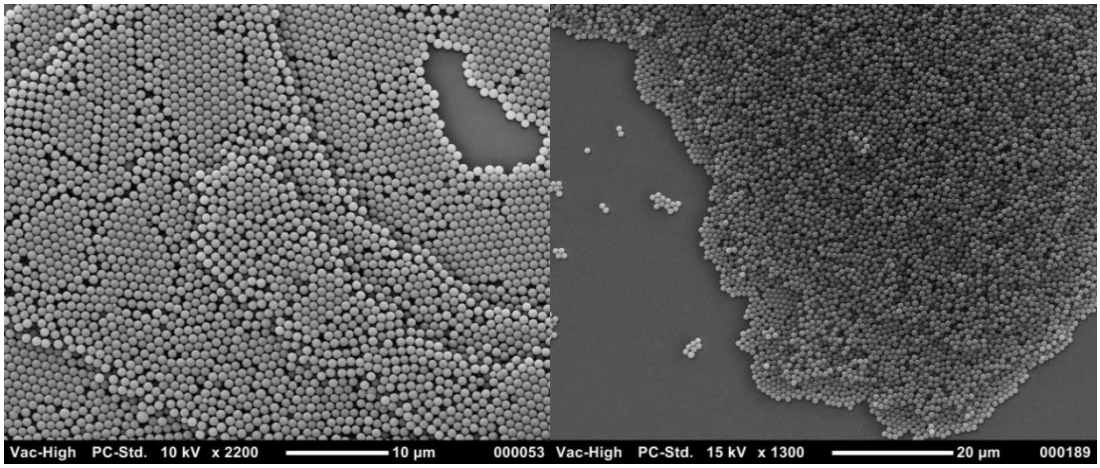

Figure 3.22: SEM images of dispersion D5 before (left) and after (right) a period of standing. The layering and order seen on the left is less defined on the right, with more areas of aggregation visible.

This was then further compounded by the discovery that if the dispersions were left standing overnight, they became completely solid. It was noticed that on heating, the dispersions became fluid again, suggesting that the particles were somehow gelating or crystallising the dodecane. It was decided that a number of tests would be undertaken to investigate this transition further, which will be discussed in Chapters 4 and 5.

3.5 Conclusions

Macroinitiators and subsequently block copolymers were successfully synthesised via ATRP, using conventional Cu(I) catalyst systems, and then Cu(0) systems. These stabilisers were then used in the synthesis of PMMA particle dispersions in dodecane, which were suitable for use as electrophoretic fluids.

Whilst end-group fidelity proved difficult to maintain when synthesising PMMA-Br macroinitiators via ATRP (confirmed by GPC from chain extensions and MALDI-TOF), controlled polymerisations using SET-LRP proved rather complex to achieve. This is supported by previous research, suggesting that whilst SET is a facile method for the controlled polymerisations of acrylates, it is not as successful for the

polymerisation of methacrylates. ATRP using zerovalent copper proved to be a suitable 'middle ground', maintaining more bromide functionality than conventional ATRP, while retaining a lower dispersity and initiator efficiency than SET-LRP. It was then relatively facile to purify the macroinitiators and use them to synthesise block copolymers of various lengths.

It was demonstrated that the stabilisers were highly effective when used in the NAD polymerisation of methyl methacrylate – the resulting particles were monodisperse, spherical and exhibited good packing capabilities (typically hexagonal closed packing). Size control was obtained by varying the monomer to solvent molar ratio, and this control will be investigated further by varying the stabiliser to monomer ratio in later NAD polymerisations. It was also shown that cross-linker and polymerisable dyes could be added to the synthesis without dramatically retarding the shape of the particles or increasing dispersity.

The presence of a thermoresponsive gelation process observed in the polymeric dispersions led to an investigation into the nature of the thermal transition, together with developing potential synthetic routes to prevent this occurring in future dispersions.

3.5 References

1. Resin and resin forming compound, *US2980483 A*, H. Rowland, 1934.
2. Electrical coil insulated with thermoplastic particles and thermoset polymer, *US2464568 A*, E. J. Flynn and F. J. Lasak, 1949.
3. Optical lens system, *US2440088 A*, D. S. Grey, 1948.
4. Surgical material, *US4588583 A*, H. Pietsch, V. Hohmann and D. Kluck, 1986.
5. L. Antl, J. W. Goodwin, R. D. Hill, R. H. Ottewill, S. M. Owens, S. Papworth and J. A. Waters, *Colloids and Surfaces*, 1986, **17**, 67-78.
6. S. J. Barsted, L. J. Nowakowska, I. Wagstaff and D. J. Walbridge, *Transactions of the Faraday Society*, 1971, **67**, 3598-3603.

7. G. Bosma, C. Pathmamanoharan, E. H. A. de Hoog, W. K. Kegel, A. van Blaaderen and H. N. W. Lekkerkerker, *Journal of Colloid and Interface Science*, 2002, **245**, 292-300.

8. J. V. Dawkins and G. Taylor, *Polymer*, 1979, **20**, 599-604.

9. R. P. A. Dullens, E. M. Claesson and W. K. Kegel, *Langmuir*, 2004, **20**, 658-664.

10. S. M. Klein, V. N. Manoharan, D. J. Pine and F. F. Lange, *Colloid Polym. Sci.*, 2003, **282**, 7-13.

11. M. E. Karaman, L. Meagher and R. M. Pashley, *Langmuir*, 1993, **9**, 1220-1227.

12. A. F. Shepard, A. L. Henne and T. Midgley, *Journal of the American Chemical Society*, 1931, **53**, 1948-1958.

13. C. Wohlfarth, in *Refractive Indices of Pure Liquids and Binary Liquid Mixtures (Supplement to III/38)*, ed. M. D. Lechner, Springer Berlin Heidelberg, 2008, vol. 47, pp. 528-530.

14. N. Sultanova, S. Kasarova and I. Nikolov, *Acta Phys. Pol., A*, 2009, **116**, 585-587.

15. S. Perrier, P. Takolpuckdee and C. A. Mars, *Macromolecules*, 2005, **38**, 2033-2036.

16. H. Willcock and R. K. O'Reilly, *Polymer Chemistry*, 2010, **1**, 149-157.

17. J. Krstina, G. Moad, E. Rizzardo, C. L. Winzor, C. T. Berge and M. Fryd, *Macromolecules*, 1995, **28**, 5381-5385.

18. J. S. Wang and K. Matyjaszewski, *Journal of the American Chemical Society*, 1995, **117**, 5614-5615.

19. B. D. Hornby, A. G. West, J. C. Tom, C. Waterson, S. Harrisson and S. Perrier, *Macromolecular Rapid Communications*, 2010, **31**, 1276-1280.

20. H. Hu and R. G. Larson, *Langmuir*, 2004, **20**, 7436-7443.

21. W. P. Hems, T. M. Yong, J. L. M. van Nunen, A. I. Cooper, A. B. Holmes and D. A. Griffin, *Journal of Materials Chemistry*, 1999, **9**, 1403-1407.

22. D. M. Haddleton, A. J. Clark, M. C. Crossman, D. J. Duncalf, A. M. Heming, S. R. Morsley and A. J. Shooter, *Chemical Communications*, 1997, 1173-1174.

23. D. M. Haddleton, M. C. Crossman, B. H. Dana, D. J. Duncalf, A. M. Heming, D. Kukulj and A. J. Shooter, *Macromolecules*, 1999, **32**, 2110-2119.

24. D. M. Haddleton, J. Lad and S. Harrisson, *Abstracts of Papers of the American Chemical Society*, 2002, **224**, 039-POLY.

25. A. T. Jackson, A. Bunn, I. M. Priestnall, C. D. Borman and D. J. Irvine, *Polymer*, 2006, **47**, 1044-1054.

26. Y. Kwak, Y. Yamamura and K. Matyjaszewski, *Macromolecular Chemistry and Physics*, **211**, 493-500.

27. E. F. Jordan, Jr., *J. Polym. Sci., Part A-1*, 1972, **10**, 3347-3366.

28. K. L. Beers and K. Matyjaszewski, *J. Macromol. Sci., Pure Appl. Chem.*, 2001, **A38**, 731-739.

29. F. Dutertre, P.-Y. Pennarun, O. Colombani and E. Nicol, *European Polymer Journal*, 2011, **47**, 343-351.

30. G. Moad, K. Dean, L. Edmond, N. Kukaleva, G. Li, R. T. A. Mayadunne, R. Pfaendner, A. Schneider, G. Simon and H. Wermter, *Macromolecular Symposia*, 2006, **233**, 170-179.

31. W. Jakubowski, J. F. Lutz, S. Slomkowski and K. Matyjaszewski, *Journal of Polymer Science Part A: Polymer Chemistry*, 2005, **43**, 1498-1510.

32. H. V. Harris and S. J. Holder, *Polymer*, 2006, **47**, 5701-5706.

33. H. V. Penfold, S. J. Holder and B. E. McKenzie, *Polymer*, 2010, **51**, 1904-1913.

34. P.-E. Millard, N. C. Mougin, A. Böker and A. H. Müller, 2008.

35. W. Tang, Y. Kwak, W. Braunecker, N. V. Tsarevsky, M. L. Coote and K. Matyjaszewski, *Journal of the American Chemical Society*, 2008, **130**, 10702-10713.

36. W. Tang and K. Matyjaszewski, *Macromolecules*, 2007, **40**, 1858-1863.

37. K. Ibrahim, B. Löfgren and J. Seppälä, *European polymer journal*, 2003, **39**, 939-944.

38. K. Matyjaszewski, A. K. Nanda and W. Tang, *Macromolecules*, 2005, **38**, 2015-2018.

39. C. A. Barson, J. C. Bevington and B. J. Hunt, *European Polymer Journal*, 1996, **32**, 1055-1059.

40. J. C. Bevington, B. J. Hunt and C. A. Barson, *European Polymer Journal*, 1998, **34**, 1387-1389.

41. J.-F. Lutz and K. Matyjaszewski, *Macromolecular Chemistry and Physics*, 2002, **203**, 1385-1395.

42. J. F. Lutz and K. Matyjaszewski, *Journal of Polymer Science Part A: Polymer Chemistry*, 2005, **43**, 897-910.

43. C. D. Borman, A. T. Jackson, A. Bunn, A. L. Cutter and D. J. Irvine, *Polymer*, 2000, **41**, 6015-6020.

44. F. Nyström, A. H. Soeriyadi, C. Boyer, P. B. Zetterlund and M. R. Whittaker, *Journal of Polymer Science Part A: Polymer Chemistry*, 2011, **49**, 5313-5321.

45. S. R. Samanta, A. Anastasaki, C. Waldron, D. M. Haddleton and V. Percec, *Polym. Chem.*, 2013, **4**, 5563-5569.

46. H. W. S. Hsieh, B. Post and H. Morawetz, *Journal of Polymer Science: Polymer Physics Edition*, 1976, **14**, 1241-1255.

47. J. C. Bevington and D. O. Harris, *Journal of Polymer Science Part B: Polymer Letters*, 1967, **5**, 799-802.

48. Particles for Electrophoretic Displays, L. D. Farrand, C. Topping and A. Lawrence, US20140320951, 2012.

49. I. Tausendfreund, F. Bandermann, H. W. Siesler and M. Kleimann, *Polymer*, 2002, **43**, 7085-7091.

50. C. L. Winzor, Z. Mrazek, M. A. Winnik, M. D. Croucher and G. Riess, *Eur. Polym. J.*, 1994, **30**, 121-128.

51. F. L. Baines, S. Dionisio, N. C. Billingham and S. P. Armes, *Macromolecules*, 1996, **29**, 3096-3102.

52. K. P. Lok and C. K. Ober, *Canadian journal of chemistry*, 1985, **63**, 209-216.

53. A. P. Richez, L. Farrand, M. Goulding, J. H. Wilson, S. Lawson, S. R. Biggs and O. J. Cayre, *Langmuir*, 2014.

54. M. M. de Villiers, P. Aramwit and G. S. Kwon, *Nanotechnology in Drug Delivery*, Springer, 2008.

55. H. T. Zhang, H. Huang, R. Lv and M. Chen, *Colloid Surf. A-Physicochem. Eng. Asp.*, 2005, **253**, 217-221.

56. J. S. Song and M. A. Winnik, *Macromolecules*, 2005, **38**, 8300-8307.

57. J. Shin, W. Bae and H. Kim, *Colloid Polym. Sci.*, 2010, **288**, 271-282.

58. K. C. Lee and S. Y. Lee, *Macromolecular Research*, 2007, **15**, 244-255.

59. S. Shen, E. Sudol and M. El-Aasser, *Journal of Polymer Science Part A: Polymer Chemistry*, 1993, **31**, 1393-1402.

60. C. M. Tseng, Y. Y. Lu, M. S. El-Aasser and J. W. Vanderhoff, *Journal of Polymer Science Part A: Polymer Chemistry*, 1986, **24**, 2995-3007.

61. W. X. Wang, R. M. T. Griffiths, A. Naylor, M. R. Giles, D. J. Irvine and S. M. Howdle, *Polymer*, 2002, **43**, 6653-6659.

Chapter 4: Synthesis of Functionalised Copolymers and Particle Dispersions

4.1 Introduction

4.1.1 Comonomers Which Disrupt Side Chain Crystallisation

The crystallisation observed in polymers with long alkyl side chains, and the subsequent gelation of solvents which can occur, has been demonstrated to be due to the ordered arrangement of the long alkyl chains.[1, 2] As discussed in Chapter 3, this process was undesirable in this work, and therefore it was necessary to explore ways in which to disrupt the crystallisation process.

Homopolymers of octadecyl acrylate and octadecyl methacrylate were shown to exhibit side chain crystallisation, which was analysed by X-ray diffraction. It was observed that when ODA was copolymerised with methyl acrylate (MA), the molar percentage of the crystalline component dictated the behaviour. Copolymers containing 30 and 60 molar % MA still exhibited crystallisation, but increasing the MA content to 80 molar % prevented the crystallisation from occurring.[3] However, the choice of comonomer has been shown to be crucial, as work looking at alternating copolymers of butadiene and long alkyl methacrylates (described as 'widely-spaced comb-like polymers') contradicted this study. It was demonstrated that even with the butadiene monomer units increasing the spacing between the long alkyl chains, crystallisation was observed, and in some cases more CH_2 units were actually involved in the crystallisation than for the homopolymers. This was attributed to the extra flexibility afforded to the long chains, allowing them to move towards each other and crystallise.[4] This flexibility can, however, be restricted by substituting groups onto the main backbone of the polymer chain, increasing the rigidity of the backbone. Comonomers such as methylstyrene and methacrylates were seen to reduce the crystallinity more dramatically than units such as styrene or acrylates, which do not possess the substituent groups.[5]

From this research, it was evident that in order to disrupt crystallisation, a comonomer must be selected which disrupted the order of the side chains, without providing them with space in which they could arrange themselves. The addition of groups onto the polymeric backbone through the addition of comonomer would also be advantageous.

4.1.2 Fluorinated Block Copolymers and Stabilisers

One type of specialised stabiliser for dispersion polymerisation is one which contains fluorinated groups in its polymeric structure. The synthesis of fluorinated block copolymers by ATRP has been discussed in the literature. A PMMA-*b*-P3FM (where 3FM was 2,2,2-trifluoroethyl methacrylate) block copolymer was synthesised using a PMMA macroinitiator, under typical ATRP conditions (toluene as a solvent, Cu(I)Br as a catalyst and PPMI as a ligand. This resulted in a controlled polymerisation with a product which had low dispersity (below 1.05), but macroinitiator was seen to remain after the reaction was finished, with an end group activity of 45% reported for the macroinitiator. For this reason, sequential monomer addition was conducted, whereby 3FM monomer was added to the polymerisation of MMA after relatively high conversions of the first monomer had been obtained. This gave product copolymers with higher dispersities (around 1.2), but no unreacted PMMA was observed.[6] It was also shown that fluorinated block copolymers could be synthesised by using a fluorinated macroinitiator, rather than adding fluorinated monomers to a standard polymeric initiator.[7, 8]

Semi-fluorinated polymer brushes (block copolymers of methyl acrylate and pentafluoropropyl acrylate) were grafted onto silica surfaces, using trifluorotoluene as a solvent. These brushes were seen to rearrange on treatment with different solvents (ethyl acetate and trifluorotoluene).[9] This arrangement of fluorinated brushes over a surface reflects the arrangement of block copolymers when used to stabilise particle dispersions – this has also been demonstrated for fluorinated block copolymers.

Of particular relevance to this work was work into colloidal dispersions of PMMA particles stabilised by fluorinated block copolymers (PMMA-*b*-PFMA). Dispersion polymerisations were carried out in supercritical carbon dioxide, and gave discrete particles, the size of which could be controlled by varying the molar concentration of monomer in the system.[10] Similar results were also demonstrated for the dispersion polymerisation of styrene stabilised by PS-*b*-PFOA.[11]

4.1.3 Functional ATRP Initiators

As the field of living radical polymerisation developed, and interest in ATRP increased, a number of functional ATRP initiators became commercially available.[12] Figure 4.1 demonstrates a number of the initiators which can now be purchased.

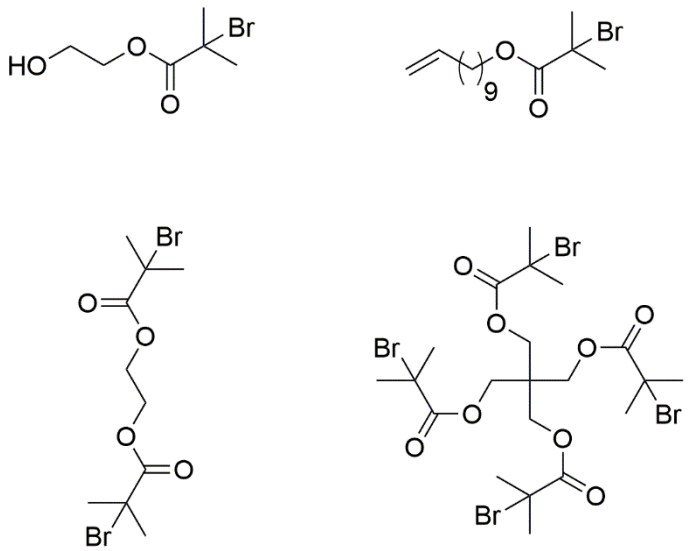

Figure 4.1: Structures of commercially available functional initiators for ATRP: hydroxy-functionalised (top left); allyl functionalised (top right); difunctional (bottom left) and tetrafunctional, to synthesis star polymers (bottom right). (Reproduced from reference [12]).

However, prior to this, numerous functional initiators were synthesised and reported in literature.[13] The hydroxy-functionalised initiator shown in Figure 4.1 has been documented in a number of different variations.[14, 15] Simple allyl halides such as allyl bromide and allyl chloride were also demonstrated to be effective initiators for the ATRP of styrene.[16] The use of this type of initiator added a polymerisable group to the end of a polymeric chain, although the reaction conditions required

optimisation to ensure that the allyl group did not react during the polymerisation. Fluorinated initiators were synthesised by the functionalization of dimethylamino chalcones which have been shown to be fluorescent compounds. After this step, the novel initiators were successfully used in the ATRP of styrene.[17] More unusual initiator structures have also been designed, such as by the modification of amino acids to incorporate conventional ATRP initiating groups, giving peptide macroinitiators. These were then used in the synthesis of biohybrid materials, with the potential to be used as drug delivery systems or in tissue engineering.[18]

Telechelic polymers, or polymers which possess a functional group at each end have also been reported. For example, a functional initiator was used to synthesise a block copolymer (PMMA-*b*-PBA) with a hydroxy group at one end and a bromo end group at the active chain end. This halide end could then be further reacted with 5-amino-1-pentanol to give a hydroxy group at both ends of the polymeric chain.[19]

The addition of these functionalities to the stabilisers, either through the use of comonomers or functional initiators, could potentially affect the stabilising behaviour of the copolymers. This would in turn affect the properties of the colloidal particles stabilised by them. This means that adjustments to the parameters of dispersion polymerisations might be necessary in order to retain the desired particle characteristics for the end application.

4.2 Aims and Objectives

The aim of the work outlined in this chapter was to develop functional stabilisers for use in NAD polymerisations, as well as particle dispersions containing dyes and cross-linking moieties.

The first challenge was to develop stabilisers which alleviated the thermoresponsive gelation observed when using PMMA-*b*-PODA copolymers, whilst maintaining the other desirable properties of the resulting dispersions. Comonomers were added in various weight percentages to the lyophilic block of the stabiliser, and these copolymers were then used in the NAD polymerisations. The effect of the changing

concentration of comonomer on any gelation observed was investigated using DLS, DSC and rheology.

The potential to add functional groups to the copolymer, and then into the polymeric dispersions was also investigated. An initiator with a hydroxy- functionality was synthesised, which was then used in ATRP to synthesise various block copolymers. This hydroxy- group was then substituted for a fluorescent moiety, and a polymerisable group. This new polymerisable stabiliser was then used in NAD polymerisations of MMA.

Another specialised copolymer stabiliser, with a PMMA lyophobic block and a fluorinated lyophilic block, was also synthesised with the aim of synthesising particle dispersions in fluorinated solvents.

4.3 Experimental

4.3.1 Materials

2-bromo-2-methylpropionyl bromide (Aldrich, 98%), ethylene glycol anhydrous (Aldrich, 99.8%), methacryloyl chloride (Aldrich, 97%), triethylamine (Aldrich, 99%), pyrene butyric acid (Acros, 97%), thionyl chloride (Acros, 99.5%), copper (I) bromide (Aldrich, 98%), copper (I) chloride (Aldrich, 97%), copper (II) chloride (Aldrich, 97%), N,N,N',N'',N''-pentamethyldiethylenetriamine (PMDETA) (Aldrich, 99%), ethyl-2-iso-bromobutyrate (EBIB) (Acros Organics, 98%), 2-methyl-2-propenoic acid, 3,3,4,4,5,5,6,6,7,7,8,8,8-tridecafluorooctyl ester (Capstone 62-MA) (DuPont, 94%), 1,1,1,3,3,3-hexafluoroisopropyl methacrylate (HFIPMA) (Aldrich, 99%), tridecafluorooctyl ester methacrylic acid (Aldrich, 99%), 2,2'-azobis(2-methylbutyronitrile) (V-59) (Wacko Chemicals, 99%), octanethiol (Aldrich, 98.5%), and ethylene glycol dimethacrylate (Aldrich, 98%) were used without further purification. Aluminium oxide (Acros Organics, activated, neutral, Brockmann 1, for chromatography, 50-200 μm), hexane (Fisher, laboratory grade), dichloromethane, toluene, methanol, xylene and tetrahydrofuran (all Fisher, analytical grade) were used as received. Polymerisable dyes (red, magenta, cyan and

black) were used as received from Merck Chemicals. In order to remove inhibitors, methyl methacrylate (Aldrich, 99%) and ethyl hexyl acrylate (Alfa Aesar, 98%) were passed directly through an aluminium oxide column, and octadecyl acrylate (Aldrich, 97%) was heated to 60°C; stirred with alumina overnight; and hot filtered. N-(n-propyl)-2-pyridyl(methanimine) (PPMI) was synthesised according to literature procedure.[20]

4.3.2 Apparatus

^{1}H and ^{13}C nuclear magnetic resonance (NMR) spectra were recorded using a JEOL ECS-400 spectrometer at 30°C from solutions in $CDCl_3$, unless specified otherwise.

Molecular weight characteristics of polymers were estimated relative to PMMA standards by gel permeation chromatography (GPC) using a PL-GPC 50 supplied by Polymer Laboratories Ltd, in conjunction with a refractive index detector. All determinations were carried out at 40°C with tetrahydrofuran (THF) as a mobile phase at a flow rate of 1 ml min-1, using a 50 mm x 7.8 mm 10 µm PLgel guard column and 2 x 300 mm x 7.8 mm 5 µm PLgel Mixed-C columns.

Scanning electron microscope (SEM) images were taken using a JCM-5000 Benchtop SEM (Neoscope), at a specimen height of 55 mm, an acceleration voltage of 15 kV and under high vacuum. Particles were sputtered by gold for 120 seconds at 18mA before being assessed in the SEM chamber. Particle sizes were measured using Image J software version 1.42q, with diameters of over 100 particles for each dispersion measured from 8-bit, binary watershed images using a feret distribution.

Dynamic light scattering (DLS) measurements were carried out on colloidal solutions and solutions of block copolymer stabilisers at a range of temperatures using a Zeta-sizer nano series (Nano-ZS) machine, supplied by Malvern Instruments. The z-average, number average and dispersity were measured at temperatures between 10°C and 45°C at a height of 0.85 cm, with measurements taken over a period of 90 seconds with an automatically generated number of scans, ranging from 12-19. Samples were all in dodecane unless otherwise stated.

TEM images were obtained using a JEOL JEM (200-fx) at 120kV. 20µl of a sample in dodecane was transferred onto a carbon coated copper grid and left to air dry.

FTIR spectra were obtained using a Shimadzu IRAffinity-1. All measurements were taken from 400-4000 cm^{-1} for 256 scans.

UV-Vis spectra were obtained using a Shimadzu UV-1800, between 900 cm^{-1} and 400 cm^{-1}, at a rate of 175 cm^{-1}/min.

4.3.3 Synthesis of Block Copolymers with Second Monomer in Lyophilic Block

4.3.3.1 Synthesis of PMMA macroinitiator (M26 and MF)

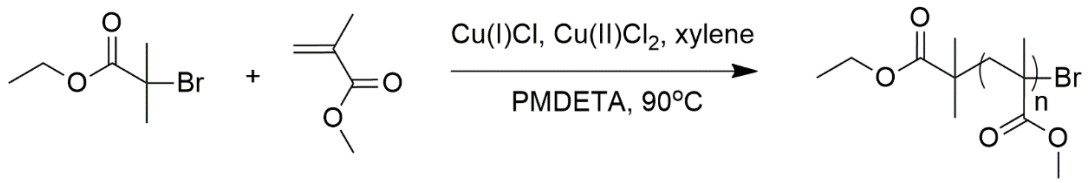

Scheme 4.1: Synthesis of PMMA-Br macroinitiator by ATRP.

A typical procedure was as follows. Synthesis as for section 3.3.3.1. Nitrogen gas was bubbled through a mixture of MMA (70g, 0.699 mol), copper (I) chloride (1.065 g, 0.011 mol), copper (II) chloride (0.072 g, 0.538 mmol), PMDETA (5.592 g, 0.033 mol) and xylene (140 ml) for an hour. Nitrogen gas was bubbled through a separate flask of ethyl-2-iso-bromobutyrate (EBIB) (1.57 ml, 0.011 mol) simultaneously. The mixture was then subjected to 4 freeze-pump-thaw cycles and then heated to 90°C, before ethyl-2-iso-bromobutyrate was injected, and the reaction mixture stirred at temperature for 150 minutes. The reaction mixture was thinned with THF, run down an alumina column and THF was removed under vacuum. The polymer was redissolved in THF and precipitated into cold stirring hexane twice to give a white powder.

Details of the macroinitiators synthesised can be found in Tables 4.1 and 4.5.

^{13}C NMR ($CDCl_3$, ppm) δ: 14.2 (**C**H_3-CH_2), 18.8 (**C**H_3-C-CO), 22.7 (**C**H_3-C-**C**H_3), 31.6 (CH_3-**C**-C=0), 44.6 (CH_3-**C**-CH_3), 44.9 (**C**H_2-C-C=O), 51.9 (**C**H_3-O), 54.5 (CH_3-**C**H_2), 177.0 (O-**C**=O-C), 178.2 (O=**C**-OCH_3).

4.3.3.2 Synthesis of PMMA-*b*-P(ODA-*co*-EHA) block copolymer (S6-S8)

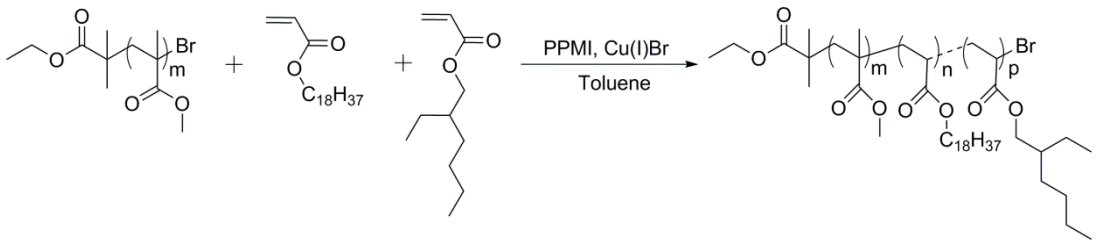

Scheme 4.2: Synthesis of PMMA-*b*-(PODA-*co*-PEHA) by ATRP.

A typical procedure was as follows. Nitrogen gas was bubbled through a mixture of ODA (7.17 g, 0.0221 mol), EHA (4.074 g, 0.0221 mol), copper (I) bromide (0.106 g, 1.37 mmol), PPMI (0.219 g, 1.47 mmol) and toluene (15 ml) for an hour. This mixture was then subjected to 4 freeze-pump-thaw cycles (heated to 35°C in the thaw stages), before mixture was heated to 95°C. Nitrogen gas was bubbled through a separate flask of PMMA-Br (5.000 g, 0.737 mmol) in toluene (10 ml) simultaneously. The solution of PMMA-Br in toluene was then injected into the reaction mixture and the reaction stirred at 95°C under a nitrogen atmosphere for 6 days. The mixture was diluted with THF (ca. 30 ml), run down an alumina column and the solvent removed under vacuum. The polymer was then redissolved in DCM and precipitated into cold stirring methanol twice to give an off-white (brownish) powder (77% yield).

The molar amounts of ODA and EHA were varied between reactions – details of products can be found in Table 4.2. Full NMR analysis for an example of this copolymer can be found in Figure 4.4.

4.3.4 Synthesis of Specialised Stabilisers with Functional Groups

There are a number of simple ways to add functionality to polymers synthesised via ATRP; functional monomers can be incorporated into the main polymer chain itself, or the structure of the initiator used in the synthesis can be modified. This method typically adds one functional group per polymeric chain, which can be altered after polymerisation to give the desired functionality.

4.3.4.1 Synthesis of Fluorinated Block Copolymers (F1 and F2)

Two different fluorinated block copolymers were synthesised via ATRP, PMMA-*b*-PHFIPMA and PMMA-*b*-PCapstone.

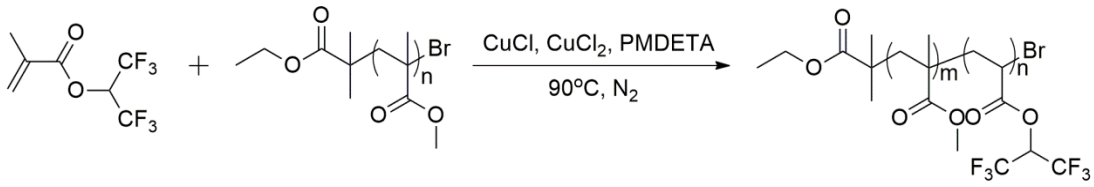

Scheme 4.3: Synthesis of PMMA-*b*-PHFIPMA by ATRP.

Nitrogen gas was bubbled through a mixture of HFIPMA (0.5 g, 2.118 mmol), PMDETA (0.0367 g, 0.212 mmol), CuCl (0.0070 g, 0.071 mmol), $CuCl_2$ (0.0005 g, 0.004 mmol) and xylene (5ml) for an hour. This mixture was then subjected to 4 freeze-pump-thaw cycles, before the mixture was heated to 90°C. Nitrogen gas was bubbled through a separate flask of PMMA-Br (0.0367 g, 0.071 mmol) in xylene (10 ml) simultaneously. The solution of PMMA-Br in xylene was then injected into the reaction mixture and the reaction stirred at 90°C under a nitrogen atmosphere for 3 days. The mixture was diluted with THF (ca. 30 ml), run down an alumina column and the solvent removed under vacuum. The polymer was then redissolved in DCM and precipitated into cold stirring methanol twice to give a white powder.

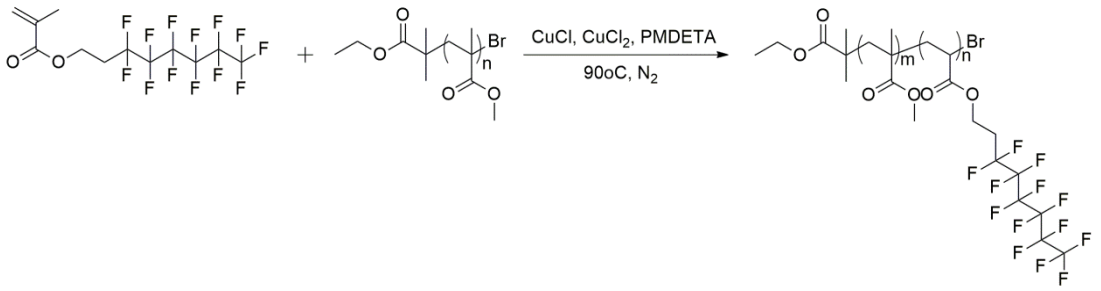

Scheme 4.4: Synthesis of PMMA-*b*-PCapstone by ATRP.

Nitrogen gas was bubbled through a mixture of Capstone 62-MA (31.523 g, 72.94 mmol), PMDETA (0.632 g, 3.647 mmol), CuCl (0.120 g, 1.216 mmol), $CuCl_2$ (0.008 g, 0.061 mmol) and xylene (20 ml) for an hour. This mixture was then subjected to 4 freeze-pump-thaw cycles, before the mixture was heated to 90°C. Nitrogen gas was bubbled through a separate flask of PMMA-Br (15 g, 2.239 mmol) in xylene (30 ml) simultaneously. The solution of PMMA-Br in xylene was then injected into the reaction mixture and the reaction stirred at 90°C under a nitrogen atmosphere for 3 days. The mixture was diluted with THF (ca. 30 ml), run down an alumina column and the solvent removed under vacuum. The polymer was then redissolved in DCM and precipitated into cold stirring methanol twice to give a white powder.

Details of fluorinated copolymers can be found in Table 4.6.

4.3.4.2 Synthesis of hydroxy-functionalised initiator (HO-EBIB)

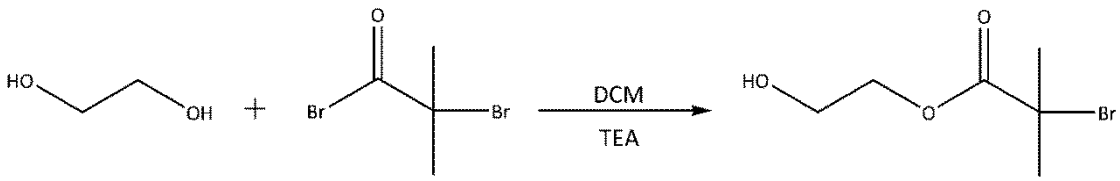

Scheme 4.5: Synthesis of hydroxy-functionalised ATRP initiator.

A mixture of 2-bromo-2-methylpropionyl bromide (40g, 0.174 mol) and dichloromethane (40 ml) was added dropwise to an excess of anhydrous ethylene glycol (107.99 g, 1.74 mol) and triethylamine (35.212 g, 0.348 mol) with stirring on ice. On complete addition, the mixture was filtered before solvent was removed under vacuum. The product was analysed using ^{1}H NMR, and if traces of starting

materials were still present, the product was redissolved in dichloromethane and purified by passing through an activated alumina column, before drying under vacuum to give a colourless oil.

^{1}H NMR (400 MHz, $CDCl_3$, ppm) δ: 4.3 (triplet, 2H, HO-CH_2-C**H$_2$**), 3.9 (triplet, 2H, HO-C**H$_2$**-CH_2), 2.7 (broad singlet, 1H, **H**O-CH_2), 1.9 (triplet, 6H, (C**H$_3$**)C(C**H$_3$**).

^{13}C ($CDCl_3$, ppm) δ: 172 (**C**=O), 68 (HO-**C**H_2), 61 (HO-CH_2-**C**H_2), 57 (**C**$(CH_3)_2$), 31 (C(**C**$H_3)_2$).

4.3.4.3 Synthesis of PMMA-Br using functionalised initiator (HO-PMMA-Br) (M27 and M28)

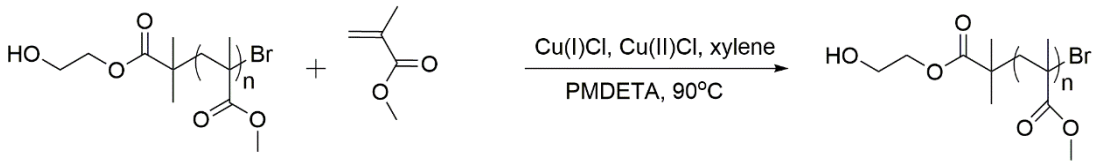

Scheme 4.6: Synthesis of HO-PMMA-Br macroinitiator by ATRP.

A typical procedure was as follows. Synthesis followed as in 4.3.3.1, but with EBIB being replaced by HO-EBIB (2.31 g, 0.011 mol). Details of macroinitiators can be found in Table 4.7.

^{1}H NMR (400 MHz, $CDCl_3$, ppm) δ: 0.9 (broad doublet, 3H, C(C**H$_3$**), 1.75 (broad doublet, 2 H, C-C**H$_2$**-C), 3.6 (singlet, 3H, O-C**H$_3$**), 3.81 (broad signal, 2H, HO-C**H$_2$**), 4.22 (broad signal, 2H, HO-CH_2-C**H$_2$**).

^{13}C NMR ($CDCl_3$, ppm) δ: 14.2 (**C**H_3-CH_2), 18.8 (**C**H_3-C-CO), 22.7 (**C**H_3-C-**C**H_3), 31.6 (CH_3-**C**-C=0), 44.6 (CH_3-**C**-CH_3), 44.9 (**C**H_2-C-C=O), 51.9 (**C**H_3-O), 54.5 (CH_3-**C**H_2), 61.2 (HO-CH_2-**C**H_2), 66.0 (HO-**C**H_2), 177.0 (O-**C**=O-C), 178.2 (O=**C**-OCH_3).

4.3.4.4 Synthesis of block copolymers using functionalised HO-PMMA-Br (S9-S11)

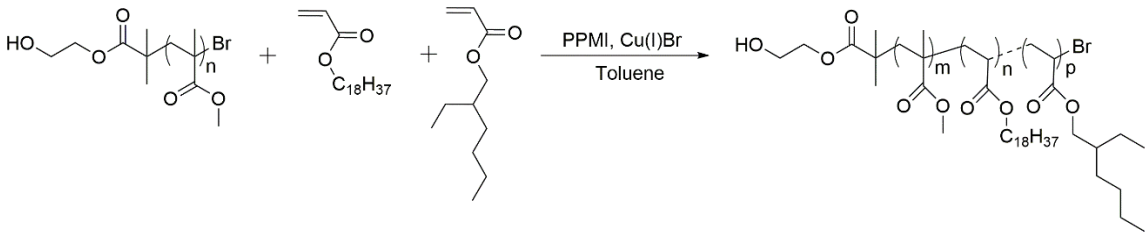

Scheme 4.7: Synthesis of HO-PMMA-*b*-(PODA-*co*-PEHA) by ATRP.

A typical procedure was as follows. Synthesis followed as for 4.3.3.2, with PMMA-Br being replaced by HO-PMMA-Br (5.00 g, 0.737 mmol). Details of block copolymers can be found in Table 4.8.

^{1}H NMR (400 MHz, $CDCl_3$, ppm) δ: 4.0 (broad singlet, 4H, CH_3-$C_{16}H_{32}$-C**H$_2$** and CH_3-C_3H_6-CH(C_2H_5)-C**H$_2$**), 3.6 (broad singlet, 3H, C**H$_3$**-O), 1.9 (multiplet, 6H, CH_3-O-CO-C(CH_3)-C**H$_2$** and CH_3-$C_{16}H_{32}$-CH_2-O-CO-CH-C**H$_2$** and CH_3-C_3H_6-CH(CH_2CH_3)-CH_2-O-CO-CH-C**H$_2$**), 1.6 (multiplet, 9H, C**H$_3$**-$C_{16}H_{32}$ and C**H$_3$**-C_3H_6-CH(CH_2C**H$_3$**), 1.3 (multiplet, 40H, CH_3-C_{16}**H$_{32}$** and CH_3-C_3**H$_6$**-CH(C**H$_2$**CH_3)), 1.0 (broad doublet, 3H, CH_3-$C_{16}H_{32}$-CH_2-O-CO-C**H** and CH_3-C_3H_6-C**H**(CH_2CH_3)-CH_2-O-CO-C**H**), 0.9 (multiplet, 3H, CH_3-O-CO-C(C**H$_3$**).

4.3.4.5 End-group substitution with UV-active pyrene based group

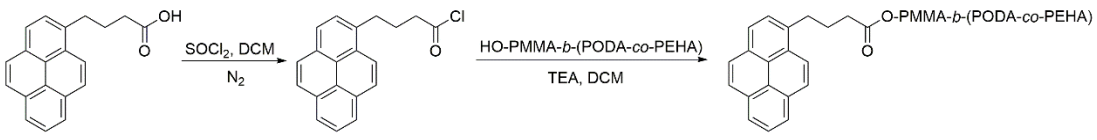

Scheme 4.8: The substitution of pyrene butyric acid onto HO-PMMA-*b*-(PODA-*co*-PEHA).

The first step of substituting a UV-active group onto the block copolymer was adapted from literature.[21] Pyrene butyric acid (1.000 g, 3.4 mmol) was stirred in DCM (40 ml) with thionyl chloride (5.126 g, 34 mmol). The mixture was refluxed for 3 hours under nitrogen atmosphere, before solvent and excess thionyl chloride were removed under vacuum. This resulted in a white solid product (pyrene butyryl

chloride). In the second step, pyrene butyryl chloride (0.155 g, 0.51 mmol) in DCM (10 ml) was added dropwise to a mixture of HO-PMMA-*b*-(PODA-*co*-PEHA) (1 g, 0.051 mmol), TEA (0.0102 g, 0.101 mmol) and DCM (10 ml), stirring on ice. The reaction was allowed to stir for 4 hours, before the mixture was filtered and solvent was removed under vacuum. The product was redissolved in THF, and then reprecipitated twice into cold stirring methanol, giving a reddish-brown solid.

NMR analysis of the product of this reaction will be discussed in section 4.4.2.3.

4.3.4.6 End-group substitution for polymerisable group

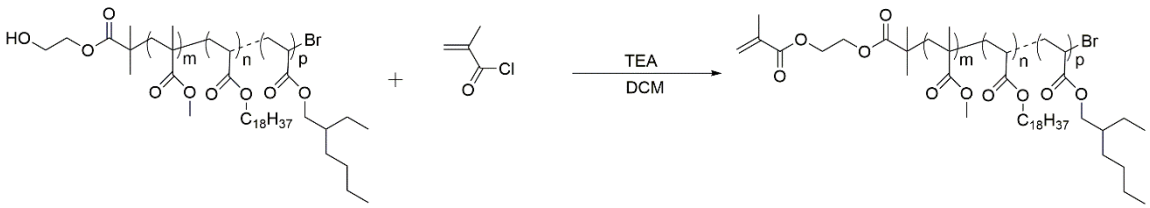

Scheme 4.9: The substitution of methacryloyl chloride onto HO-PMMA-*b*-(PODA-*co*-PEHA).

Hydroxy-functionalised stabiliser HO-PMMA-b-P(ODA-co-EHA) (20.00 g, 0.0012 mol) was added to a mixture of methacryloyl chloride (6.272 g, 0.060 mol), triethylamine (0.243 g, 0.0024 mol) and dichloromethane (20 ml) and allowed to stir at room temperature for 4 hours. The mixture was filtered, and then precipitated twice into cold stirring methanol, to produce an off-white (brownish) powder.

NMR analysis of the product of this reaction will be discussed in section 4.4.2.4.

4.3.5 Syntheses of PMMA Particle Dispersions

Details of individual reactions for all types of PMMA dispersions (to follow) can be found in Table 4.3 (PMMA-*b*-(PODA-*co*-PEHA) stabilised), and Table 4.6 (HO-PMMA-*b*-(PODA-*co*-PEHA) stabilised).

4.3.5.1 Synthesis of PMMA dispersions (D19-D24)

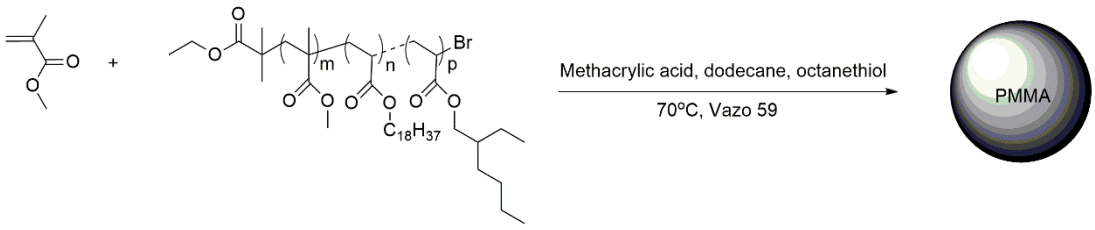

Scheme 4.10: The synthesis of PMMA particles via NAD polymerisation, using a PMMA-*b*-(PODA-*co*-PEHA) stabiliser.

A typical procedure was as follows. Methyl methacrylate (20.580 g, 0.205 mol), copolymer stabiliser (1.050 g, 0.508 mmol), octanethiol (0.125 ml, 0.715 mmol), methacrylic acid (0.416 ml, 4.859 mmol) and dodecane (25.195 g, 0.146 mol) were added together and heated to 70°C under nitrogen. V-59 initiator (0.200 g, 1.036 mmol) was then added, and the mixture was stirred under nitrogen for two hours, before being removed from the heat and allowed to cool to room temperature. The reaction mixture was then passed through 50 µm cloth (purchased from Sefar) to remove fused particles, and washed in dodecane, centrifuged and redispersed three times before analysis by SEM and DLS.

4.3.5.2 Synthesis of dyed PMMA particle dispersions (D25-D30)

A typical procedure was as follows. Commercially available polymerisable dyes (Figure 4.2) were used in NAD polymerisations.[22, 23] The method detailed in 4.3.5.1 was followed, with the dyes added at the beginning of the synthesis at either 5 or 10 wt % with regard to the monomer weight used in the synthesis. The particles were washed in the same manner as those synthesised without dyes, and the solvent which was decanted after each round of centrifugation was observed for any traces of leached dyes. Details of all particle dispersions can be found in Table 4.9.

Figure 4.2: Structures of polymerisable dyes; a) red; b) black; c) cyan; d) magenta.

4.4 Results and Discussion

4.4.1 Synthesis of PMMA-b-(PODA-co-PEHA) Stabilisers, and Their Use in NAD Polymerisations

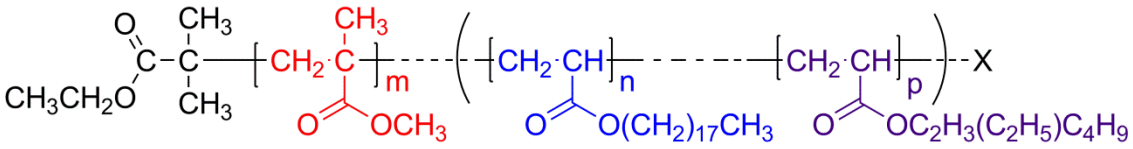

Figure 4.3: Structure of PMMA-*b*-(PODA-*co*-PEHA), as synthesised by ATRP.

As the synthesis of PMMA-Br macroinitiators was previously optimised (Chapter 3), only one macroinitiator was synthesised, on a scale large enough to facilitate the synthesis of numerous block copolymers. The details of this macroinitiator are shown in Table 4.1.

Table 4.1: PMMA-Br macroinitiator synthesised by ATRP. ([a] – Measured by GPC)

Macroinitiator	Initiator	Ligand	Catalyst	Solvent	Monomer (g)	Time (hrs)	Temp (°C)	Target M_n	M_n [a]	Conversion (%)	I_{Eff}	M_w/M_n [a]
M26	EBIB	PMDETA	$CuCl/CuCl_2$	Xylene	10	2.5	90	6700	6780	62	0.62	1.22

Methyl methacrylate has been demonstrated to have a considerably higher reactivity ratio than ethyl hexyl acrylate, with a value of 2.00 in comparison to 0.13.[24] As discussed in Chapter 3, MMA has also been shown to be considerably more reactive than ODA. These values indicated that a copolymer of EHA and ODA would be more of a random copolymer than a gradient copolymer, as the reactivities of EHA and ODA do not differ dramatically. The details of a number of block copolymer stabilisers are shown in Table 4.2.

Table 4.2: Block copolymers synthesised by ATRP using a PMMA-Br macroinitiator, and various ratios of ODA and EHA. ([a] – Measured by GPC)

Stabiliser	Macroinitiator	Macroinitiator (g)	ODA (g)	EHA (g)	Target DP	M_n [a]	M_w/M_n [a]
S6	M26	5	14.35	-	60	12280	1.60
S7	M26	5	13.63	0.41	57+3	14400	1.32
S8	M26	5	7.18	4.07	30+30	16910	1.29

Figure 4.4 shows the fully assigned ^1H NMR spectrum for stabiliser S8, PMMA-*b*-(PODA-*co*-PEHA). The signals corresponding to the end group from the original ethyl-2-iso-bromobutyrate initiator were seen to fall underneath broad polymeric peaks, making molecular weight calculations relative to these protons impossible.

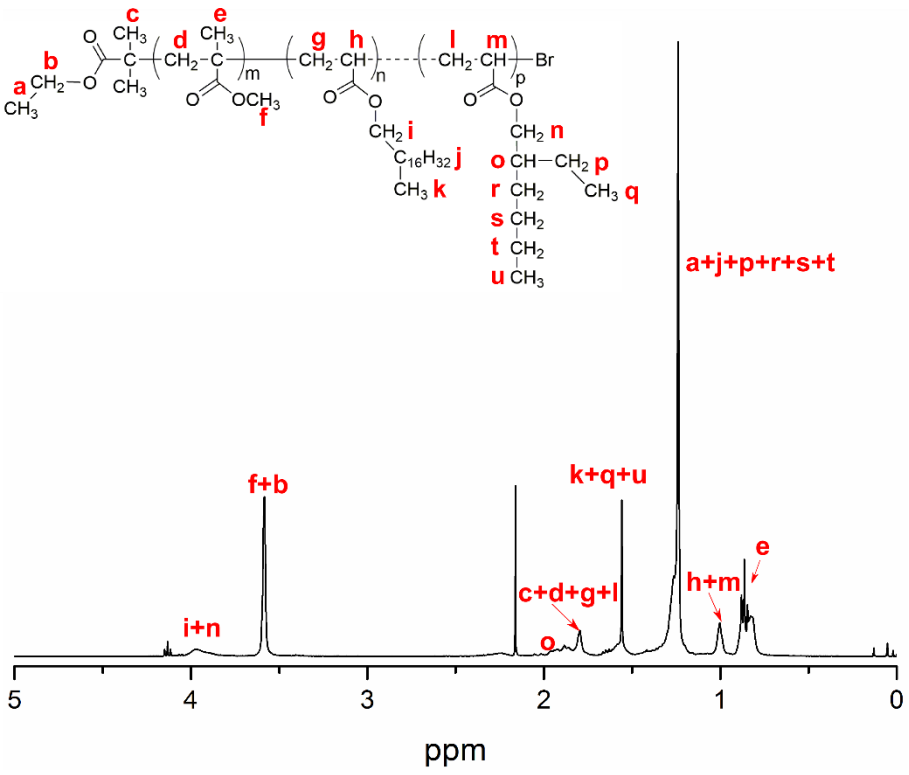

Figure 4.4: ^{1}H NMR of stabiliser S8, with full peak assignments.

The ratio of octadecyl acrylate to ethyl hexyl acrylate in the lyophilic block was calculated from NMR integrals. The signal at 4.0 ppm corresponded to the CH_2 closes to the ester group for both the ODA and the EHA, whilst the CH group at the branching point of the ethyl hexyl acrylate gave a signal at 1.6 ppm. This integral was set to correspond to 1 proton, giving the signal at 4.0 ppm a value of 2 CH_2 protons from EHA, and the remainder of that signal was then attributed to the CH_2 group of the ODA. This could then be converted into a percentage of ODA groups in comparison to the total number of monomer units in the lyophilic block. These values were then converted to give a degree of polymerisation for each component, using the molecular weight of each respective unit. The values for each stabiliser are shown in table 4.3.

The values in this table indicated that ethyl hexyl acrylate was more reactive than octadecyl acrylate, with the content of EHA in the lyophilic block higher for both stabilisers than was targeted.

Table 4.3: MMA, ODA and EHA content of stabilisers S6, S7 and S8. ([a] – Measured by GPC, [b] – Calculated from NMR, [c] – Calculated from both NMR and GPC data)

Stabiliser	M_n[a]	DP MMA[c]	DP ODA[c]	DP EHA[c]	Molar Ratio[b] ODA:EHA
S6	12280	65	23	-	-
S7	14400	65	13	18	42:58
S8	16910	65	12	33	27:73

The stabilisers containing various ratios of ethyl hexyl acrylate were then used in numerous non-aqueous dispersion polymerisations (shown in Table 4.4). As in previous chapters, particle dispersions were synthesised at Merck Chemicals, and a number of samples were kept there in order to be subjected to a number of tests as to their viability in electrophoretic cells. For this reason, size and dispersity measurements were only obtained from SEM images and not from DLS analysis.

Table 4.4: Dispersions synthesised by NAD polymerisation using stabilisers with varying ratios of ODA to EHA. Shaded squares indicate DLS data which could not be obtained due to samples being retained at Merck for EPD testing.

Dispersion	Stabiliser	Wt % monomer	Reactant	D_{SEM}	% SD	D_{DLS}	Đ
D12	S6	42	None	1082	17.1	1442	0.472
D13	S7	42	None	611	8.51	736.4	0.204
D14	S8	42	None	763	19.69	1463	0.283
D15	S8	42	2% EGDMA	955	8.06		
D16	S8	42	10% Magenta	1074	5.21	1045	0.176
D17	S8	42	5% Cyan	1273	11.55	965.7	0.393
D18	S7	42	3% EGDMA	584	14.9		

Figure 4.5 shows SEM images of dispersions D12, D13 and D14, which were stabilised by block copolymers with various EHA contents. The chain length of

PMMA did not vary between stabilisers, and the number of ODA units were also nearly identical between S7 and S8. However, the EHA content of S8 was considerably higher than for S7 (33 and 18 EHA units respectively). Whilst all dispersions were seen to consist of monodisperse particles, those stabilised by block copolymers containing EHA were somewhat smaller than those stabilised by PMMA-*b*-PODA. This could be attributed to the branched component of the EHA, which would form more of a barrier at the solvent/particle interface during the reaction than long alkyl chains, preventing monomer from entering the growing particle. This would result in more, smaller particles.

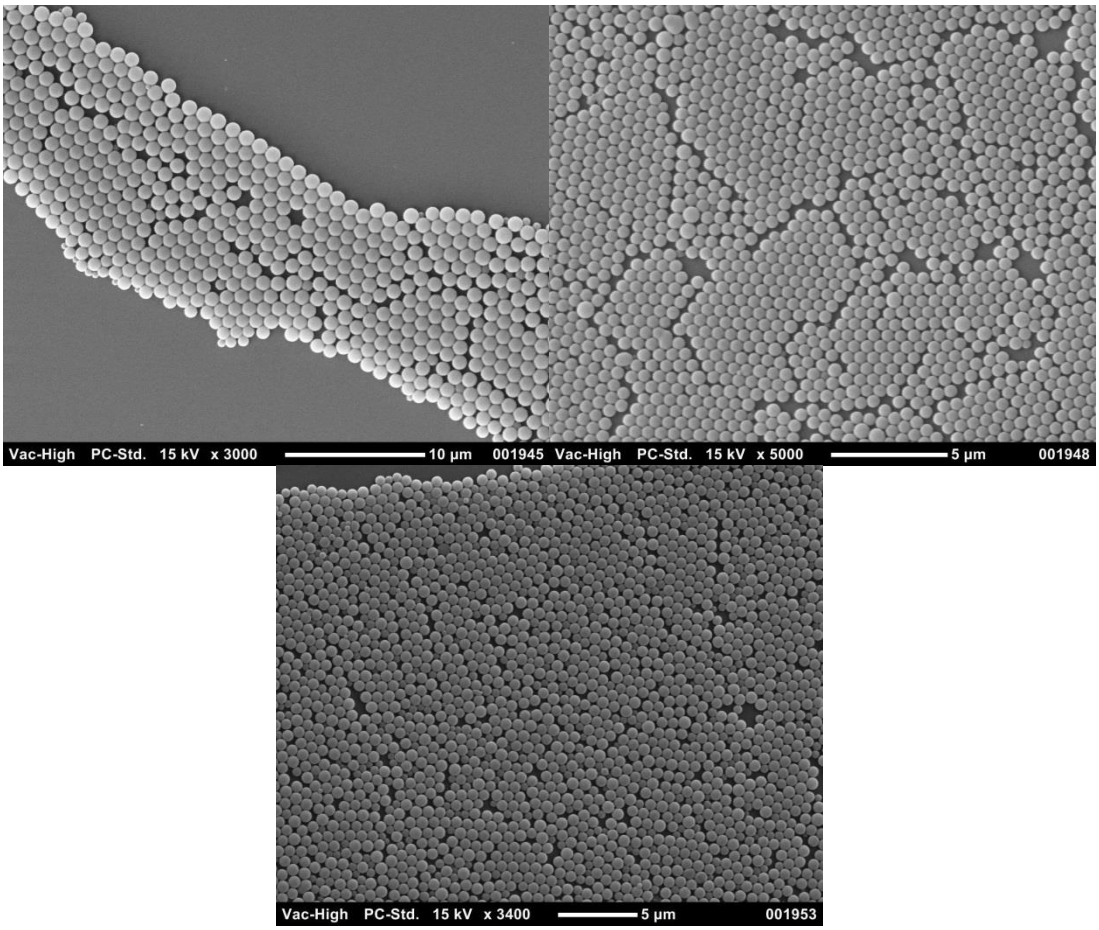

Figure 4.5: SEM images showing dispersions D12 (top left), D13 (top right) and D14 (bottom centre).

A number of dispersions were synthesised which incorporated the cross-linker ethylene glycol dimethacrylate (EGDMA) or cross-linking dyes. SEM images of these dispersions are shown in Figure 4.6. In the top left, D15 shows particles synthesised with 2 molar % EGDMA, and D16 in the top right shows particles

incorporating 10 molar % magenta dye. Whilst the addition of these components increased the particle size in both cases (from 760 nm without the extra reactants to 960 nm for the cross-linked dispersion and 1070 nm for the dyed dispersion), this appeared to be the only property that was affected. Particles in both dispersions were seen to be highly monodisperse and spherical, and packed in hexagonal arrangements.

The middle images (D17) and the bottom images (D18) show dispersions containing cyan dye and 3 molar % EGDMA respectively. The addition of cyan dye increased the particle size in much the same way as the magenta dye, but in this case the dispersity was also increased. The magnified SEM image also showed that the surfaces of the particles were rough and less spherical than observed for previous samples. The morphology of the particles containing 3% cross-linker was also different, with the SEM images showing regions where particles had coagulated to form non-spherical, fused together particles. Although the majority of the dispersion was observed to be monodisperse, these fused particles increased the overall dispersity of the sample and would affect the viability of the dispersion for use as an electrophoretic fluid. These results indicated that there may be an upper limit to the amount of cross-linking reactant that can be incorporated before the dispersion becomes unstable. This was in agreement to D9 (discussed in Chapter 3), where 5 molar % EGDMA was sufficient to cause irreversible coagulation of particles and therefore a very polydisperse sample.

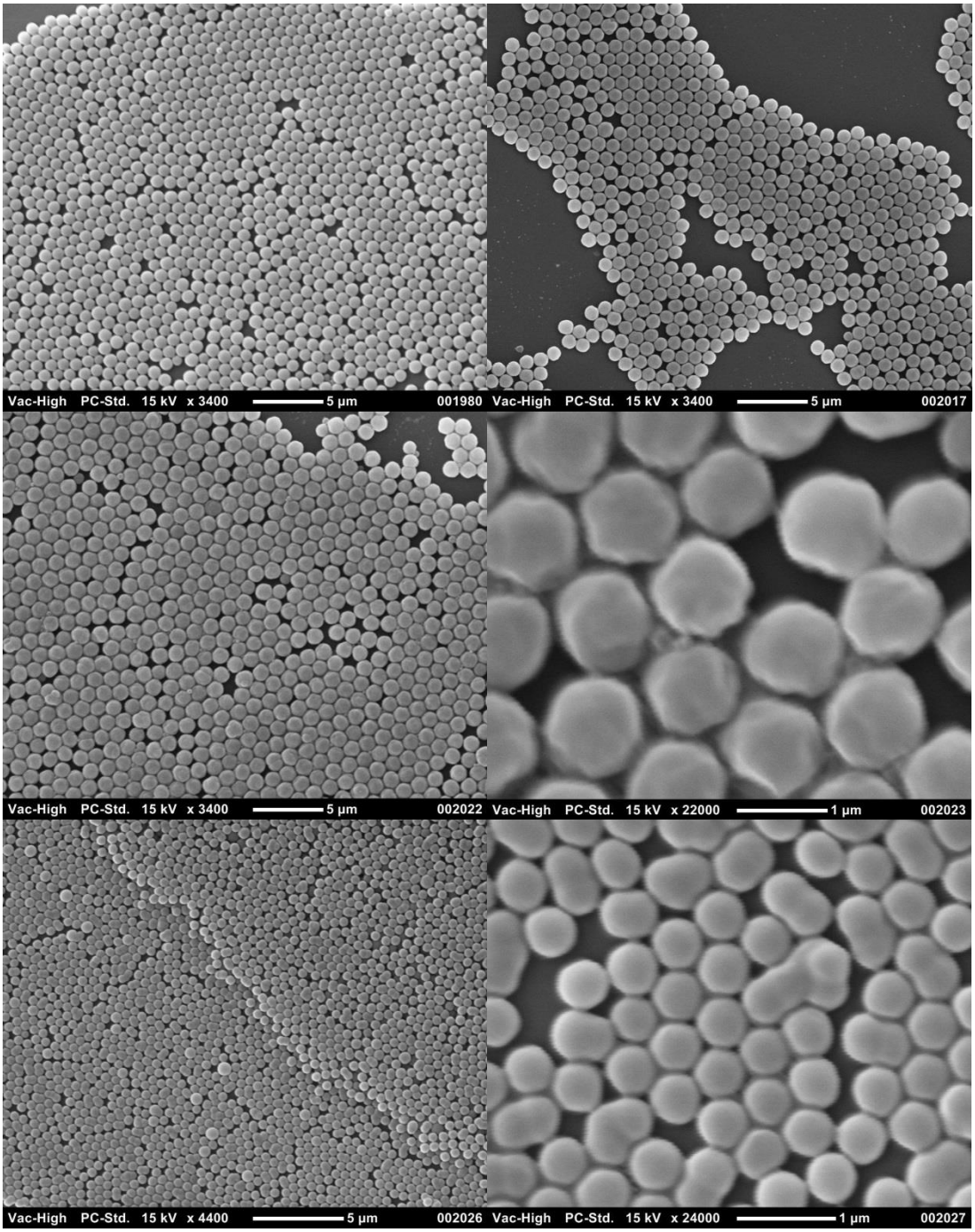

Figure 4.6: SEM images showing dispersions D15 (top left), D16 (top right), D17 (both centre images, at different magnifications) and D18 (both bottom images, different magnifications).

4.4.2 Synthesis of Functionalised Stabilisers

4.4.2.1 Synthesis of Fluorinated Block Copolymers

A PMMA-Br macroinitiator was synthesised following the method in 4.3.3.1, details of which are found in Table 4.5.

Table 4.5: PMMA-Br macroinitiator synthesised by ATRP. ([a] – Measured by GPC)

Macroinitiator	Initiator	Ligand	Catalyst	Solvent	Monomer (g)	Time (hrs)	Temp (°C)	Target M_n	M_n [a]	Conversion (%)	I_{Eff}	M_w/M_n [a]
MF	EBIB	PMDETA	$CuCl/CuCl_2$	Xylene	10	2.5	90	6700	6699	66	0.66	1.24

This macroinitiator was then used in the synthesis of two block copolymers, one with HFIPMA and one with Capstone 62-MA – the details of these products can be found in Table 4.6. It was observed that the fluorinated monomers were less soluble in THF than typical polymeric samples, and as such GPC data was collected at 50°C instead of 40°C. This was to ensure that all of the copolymer was dissolved and to allow accurate measurement of the M_n and Đ.

Table 4.6: Fluorinated block copolymers synthesised by ATRP. ([a] – Measured by GPC at 50°C)

Stabiliser	Macroinitiator	Monomer	Macroinitiator (g)	Monomer (g)	Target DP	M_n [a]	M_w/M_n [a]
F1	MF	HFIPMA	0.0367	0.5	30	11770	1.22
F2	MF	Capstone 62-MA	15.000	31.5	30	14760	1.33

Figure 4.7 shows the GPC traces for the PMMA macroinitiator, in together with the fluorinated copolymers. It was observed that in both cases, the M_n of the sample had increased, confirming that block copolymers had been synthesised. However, a

shoulder was observed for both of the fluorinated samples, indicating that some macroinitiator remained unreacted. This was in agreement with previous studies which suggested that sequential monomer addition was often necessary to ensure that all chains contained fluorinated regions.[6]

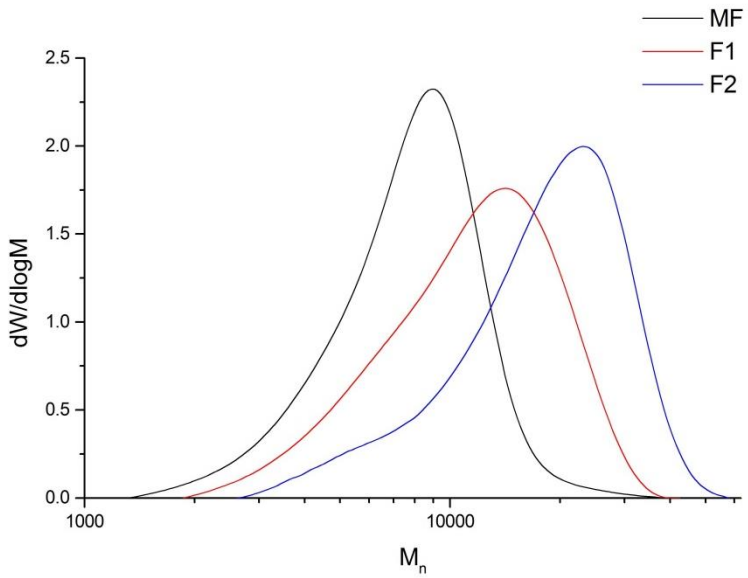

Figure 4.7: GPC traces showing MF (black), copolymers F1 (red) and F2 (blue).

To further confirm that the block copolymerisation had been successful, FTIR spectra were obtained for both the Capstone 62-MA monomer and F2 (Figure 4.8). C-F stretches are typically observed in the region of 1200-1400 cm^{-1},[25] which has been magnified in this figure. The strong, sharp signals centring around 1180 cm^{-1} were assigned as the C-F stretches within the Capstone 62-MA monomer units, and were also observed for the PMMA-*b*-PCapstone block copolymer.

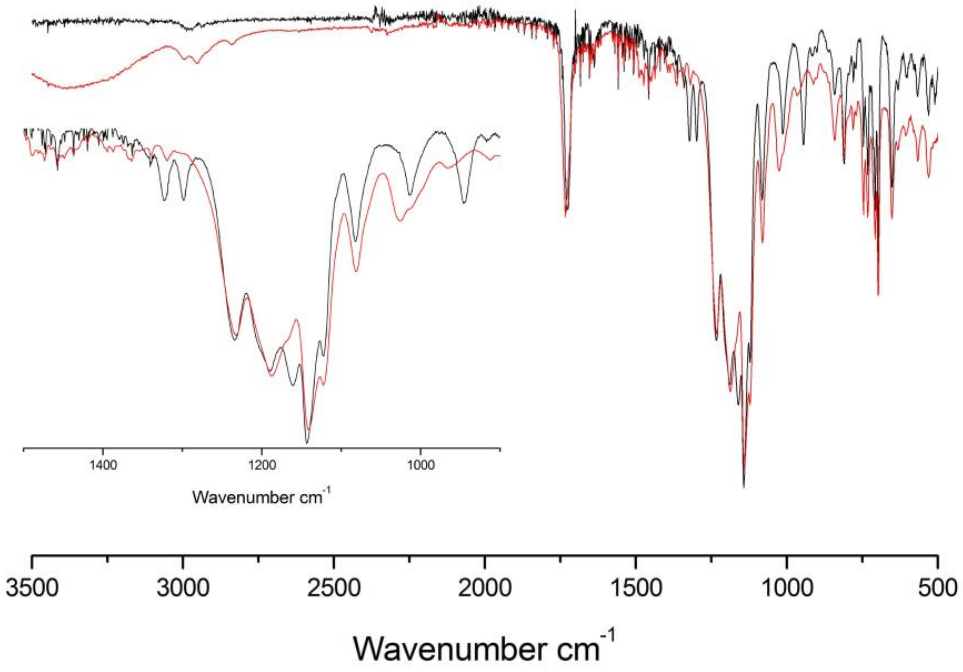

Figure 4.8: FTIR spectra of Capstone 62-MA (black) and F2 (red), with magnification on the region 1000-1400 cm^{-1}, corresponding to C-F stretches.

Figure 4.9 shows a magnification of the signals obtained by ^{1}H NMR for the block copolymer F2. As was observed by GPC, the temperature at which the data was collected was seen to affect the intensity of the signals, due to the poor solubility of the fluorinated groups. This figure demonstrates the increased signal at 4.2 ppm as a function of temperature – the signal was not seen to increase further on increasing the temperature above 50°C, and so all subsequent NMR spectra were obtained at this temperature. Signals corresponding to groups in the PMMA block were not seen to increase in the same manner as those attributed to the fluorinated block.

This broad signal at 4.25 ppm for the PMMA-*b*-PCapstone F2 block copolymer corresponds to the CH_2 group next to the ester group in the Capstone units (shown in figure 4.10). Using the integrals obtained for the block copolymer at 50°C in comparison with the CH_3 group of the MMA units at 3.60, a degree of polymerisation of 18 Capstone units was calculated. This was in agreement with the M_n obtained for the copolymer by GPC. 18 Capstone units attached to the PMMA macroinitiator would result in a M_n of 14526, and the measured M_n was 14760.

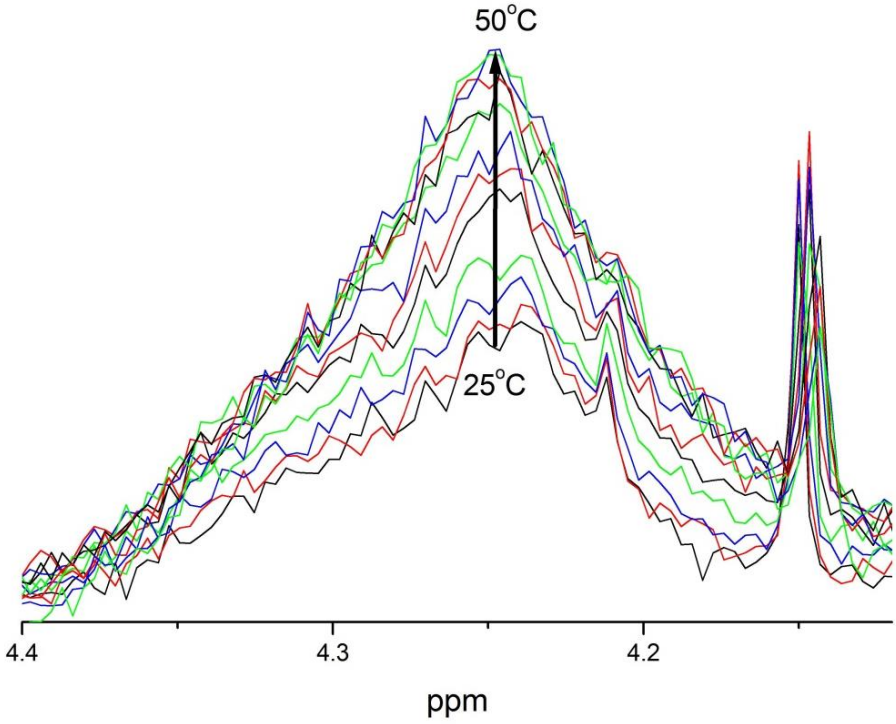

Figure 4.9: ^{1}H NMR signals at 4.25 ppm for copolymer F2, showing an increasing signal as the temperature was increased, until the signals remained the same on increasing from 47.5°C to 50°C.

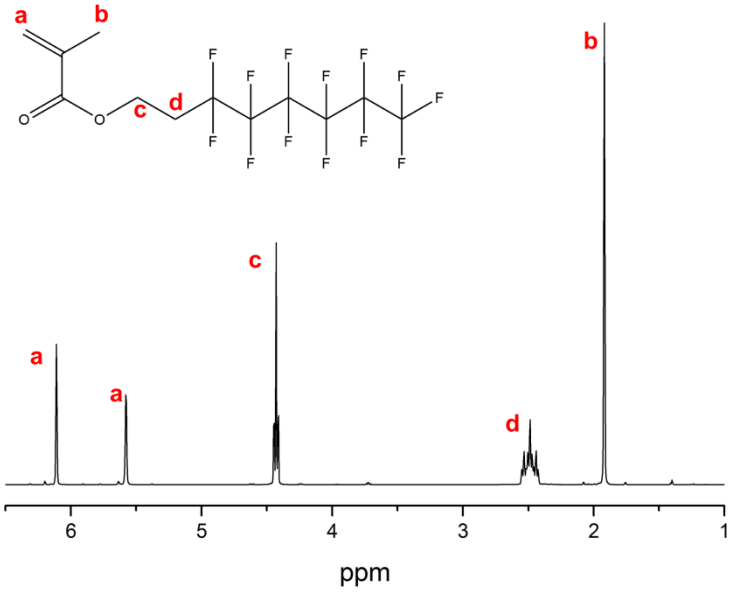

Figure 4.10: ^{1}H NMR of Capstone 62-MA monomer, with full peak assignments. NMR collected at 50°C.

The block copolymer samples were sent to Merck to be used in dispersion polymerisations of MMA in both alkyl and fluorinated solvents. However, these reactions were unsuccessful, and stable particle dispersions could not be synthesised. For this reason, fluorinated copolymers were not investigated further in this work.

4.4.2.2 Synthesis of HO-PMMA-*b*-(PODA-*co*-PEHA)

The synthesis of the HO-functionalised initiator (2-hydroxyethyl bromoisobutyrate) was adapted from literature.[14, 15] It was observed that if the reaction was allowed to progress for longer than 4 hours, or if the excess of ethylene glycol was not substantial enough, a diester would form. This was due to an initiating halide group substituting onto both ends of the ethylene glycol molecule, indicated by an extra proton signal at 4.4 ppm. Whilst it is possible that this by-product could have been isolated by chromatography, it was discovered that increasing the molar excess and reducing the reaction time prevented the by-product from forming.

The ^{1}H and ^{13}C NMR spectra are shown in Figure 4.11 with full peak assignments. The new peaks at 4.22 and 3.81 ppm on the ^{1}H spectrum, and at 66.0 and 61.2 ppm on the ^{13}C spectrum indicate the substitution of the ethylene glycol molecule for the bromine, forming the ester. Ethylene glycol itself exhibits one carbon signal at 63.79 ppm,[26] but it was clear from the ^{13}C NMR that this signal was not present, with the two CH_2 signals observed instead.

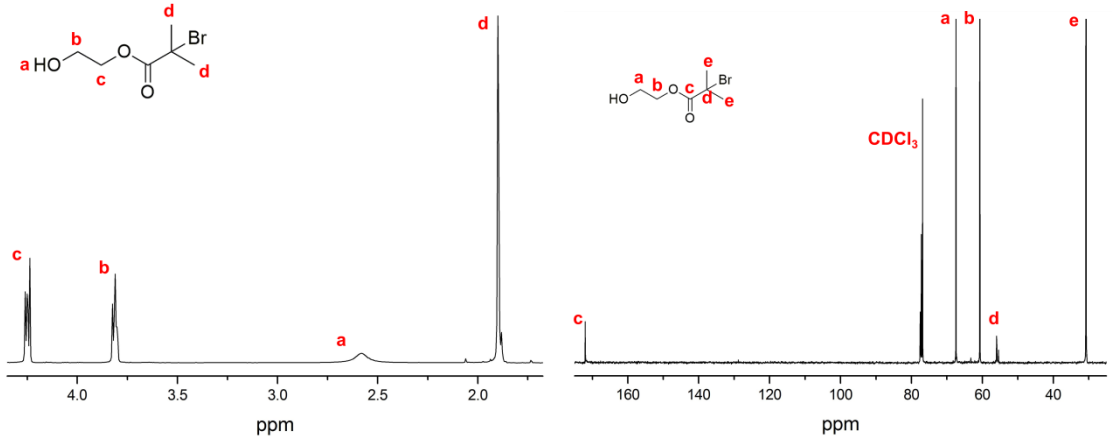

Figure 4.11: ^{1}H NMR (left) and ^{13}C NMR (right) spectra of HO-initiator with full peak assignments.

Figure 4.12 shows the FTIR spectra of both the starting material and the product of the reaction to synthesise the functional initiator. The starting material contained a C-Br bond, which would appear at around 500-800 cm^{-1}, and there are a number of

stronger signals in the spectrum for the starting compound in this region which are not present in the product. However, the more easily identifiable signals were the stretch corresponding to O-H at 3402 cm^{-1}, and the C-O stretch at 1273 cm^{-1}. Neither of these stretches were observed for the starting material, but were both present in the spectra of the product, supporting NMR evidence that the initiator 2-hydroxyethyl bromoisobutyrate was formed.

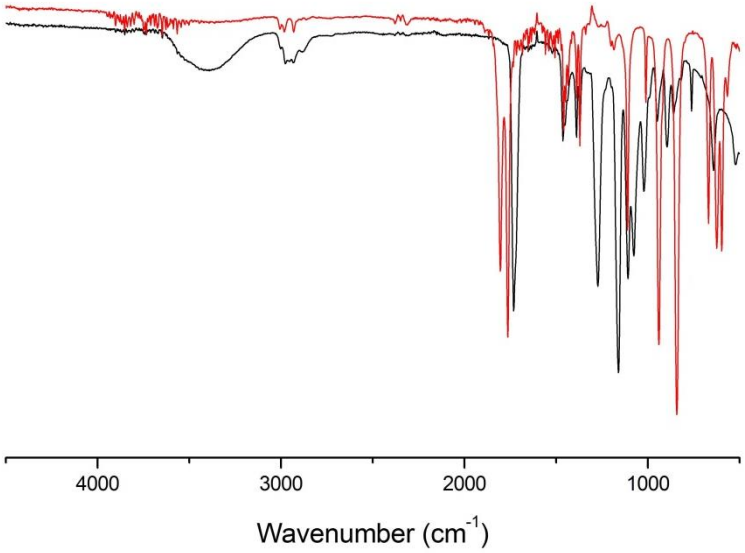

Figure 4.12: FTIR of the starting material α-bromoisobutyrl bromide (red) and the hydroxy-functionalised initiator 2-hydroxyethyl bromoisobutyrate (black). The reaction was confirmed by the presence of the OH stretch at 3400 cm^{-1} and the C-O stretch at 1280cm^{-1}.

This initiator was then used in the synthesis of a number of HO-PMMA-Br macroinitiators, shown in table 4.7. Again, these syntheses followed the optimised method from Chapter 3. The dispersity of these macroinitiators was not seen to be larger than those synthesised without the functional group.

Table 4.7: Hydroxy-functionalised PMMA-Br macroinitiators synthesised by ATRP. ([a] – Measured by GPC)

Macroinitiator	Initiator	Ligand	Catalyst	Solvent	Monomer (g)	Time (hrs)	Temp (°C)	Target M_n	M_n [a]	Conversion (%)	I_{Eff}	M_w/M_n [a]
M27	HO-1	PMDETA	$CuCl/CuCl_2$	Xylene	70	2.5	90	6700	10580	78	0.49	1.33
M28	HO-1	PMDETA	$CuCl/CuCl_2$	Xylene	70	2	90	6700	7870	65	0.55	1.23

Using molar ratios of ODA to EHA previously used in section 4.4.1, the PMMA macroinitiators were reacted to give block copolymer stabilisers, details of which are shown in Table 4.8.

Table 4.8: Hydroxy-functionalised stabilisers synthesised by ATRP. ([a] – Measured by GPC)

Stabiliser	Macroinitiator	Macroinitiator (g)	ODA (g)	EHA (g)	Target DP	M_n [a]	M_w/M_n [a]
S9	M27	5	8.74	0.26	57+3	19780	1.29
S10	M28	30	43.6	24.8	30+30	18310	1.63
S11	M28	20	24.8	14.1	30+30	17100	1.49

These functional copolymers were then subjected to a number of different substitution reactions, before being used as stabilisers in further dispersion reactions.

4.4.2.3 Addition of Fluorescent Group to Stabiliser Structure

With NMR confirming the structure of the hydroxy-functionalised initiator, stabiliser S9 was synthesised via ATRP according to sections 4.3.4.3 and 4.3.4.4. Pyrene butyric acid was converted from the carboxylic acid to the acyl chloride (pyrene butyryl chloride), which was substituted onto the block copolymer in place of the

alcohol moiety. GPC traces from before and after the substitution show that the molecular weight and dispersity of the sample was not affected (Figure 4.13).

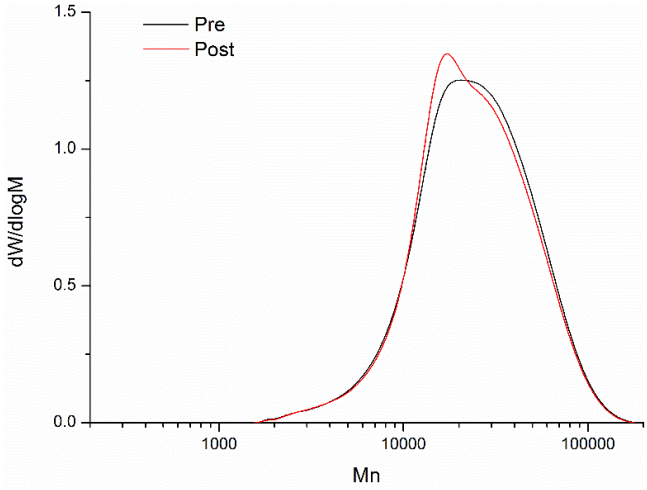

Figure 4.13: GPC traces for S9 'pre' substitution with pyrene butyryl chloride (black) and 'post' substitution (red).

These samples were then also analysed by UV-Vis spectroscopy. The spectrum for pyrene butyric acid clearly showed 7 peaks between 225 nm and 350 nm, whilst the S9 sample (pre-substitution) showed no absorption in this region (Figure 4.14). The 7 peaks from the pyrene butyric acid were also observed for the S9 sample after substitution, albeit slightly broader and less intense. This was, however, expected, as for one polymer chain (M_n of nearly 20000), only one UV-active pyrene group would be present.

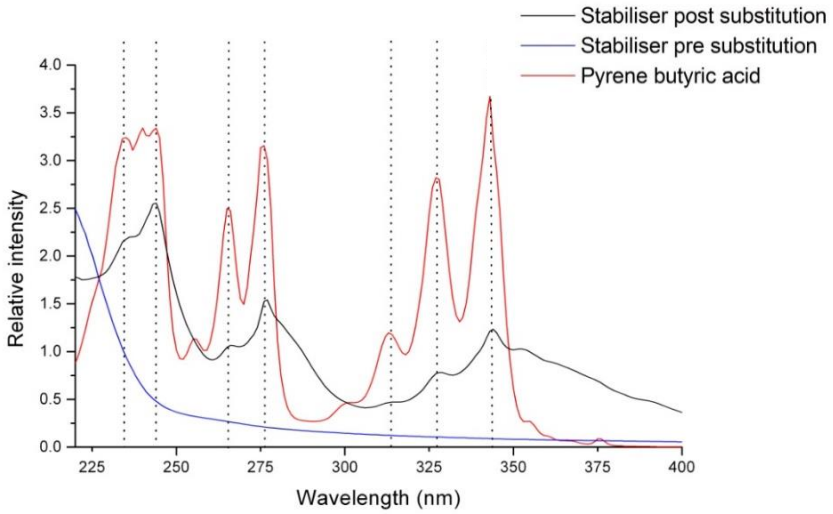

Figure 4.14: UV-visible spectra showing the absorption bands for pyrene butyric acid, and stabiliser S9 before and after substitution.

The presence of the pyrene functional group was also supported by ^{1}H NMR – the signals corresponding to the aromatic groups of the pyrene butyric acid were observed between 7.8 and 8.4 ppm (Figure 4.15). There were no signals observed in this region for S9, but after substitution a small, broad signal was visible in this region. Again, this was to be expected, as the number of protons in the pyrene group is considerably smaller than the protons in the rest of the polymer chain, and polymeric NMR signals are typically broader than monomeric or small molecule signals. The other signals expected for the pyrene butyric acid fall underneath signals observed for the polymeric structure, making identification of these unfeasible. However, there was sufficient evidence from UV-Vis and NMR spectroscopies to deduce that the substitution of the pyrene functional group onto the stabiliser was successful.

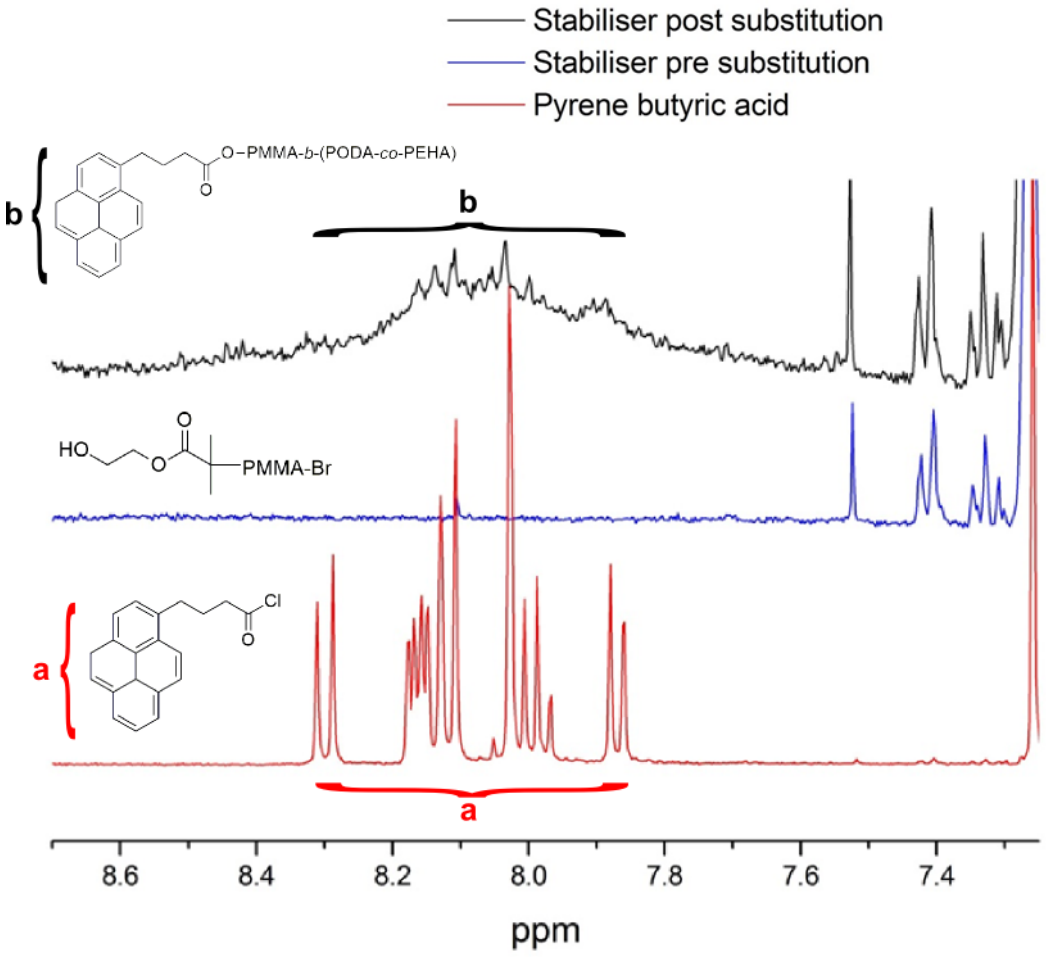

Figure 4.15: NMR spectra showing the region between 7.25 and 8.7 ppm, for pyrene butyric acid (bottom), S9 before substitution (middle), S9 after substitution (top).

4.4.2.4 Addition of Polymerisable Group to Block Copolymer

With the structure of the functionalised initiator confirmed, and the ability to demonstrate substitution of a different functional group onto the hydroxy- moiety, stabiliser D11 was reacted with methacryloyl chloride in an attempt at adding a polymerisable group to the stabiliser structure.

NMR spectra were obtained using the 400 MHz spectrometer, but the sensitivity of the machine was not sufficient to obtain fine detail without running excessively long experiments. For this reason, the spectra presented in this section were obtained using a 14.1 T (600 MHz ^{1}H) Bruker Avance III NMR spectrometer equipped with a 5 mm QCI-F cryoprobe. Data was collected at 25°C, for samples in $CDCl_3$.

Unfortunately, the signals for the two CH_2 groups initially at the end of the polymeric chain from the ethylene glycol group (at 4.22 and 3.81 ppm) fall directly under signals corresponding to the polymeric backbone and could not be observed. If there were no other groups in this region, it would be expected that these signals would both be seen to have shifted slightly downfield due to being between two ester groups.

There were no polymeric peaks in the region where protons attached to a doubly bonded carbon would be expected to fall. Figure 4.16 shows the ^{1}H NMR spectra for M28, S11 'pre' and 'post' substitution, in the region where the new signals corresponding to the presence of a new double bond would be expected. Unfortunately, even after multiple precipitations, the concentrated NMR spectra shown in this figure still show traces of monomer (Figure 4.17 shows the ^{1}H spectra of MMA, ODA and methacryloyl chloride in this region for comparison). The signals at 5.8, 6.1 and 6.4 ppm in both of the copolymer spectra correspond to unreacted acrylate monomer, and the signals at approximately 5.45 and 6.2 ppm in the spectra correlate with MMA peaks. Disregarding these signals from impurities, two larger signals at 6.18 and 5.64 ppm were observed for the copolymer after the substitution reaction. These signals were assigned as the two protons attached to the double bond in the methacrylate functional group which would be present at the end of the stabiliser structure after reaction with methacryloyl chloride to give a polymerisable group.

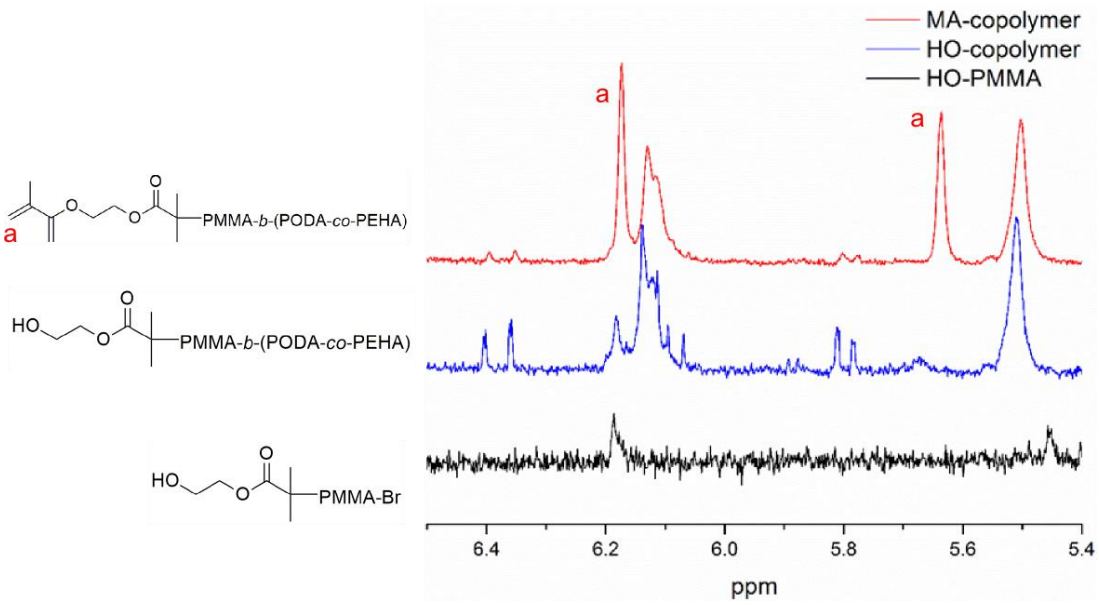

Figure 4.16: ^{1}H NMR spectra showing the functionalised macroinitiator M28 (black), the functionalised copolymer S11 (blue) and S11 after substitution with methacryloyl chloride (red).

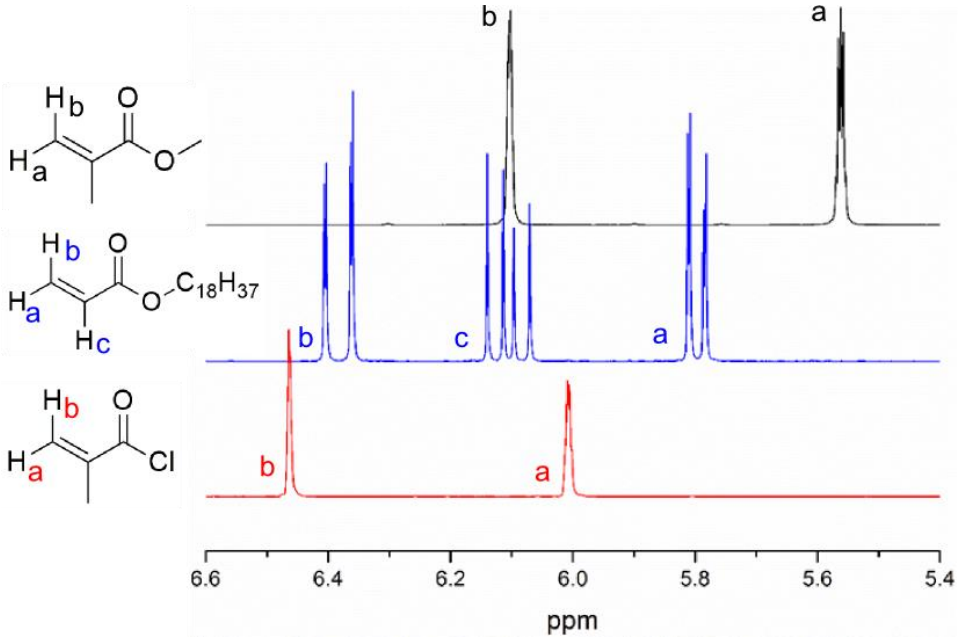

Figure 4.17: ^{1}H NMR spectra of methyl methacrylate (black), octadecyl acrylate (blue) and methacryloyl chloride (red), concentrating on the region where signals corresponding to protons around the double bond were observed.

Figure 4.18 shows the ^{13}C NMR spectra of HO-PMMA-Br macroinitiator M28, HO-PMMA-*b*-(PODA-*co*-PEHA) stabiliser S11, and the same stabiliser after the substitution with methacryloyl chloride. Signals at 61.2 ppm and 66.0 ppm for M28 correspond to the two CH_2 groups which were added to the initiator structure during

the esterification reaction. These signals were still observed for the block copolymer stabiliser, alongside the two CH_2 groups corresponding to the CH_2 next to the ester in both ODA and EHA units (64.6 ppm and 67.2 ppm). This was evidence to suggest that the functional group had not changed during the block copolymerisation.

If substitution for the polymerisable group was successful, the signals at 61.2 ppm and 66.0 ppm would be expected to shift. They would no longer be next to an alcohol moiety, but instead would be between the ester group from the initiator and the ester of the polymerisable group. The NMR for the 'post' substitution stabiliser gave evidence to suggest this had occurred, as the signals at 61.2 ppm and 66.0 ppm were no longer present. In their place was one signal at 64.1 ppm, consistent with CH_2 groups between two ester groups.

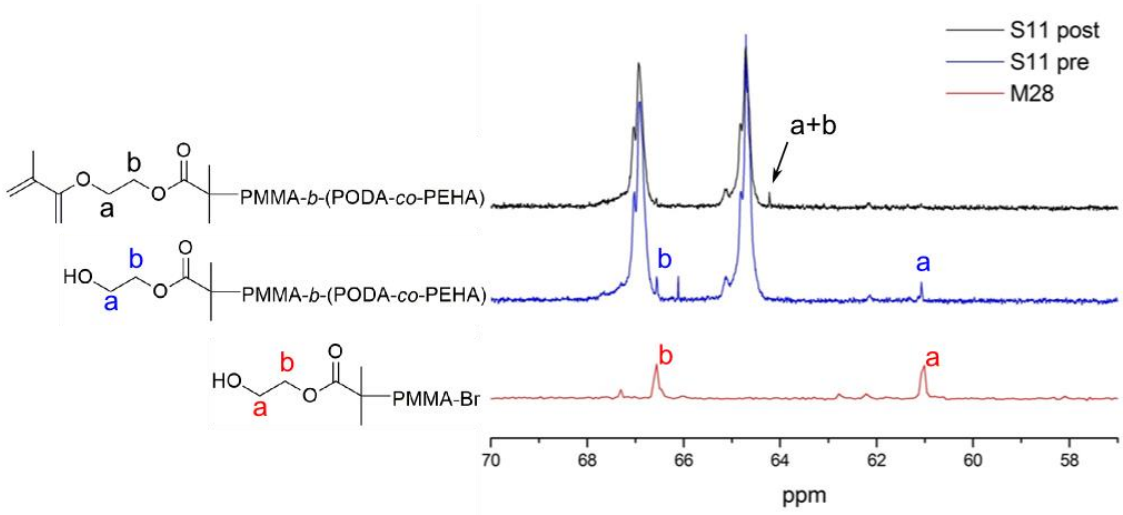

Figure 4.18: ^{13}C NMR spectra showing the region between 70 and 57 ppm, of PMMA-Br macroinitiator M28 (red), PMMA-*b*-(PODA-*co*-PEHA) (S11) 'pre' substitution (blue) and S11 'post' substitution (black).

Further NMR studies of these samples such as the use of 2D NMR (e.g. HSQC) would also be valuable to confirm the correlation between the carbon and protons of the functional group.

4.4.2.5 Particle Dispersions Using the Polymerisable Stabiliser

A range of dispersions were synthesised using the PMMA-*b*-(PODA-*co*-PEHA) stabilisers with the added polymerisable group – details of the particle dispersions are shown in Table 4.9.

Table 4.9: Dispersions synthesised by NAD polymerisation using hydroxy-functionalised stabilisers, with varying molar ratios of stabiliser to monomer, and the addition of dyes and cross-linkers. Shaded squares indicate DLS data which could not be obtained due to samples being retained at Merck for EPD testing. * indicates SEM data which could not be obtained due to particles being too small to size at the resolution of the SEM.

Dispersion	Stabiliser	Wt % monomer	Wt % stabiliser	Reactant	D_{SEM} (nm)	% SD	D_{DLS} (nm)	Đ
D19	S10	42	5.1	None	619	11.79		
D20	S10	42	7.5	None	331	14.8		
D21	S10	42	6	None	673	9.81		
D22	S10	42	5.1	None	599	9.85		
D23	S11	42	5.1	None	491	13.44	461.3	0.409
D24	S11	42	7.5	None	350	17.43	305.7	0.578
D25	S10	42	7.5	10% Magenta	764	19.24	844.2	0.094
D26	S10	42	6	10% Magenta	831	12.27	933.0	0.109
D27	S10	42	8.5	10% Magenta	662	7.25	797.9	0.224
D28	S11	42	8.5	10% Magenta	505	6.73	519.8	0.073
D29	S10	42	25	10% Black	*	*	178.2	0.194
D30	S10	42	15	10% Black	*	*	152.5	0.211

Figure 4.18 shows SEM images of the dispersions in table 4.9 that were synthesised without the addition of extra reactants such as cross-linker or dyes. The two images at the top of Figure 4.19 demonstrate the reproducibility of the particle syntheses – D19 and D22 were both stabilised by S10, with 5.1 molar % stabiliser and 42 molar % monomer. The resulting particles were measured to be 620 nm and 600 nm for

the two dispersions, showing the level of control that the stabiliser provides over the system.

The middle images show the effect of varying the weight % stabiliser included in the particle syntheses – the image on the left is D20 (7.5% stabiliser) and the image on the left is D21 (6% stabiliser). These images, and the subsequent size analysis of the particles, supported the theory that an increased amount of stabiliser can stabilise a larger surface area – this therefore results in smaller particles. Increasing the weight % of stabiliser from 6% to 7.5% resulted in particles that were 330 nm, in comparison to 670 nm. However, this theory did not hold when dispersions D19 and D22 were included in the 'trend', as at 5.1% stabiliser the particles would be expected to be larger than for either D20 or D21. This is not the case, as particles for D19 and D22 were actually measured to be in between these sizes. One possible explanation for this observation is that there is an optimum concentration of stabiliser to prevent aggregation of particles during the polymerisation reaction. Either side of this optimum, some aggregation may occur. If growing particles come into contact towards the beginning of the reaction, this does not necessarily lead to irreversible coagulation, but can instead result in larger, stable particles. This is similar to an observation made for PMMA latices, where an 'unstable region' (dictated by stabiliser and monomer concentration) was discovered. In this region, particles were seen to coagulate during the polymerisation.[27]

The bottom two images show dispersions D22 and D23, both of which were stabilised by S11. These dispersions were synthesised with varying molar percentages of stabiliser, and the resulting particles were seen to follow the general trend with regards to size as a function of stabiliser content.

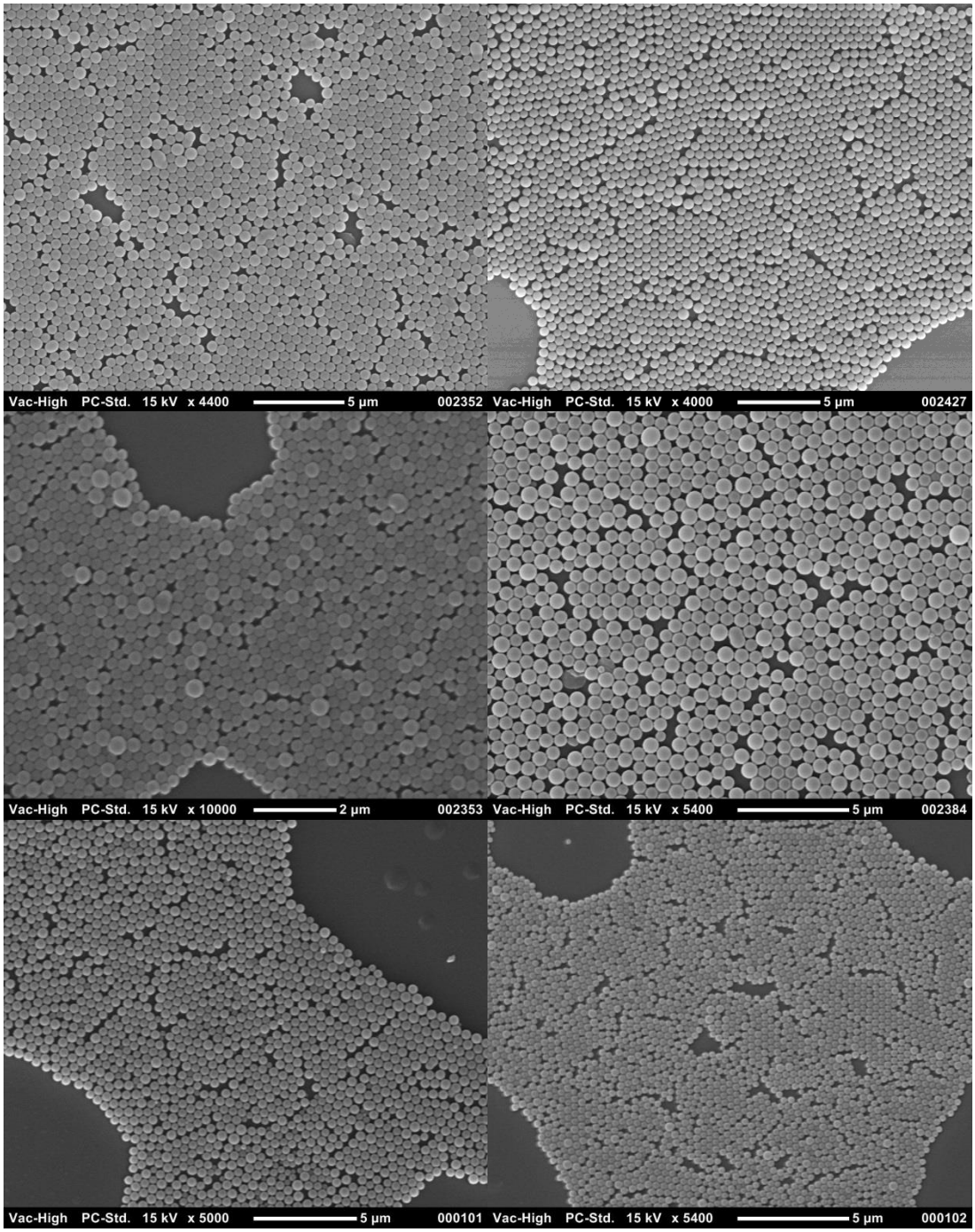

Figure 4.19: SEM images of particle dispersions: D19 (top left), D22 (top right), D20 (middle left), D21 (middle right), D22 (bottom left) and D23 (bottom right).

Dispersions were also synthesised to incorporate the polymerisable dyes used previously into particles stabilised by the polymerisable stabiliser – SEM images of dispersions D26, D26, D27 and D28 are shown in Figure 4.20. All of these dispersions incorporated 10% magenta dye, and were seen to be monodisperse and pack in the desired manner. The particles also did not appear to have rough surfaces

in the same way as some previous coloured particles; the surface of all particles in dispersions stabilised by S10 and S11 had smooth, even surfaces. These dispersions followed the expected trend, whereby decreasing the molar percentage of stabiliser increased the particle size – 8.5 %, 7.5 % and 6 % stabiliser S10 resulted in particles of 660 nm, 760 nm and 831 nm respectively. The varying amounts of stabiliser also did not appear to correlate to the changing dispersity between samples.

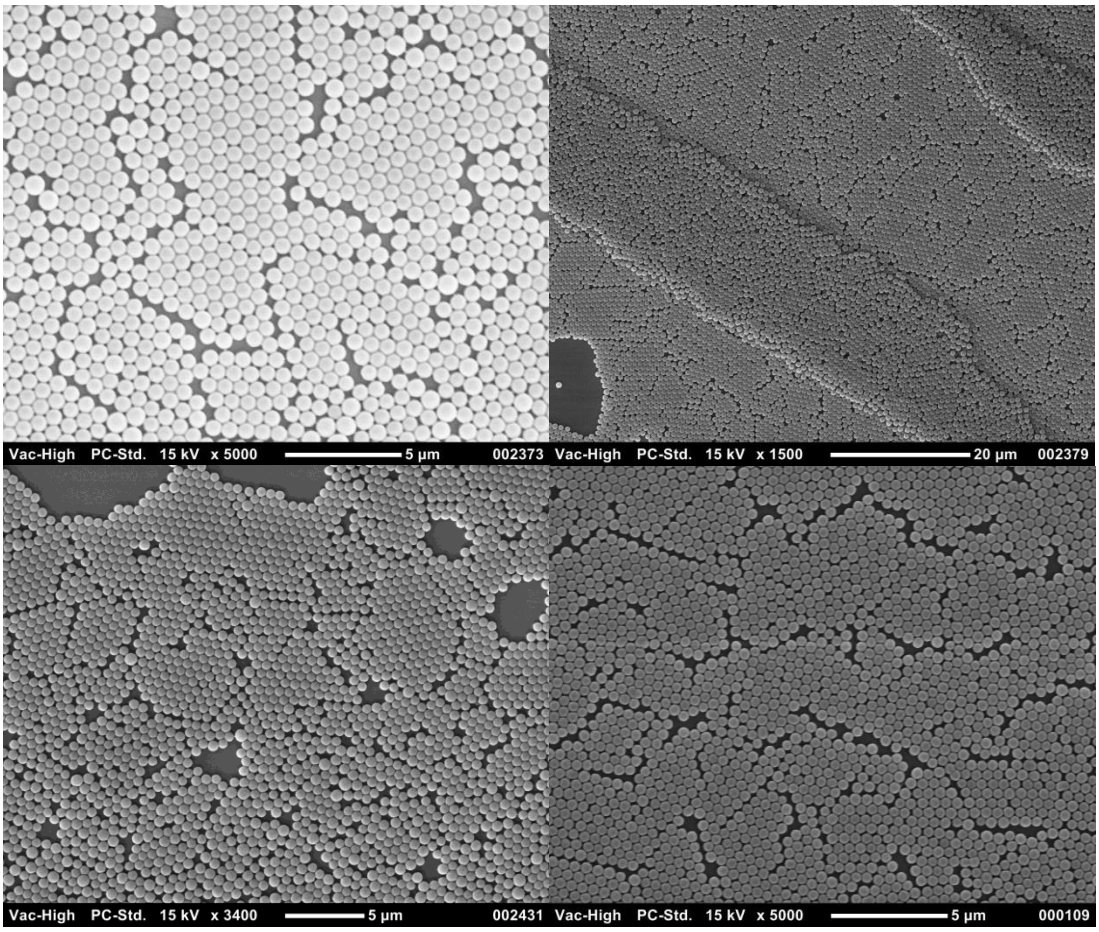

Figure 4.20: SEM images of dispersions: D25 (top left), D26, (top right), D27 (bottom left) and D28 (bottom right).

Stabiliser S10 was also used in the synthesis of ~100 nm dyed black PMMA particles (D29 and D30 in Table 4.9). Particles of this size were obtained by increasing the ratio of stabiliser: monomer, with 25% and 15% stabiliser (D29 and D30 respectively) being included in the NAD reaction with K8 black dye.

SEM images were obtained for these particles, but due to the resolution of the microscope it was not possible to obtain D_{SEM} values for these samples. However,

TEM images were obtained in an attempt at measuring discrete particle sizes to compare with the hydrodynamic radii measured by DLS. Both TEM and SEM images are shown in Figure 4.21. DLS gave N average size measurements of approximately 180 nm and 150 nm for D29 and D30, which was in agreement with TEM and SEM observations (with the expected increase in measurement by DLS due to the larger hydrodynamic radii of particles).

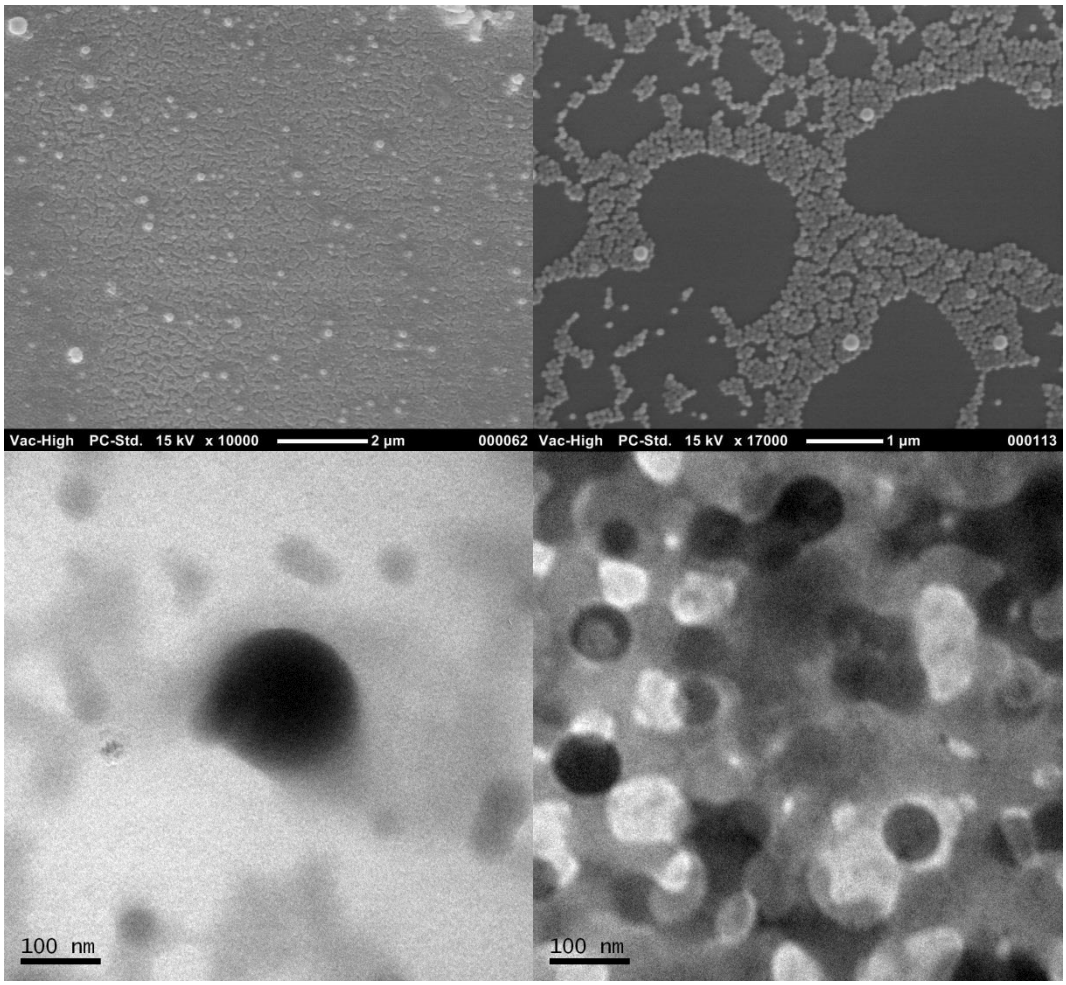

Figure 4.21: Microscopy images of D29 (left) and D30 (right), obtained by SEM (top) and TEM (bottom).

Although the resolution of the SEM was not sufficient to enable size measurements, a number of other observations could be drawn about the particles from the images. For both dispersions, there appeared to be a bimodal distribution of particle sizes, with the majority of the particles being around 100 nm in size, but a number of larger particles (approximately 200 nm in size) also being present. The smaller particles appeared to be monodisperse, and were also packing hexagonally as has been

observed for other dispersion samples. These dispersions indicate the versatility of this method of synthesising coloured monodisperse particle dispersions, as control over size was obtained down to smaller particles than have typically been synthesised by non-aqueous dispersion polymerisation.

The dispersions D19 to D30 were all synthesised using stabilisers which containined a polymerisable group at the end of the chain. This slight change in stabiliser structure could potentially have disrupted the size, dispersity and morphology of particles stabilised by it, but this was not observed to be the case. Imvariably, particles synthesised were observed to be monodisperse, smooth and spherical.

4.4.3 Particle Testing for Display Applications

Particle dispersions which had shown to be monodisperse, of a suitable size and which did not exhibit colour leaching when repeatedly washed in dodecane were subjected to testing in electrophoretic cells to assess their viability for use in displays. The dispersions were made into electrophoretic fluids at Merck Chemicals by the addition of a charge carrier agent, dioctyl sulfosuccinate sodium salt, and increasing the volume of dodecane. Colour data was measured using an x-rite, and the electrophoretic mobility and zeta potential for each dispersion were also measured using the DLS Zetasizer.

The resulting videos of particle switching are accessible on the attached CD (inside the back cover of this thesis). Video 1 is of a sample of PMMA particles stabilised by PHSA-*g*-PMMA stabiliser, and represents the original standard of switching quality prior to this project. It was included to give a comparison to the samples synthesised in this work. The electrophoretic fluids switching in videos 2 and 3 were made up from dispersions D27 and D28 respectively. Video 4 shows the switching of D17, synthesised with cyan polymerisable dye at 5 molar %. All three of these videos showed relatively quick switching times, and clean transitions, with little to no adsorption at the electrodes after the particles have switched to the other electrode. Both videos 5 and 6 show dispersion D29 under slightly different conditions. These videos demonstrated that a smaller particle size could still result

in a viable electrophoretic system – video 5 demonstrated a quicker switching speed, with some residual particles remaining between the electrodes, whilst video 6 demonstrated a much cleaner switch, although the switching time was seen to be slightly increased. All of these videos were comparable, if not marginally better in some cases, to the video presented by Merck as their current example of electrophoretic cells.

Video 7 shows an attempt at a two component system, with oppositely charged cyan and magenta electrophoretic fluids combined in one cell. Whilst each electrode were seen to only attract particles of one colour (as intended) after a current switch, the movement of the particles between the electrodes was slower, which can be attributed to interaction between the two fluids. Although this video does not demonstrate optimum electrophoretic behaviour, it was a very positive indication that this system had good potential for use in electrophoretic displays.

4.5 Conclusions

There were three main aims of this chapter; the first was to synthesise block copolymers with a comonomer in the lyophobic block, in an attempt to disrupt the gelation observed for dispersions synthesised in Chapter 3. The second was to synthesise a functional ATRP initiator, and use this in the synthesis of a number of functional block copolymer stabilisers. These stabilisers were then used in non-aqueous dispersion polymerisations, as in Chapter 3, to investigate the influence of the stabiliser on the properties of the resulting particle dispersions. Finally, a stabiliser with a fluorinated block for use as a stabiliser in fluorinated solvents was synthesised.

By adapting the synthesis optimised in Chapter 3, a number of block copolymer stabilisers were synthesised with PMMA as the lyophobic block, and a copolymer of ODA and EHA as the lyophilic block. The ratio of EHA was varied slightly between copolymers (0 molar %, 5 molar % and 50 molar %). Each copolymer was isolated via precipitation, and then used to synthesise PMMA particle dispersions. In every case, monodisperse, spherical particles were produced, including reactions using 3%

EGDMA cross-linker, and 10% cross-linking magenta dye. The dispersions synthesised using the stabiliser with 50 molar % EHA did not appear to gelate at room temperature, but the thermal properties of these samples will be discussed in Chapter 5.

A hydroxy-functionalised initiator was successfully synthesised, isolated and analysed via NMR. This was then used in the synthesis of a number of block copolymers, all with EHA incorporated into the lyophilic block. The hydroxy-moiety of one such stabiliser was then substituted for pyrene butyryl chloride as a test to see how facile end group substitution was. The presence of this UV-active group was then confirmed by both UV-Vis and NMR spectroscopies.

This led to the ultimate target of substituting a polymerisable group onto the end of the block copolymer stabiliser, which was achieved by reacting the stabiliser with methacryloyl chloride. This would enable the stabiliser to be 'locked in' to the PMMA particles in subsequent NAD polymerisations, due to the methacrylate group becoming incorporated into the PMMA chains which formed the PMMA particles. Whilst ^{13}C NMR confirmed the presence of the signals corresponding to the methacrylate monomer being present at the end of the chain, the signals were very weak in comparison to the large signals due to the groups within the polymeric chain. This was evidence to suggest the group was present, although identification of this group was less straightforward than for the pyrene-based group. One way to circumvent these difficulties would be the use of hydroxyethyl methacrylate (HEMA) as a comonomer in the PMMA block of the stabiliser. This would result in a statistical number of polymerisable groups within the stabiliser chain, which would potentially increase the number of sites in which the stabiliser was physically bound to the particle, but this could affect the dispersity and shape of product particles when used in dispersion polymerisations. For this reason, it was not investigated in this work, but could be a potentially interesting extension.

Stabilisers containing the polymerisable group at the end of the chain were then used in a number of NAD polymerisations, to investigate the effect (if any) on the morphology and dispersity of particles synthesised. In all cases, these reactions resulted in monodisperse spherical particles which packed in the same manner as

previous dispersions. Size control was maintained, by varying the molar percentage of stabiliser as opposed to the molar percentage of monomer (as presented in Chapter 3).

A number of dispersions were then used to produce electrophoretic fluids, and placed into electrophoretic cells at Merck. Numerous one colour systems were produced, as well as a mixed colour system. These tests gave promising results as to the viability of sterically stabilised PMMA particles as electrophoretic inks.

4.6 References

1. E. F. Jordan, B. Artymyshyn, A. Speca and A. N. Wrigley, *Journal of Polymer Science Part A-1: Polymer Chemistry*, 1971, **9**, 3349-3365.
2. S. Roke, O. Berg, J. Buitenhuis, A. van Blaaderen and M. Bonn, *Proceedings of the National Academy of Sciences*, 2006, **103**, 13310-13314.
3. H. W. S. Hsieh, B. Post and H. Morawetz, *Journal of Polymer Science: Polymer Physics Edition*, 1976, **14**, 1241-1255.
4. K. Yokota, T. Kougo and T. Hirabayashi, *Polym J*, 1983, **15**, 891-898.
5. T. Hirabayashi, T. Kikuta, K. Kasabou and K. Yokota, *Polym J*, 1988, **20**, 693-698.
6. N. M. L. Hansen, M. Gerstenberg, D. M. Haddleton and S. Hvilsted, *J. Polym. Sci., Part A: Polym. Chem.*, 2008, **46**, 8097-8111.
7. B. S. Shemper and L. J. Mathias, *Eur. Polym. J.*, 2004, **40**, 651-665.
8. Z. Shi and S. Holdcroft, *Macromolecules*, 2004, **37**, 2084-2089.
9. A. M. Granville and W. J. Brittain, *Macromol. Rapid Commun.*, 2004, **25**, 1298-1302.
10. W. P. Hems, T. M. Yong, J. L. M. van Nunen, A. I. Cooper, A. B. Holmes and D. A. Griffin, *Journal of Materials Chemistry*, 1999, **9**, 1403-1407.
11. D. A. Canelas, D. E. Betts and J. M. DeSimone, *Macromolecules*, 1996, **29**, 2818-2821.

12. W. Jakubowski, N. V. Tsarevsky, P. McCarthy and K. Matyjaszewski, *Mater. Matters (Milwaukee, WI, U. S.)*, 2010, **5**, 16-24.

13. V. Coessens, T. Pintauer and K. Matyjaszewski, *Prog. Polym. Sci.*, 2001, **26**, 337-377.

14. N. A. A. Rossi, R. G. Jones and S. J. Holder, *J. Polym. Sci., Part A: Polym. Chem.*, 2002, **41**, 30-40.

15. W. Jakubowski and K. Matyjaszewski, *Macromolecules*, 2005, **38**, 4139-4146.

16. Y. Nakagawa and K. Matyjaszewski, *Polym J*, 1998, **30**, 138-141.

17. Q. Zhou, P. Gu, Y. Zhang, N. Li, Q. Xu, Y. Zhang and J. Lu, *Chinese Journal of Chemistry*, 2014, **32**, 573-578.

18. R. M. Broyer, G. M. Quaker and H. D. Maynard, *Journal of the American Chemical Society*, 2007, **130**, 1041-1047.

19. H. Zhang, X. Jiang and R. van der Linde, *Polymer*, 2004, **45**, 1455-1466.

20. D. M. Haddleton, M. C. Crossman, B. H. Dana, D. J. Duncalf, A. M. Heming, D. Kukulj and A. J. Shooter, *Macromolecules*, 1999, **32**, 2110-2119.

21. C. Hou, Y. Xiong, N. Fu, C. C. Jacquot, T. C. Squier and H. Cao, *Tetrahedron Lett.*, 2011, **52**, 2692-2696.

22. Coloured particles for electrophoretic displays, N. Greinert, L. D. Farrand, M. James, A. N. Smith, M. J. Goulding, D. Walker, S. Khan, P. Reynolds, S. Hawkins and R. Hughes, 2010.

23. Particles for electrophoretic displays, L. D. Farrand, M. James, E. J. Markham, C. Topping and J. H. Wilson, 2012.

24. A. Aymonier, E. Papon, J. J. Villenave, P. Tordjeman, R. Pirri and P. Gerard, *Chem. Mater.*, 2001, **13**, 2562-2566.

25. G. Socrates, *Infrared and Raman Characteristic Group Frequencies: Tables and Charts*, Wiley, 2004.

26. G. R. Fulmer, A. J. M. Miller, N. H. Sherden, H. E. Gottlieb, A. Nudelman, B. M. Stoltz, J. E. Bercaw and K. I. Goldberg, *Organometallics*, 2010, **29**, 2176-2179.

27. L. Antl, J. W. Goodwin, R. D. Hill, R. H. Ottewill, S. M. Owens, S. Papworth and J. A. Waters, *Colloids and Surfaces*, 1986, **17**, 67-78.

Chapter 5: Thermoresponsive Gelation of Particle Dispersions and Block Copolymers in Non-Polar Solutions

5.1 Introduction

5.1.1 Semi-crystalline Side Chain Polymers

Side-chain crystallisation of 'comb-like' or 'brush-like' polymers has been well documented,[1-3] and has been described as 'crystallisation of alkanes in the presence of external constraints'.[4] Whilst crystallisation of the main backbone chain of a polymer also occurs, the presence of long side chains often inhibits or reduces the main chain crystallisation.[5]

Differential scanning calorimetry (DSC) measurements were taken of homopolymers of acrylates with alkyl side chains of varying length (C12 – C22). The crystallinity of the side chains could be calculated by comparing the heat of fusion for the homopolymer with the heat of fusion for the pure crystalline unit. This work showed that in bulk, the first 8.7 CH_2 groups were amorphous, with the remaining groups in the alkyl side chain found to be crystalline, demonstrated in Figure 5.1. It was also shown that as the chain length increased, the number of crystalline units also increased, whilst little variation in the amorphous region was observed.[6] This crystallisation typically occurs upon cooling 10 to 15ºC below the melting point of the homopolymer.[7]

It has also been shown that the crystalline and amorphous phases of homopolymers have different gas permeabilities. Octadecyl acrylate was found to be non-permeable to gases when in the crystalline state, but when the polymer was in a molten state, the permeability was seen to dramatically increase. This potential to store and transport gases gives the semi-crystalline material the potential to be a thermally responsive delivery system.[8]

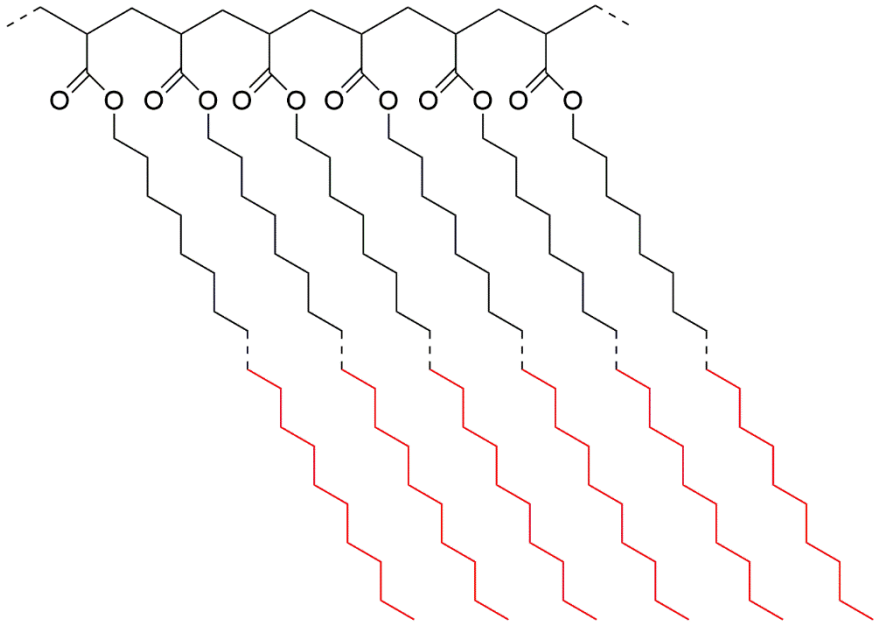

Figure 5.1: Structure showing the amorphous (black) and crystalline (red) regions of a chain of poly(octadecyl acrylate) according to literature studies.[6]

The addition of functional groups to the polymeric backbone has also been demonstrated to have an effect on side chain crystallisation.[1] For copolymers of styrene, substitutions onto the main chain were suggested to lead to a less flexible backbone, making the side chain crystallisation less favourable.[2] The addition of a comonomer to the crystallisable block was investigated for octadecyl styrene – the copolymers were seen to have different T_m values in comparison to those of the homopolymer, and the position of the comonomer in the chain was also seen to have an effect on the thermal properties.[9]

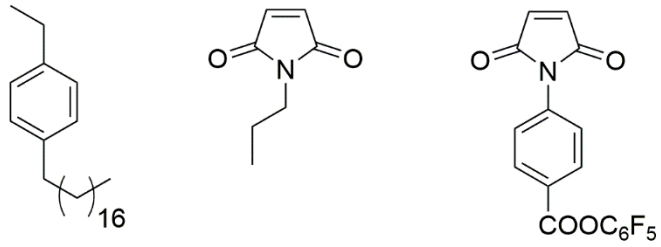

Figure 5.2: structure of comonomers used to disrupt the crystallisation of poly(octadecyl styrene) (shown on the left): N-(n-Propyl)maleimide (centre) and 4-(N-maleimido)-azobenzene.

A number of potential arrangements of the long side chains leading to the crystallisation have been proposed, shown in Figure 5.3, each supported by different

analyses of semi-crystalline polymers. End-to-end packing shows the amorphous region closest to the backbone chain, and then the crystalline regions extending towards the side chains of a different polymer chain.[7] Interdigitating or intercalating crystalline regions were proposed from SAXS measurements.[10] The hexagonal packing lattice later proposed does not necessarily contradict either of the first two proposals – layers of polymeric chains can either form in an end-to-end manner, or with intercalating chains, but these chains can be arranged in a hexagonal lattice when the 3-dimensional arrangements are viewed.[11] This arrangement is often caused by a heating process, where side chains arrange themselves in different directions from the central polymeric backbone after the ordered structure has been disrupted by melting.

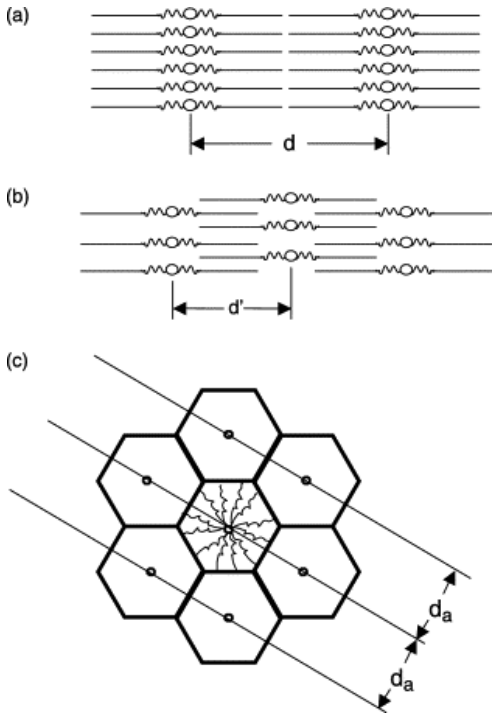

Figure 5.3: Schematic showing proposed packing arrangements for side chains: a) end-to-end; b) interdigitating; and c) hexagonal packing lattice (Reproduced with permission from K. A. O'Leary and D. R. Paul, Polymer, 2006, 47, 1226-1244).[11]

There has, however, been some disagreement as to whether or not the backbone of the polymer chain is included in the crystallisation. Some research groups found that in the case of poly(n-alkyl acrylates), the backbone of the polymer is indeed included in the crystallisation process,[7, 12] while other bodies of work suggest that only the ends of the alkyl chains are involved.[6]

It has been shown that, specifically in the case of poly(octadecyl acrylate) (PODA), a greater crystallinity was observed when the polymer was synthesised via controlled polymerisation techniques instead of conventional polymerisation methods.[13] This was a particularly valuable observation with regards to this research, as the block copolymer stabilisers discussed in this work were synthesised via ATRP.

5.1.2 Gelation of Solvent by Semi-Crystalline Side-Chain Polymers

It was demonstrated that polymers which exhibit side-chain crystallisation can exhibit gelation behaviour once dissolved in a suitable solvent. This process has been attributed to the fact that as the chains arrange into a 'semi-crystalline' structure, they can become swollen and trap solvent between them.[14] There have been examples in the literature of long side chain polymers forming thermally responsive gels in solutions such as alcohols and alkanes. The gelation process is often seen as being temperature dependent – typically, an increase in temperature breaks the gel structure and dramatically reduces the viscosity. A reversible order-disorder transition is observed by X-ray diffraction, where the chains form an ordered structure below a certain temperature, but above this temperature the chains become disordered and amorphous. This was demonstrated for copolymers of octadecyl acrylate and acrylic acid, the structure of which is shown in Figure 5.4.[14]

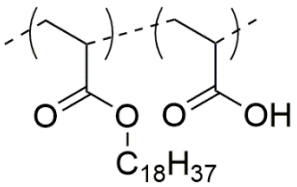

Figure 5.4: the structure of a copolymer of octadecyl acrylate and acrylic acid.

The work which first measured the number of crystalline CH_2 groups in a side chain also showed that solvating both the backbone and the side chains increased the fraction of the chain which was crystalline, with 7.8 CH_2 groups found to be amorphous in the presence methanol, in comparison to the 8.7 when the material was in bulk.[6] Another observation made was that the melting temperature of gels of comb-like homopolymers in alkane solvents increases as the chain length of the solvent increases.[15]

5.1.3 Gelation of Particle Dispersions Stabilised by Long Alkyl Chains

Alkyl chain s have been used to stabilise particle dispersions for decades. However, it has been observed that gelation often occurred at defined temperatures. Neutron scattering experiments have investigated the phase behaviour of long alkyl chains tethered to a silica surface in a brush-like arrangement, which were shown to gelate below certain temperatures. It was shown that above the phase transition, the alkyl chains were consistent with a solvated layer of disordered chains, but below this temperature the chains straightened into a rigid arrangement. This was observed by an increase in the shell thickness and an increased concentration of solvent present in the brush layer, with the solvent molecules assumed to be interdigitating between the tethered alkyl chains (shown in Figure 5.5). This led to particle aggregation, before a gel was formed (above a certain concentration of stabiliser chains).[16]

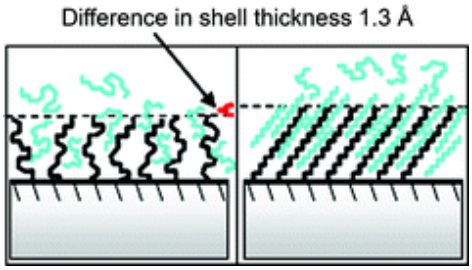

Figure 5.5: schematic to show the disordered arrangement of tethered alkyl chains above (left) and the crystalline, extended arrangement below (right) the temperature of phase transition (Reproduced with permission from A. P. R. Eberle et al, Langmuir, 2010, 26, 3003-3007. Copyright American Chemical Society 2010).[16]

Gelation of polymer based colloids has reported in literature for a variety of different systems.[17-19] The graft density of the stabilising poly(ethylene oxide) chains for a dispersion of polystyrene particles was seen to affect the temperature at which gelation was observed. Samples with a lower graft density were shown to be gels at room temperature, whilst a higher grafting density caused samples to be stable dispersions down to much lower temperatures.[18] It has also been presented that the high surface area of concentrated colloidal systems, which have small interparticle distances, are the most suitable to give a temperature induced gelation, and that this gelation is usually observed at the cloud point for the corresponding polymeric stabiliser.[19]

Spectroscopic analysis of silica particles stabilised by octadecyl chains in hexadecane solvent supported the assertion which has previously been discussed[16] that the stabiliser chains form an ordered structure once the sample has gelated, whilst they are randomly ordered when they are dispersed. It was also shown that this process involved the layer of polymeric chains to be 'filled' with solvent molecules to a concentration of at least 40%.[20]

Crystallisation and gelation behaviour of polymers has been investigated via a number of analytical techniques, with the most commonly used being dynamic light scattering, differential scanning calorimetry and rheological methods.

5.1.4 Dynamic Light Scattering

Dynamic light scattering (DLS) can be used to monitor the long term stability of sterically stabilised polymeric particles. Polypyrrole particles were left to stand for a period of 5 weeks, and the size of the particles was monitored weekly. An increase in particle size was observed for the less stable colloidal system (which was stabilised by an imine-based stabiliser), indicating that flocculation occurred over a period of weeks. This was in contrast to a more stable system (stabilised by an amine-based stabiliser), where particle size remained relatively constant over time.[21]

DLS can also be used to measure the stability of a colloidal system at different temperatures. It has been shown that at higher temperature, some stabilisers had a lower affinity for solid colloidal material, lowering the amount of stabiliser adsorbed to the particles which led to aggregation as the temperature was increased.[22] In a similar manner, DLS was also used to investigate the phase transitions due to temperature in particles of poly(N-isopropylacrylamide) and poly(acrylic acid)[23], as well as of iron oxide nanoparticles.[24] In both instances, it was observed that as temperature increased, the radius of the particles decreased due to a 'shrunken state', as opposed to the 'swollen state' at lower temperatures.

5.1.5 Differential Scanning Calorimetry

Differential scanning calorimetry (DSC) has been used in a number of different ways to monitor colloidal dispersions during thermal transitions. The cloud point of polymeric samples and the aggregation of particles can be measured as a function of temperature.[20] It was also demonstrated that dispersity of polymeric samples affected the temperature at which the thermal gelations occurred – surfactants with a broader dispersity were seen to gelate at lower temperatures (due to the higher molecular weight fractions having a higher tendency to order and induce a gelation).[25]

5.1.6 Rheology

Rheology measurements on colloidal dispersions of particles can provide information on a number of properties of the dispersion. For example, it is well documented that the viscosity of a liquid increases as the volume fraction of solid spheres increases. A number of theoretical studies have shown that the viscosity of a system dramatically increases once the volume fraction is above 0.5, suggesting a theoretical upper limit to the fraction of spheres which can be added without the liquid becoming solid.[26] Once the interactions which occur within a stable colloidal suspension are taken into account, these models become inaccurate and require the addition of a number of other parameters.[27] A combination of rheological measurements, volume fraction calculations and DLS data has also been used to calculate the thickness of the stabilising layer in colloidal dispersions.[28, 29]

Studies have been carried out into how interactions between sterically stabilised particles affect the rheological properties of the colloidal system. The length of the alkyl chain was seen to affect the rigidity of a gel or network formed by the dispersion – a longer chain resulted in a higher elastic modulus, indicating that these networks are stiffer than ones with shorter side chains. However, this effect is seen to lessen once the chain length increases above 8 carbon atoms[30], consistent with the length necessary for chains to crystallise.[6]

Oscillatory measurements were used to examine the process of flocculation in sterically stabilised dispersions – this highlighted that the nature and strength of the

adsorption of the stabilising molecule dramatically affected the stability. Higher surface coverage of particles was shown to produce a more stable system, with the chain length of the stabiliser also seen to have a dramatic effect on stability. For example, for silica particles, a PMMA stabilising layer of chains of M_w 88000 produced a more stable dispersion than chains of M_w 58000, but also more stable than M_w 330000 (stability was derived from the change in G' values). This was attributed to the longer chains entangling, leading to greater flocculation. This work showed the necessity to tune each aspect of a sterically stabilised dispersion in order to maintain stability.[31]

5.2 Aims and Objectives

The work in Chapter 3 highlighted one of the drawbacks of using long-chain aliphatics as one of the components of block copolymer stabilisers. Dispersions stabilised by these copolymers were observed to solidify over time if left standing (rather than on a continuous roller-mixer, where this behaviour was not observed). This gelation process was seen to be thermoresponsive, with particles redispersing as the temperature was increased. However, when stabilisers were synthesised with a comonomer in the lyophilic block (Chapter 4), dispersions were seen to remain liquid, even after refrigeration.

This chapter investigates the nature of the thermoresponsive transition observed in the initial samples, utilising dynamic light scattering (DLS), differential scanning calorimetry (DSC) and rheometry. This analysis was then continued to examine how modifying the structure of the stabiliser with the addition of a comonomer affected the aggregation behaviour, thermal transitions and rheological properties of the dispersions. This work indicated that the modified stabiliser allowed for the synthesis of polymeric particle dispersions which could be used as electrophoretic fluids, without the undesirable gelation occurring.

5.3 Experimental

5.3.1 Apparatus

Dynamic light scattering (DLS) measurements were carried out on colloidal solutions and solutions of block copolymer stabilisers at a range of temperatures using a Zeta-sizer nano series (Nano-ZS) machine, supplied by Malvern Instruments. The z-average, number average and dispersity were measured at temperatures between 10°C and 45°C at a height of 0.85 cm, with measurements taken over a period of 90 seconds with an automatically generated number of scans, ranging from 12-19. Samples were all in dodecane unless otherwise stated.

DSC measurements were obtained using a Netzsch DSC 200 PC, with a protective and purge environment of nitrogen gas. Measurements were taken between -30ºC and 150ºC, at a heating or cooling rate of 10ºC min^{-1}, with cooling regulated by liquid nitrogen. An empty aluminium pan was used as a reference sample, and the machine was calibrated against 5 standards provided by Netzsch.

Rheology measurements were obtained using a Bohlin Gemini rheometer, on loan from the EPSRC (Engineering and Physical Sciences Research Council) Engineering Instrument Pool, with a Peltier plate temperature control unit installed. A 40 mm parallel plate geometry was used for oscillatory measurements, and a 25 mm cone and plate geometry with an angle of 2.5º was used for rotational measurements. Data was processed using Bohlin software.

5.4 Results and Discussion

A number of different stabilisers, dispersions, and related compounds were analysed via DLS, DSC and rheology – these were summarised in Table 5.1.

Table 5.1: summary of samples to be discussed in the following analysis section ([a]- measured by GPC. [b]- measured by SEM, [c]- measured by DLS).

Identity	Type	Structure	M_n	$Đ^a$	D_{SEM}	% SD^b	D_{DLS}	$Đ^c$
S3	Stabiliser	PMMA-*b*-PODA	31130	1.42				
S6	Stabiliser	PMMA-*b*-PODA	12280	1.6				
S7	Stabiliser	PMMA-*b*-(PODA-*co*-PEHA)	14400	1.32				
S8	Stabiliser	PMMA-*b*-(PODA-*co*-PEHA)	16910	1.29				
S10	Stabiliser	HO-PMMA-*b*-(PODA-*co*-PEHA)	18310	1.63				
C2	Stabiliser	PMMA-*co*-PODA	59990	1.39				
D1	Dispersion	PMMA particles			470	7.23	748.8	0.112
D12	Dispersion	PMMA particles			1082	17.1	1442	0.472
D13	Dispersion	PMMA particles			611	8.51	736.4	0.204
D14	Dispersion	PMMA particles			763	19.7	1463	0.283
D26	Dispersion	PMMA particles with 10% MM12			831	12.3	933.0	0.109
D29	Dispersion	PMMA particles with 10% K8			8.31	12.3	178.2	0.194

As described in chapter 3, the gelation of particle dispersions with a solid content of 39 – 47% stabilised by PMMA-*b*-PODA was visible by eye once they had been allowed to stand overnight. One dispersion (D1) was then systematically diluted, from the original 42 % solid content, to roughly 20 %, 10 % and 1 %, and the resulting dispersions were allowed to stand overnight. Only the original dispersion was seen to solidify, whilst the particles in the diluted samples were seen to settle out to the bottom of the vials (shown in Figure 5.6).

Figure 5.6: Settling and gelating processes observed when dilutions of a dispersion (D1) stabilised by PMMA-*b*-PODA (S3) were allowed to stand for a period of time; from left to right - 1%, 10%, 20% and 40% solid content.

In contrast, dispersions synthesised with PMMA-*b*-(PODA-*co*-PEHA) stabilisers exhibited differing behaviour. Figure 5.7 shows these dispersions after varying periods of time. Dispersion D12, stabilised by PMMA-*b*-PODA, showed the expected gelation at room temperature. Dispersion D13, stabilised by PMMA-*b*-(PODA-*co*-PEHA) with 58 molar % EHA in the lyophobic block, exhibited gelation after refrigeration for a short period of time. However, once this dispersion was warmed to room temperature, the dispersion was liquid again, indicating that even a small amount of comonomer was sufficient to reduce the temperature at which gelation occurred. Dispersion D14, stabilised by PMMA-*b*-(PODA-*co*-PEHA) with 73 molar % EHA in the lyophobic block, remained liquid even after a considerable length of time at 4°C. This supported the proposition that the addition of the comonomer disrupts the gelation process, and if the gelation were to occur at all, it would be at a much lower temperature than previously observed.

Figure 5.7: Images of dispersions with varying ratios of EHA comonomer: 1) D12 – stabilised by PMMA-*b*-PODA S6 ; 2) D13 – stabilised by PMMA-*b*-(PODA-*co*-PEHA) S7 after refrigeration; 3) D13 – stabilised by PMMA-*b*-(PODA-co-PEHA) S7 after 30 seconds at room temperature; 4) D14 – stabilised by PMMA-*b*-(PODA-*co*-PEHA) S8 after 24 hours refrigeration.

5.4.1 Dynamic Light Scattering

5.4.1.1 DLS of PMMA-*b*-(PODA) Stabilisers and Dispersions

Dispersions were analysed using DLS to investigate the temperature at which an increase in particle size and dispersity could be observed, which was thought to be due to the aggregation and subsequent gelation of the dispersion. Particle sizes reported were the N_{ave} values – these were chosen due to the highly monodisperse nature of the dispersions, and they were also seen to be in agreement with values obtained by SEM. Figure 5.8 shows the DLS plot for dispersion D1 on cooling from 45ºC to 10ºC. Whilst a considerable increase in dispersity was observed below 20ºC, the same was not immediately obvious for particle size. A slight increase in size was observed, before a dramatic decrease was seen below 15ºC – this is due to aggregates being formed which were larger than the spectrometer could measure, presumably due to the total gelation of the dispersion due to the cessation of Brownian motion.

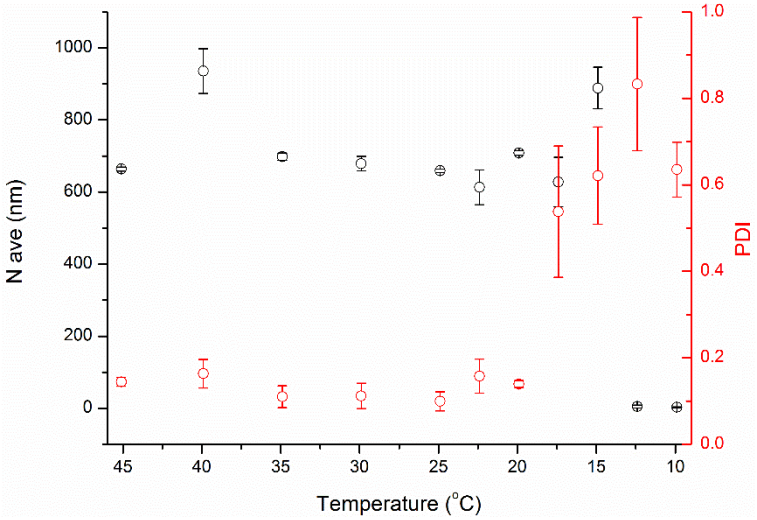

Figure 5.8: DLS results of Nave size and Đ for dispersion D1 with varying temperature.

The weight percentage of solids necessary to cause this gelation was also investigated. To correspond with images presented in Figure 5.6, different dilutions of the PMMA particles of dispersion 1 were made up, and analysed by cooling runs (shown in Figure 5.9). All samples (containing 20 wt %, 10 wt% and 1 wt% solids) exhibited an increased particle size as predicted for a solution being cooled. The decreased particle size for the sample containing 20 wt % solids was thought to be

due to aggregates forming which were larger than could be measured by the spectrometer. Smaller aggregates were also observed for the more dilute 1 wt% dispersion, which was as expected, due to fewer particles present in the sample to form aggregates. For all concentrations, the increased size was observed when the sample was cooled below 15ºC. The precise temperature at which the aggregation occurs can be more accurately observed via other analytical techniques, such as DSC. Although the transitions were seen to occur slightly earlier when analysing Đ for all three samples (shown in Figure 5.10), the trend was the same as for the aggregate size.

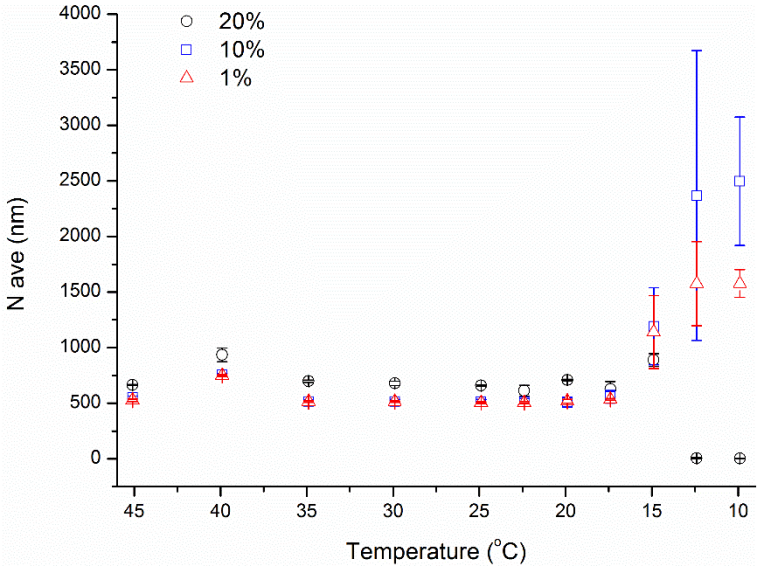

Figure 5.9: DLS results for dilutions of D1, containing 20 wt%, 10 wt% and 1 wt% solids.

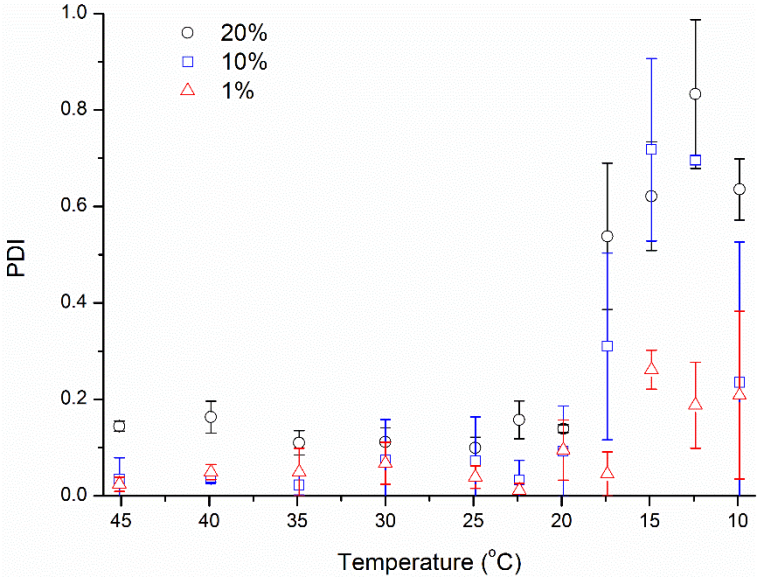

Figure 5.10: Đ results for dilutions of D1, containing 20 wt%, 10 wt% and 1 wt% solids.

These observations of increased aggregate size were confirmed by the N-average intensity plot shown in Figure 5.11, with the measurements at 45ºC (dashed lines) confirming the particle size remains constant regardless of the dilution. The solid lines show the differing aggregate sizes for the diluted dispersions at 10ºC – the smallest aggregates (around 2000 nm) were seen at 1 wt%, with larger aggregates (around 3000 nm) at 10 wt%, whilst at 20 wt% solids the aggregates formed were larger than the capability of the spectrometer. This measurement suggests that there were particles as small as 1 nm present in solution which was attributed to either the Zetasizer attempting to calculate a size for a sample which was no longer exhibiting any Brownian motion (as all large aggregates had settled out), or the presence of small isolated polymer chains in solution.

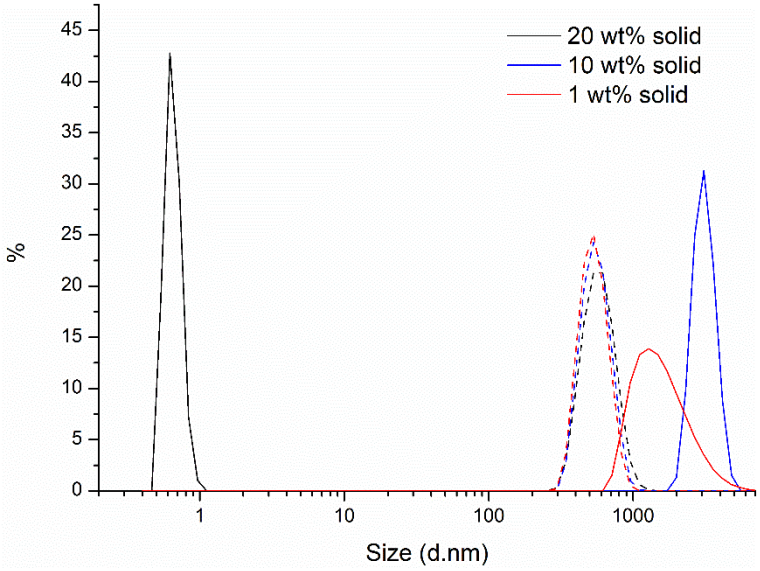

Figure 5.11: N-average plots of D1 at various dilutions and temperatures, with dashed lines representing data for 45ºC (above gelation) and solid lines representing data at 10ºC (below gelation).

A sample of stabiliser S3 (10 wt %) in dodecane was made up, and allowed to stand for a period of two days. This sample was also seen to solidify, but on increasing the temperature the sample was seen to redisperse. This was not unexpected, as the side chains in the copolymer could order themselves once in solution, and the ODA content of 10 % stabiliser in dodecane was actually higher than the ODA content of a dispersion, where only 5 wt % stabiliser was added.

Figure 5.12 shows a comparison for a solution of PMMA-*b*-PODA stabiliser (S3) (10 wt %) in dodecane and the PMMA dispersion (D1) which was stabilised by it.

Above the temperature of gelation, the stabiliser was seen to produce aggregates of around 30 nm – this was consistent with the expected size of micelles of PMMA-*b*-PODA in solution. The characteristic increase in size attributed to the aggregation or gelation process was observed for both the stabiliser and the dispersion, but was considerably sharper for the stabiliser alone, starting below 22.5ºC and reaching a maximum at 15ºC. However, for the particle dispersion, not only was the onset of the increase much later, not occurring until below 17.5ºC, but it was also noticeably less dramatic. While the largest aggregates measured for the stabiliser were up to 450 times the size of the stabiliser at higher temperature, the dispersion only exhibited a 5 fold increase. One possible explanation for this was that the stabiliser micelles were considerably smaller than the stabilised particles, meaning they can move faster through solution and arrange themselves more readily. It should be noted that this data was for a diluted dispersion of 10 wt% solid, due to the inability of the spectrometer to 'size' the aggregates formed in a 20 % solid content dispersion sample.

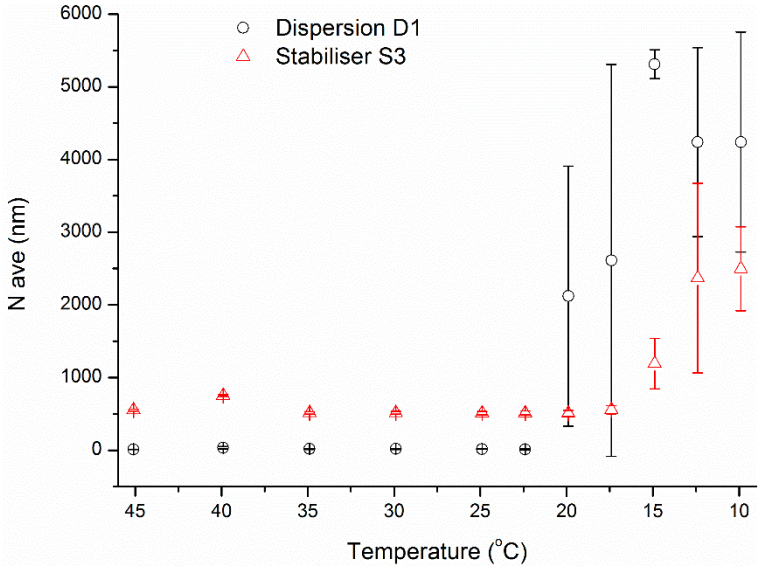

Figure 5.12: Comparison of DLS results for dispersion D1 and stabiliser S3 in dodecane (S3 was the stabiliser used in the synthesis of D1). Due to the large aggregates formed for 20 wt% solids, this comparison is for D1 at 10 wt% solids.

In order to determine which component of the dispersion was causing the gelation, a number of different samples were analysed by DLS. The N_{ave} sizes for octadecane, octadecyl acrylate and PODA are shown in Figure 5.13 – the dramatic increase in size below 20ºC was only observed for the polymeric sample, with no variation seen

for either octadecane and octadecyl acrylate. This suggested that the process was not solely due to long alkyl chains being present, as this could be said of both ODA and octadecane, but due to the arrangement of these chains once they have been polymerised.

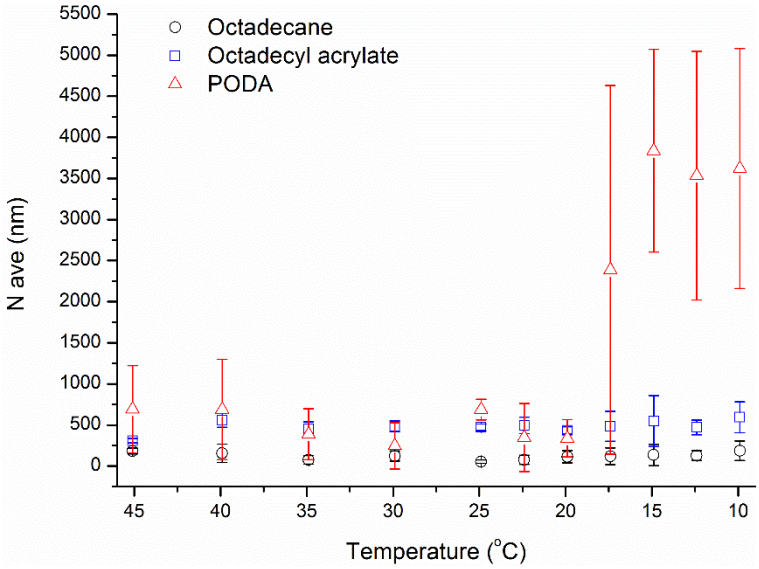

Figure 5.13: Nave particle sizes for octadecane, octadecyl acrylate and poly(octadecyl acrylate).

Whilst these DLS measurements support the findings that the dispersion sample undergoes a thermoresponsive transition which was directly related to the arrangement of the long alkyl side chains of the copolymer stabiliser, the exact temperature at which this occurs and further details of the type of transition required DSC and rheological analysis.

5.4.1.2 DLS of PMMA-*b*-(PODA-*co*-PEHA) Stabilisers and Dispersions

Dispersions stabilised by PMMA-*b*-(PODA-*co*-PEHA) were then subjected to the same DLS testing as previous dispersions, with D12 used as a comparison (as the stabilisers in dispersions D12, D13 and D14 were all synthesised from the same PMMA macroinitiator). Figure 5.14 shows the results of these cooling runs. D12, stabilised by PMMA-*b*-PODA showed the expected increase in both particle size and dispersity below 22.5°C, resulting in complete gelation which the DLS was unable to measure. D13, stabilised by PMMA-*b*-(PODA-*co*-PEHA) with 58 molar % EHA, showed an aggregation (by both particle size and Đ) which did not occur until after

17.5°C. This was consistent with what was observed when the sample was refrigerated and then heated back to room temperature. D14, stabilised by PMMA-*b*-(PODA-*co*-PEHA) with 73 molar % EHA, did not appear to exhibit any increase in particle size or dispersity even when cooled to 10°C. The fluctuations observed were to be expected for any colloidal dispersion due to the inherent Brownian motion of the particles.

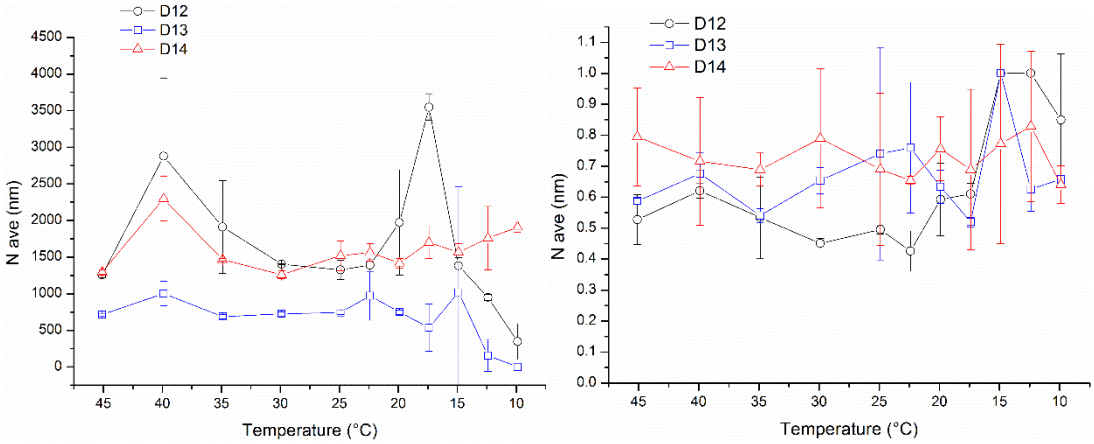

Figure 5.14: DLS data for dispersions D12 (black), D13 (red) and D14 (blue) showing Nave (left) and Đ (right) during a cooling run. For both cases it was clear that aggregation and gelation occurred at a higher temperature for D12 than D13, whilst both size and Đ remain relatively constant for D14, indicating an absence of gelation.

The stabilisers used in the synthesis of dispersions D12, D13 and D14 were also placed into solution (in dodecane) and analysed by DLS. The same trends were observed for these samples (shown in Figure 5.15), with one exception. Although it was observed that the Đ of stabiliser S7 increased at a lower temperature than S6, the size data suggested that aggregation occurred at roughly the same temperature for both samples. The temperature at which this increase occurred for both S6 and S7 was also observed to be lower than for their respective dispersions D12 and D13. This was in contrast to the observations made about the previous set of samples, where S3 was seen to aggregate at a higher temperature than its corresponding dispersion D1. However, this can be justified for two reasons – in this case, the dispersions measured were at a higher solids concentration than for the previous samples (42% as opposed to 20%), meaning there were more particles with stabilising side chains to participate in the gelation process. The alkyl chains would also be more ordered when at a particle surface than when they form stabiliser micelles, and this order would further aid gelation.

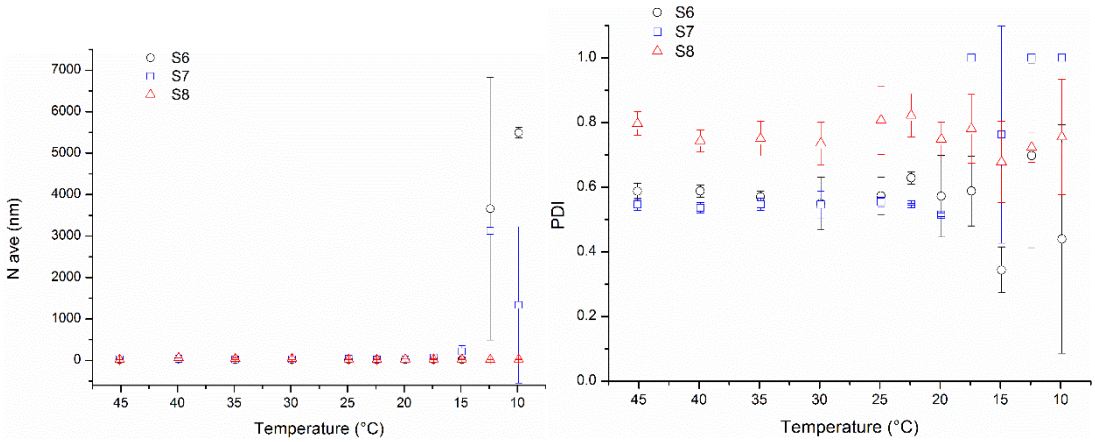

Figure 5.15: DLS data for stabilisers S6 (black), S7 (red) S8 (blue) showing Nave (left) and Đ (right) during a cooling run. As for the dispersion data, it was clear that aggregation and gelation occurred for S6 and S7, whilst both size and Đ remain relatively constant for S8, indicating an absence of gelation.

To further confirm these findings, DSC and rheological data was obtained for the range of dispersions and stabilisers containing various molar percentages of ethyl hexyl acrylate.

5.4.2 Differential Scanning Calorimetry

5.4.2.1 DSC of PMMA-*b*-(PODA) Stabilisers and Dispersions

Thermograms were first obtained for the homopolymers of PMMA and PODA in order to determine their thermal transitions. Whilst PMMA has a small thermal transition, corresponding to its T_g at around 100ºC, PODA has a considerably larger transition at around 50ºC. Data was also obtained for dodecane (as it was the solvent for all particle dispersions), and two transitions were observed – the T_m at around -11ºC, and another at approximately 180ºC, corresponding to the temperature at which dodecane is known to evaporate. All data regarding thermal transitions discussed in this section is reported in Table 4.2.

It was important to determine the transitions for each individual component within the system, in order to interpret data for copolymers and dispersions effectively.

Table 5.2: Table to show the onsets, peaks and ΔH values measured by DSC for various samples. Data shown was taken from a heating run.

Identity	T_m			T_m and T_{gel}			T_g		
	Onset (ºC)	Peak (ºC)	ΔH (J/g)	Onset (ºC)	Peak (ºC)	ΔH (J/g)	Onset (ºC)	Peak (ºC)	ΔH (J/g)
PMMA							98.9	109	-2.010
PODA				46.6	54.5	-98.3			
Dodecane	-11.0	-2.1	-249.3						
C2				21.0	27.3	-16.11			
S3				44.9	49.8	-77.98	103.1	109.9	-1.985
S3 in dodecane	-12.8	-5.7	-220.4	26.0	28.6	-63.70			
D1	-13.4	-8.0	-183.5	23.1	24.7	-13.49			

The transitions for the homopolymers of PMMA and PODA, together with dodecane, are shown in Figure 5.16. The melting transitions of PMMA observed at 98.9°C, PODA observed at 46.6°C and the two transitions of dodecane observed at -12.7°C and 178.3°C were consistent with literature values.[6, 32, 33]

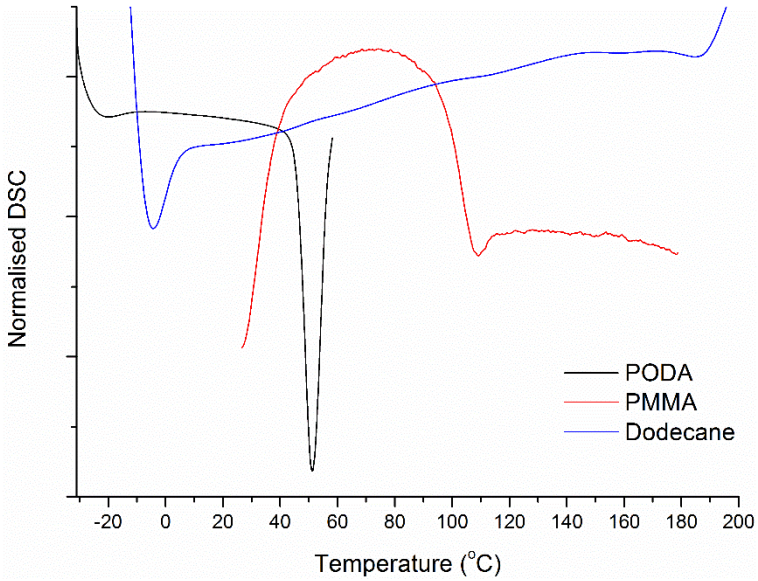

Figure 5.16: DSC thermogram showing transitions for the bulk materials of: homopolymers PMMA and PODA, and dodecane. Data was taken from a heating run.

Figure 5.17 shows a comparison of the thermal transitions observed for block copolymer S3 when analysed alone, and also when dissolved in dodecane. Two transitions can be observed for the stabiliser – one with an onset of 44.9°C, which

corresponds to the T_m of PODA, and one (much smaller transition) with an onset of 103.1°C which corresponds to the T_g of PMMA. This data was expected, as the blocks of the copolymer are made of components with significantly different properties, resulting in phase separation and multiple transitions. However, as expected when the stabiliser S3 was dissolved in dodecane, these transitions were no longer observed. A large transition with a ΔH value of -220.4 J/g was observed at -12.8°C, consistent with the T_m of dodecane.[33] A new transition was also observed with a ΔH value of -63.7 J/g. The onset of this transition was at 26°C, which was in the same region as the transition observed for the stabilised dispersion D1 (Figure 5.16). The values of ΔH were calculated from the area above the curve for each transition, and then adjusted to attribute each transition to only one component of the system i.e. the transition at -12.8°C was solely attributed to the dodecane, and the transition at 26°C was attributed to the stabiliser.

Once the stabiliser was dissolved in dodecane, DLS size analysis suggested that the stabiliser was forming micelles of around 30 nm (Figure 5.12). This arrangement of the stabiliser molecules would mirror the brush-like arrangement of the stabiliser at a particle surface. This arrangement was seen to be crucial for gelation to occur by DLS analysis – octadecane and octadecyl acrylate did not exhibit any temperature responsive aggregation, but once the units were aligned with each other in a polymeric arrangement, the aggregation occurred at around 20°C. This was supported by this DSC analysis, whereby the normal T_m values of the components in the stabiliser were no longer observed, whilst the new transition corresponding to the gelation of the block copolymer was seen. This transition had an onset of 26.0°C.

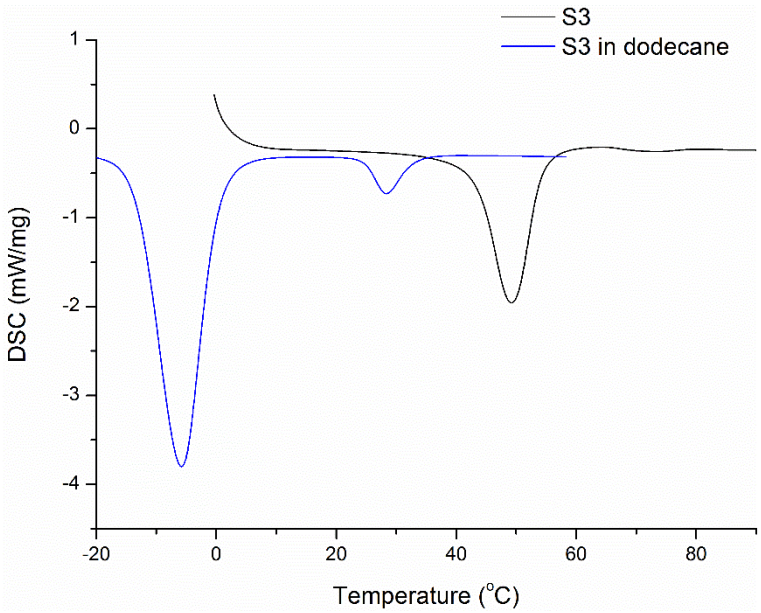

Figure 5.17: DSC thermogram showing the transitions observed for stabiliser S3 alone (black), and when solubilised by dodecane (10 wt %) (blue). Data was taken from a heating run.

The thermogram for the transitions of the dispersion D1 are shown in Figure 5.18 – the large transition (ΔH of -183.5 J/g) corresponds to the melting temperature of the dodecane within the dispersion. There was also a much smaller transition at 23.1°C (ΔH value of -13.49 J/g), consistent with the temperature at which gelation was observed for the stabiliser in dodecane (Figure 5.15), and close to the gelation by DLS.

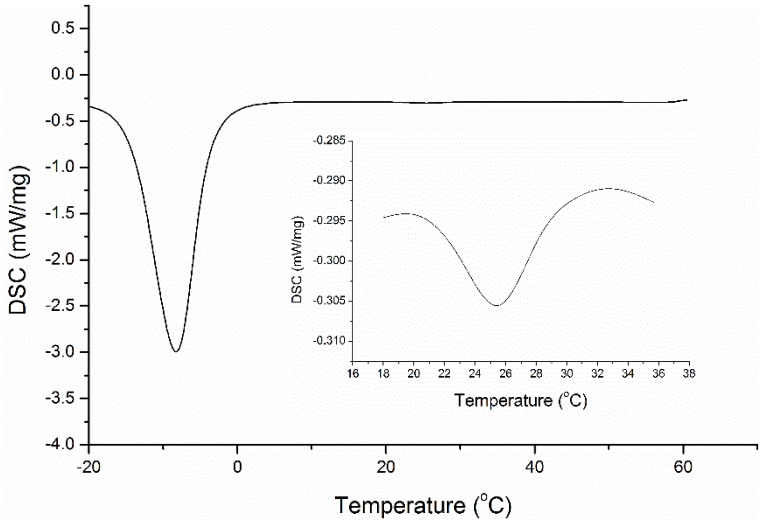

Figure 5.18: DSC thermogram showing the transitions observed for the polymeric dispersion D1 – inset is a magnification of the transition at 23.1°C. Data was taken from a heating run.

The transitions seen by DSC all occurred slightly higher values than by DLS, but this was due to the fact that DSC measurements were taken for heating runs, whilst DLS data was obtained by cooling runs. This means that the DSC data was showing melting transitions (endothermic), whilst DLS was recording exothermic transitions. For this reason, cooling measurements were also obtained, shown in Table 5.3. The temperature at which the particles were seen to redisperse, T_{degel}, correlated more closely for these cooling measurements with the DLS cooling data for both S3 in dodecane and D1.

Table 5.3: Table showing the onsets, peaks and ΔH values measured by DSC for various samples. Data shown was taken from a cooling run.

Identity	T_c			T_c and T_{gel}		
	Onset (ºC)	**Peak (ºC)**	**ΔH (J/g)**	**Onset (ºC)**	**Peak (ºC)**	**ΔH (J/g)**
PODA	41.2	36.3	112.3			
Dodecane	-14.2	-16.4	43.43			
C2	16.2	9.2	11.3			
S3	39.7	35.7	87.17			
S3 in dodecane	-19.9	-21.5	131.8	17.7	15.4	65.45
D1	-21.2	-22.2	162.6	11.8	10.7	10.94

5.4.2.2 DSC of PMMA-*b*-(PODA-*co*-PEHA) Stabilisers and Dispersions

DSC data was then obtained for stabiliser S8, containing 73 molar % EHA in the lyophobic block (Figure 5.19). This stabiliser showed a considerably broader transition between 25°C and 50°C than for PMMA-*b*-PODA stabilisers in dodecane, which was due to the EHA disrupting the order of the ODA side chains, meaning the transition occurred over a much wider temperature range. The ΔH value for the T_m was measured to be -60.36 J/g (and 69.35 J/g for the T_c of the cooling run), which was comparable to the T_m observed in the same region for S3.

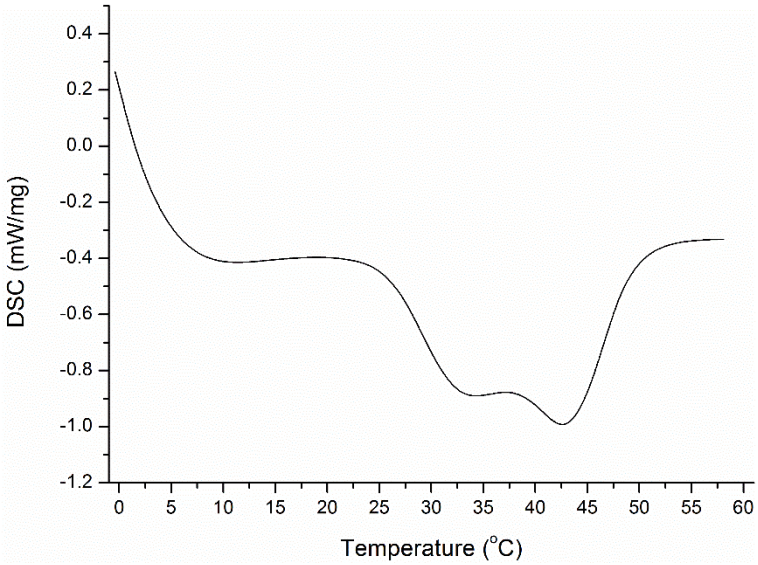

Figure 5.19: DSC thermogram showing the transition observed for the stabiliser S8. Data was taken from a heating run.

Data was not collected for the PMMA-*b*-(PODA-*co*-PEHA) stabilisers in dodecane or dispersions stabilised by them, as DLS data and rheology data (presented in section 5.4.3.2) agreed with the observations made by eye.

5.4.3 Rheology

5.4.3.1 Rheology of PMMA-*b*-(PODA) Stabilisers and Dispersions

Measurements of polymeric stabilisers and dispersions were taken via both rotational and oscillatory modes of the rheometer, allowing for data about the viscosity of the samples to be obtained, together with data on the viscoelastic properties of the materials.

Firstly, measurements of D1 were taken in rotational mode, steadily decreasing the temperature from 45ºC to 5ºC. This was to determine the temperature at which the viscosity of the dispersion increased, consistent with the gelation observed by eye and by DLS. The plot for viscosity with decreasing temperature is shown in Figure 5.20, with a constant low viscosity observed until 16.3ºC – at this point a dramatic increase in viscosity was observed. As the temperature was further decreased, the viscosity was seen to decrease again, which would suggest the 'gel' became more fluid at a lower temperature. However, this was not observed either by eye or by

DLS measurements, meaning this reduced viscosity was unexpected. During this measurement, shear stress required to keep the shear strain at a consistent level was measured, allowing for the calculation of viscosity according to equation 4.4 (viscosity = shear stress/shear rate). Once the sample solidified, a greater amount of shear stress was required - it is possible that, due to the sample being a gel rather than completely solid, the amount of stress required varied due to the flexible nature of the sample and its capability to move. Another possible explanation was that the sample actually possesses a yield stress, and that once this level of stress was applied to the sample after the increase in viscosity, the material was again capable of flowing.

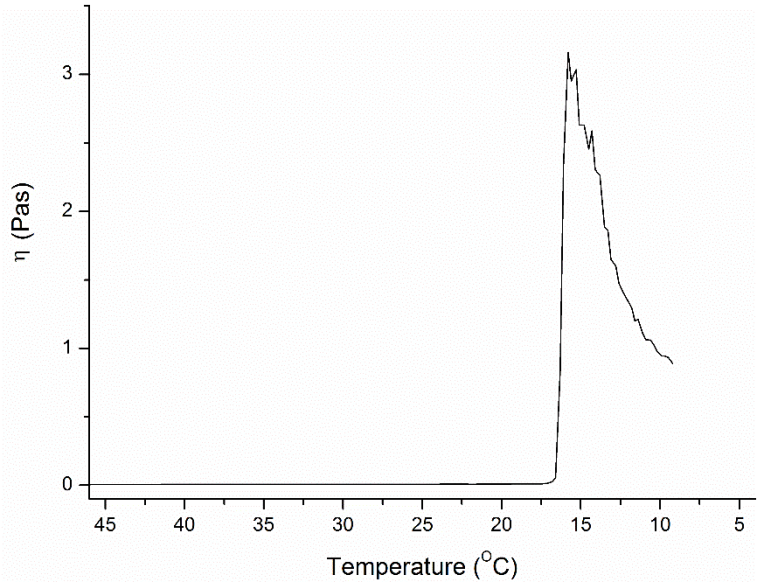

Figure 5.20: Plot showing the change in viscosity of D1 with change in temperature.

Next, oscillatory measurements were taken of D1 to investigate the viscoelastic nature of the sample, shown in Figure 5.21. At high temperatures, G'' was seen to be larger than G', giving a high phase angle (of around 70º), which was consistent with a sample which could flow and was behaving as a liquid. Below 20ºC, a slight increase in both G' and G'' was observed, before a dramatic increase was seen at 17.5ºC, with G' being greater than G''. This lead to a drop in phase angle, initially down to around 10°, showing that the sample was behaving more as a solid. However, this phase angle was seen to fluctuate, averaging at closer to 45°. This was not entirely unexpected, as a phase angle of 45° indicates a sample which has both solid-like and liquid-like behaviour, also known as a gel.

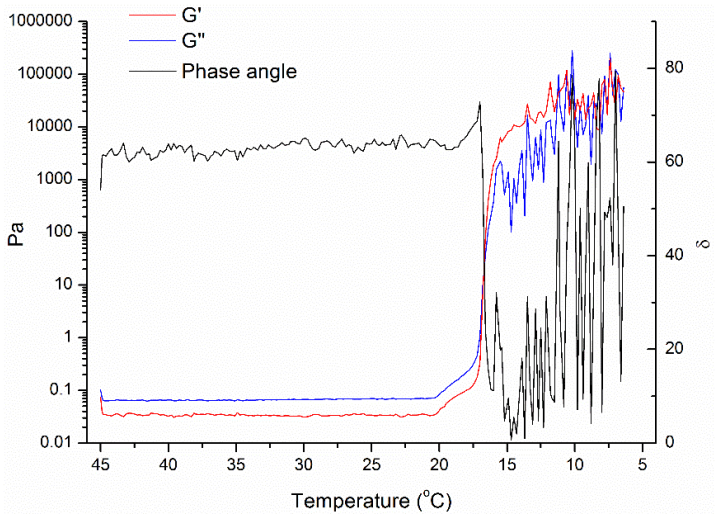

Figure 5.21: plot showing the change in viscous modulus, storage modulus and phase angle of D1 with change in temperature.

The temperature at which the increase in viscosity and decreased phase angle was observed for D1 was consistent with the temperature at which increased aggregate size was seen by DLS measurements.

Colloidal dispersions are typically stable under shear – at up to 20% volume concentration, dispersions exhibit Newtonian behaviour. Above this concentration, samples are seen to be stable only under smaller shears. Typically the particle dispersions produced in this work contain around 40% solids, but they appeared stable to relatively large levels of shear if a constant temperature was maintained. This data is shown in Figure 5.22. As the rate of shear was increased, the shear stress increased proportionally, but without any increase in the sample viscosity.

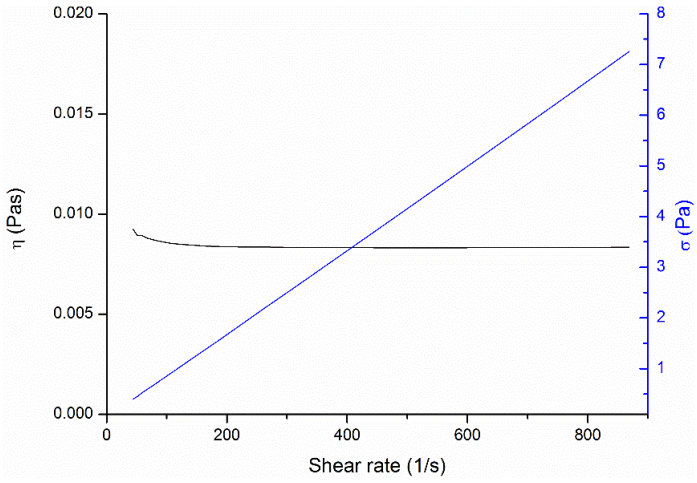

Figure 5.22: Plot showing the shear stress and viscosity of D1 with increasing shear rate (measured at 25°C, which is above the temperature at which the thermal transition is observed).

It would potentially be possible to calculate the thickness of the stabiliser barrier using data obtained for the hydrodynamic volume of the particles in the dispersion (from DLS), together with the measured viscosity.[34] However, this would require measurements of viscosity under a wider range of conditions than the time with the rheometer allowed.

5.4.3.2 Rheology of PMMA-*b*-(PODA-*co*-PEHA) Stabilisers and Dispersions

Dispersion D14, stabilised by PMMA-*b*-(PODA-*co*-PEHA) containing 73 molar % EHA, was tested by rotational measurements in order to determine the change in viscosity as a function of temperature (Figure 5.23). Whilst a slight increase in viscosity was observed when the temperature was decreased from 50°C to 5°C, there was no dramatic increase consistent with a thermoresponsive gelation as previously observed for dispersion D1. The increase was also of a considerably smaller magnitude to that of D1 – D1 increased from 0.007 Pas to 0.9 Pas, whilst D14 only increased from 0.008 Pas to 0.02 Pas. As such, this small increase in viscosity can be attributed to the reduced velocity of the particles at a reduced temperature.

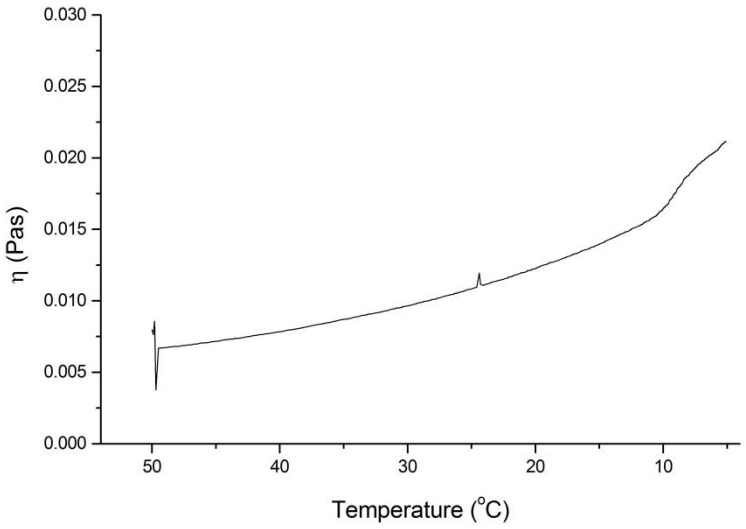

Figure 5.23: Plot showing the change in viscosity of D14 with change in temperature.

The same was true for dispersions D26 and D29 – whilst there was a small increase in viscosity as the temperature was decreased, no dramatic increase which would correspond to a gelation process was observed (Figure 5.24). This further indicated

that the addition of dyes (D26) and the particle size (D29 – *ca*. 100 nm particles) did not contribute to the gelation.

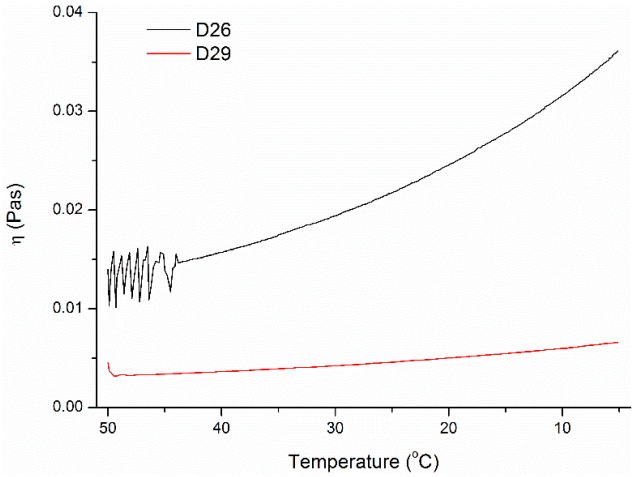

Figure 5.24: Plot showing the change in viscosity of D26 and D29 with change in temperature.

Dispersions D13 and D14 were then analysed using oscillatory measurements in order to observe the differing viscoelastic properties arising from the EHA content of the stabiliser (shown in Figures 5.25 and 5.26). D13 exhibited an increase in both G' and G'' below 15°C, giving the decreased phase angle consistent with the sample behaving more as a solid than as a liquid (Figure 5.25). As expected, this transition occurred at a lower temperature than for dispersions containing no comonomer, and the increase in the values of G' and G'' was 2 orders of magnitude smaller than the same transition for PMMA-*b*-PODA stabilised dispersions. This was in agreement with measurements obtained by DLS for the gelation process.

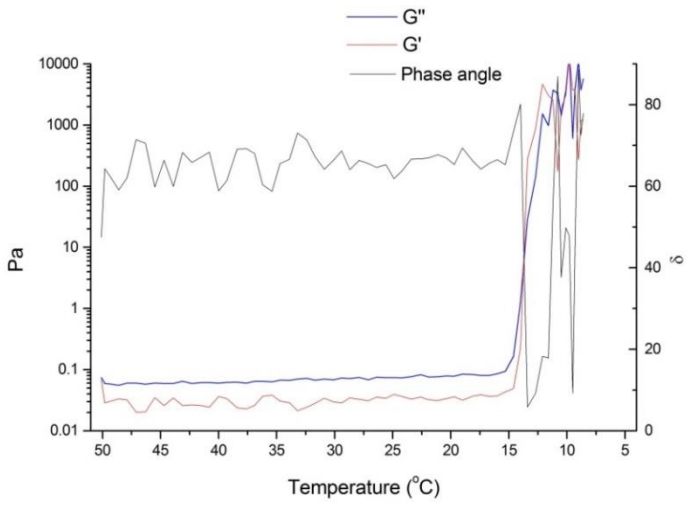

Figure 5.25: plot showing the change in viscous modulus, storage modulus and phase angle of D13 with change in temperature.

D14, in contrast, did not exhibit the dramatic increase in G' and G'', with the values for both of these moduli and the value for phase angle remaining relatively constant down to a temperature of 5°C (Figure 5.26). The phase angle was consistently at around 70°C, indicating the sample was more 'liquid-like' than 'solid-like' across all temperatures measured.

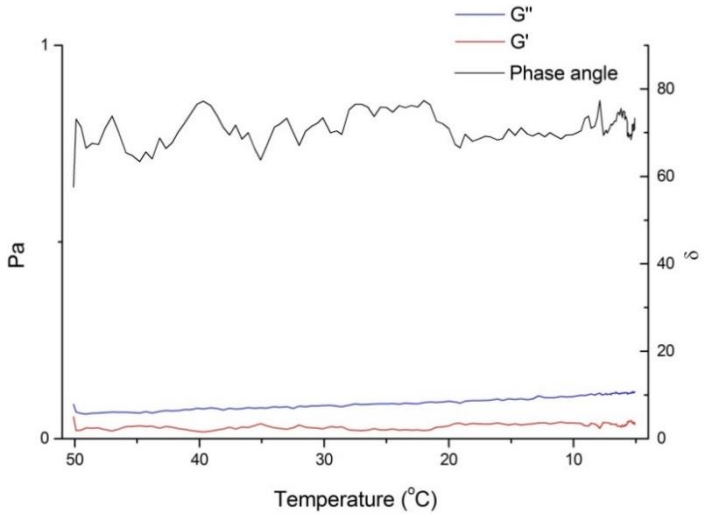

Figure 5.26: plot showing the change in viscous modulus, storage modulus and phase angle of D14 with change in temperature.

5.5 Conclusions

The various analyses of PMMA-*b*-PODA stabilisers themselves, together with data for the stabilised dispersions have eliminated a number of possible explanations for the observed gelation. Firstly, the temperature at which the gelation was observed did not correlate with the T_m of dodecane, so a purely solvent based transition can be dismissed. Neither did it directly correspond to the T_m of PMMA or PODA, indicating that the transition was not just a melting transition. A table summarising the transitions seen for each sample shown below (Table 5.4).

Table 5.4: Summary of thermal transitions observed by various samples, obtained by DLS, DSC and rheology. Data was all for cooling runs, except for values marked with *, which were obtained during heating runs. Shaded squares denote measurements which were not taken.

	Thermal transition observed at (°C)				
	DLS	DSC			Rheology
	T_{gel}	T_g*	T_c	T_{gel}	T_{gel}
PMMA	None observed	98.9	-	-	
PODA	None observed	-	46.6	-	
Dodecane		-	-16.4	-	
C2	None observed	-	16.2	-	
S3	None observed	-	39.7	-	
S3 in dodecane	22.5	-	-21.5	17.7	
D1	15.0	-	-22.2	11.8	17.5

The DLS data for samples containing 18 carbon alkyl chains (octadecane and ODA) that were not ordered or arranged in any particular manner did not show the same increase in aggregation under reduced temperature as was observed for the block copolymer and dispersion. This suggested that the steric arrangement of the alkyl chains was crucial for the gelation to occur, and not just the presence of long carbon chains.

DSC results indicated that in bulk, the block copolymer S3 exhibited thermal transitions corresponding to both the blocks incorporated within it. However, this was not the case when the PMMA-*b*-PODA was dissolved in dodecane. At low temperatures, the polymer chains were seen to precipitate out, and at sufficiently high quantities of stabiliser (10 weight %), the sample was seen to gelate. This precipitation process was due to the upper critical solution temperature (UCST) of the PMMA-*b*-PODA, and resulted in the ordering and crystallisation of the side chains and ultimately the gelation of the sample. This was observed as a transition at 17.7°C by DSC, and approximately 22.5°C by DLS.

DSC analysis of the particle dispersion D1 showed a thermal transition at 11.8°C, which was close to that observed for S3 in dodecane – this was supported by DLS data which measured a dramatic increase in particle size at approximately the same temperature for both of these samples. This transition was confirmed as a gelation by the changes in phase angle (from behaving as a solid-like material with a phase

angle of nearly 90° to a gel-like material with a phase angle of approximately 45°) and a dramatic increase in viscosity measured by rheology. Perhaps the key observation was the presence of a transition for both samples (D1 and S3 in dodecane) which corresponded to the crystallisation of previously amorphous regions of dodecane.

All of these findings were in agreement with literature discussing long alkyl chains at the surface of silica particles or silicon wafers. This work found that at high temperatures, alkyl chains were relaxed and disordered with solvent molecules present within the brush. However, at low temperatures, a phase transition occurred which resulted in an increased brush thickness due to the alkyl chains straightening and becoming ordered, interdigitating with the solvent molecules.[16] This was in turn demonstrated to increase the particle-particle attraction due to Van der Waals forces, resulting in aggregation and then gelation of the colloidal system.[20]

The addition of a second monomer to the lyophilic block of the stabiliser, specifically chosen to disrupt the packing order of the alkyl chains, was seen to disrupt the gelation process of dispersions. Gelation was seen to occur in dispersions containing stabiliser S7 (58% EHA) at a lower temperature than those stabilised by PMMA-*b*-PODA, whilst no gelation was observed down to 5°C for dispersions stabilised by S8 (73% EHA). This was confirmed by DLS, which showed the same trends for both the particle dispersions D12 – D14, and their stabilisers S6 – S8. Rheology of D14 showed that the EHA content of 73% was sufficient to prevent any increase in viscosity or decrease in phase angle down to temperatures of 5°C.

Although for this industrially based project the observed thermally responsive nature was undesirable, there are a number of applications in which it could be valuable. If the temperature at which the gelation occurs could be tuned, there is the potential that this system could find uses in a number of areas, mainly within biomedical applications, such as for temperature responsive drug delivery systems and cell carriers.[35] A starting point for this investigation would to be look at how the temperature of this gelation changes in relation to the ratio of PMMA to PODA.

5.6 References

1. E. F. Jordan, B. Artymyshyn, A. Speca and A. N. Wrigley, *Journal of Polymer Science Part A-1: Polymer Chemistry*, 1971, **9**, 3349-3365.
2. T. Hirabayashi, T. Kikuta, K. Kasabou and K. Yokota, *Polym J*, 1988, **20**, 693-698.
3. Y. Kagami, J. P. Gong and Y. Osada, *Macromol. Rapid Commun.*, 1996, **17**, 539-543.
4. G. Reiter and G. R. Strobl, *Progress in Understanding of Polymer Crystallization*, Springer, 2007.
5. W. M. Groenewoud, *Characterisation of Polymers by Thermal Analysis*, Elsevier Science, 2001.
6. E. F. Jordan, D. W. Feldeisen and A. N. Wrigley, *Journal of Polymer Science Part A-1: Polymer Chemistry*, 1971, **9**, 1835-1851.
7. V. P. Shibaev, B. S. Petrukhin, Y. A. Zubov, N. A. Plate and V. A. Kargin, *J. Polym. Sci., Part A-1: Polym. Chem.*, 1971, **9**, 2291-2298.
8. Z. Mogri and D. R. Paul, *Polymer*, 2000, **42**, 2531-2542.
9. S. Srichan, N. Kayunkid, L. Oswald, B. Lotz and J.-F. Lutz, *Macromolecules (Washington, DC, U. S.)*, 2014, **47**, 1570-1577.
10. H. W. S. Hsieh, B. Post and H. Morawetz, *Journal of Polymer Science: Polymer Physics Edition*, 1976, **14**, 1241-1255.
11. K. A. O'Leary and D. R. Paul, *Polymer*, 2006, **47**, 1226-1244.
12. D. Curcó and C. Alemán, *Journal of Polymer Science Part B: Polymer Physics*, 2006, **44**, 953-966.
13. X. Zhu, Y. Gu, G. Chen, Z. Cheng and J. Lu, *Journal of Applied Polymer Science*, 2004, **93**, 1539-1545.
14. A. Matsuda, J. i. Sato, H. Yasunaga and Y. Osada, *Macromolecules*, 1994, **27**, 7695-7698.
15. N. A. Plate and V. P. Shibaev, *J. Polym. Sci., Macromol. Rev.*, 1974, **8**, 117-253.

16. A. P. R. Eberle, N. J. Wagner, B. Akgun and S. K. Satija, *Langmuir*, 2010, **26**, 3003-3007.

17. K. Loyen, I. Iliopoulos, R. Audebert and U. Olsson, *Langmuir*, 1995, **11**, 1053-1056.

18. J. S. Shay, S. R. Raghavan and S. A. Khan, *J. Rheol. (N. Y., NY, U. S.)*, 2001, **45**, 913-927.

19. C. Alava and B. R. Saunders, *J. Colloid Interface Sci.*, 2006, **293**, 93-100.

20. S. Roke, O. Berg, J. Buitenhuis, A. van Blaaderen and M. Bonn, *Proceedings of the National Academy of Sciences*, 2006, **103**, 13310-13314.

21. M. Morgan, Fielding, L.A. and Armes, S.P., *Colloid Polym. Sci.*, 2013, **291**, 77-86.

22. A. Tiwari and A. Tiwari, *Bioengineered Nanomaterials*, Taylor & Francis, 2013.

23. V. Nigro, R. Angelini, M. Bertoldo, V. Castelvetro, G. Ruocco and B. Ruzicka, *Journal of Non-Crystalline Solids*, 2015, **407**, 361-366.

24. C. Manuela, A. Katel Hervé, A. Amélie, F. Jean-François, S. Martin and C. Igor, *Nanotechnology*, 2013, **24**, 395605.

25. K. Nishinari, *Colloid Polym. Sci.*, 1997, **275**, 1093-1107.

26. P. A. Nommensen, M. H. G. Duits, J. S. Lopulissa, D. Van den Ende and J. Mellema, *Prog. Colloid Polym. Sci.*, 1998, **110**, 144-149.

27. J. Mewis and N. J. Wagner, *Colloidal Suspension Rheology*, Cambridge University Press, 2011.

28. G. Fritz, V. Schädler, N. Willenbacher and N. J. Wagner, *Langmuir*, 2002, **18**, 6381-6390.

29. A. Ponton, D. Quemada, F. Lafuma and O. Neel, *Colloids and Surfaces A: Physicochemical and Engineering Aspects*, 1996, **119**, 255-259.

30. S. R. Raghavan, J. Hou, G. L. Baker and S. A. Khan, *Langmuir*, 2000, **16**, 1066-1077.

31. G. S. Grover and S. G. Bike, *Langmuir*, 1995, **11**, 1807-1812.

32. B. H. Stuart, *Polymer Analysis*, Wiley, 2002.

33. NIST Webbook - Dodecane. (accessed 2 January 2015), http://webbook.nist.gov/cgi/cbook.cgi?ID=C112403&Mask=1EFF.

34. D. J. Walbridge and J. A. Waters, *Discussions of the Faraday Society*, 1966, **42**, 294-300.

35. L. Klouda and A. G. Mikos, *European journal of pharmaceutics and biopharmaceutics : official journal of Arbeitsgemeinschaft fur Pharmazeutische Verfahrenstechnik e.V*, 2008, **68**, 34-45.

Chapter 6 – Conclusions and Further Work

6.1 Conclusions

The main aim of the work presented in this thesis was to develop block copolymer stabilisers for use in non-aqueous dispersion polymerisations. PMMA was chosen as the lyophobic block (or 'anchor component') of the stabiliser, which would become incorporated into the particle, and PODA was chosen as the lyophilic block, which would remain at the particle solvent interface. The aim was to use these stabilisers in NAD polymerisations together with polymerisable dyes and cross-linkers, ultimately to synthesise dispersions which could be converted into electrophoretic inks. This work also aimed to allow for the functionalization of the stabiliser in various different ways to add desirable properties to the particles.

PMMA-*b*-PODA block copolymers were synthesised via ATRP. Firstly, PMMA macroinitiators were synthesised on a small scale, with components of the reaction being systematically varied until the optimum polymeric properties (low dispersity and reproducibility of the reaction) were obtained. Macroinitiator samples were obtained with dispersities as low as 1.11, with molecular weights ranging from 2600 to 12500 $gmol^{-1}$. It was shown that adapting the catalyst system from CuBr to CuCl with 5 molar % $CuCl_2$, and changing the ligand from PPMI to PMDETA, provided the best control over the polymerisation. A number of attempts at synthesising PMMA macroinitiators using Cu(0) mediated ATRP and SET-LRP were made, with the aim of improving the dispersity and the 'livingness' of the polymers. The polymers synthesised by Cu(0) ATRP produced polymers with very low dispersities (1.1), but these reactions were seen to be very slow (up to 72 hours). On the other hand, those synthesised by SET-LRP were seen to be quicker but much less controlled with regards to dispersity (around 1.5) and chain length (in some cases double that which was targeted). MALDI analysis also showed that the polymers

synthesised by SET had a greater proportion of terminated chains than those synthesised by ATRP, and as such SET was not considered further.

These initiators were then used to polymerise ODA to synthesise the block copolymers – this second step was seen to be considerably slower than the PMMA synthesis (up to 6 days) due to the lower reactivity of ODA. Initially, bimodal samples were observed by GPC analysis – this was due to the macroinitiator synthesis reaching near completion and a proportion of the PMMA chains losing their halide end cap, meaning they could not be further polymerised. It was found that a 'backwards precipitation' could remove these unreacted macroinitiator chains from the block copolymer sample, although after the macroinitiator synthesis was optimised this step became unnecessary. Block copolymers were synthesised with molecular weights ranging from 12300 to 54200 $gmol^{-1}$, and with dispersities between 1.2 and 1.6.

The PMMA-*b*-PODA block copolymers were then used as the stabiliser in the non-aqueous dispersion polymerisation of MMA in place of the stabiliser which had previously been used, PHSA-*g*-PMMA. The dispersion samples prepared by NAD polymerisation were seen to contain particles which were very monodisperse, and to pack hexagonally when observed by SEM. Control over particle size was obtained by adjusting the ratio of monomer to solvent (varying monomer content from 39% up to 47%). This enabled the synthesis of monodisperse particles from 350 to 1100 nm. At this stage, dispersions were synthesised containing EGDMA at various molar percentages (1-5%) and polymerisable dyes (up to 10%). Monodisperse spherical particles were obtained in all cases, with the exception of the dispersion which contained 5% EGDMA, indicating an upper limit to the amount of cross-linker that can be added which will still result in a stable dispersion. It was also demonstrated that polymerisable dyes (red and magenta) could be incorporated into the particles without affecting the dispersity and particle size of the dispersions.

These dispersions were seen to solidify if left to stand for a period of time, but were observed to redisperse if they were warmed up. This thermoresponsive transition was believed to be due to the crystallisation of the side chains of the PODA block, and as such, modified stabilisers were designed. A new range of stabilisers were synthesised containing EHA as a comonomer in the PODA block, in an attempt to

disrupt the crystallinity that the PODA possessed, and in turn prevent the gelation process observed for the stabilised particles. These stabilisers had molecular weights between 12300 and 19800 $gmol^{-1}$, and dispersities below 1.63. The PMMA-*b*-(PODA-*co*-PEHA) stabilisers synthesised were then used in NAD polymerisations, and were again seen to produce monodisperse, spherical particles, with the addition of cross-linkers and dyes not affecting the crucial properties of these particles. Stable dispersions of particles as small as 150 nm (measured by DLS) were synthesised using these stabilisers.

The gelation process was further investigated using DLS, DSC and rheological analysis. Dispersions stabilised by PMMA-*b*-PODA block copolymers were seen to gelate at around 20°C, and the same transition was observed when the stabiliser alone was dissolved in dodecane. However, other long chain molecules such as octadecane and octadecyl acrylate were not seen to go through a thermal transition in the same region. This indicated that the gelation process was related to the ordering of the long chains into a 'brush-like' arrangement. The temperature at which this transition occurred did not correspond to the melting/crystallisation temperatures of any of the individual components, so this transition was assigned as a T_{gel} rather than a T_g or T_m.

The determination of the transition as a 'gelation' was supported by evidence from DSC and rheology. A transition corresponding to the T_c of the dodecane was observed for both a sample of a PMMA-*b*-PODA stabiliser in dodecane, and of the corresponding dispersion D1. This indicated that the structures formed were in fact gels, with the alkyl chains of the PODA crystallising, with amorphous regions of dodecane present within the samples. This gelation was also observed by a dramatic increase in viscosity as the dispersion samples were cooled, as well as a drop in phase angle to around 45°, indicating the material behaved more like a liquid above the T_{gel} but as a solid-like gel below this temperature.

The addition of the comonomer EHA was seen to change the temperature at which these transitions occurred. Dispersions synthesised with copolymers with the lowest contents of EHA (58 molar %) still exhibited a thermoresponsive gelation process, but at a lower temperature than those stabilised by PMMA-*b*-PODA. Stabilisers with increased EHA concentration (73 molar %) produced dispersions which did not

exhibit any gelation, even after refrigeration. This was confirmed by rheology, where decreasing the temperature of a dispersion to as low as 5°C did not induce an increase in viscosity or a drop in phase angle (other than the slight changes expected due to reduced molecular movement at reduced temperatures).

PMMA macroinitiators were also used to synthesise block copolymers with a fluorinated block. These block copolymers were synthesised by ATRP, but characterisation proved to be difficult as the fluorinated components were not soluble at temperatures at which analysis was typically carried out. For this reason, GPC and NMR data was collected at 50°C. The intention was to use these as stabilisers for PMMA particles in fluorinated solvents, but attempts at this were unsuccessful.

A potential difficulty in using sterically stabilised particles in electrophoretic displays is the possibility that the stabiliser chains could become detached from the particles after numerous 'switches' under the changing field of the device. For this reason, the ability to bind the stabiliser onto the particle would be valuable. This began with the synthesis of hydroxyethyl bromoisobutyrate, an initiator to be used in ATRP which possessed a hydroxy- group at the end. This group would not react during the synthesis of the stabiliser, but could then be substituted for a wide range of other functional group. This initiator was used in the synthesis of a range of block copolymer stabilisers by ATRP, also incorporating EHA into the lyophilic block.

The HO- group at the end of one block copolymer stabiliser was substituted for pyrene butyryl chloride, which was confirmed by ^{1}H NMR and UV-Vis spectroscopy. This indicated that replacement of the functional group was relatively facile, so the hydroxy- group of another stabiliser was substituted with methacryloyl chloride to add a polymerisable group. Evidence that this substitution was successful was obtained from ^{1}H and ^{13}C NMR, and these polymerisable stabilisers were then used in the NAD polymerisations. No adverse effects were observed by using these stabilisers, and particles were synthesised with low dispersities, even when dyes and cross-linkers were incorporated.

To summarise, Figure 6.1 shows the flexible characteristics of the stabiliser and of this method of particle synthesis. It demonstrates that not only does increasing the weight percentage of stabiliser (relative to solvent) increase the resulting particle

size, but that these results are also in agreement with work previously published with regard to size control. The ○ represents syntheses presented in this work, whilst □ are results from previous literature in this field.[1] Figure 6.1 also displays the sizes of all particle dispersions presented in this work – particles from 200 nm to 1.3 µm have been synthesised via NAD polymerisation, and the change in particle size is due to changes in reaction conditions, mainly the variation of molar ratios of starting materials, or occasionally the addition of cross-linkers and polymerisable dyes.

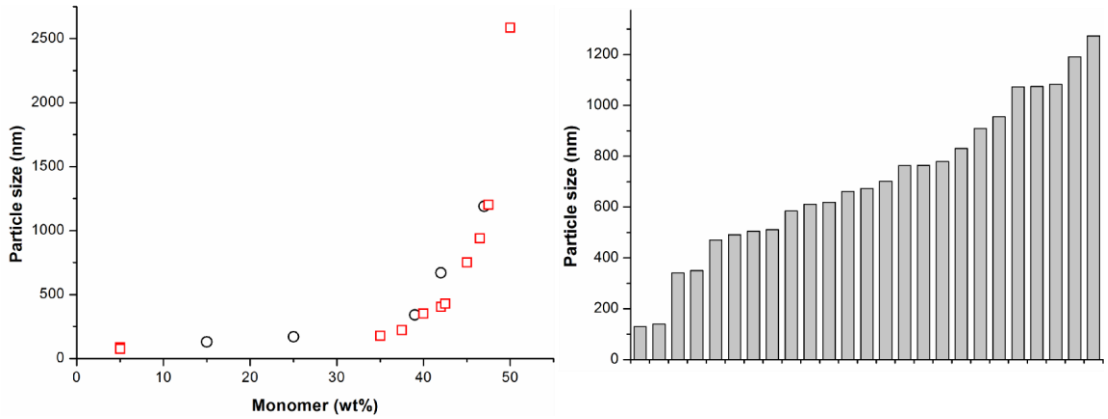

Figure 6.1: the PMMA-*b*-PODA based stabiliser system is versatile – a) particle size is directly linked to the wt. % monomer added to the reaction; b) by simply varying the experimental conditions of NAD polymerisation, it is possible to synthesise particles from 200 nm to 1.3 µm.

Figure 6.2 demonstrates the range of coloured dispersions which were synthesised by NAD polymerisation, and shows the SEM images for each, demonstrating the monodisperse, spherical nature of the particles for each dispersion.

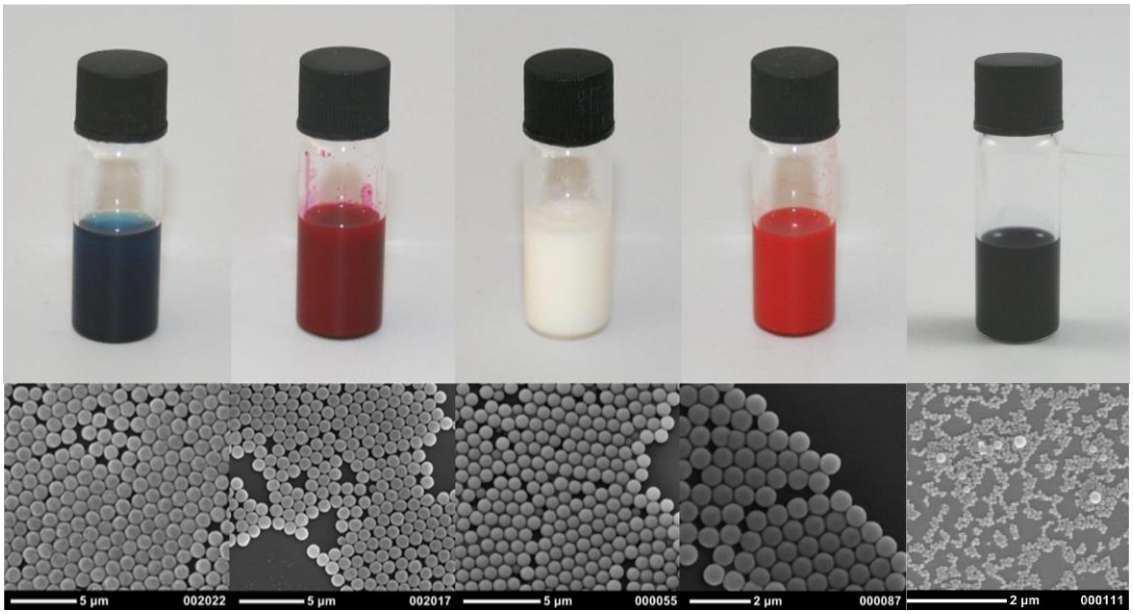

Figure 6.2: a summary showing the range of coloured particles synthesised, with corresponding SEM images.

This work has resulted in the publication of a patent, entitled 'Particles for Electrophoretic Displays'[2], as well as a paper looking into the gelation process, which is in preparation for submission to Langmuir.

6.2 Further Work

Single electron transfer living radical polymerisation (SET-LRP) has been reported to synthesise polymers with high chain end fidelity and low dispersities, as well as requiring less metal catalyst.[3] However, success of this method with methacrylates has been rather more limited.[4] If the SET system trialled briefly in this work could be modified in order to prevent the termination which was observed by MALDI analysis, the synthesis of the stabilisers would become more commercially viable. The amount of metal catalyst required for the synthesis via ATRP is undesirable for scaling up the reactions to industrial scale, and SET would be a possible solution to this. Another would be to ensure that the purification of the products allowed for the catalyst to be recycled, as discussed in Chapter 1.

One potential area which was not considered during this work was that the thermoresponsive gelation (which was undesirable for the present application) could

be potentially valuable for a number of other applications. Thermoresponsive colloidal microgels have found applications as carrier systems for drugs, diagnostic agents and nanoparticles[5], and research could be conducted into whether the PMMA particles in dodecane system could be adapted to find a role in these areas.

Whilst including EHA in the lyophilic block of the copolymer stabilisers was sufficient to prevent the gelation of dispersions, EHA was only added in two different molar ratios in relation to the ODA content of the block. Adding 58% EHA reduced the temperature at which the gelation occurred, whilst 73% EHA content prevented the gelation at temperatures down to 5°C. It would be of interest (particularly if studying potential applications related to thermoresponsive nature) to investigate in greater depth if varying the EHA content of the stabiliser allowed for the temperature of gelation to be tuned more accurately. A copolymer of PMMA-*b*-PEHA could also be synthesised – this copolymer should not exhibit crystallisation, and therefore should not induce gelation of colloidal dispersions. However, it is possible that this copolymer would not have the same stabilising behaviour as the PMMA-*b*-PODA stabilisers, which could result in larger, more polydisperse particle dispersions. This would indicate that a balance is required between stabilising behaviour and disruption of order in the polymeric side chains.

The synthesis of fluorinated block copolymers was discussed briefly in this work, but was not pursued further as researchers at Merck were unable to synthesise stable dispersions when using them as stabilisers, even when using fluorinated solvents. However, it has since become apparent that fluorinated dispersions are possible when the reactions are conducted using supercritical carbon dioxide. To complete this branch of the current research, it would be interesting to look at the properties of particles stabilised with the fluorinated stabilisers which were successfully synthesised.

A more in depth study into the structure of the stabilisers before and after substitution would be valuable, potentially using 2D techniques such as HSQC. This would require more time using the 600 MHz NMR equipped with a cryoprobe. It would also be an interesting extension of this work to look into the possibility of adding HEMA as a comonomer in the PMMA block to add multiple polymerisable sites along the stabiliser structure. The ‘methacryloylation’ of hydroxy groups has

already been reported,[6] and research into the effect (if any) of using stabilisers with multiple sites for polymerisation on the properties of particles synthesised would be useful. This could also allow for a detailed study into the long-term stability of particles after repeated electrophoretic switching, with a comparison between particles stabilised by unbound stabiliser, and those stabilised with block copolymers bound in one, and more than one, site. The synthesis of PMMA-*co*-PHEMA has also been reported for use in biological applications,[7] so this work could potentially extend the areas in which this copolymer could be utilised.

Finally, work into 'one-pot' dispersion polymerisations, where the stabiliser is synthesised in-situ before the particles are formed in the same reaction vessel, has been presented.[8] There are, however, limitations to this technique. The size of particles produced is dictated by the length of the polymeric stabiliser synthesised. This means that considerably longer stabiliser chains would be required in order to synthesise particles of the same size as those produced by NAD in this work. This would be an attractive route to sterically stabilised PMMA particles, which would improve ease of synthesis, and in turn commercial viability. This would require the synthesis of PODA homopolymers by ATRP, and on completion of this reaction MMA would be added. If the conditions were accurately controlled, this would drive the synthesis of a block copolymer, before the PMMA portion of the chains became entangled and formed particles. If this was successful, despite the size limitation, theoretically the addition of dyes to these reactions would be trivial, allowing for the synthesis of full colour, polymeric dispersions for use in electrophoretic displays, in just one reaction step.

6.3 References

1. L. Antl, J. W. Goodwin, R. D. Hill, R. H. Ottewill, S. M. Owens, S. Papworth and J. A. Waters, *Colloids and Surfaces*, 1986, **17**, 67-78.
2. Polymer particles for electrophoretic displays, *WO2014166583A1*, L. D. Farrand, C. Topping, K. Belsey and S. Holder, 2014.

3. V. Percec, T. Guliashvili, J. S. Ladislaw, A. Wistrand, A. Stjerndahl, M. J. Sienkowska, M. J. Monteiro and S. Sahoo, *Journal of the American Chemical Society*, 2006, **128**, 14156-14165.

4. S. R. Samanta, A. Anastasaki, C. Waldron, D. M. Haddleton and V. Percec, *Polym. Chem.*, 2013, **4**, 5563-5569.

5. Y. Hertle and T. Hellweg, *Journal of Materials Chemistry B*, 2013, **1**, 5874-5885.

6. J.-S. Koo, P. G. R. Smith, R. B. Williams, M. C. Grossel and M. J. Whitcombe, *Chemistry of Materials*, 2002, **14**, 5030-5036.

7. E. Vargün, M. Sankir, B. Aran, N. D. Sankir and A. Usanmaz, *Journal of Macromolecular Science, Part A*, 2010, **47**, 235-240.

8. L. P. D. Ratcliffe, A. J. Ryan and S. P. Armes, *Macromolecules*, 2013, **46**, 769-777.